POLYSACCHARIDE BASED PACKAGING FILM FOR FRESH CUT PRODUCE

A Thesis Submitted to
The Graduate School of Engineering and Sciences of
İzmir Institute of Technology
In Partial Fulfillment of the Requirements for the Degree of

DOCTOR OF PHILOSOPHY

In Food Engineering

By
Merve ŞAMLI

February, 2017
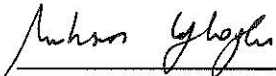İZMİR

We approve the thesis of **Merve ŞAMLI**

Prof. Dr. Şebnem HARSA
Department of Food Engineering
Izmir Institute of Technology

Prof. Dr. Figen KOREL
Department of Food Engineering
Izmir Institute of Technology

Prof. Dr. Yekta GÖKSUNGUR
Department of Food Engineering
University of Ege

Prof. Dr. Muhsin ÇİFTÇİOĞLU
Department of Chemical Engineering
Izmir Institute of Technology

Assoc. Prof. Dr. Seda ERSUS BİLEK
Department of Food Engineering
University of Ege

1 February 2017

Prof. Dr. Şebnem HARSA
Supervisor
Department of Food Engineering
Izmir Institute of Technology

Assist. Prof. Oğuz BÜYÜKKİLECİ
Co-Supervisor
Department of Food Engineering
Izmir Institute of Technology

Prof. Dr. Ahmet YEMENİCİOĞLU
Head of the Department of
Food Engineering

Prof.Dr. Aysun SOFUOĞLU
Dean of the Graduate School
of Engineering and Sciences

ACKNOWLEDGEMENTS

ABSTRACT

POLYSACCHARIDE BASED PACKAGING FILM FOR FRESH CUT PRODUCE

In this thesis, agro industrial wastes such as bracts and leaves of artichoke were used to develop biodegradable packaging materials for fresh-cut artichokes. As film forming materials; cellulose, hemicellulose, lignin and wax fractions were extracted by using mild alkaline treatment applied to artichoke wastes. Carboxy methyl cellulose was chemically synthesized from extracted cellulose fiber. A mechanical process (Masuko Supermasscolloider, at -100 μm grind size *via* 5 times feeding) with minimum environmental impact was selected to obtain cellulose micro fibrils with micro sized dimensions (50-200 μm in length and 10-30 μm in width). These fractions used as polysaccharide sources in film forming solutions. Different combinations of these polysaccharide based film materials were optimized using General Factorial Design and four film combinations were selected among the films produced. Selected films were MFC and CMC based having good elasticity (16 % strain), tensile strength and low gas permeability properties (150ml O_2 / m^2.day). Different concentrations of additives such as wax, stearic acid, chitosan were used with the glycerol addition of plasticizer. SEM analyses of selected films showed films having smooth surface and dense structure by looking their cross sectional area. Thermal analyses proved sealability of films obtained by extracted fractions from artichoke at 200-250 °C temperature intervals. But, presence of MFC in films hindered the heat sealing ability. Therefore, MFC and CMC based films successfully showed optimal properties when they were combined with glycerol, stearic acid and wax.

ÖZET

TÜKETİME HAZIR MEYVE SEBZELER İÇİN POLİSAKKARİT BAZLI AMBALAJ FİLMİ

Bu tezde, enginarın kullanılmayan kısımlarından (sapları, yaprakları) yararlanılarak taze kesilmiş enginarda kullanılabilecek nitelikte biyobozunur paketleme malzemesi geliştirilmiştir. Enginar atıklarının hafif bazik koşullarda muamele edilmesi sonucunda elde edilen selüloz, hemiselüloz, lignin ve vaks fraksiyonları film oluşturulmasında kullanılmıştır. Ayrıca, enginardan özütlenen selüloz liflerine uygulanan kimyasal dönüşüm işlemi ile sodyum karboksimetil selüloz elde edilmiştir. Mikro boyutta selüloz liflerinin (boyu 50-200 μm ve eni 10-30 μm) üretimi için çevre dostu mekanik bir işlem (Masuko mekanik parçalayıcı, -100 μm aralığında dişlilerden 5 kez besleme) kullanımının uygun olduğu gösterildi. Bu fraksiyonlar, film çözeltilerinde polisakkarit bazlı hammadde olarak kullanıldı. Faktoriyel tasarım temelli deneysel tasarım tekniğinden yararlanılarak, tüm denemeler içerisinden dört adet en uygun içerik belirlendi. Temelde mikrofibril selüloz ve karboksi metil selülozdan oluşan ve önceki denemeler sonucunda belirlenen en uygun koşullarda üretilen filmlerin tercih edilebilir nitelikte esneklik (%16 uzama), kopma mukavemeti ve düşük gaz geçirgenliği (150ml O_2 / m^2.gün) özellikleri gösterdiği tespit edildi. Vaks, stearik asit, kitosan gibi katkıların ve plastikleştirici olarak gliserolün değişik konsantrasyonlarda ilaveleri ve bunların film oluşturabilme özellikleri üzerine etkileri incelendi. Seçilen filmlerin, taramalı elektron mikroskobu görüntüleri filmlerin pürüzsüz yüzeye, yoğun, sıkı ve tekdüze bir kesite sahip olduğunu gösterdi. Termal analizler sonucunda, enginardan elde edilen - mikrofibril selüloz haricindeki- tüm ürünlerle yapılan filmlerin 200- 250°C sıcaklık aralığında ısıl yapışma özelliği gösterdiği, ancak mikrofibril selüloz ilavesi yapılan filmlerin, ısıl yapışma özelliğini kaybettiği görüldü. Sonuç olarak, mikrofibril selüloz ve karboksil metil selüloz içeren karışıma gliserol, stearik asit ve vaks ilavesi halinde elde edilen filmin üretilen filmler arasında en uygun malzeme olduğuna karar verildi.

TABLE OF CONTENTS

LIST OF FIGURES

LIST OF TABLES

ABBREVIATIONS

# T.D.	# Times diluted sample
AA	ascorbic acid
AFM	Atomic force microscopy
ALP	artichoke leaf powder
ANOVA	analysis of variance
ARTLP	artichoke leaf micro powder
Aq Chi	Chitosan dissolved in ultrapure water
ATR	Attenuated Total Reflection
AVG	average
Aw	water activity
CA	citric acid
CF	extracted cellulose fiber
CHI	chitosan
CIELAB	Hunter 1948 colour space (L*, a*, b)
CLS	micro granular cellulose (cellulose standard)
CMC	carboxylmethylcellulose
CPF	cellulose pulp film
Cys	cysteine
DALP	dewaxed artichoke leaf powder
DCF	de-ashed cellulose fiber
df	degrees of freedom
DSC	Differential Scanning Calorimetry
DTA	Differential Thermal Analysis
dTG	Derivative Thermal Gravimetry
DW	distilled water
ETOH	ethanol
FDMFDC	freeze-dried micro fibrillated de-ashed cellulose
FDMFC	freeze-dried micro fibrillated cellulose
FTIR	Fourier Transform Infrared spectroscopy
GDL	Glucono delta-lactone
GLY	glycerol

HMC	hemicellulose extract from artichoke waste
IR	Infrared Radiation
LH	Lignin-hemicellulose extract from artichoke waste
LHW	Lignin-hemicellulose-wax extract from artichoke waste
MCC	microcrystalline cellulose
MFC	micro fibrillated cellulose
MFDC	micro fibrillated de-ashed cellulose
MFFT	minimum film forming temperature
MFT	microfluidized+microfibrillated cellulose
MIR	Middle Infrared Radiation
MRTR	mortared+diluted+freezedried microfibrillated cellulose/its film
MS	Mean square
MW	Molecular Weight
NCMC	synthesized carboxyl methylcellulose from artichoke waste
Na-CMC	sodium carboxyl methylcellulose from Sigma Aldrich
nD	refractive index
N-TR	diluted+freeze-dried micro fibrillated cellulose/its film
OTR	oxygen transmission rate
PAL	Phenylalanine ammonia lyase
PCA	principal component analyses
PCM	Inverted phase contrast microscope
PEG 400	polyethylene glycol 400
PPO	polyphenoloxidase
SEM	Scanning Electron Microscopy
SMBS	Sodium Metabisulphite
SS	Sum of Squares
StA	Stearic acid
STDDEV	Standard deviation
STD sol'n	Standard solution
UPW	ultra-pure water
TGA	Thermal gravimetric analyses
Tw80	Tween 80
XRD	X Ray Powder Diffractometry
WVTR	Water Vapour transmission rate

CHAPTER 1

INTRODUCTION

Today, there is an increasing demand for fresh or minimally processed, healthy and functional fruit and vegetables. Therefore, enhancing the nutritional, microbiological and organoleptic qualities of fresh cut fruits and vegetables is drawing greater attention. However fresh cut products are more prone to rapid degradation than whole products, and are characterized by a limited shelf life.

Artichokes are an important component of the Mediterranean diet, and a good source of health-promoting compounds, mainly polyphenols. The artichoke is classified as Cynara scolymus. It grows wild in the south of Europe and is also cultivated in the United States. The edible fraction of artichoke plants is represented by the inner part of immature flowers, which accounts for about 15–20% of its fresh weight, depending on the variety and the harvesting time, and about 50% of the whole head (Cabezas-Serrano et. al 2009). In Turkey, artichoke is cultivated in Mediterranean, Aegean, Marmara regions. With a production value of 35000 metric tons, Turkey ranks 12th in the world and 4th in Europe.

Processing artichokes as fresh-cut would provide convenience due to the high percentage of discarded plant waste, and the complexity of preparation and trimming operations. The main problem with fresh-cut artichokes is the high browning rate of the cut surfaces (receptacle and bracts) caused by oxidation of phenolics catalysed by polyphenol oxidase enzymes, with subsequent formation of dark compounds (Amodio et. al 2011). It is well known that the dual role of phenol compounds as antioxidants and as substrates for oxidative enzymatic and non-enzymatic browning reactions may cause a severe shelf-life reduction of both whole and fresh-cut products. Browning is the main process responsible for quality loss during postharvest handling, storage and a limiting factor to processing artichoke (Todaro et. al 2010). Further, in the case of artichokes, the enzymatic browning is so rapid that the methods used for other fresh cut products are not as effective.

Therefore new approaches are needed to solve the rapid browning problem in artichokes. Coating methods; in which products are either sprayed with or dipped into various protective solutions (containing antioxidant, antimicrobial or chelating agents), help fresh cut produce to control / prevent browning or microbial deterioration (Todaro et al. 2010). Most browning reactions are promoted by oxygen; therefore avoiding oxygen in the food environment can slow down deterioration of the product. This can be achieved by using a packaging material with low oxygen permeability. Such packaging can be combined with a mild pre-treatment in order to provide a minimally processed food with a high quality and which has a relatively long shelf life. Cutting operation decreases shelf life of fruit and vegetables significantly, due to increased surface area, formation of injured tissues compared to whole product (Niranjan and Harsa 2013).

Polysaccharides can be extracted from many plants, however using agricultural wastes, particularly the waste from the same source as the product being packaged can have considerable economic and environmental impacts. Most of the agro-based wastes are dumped or utilized as animal feed, which has low economic value. Utilization of wastes for obtaining high value compounds like polysaccharides can enhance the value of the wastes which under the right circumstances can become co-products.

Biopolymers originating from renewable raw materials can be used to develop a wide range of environmentally friendly products. Bio based polymers, which are compostable, renewable and independent from fossil fuels, have the potential to reduce the carbon dioxide release into the atmosphere and therefore hinder greenhouse effect and global warming while alleviating the concern about recycling.

Gas barriers of packaging materials become essential when the gas composition inside the package has to be kept constant or free from oxygen. Many polysaccharides (natural polymeric carbohydrates) are known to be good oxygen barriers, explained by their hydrogen-bonded network which leads to small free volume that makes the oxygen transmission low (Miller 1997).

Hemicelluloses and many other polysaccharides are also known to be good oxygen barriers. Hemicelluloses of mannan type have been successfully used in packaging films preparation, demonstrating good film-forming properties and resistance toward oxygen diffusion (Edlund 2010).

Micro fibrillated cellulose (MFC), also called cellulose micro fibril, micro-fibrillar cellulose or Nano-fibrillated cellulose (NFC), can be viewed as a cellulosic material, composed of expanded high-volume cellulose, moderately degraded and

greatly expanded in surface area, and obtained by a homogenization process. MFC actually consists of aggregates of cellulose micro fibrils. Micro-fibrillated cellulose thus has a very good ability to form a rigid network. It is obtained by the mechanical disintegration of cellulosic materials without the use of hydrolysis (Lavoine et al. 2011).

Consequently, the enzymatic browning will be retarded, and the shelf life of the artichokes will be extended. Finding strategic ways to enhance the shelf life and keeping quality of fresh cut produce without unduly burdening the environment, must be a key part of any Food Security strategy.

The aim of this study is to develop packaging films with improved gas barrier properties in order to extend the keeping quality of minimally processed fresh cut vegetables, such as artichoke, which is a good source of several nutritional compounds. The packaging material formed was targeted to extend shelf life of fresh cut artichokes for retarding browning by providing O_2 barrier platform in form of package. Based on these objectives; packaging films from artichoke wastes were prepared *via* environmentally friendly process steps with less expense. Micro fibrillated cellulose may meet these expectations; therefore, the thesis was set to obtain cellulose and microfibrillated cellulose by using mild chemical combined with mechanical methods. Films were produced using the polysaccharides extracted from artichoke leaves. The extracts were casted into films either singly or in combination with a plasticizer compound. Other polysaccharide based film materials were also introduced into the film combinations in order to be able to tolerate surface moisture of artichokes. Films were characterized in terms of their mechanical, thermal, crystalline, morphological, and visual and gas permeability properties.

CHAPTER 2

PACKAGING

In today's food market packaging is an essential concept for handling, storage and distrubution of food products securely to the consumers. Package is any kind of protective material enclosing consumable entity in order to maintain security and safety of a specific product. In case of food packaging, there are some different concerns for providing extra safety across physical, chemical, microbial and sensorial deteriorations, since food components are very perishable materials. Any unwanted changes of food product directly affect consumer acceptability and may risk consumer health. Packaging with labels is also important for providing knowledge about content, shelf life, storage conditions of that food product (Robertson 2005).

There are various packaging materials (such as paper, glass, metal or plastic) and techniques applied for food products. Application technique or used material may vary among needs of food product. In some cases, combination of different materials might used in order to reach best protection for longest time period. Atmosphere enclosed within package material is critical for maintaining protection. That's why modified atmosphere or vacuum packaging techniques are applied due to needed atmosphere composition of selected food material.

While packaging protects the food material from environment it may interact and negatively affect food product, these submicroscobic interactions termed as migration. Migration is an important unwanted reaction chain that may result in chronic dieseases within human body *via* accumulation of risky compounds within liver in long term period (Lee et al. 2008).

Besides traditional packaging applications there are many researches on intelligent and active packaging systems providing extra functional properties to packaging material i.e. absorbing excess oxygen/carbondioxide within package, releasing antioxidant/ antimicrobial compounds, adsorbing/releasing flavor components, etc.

2.1. Agropolymers for edible and biodegradable films

Agriculture is one of the major industries in Turkey. Tea, sunflower, olive, nuts, many cereals (wheat, barley, corn, and rice), legumes (lentils, beans, and soy), industrial plants (cotton, sugar beet, tobacco) and fruits are widely cultivated. Consequently, there is a significant amount of waste material after harvesting or processing, composed of leaves, stalk, cob, stover, husk, bran, straw, trimmings, peels, etc. Although some of these materials are used in low economic value applications (feedstock or burning as fuel), they are predominantly unutilized. Therefore, there is substantial amount of cheap and year round available plant polysaccharide sources in Turkey, which can be exploited for use in bio packaging applications.

Polysaccharides can be extracted from many plants, however using agricultural wastes, particularly the waste from the same source as the product being packaged can have considerable economic and environmental impacts. Most of the agro-based wastes are dumped or utilized as animal feed, which has low economic value. Utilization of wastes for obtaining high value compounds like polysaccharides can enhance the value of the wastes which under the right circumstances can become co-products.

Biopolymers originating from renewable raw materials can be used to develop a wide range of environmentally friendly products. Bio based polymers, which are compostable, renewable and independent from fossil fuels, have the potential to reduce the carbon dioxide release into the atmosphere and therefore hinder greenhouse effect and global warming while alleviating the concern about recycling.

2.1.1 Lignocellulosic Biomass

Ligno-cellulosic biomass is the most abundant source of unutilized biomass and their availability does not necessarily impact land use. Biomass in general consists of 40-50% cellulose, 25-30% hemicellulose and 15-20% lignin and other extractable components (Menon and Rao 2012). Lignocellulose framework within cell wall was illustrated in Figure 2.1.
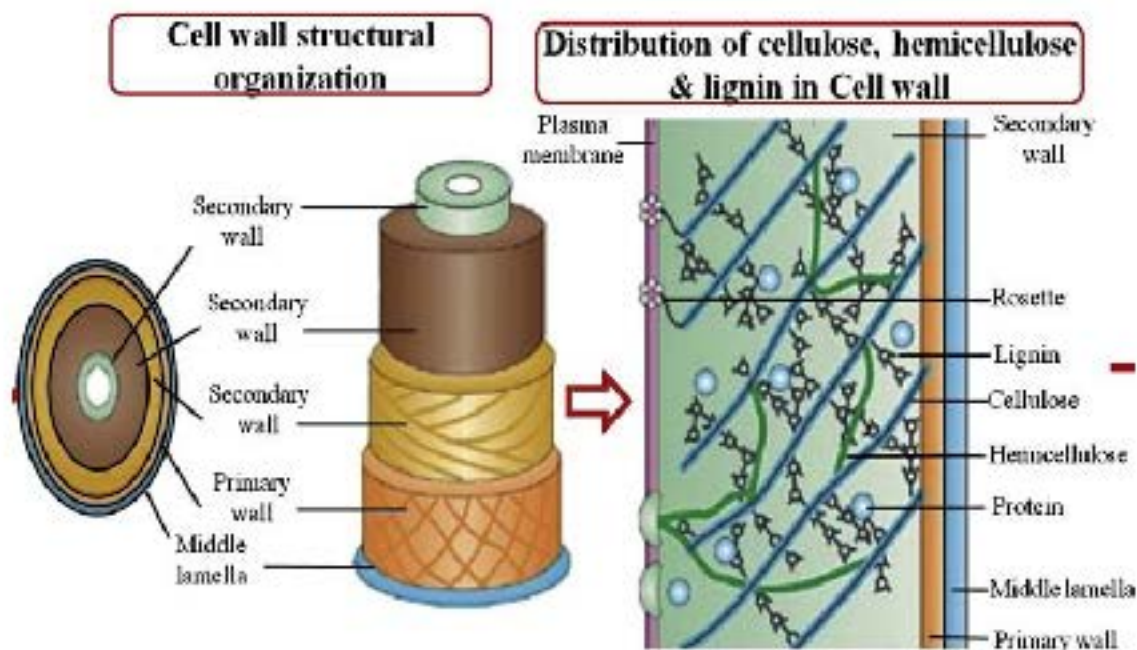
Figure 2.1 Diagrammatic illustration of the framework of lignocelluloses
(Menon and Rao 2012)

Cellulose is the most abundantly occurring natural polymer on earth and is almost linear polymer of anhydroglucose. The worldwide production of cellulose is estimated to be between 10^{10} and 10^{11} tonnes each year (Lavoine *et al.*).

Cellulose is a linear homopolysaccharide of β-1,4-linked anhydro-D-glucose units with a degree of polymerization (DP) of approximately 10,000 for cellulose chains in nature and 15,000 for native cellulose cotton. Cellobiose units construct basic structure of cellulose; these dimers were presented in Figure 2.2-(A) below. The anhydroglucose unit (monomer), contains three hydroxyl groups having ability to form strong hydrogen bonds confer upon cellulose its most important properties, in particular its (i) multi-scale micro fibrillated structure, (ii) hierarchical organization (crystalline vs. amorphous regions), and (iii) highly cohesive nature (with a glass transition temperature higher than its degradation temperature) (Lavoine *et al.*).

Tight packing of polymer chains of anhydroglucose causes a crystalline structure that restricts hydrophilicity. Treating cellulose with alkaline followed by reaction with mono chloro acetic acid to yield carboxyl methyl cellulose (CMC) would lead an increase in water solubility of cellulose (Dhall 2012). Detailed structure of CMC was shown in Figure 2.2-(B).

6
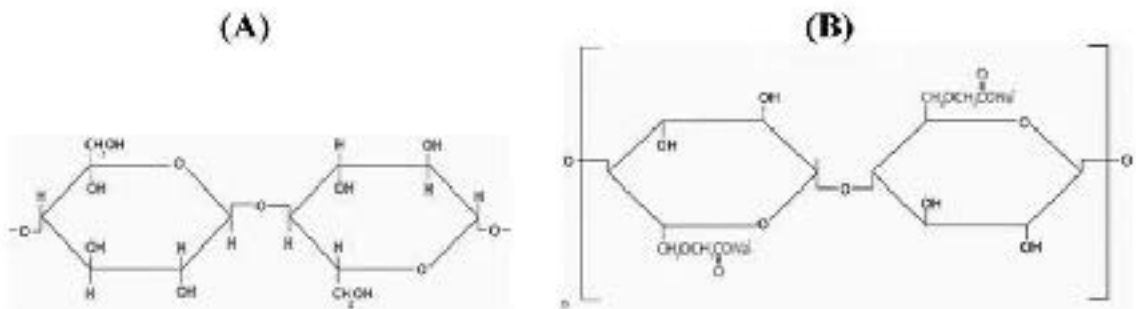
Figure 2.2 Structure of (A) cellulose, (B) carboxyl methyl cellulose (Laaman 2011).

The cellulose chains are packed into micro fibrils which are stabilized by hydrogen bonds. These fibrils are attached to each other by hemicelluloses and amorphous polymers of different sugars (Menon and Rao 2012). Hemicelluloses are hetero-polysaccharides and they represent up to 50% of the biomass of annual and perennial plants.

While the cellulose basic chemical structure is identical in plants, the composition of hemicelluloses can vary within tissues of the same plant (e.g., roots, stems, leaves and seeds) and between different plant species, differences presented in Table 2.1. In contrast to cellulose, hemicelluloses are amorphous, often branched and have different solution properties (Albertsson *et al.* 2011). Xylan, glucuronoxylan, arabinoxylan, glucomannan, and xyloglucan could be listed as types of hemicelluloses. While cellulose contains simply anhydrous glucose; hemicelluloses may contain xylose, mannose, rhamnose, arabinose and galactose.

Hemicelluloses are usually divided into four major groups in view of their structural conformation: D-xyloglycans (xylans), mannans, mixed-linkage β-glucans and xyloglucans (Heinze *et al.* 2005). The monosaccharide building blocks of hemicelluloses can be pentose and hexose sugars as well as acid sugars (J. M. Fang *et al.* 1999). Common molecular motif of hemicelluloses was given in Figure 2.3. Hemicelluloses' composition vary due to the differences in extraction/isolation steps (Hansen and Plackett 2008).
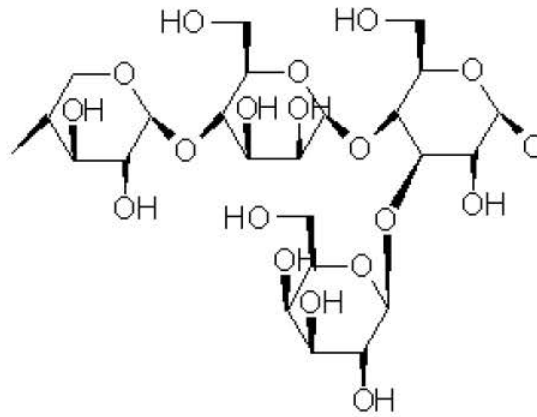
Figure 2.3 Common molecular motif of hemicelluloses [-Xylose-β (1, 4)-Mannose-β(1,4)-Glucose-α(1,3)] (Anon 2013-H)

Lignin is a class of complex, high molecular weight polymers whose exact structure varies. It is an amorphous, i.e., not crystalline, polymer that acts as a binding agent to hold cells together. Lignin also occurs within cell walls to impart rigidity. Like cellulose and hemicelluloses, lignin is made from carbon, oxygen, and hydrogen. However, these elements are arranged differently so that they are not classified as carbohydrates. They are instead classified as phenolics, and the polymer is based on the phenyl propane unit (Adler 1977). Molecular structure of lignin was shown in Fig 2.4.
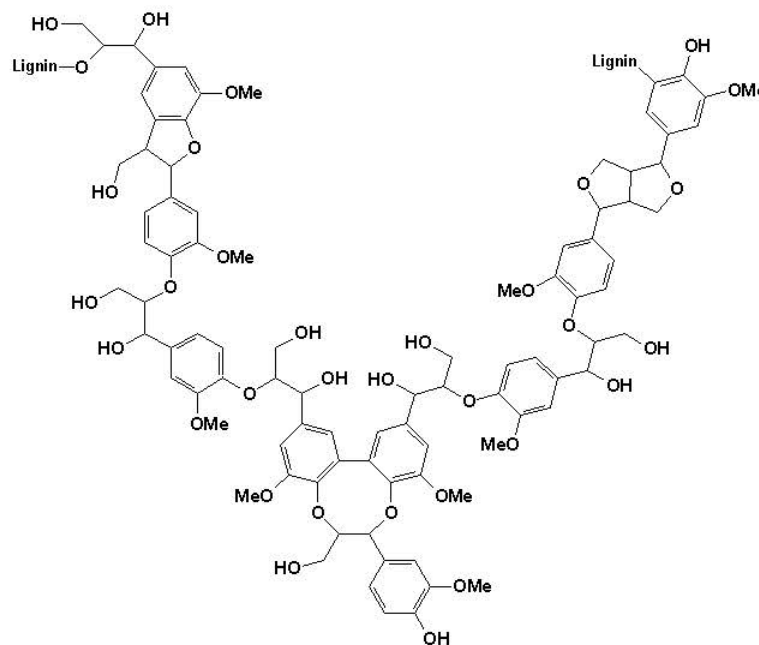
Figure 2.4 A small piece of lignin polymer (Anon 2013-L).

Table 2.1 The main types of polysaccharides present in hemicelluloses (Peng et al. 2012).

Polysaccharide	Biological origin	Amount (% dry biomass)	Backbone	Side chain	Degree of polymerization
Arabinogalactan	Softwoods	5-35	β-D-Galp	β-D-Galp	100-600
				α-L-Araf	
				β-L-Arap	
Xyloglucan	Hardwoods, softwoods, and grasses	2–25	β-D-Xylp	β-D-Xylp	
			β-D-Glcp	β-D-Galp	
				α-L-Araf	
				α-L-Fucp	
				Acetyl	
Galacto glucomannan	Softwoods	10–25	β-D-Manp	β-D-Galp	40–100
			β-D-Glcp	Acetyl	
Glucomannan	Hardwoods	2-5	β-D-Manp		40-70
			β-D-Glcp		
Glucuronoxylan	Hardwoods	15-30	β-D-Xylp	4-O-Me-α-D-GlcpA	100-200
				Acetyl	
Arabino glucuronoxylan	Grasses and softwoods	5–10	β-D-Xylp	4-O-Me-α-D-GlcpA	50–185
				α-L-Araf	
Glucurono arabinoxylan	Grasses	15–30	β-D-Xylp	α-L-Araf	
				4-O-Me-α-D-GlcpA	
				Acetyl	
Arabino glucuronoxylan	Grasses and softwoods	5–10	β-D-Xylp	4-O-Me-α-D-GlcpA	50–185
				α-L-Araf	
Glucurono arabinoxylan	Grasses	15–30	β-D-Xylp	α-L-Araf	
				4-O-Me-α-D-GlcpA	
				Acetyl	
Homoxylan	Algae		β-D-Xylp		
β-(1→3, 1→4)-glucan	Grasses	2-15	β-D-Glcp		

Lignin is composed of three major phenolic components, namely p-coumaryl alcohol, coniferyl alcohol and sinapyl alcohol. Lignin is synthesized by polymerization of these components and their ratio varies between different plants, wood tissues and cell wall layers. Lignin is a complex hydrophobic, cross-linked aromatic polymer that interferes with the hydrolysis process (Menon and Rao 2012).

2.1.2 Microfibrillated cellulose

Micro fibrillated cellulose (MFC), also called cellulose micro fibril, micro-fibrillar cellulose or nano-fibrillated cellulose (NFC), can be viewed as a cellulosic material, composed of expanded high-volume cellulose, moderately degraded and greatly expanded in surface area, and obtained by a homogenization process. MFC actually consists of aggregates of cellulose micro fibrils. Its diameter is in the range 20–60 nm and it has a length of several micrometers. If we consider that the micro fibrils have around 2–10 nm thickness fibrous cellulose structure and have length around several tens of microns, and then MFC is composed of 10–50 micro fibrils. MFC exhibits both amorphous and crystalline parts and presents a web-like structure. Micro-fibrillated cellulose thus has a very good ability to form a rigid network. It is obtained by the mechanical disintegration of cellulosic materials without the use of hydrolysis (Lavoine *et al.*).

MFC is produced *via* mechanical refining of highly purified wood and plant fibre pulps. Mechanical treatment of cellulose to convert it to nanofibrillated form could be applied with supermasscolloider (Figure 2.5) or microfluidizer (Figure 2.6) or ultrasic homogenizer (Figure 2.7). There are various studies in the literature for obtaining micro/nanofibrillated cellulose by using ultrasonic treatment, detailed production procedures were summarized in Table 2.2.

Table 2.2 Ultrasonic grinding applications for cellulose

Source of Cellulose	Treatment Conditions	Reference
bleached pine kraft pulp	0.012g/300 ml dw;4°C;20kHz; 30,60,120, 240 min	Li 2009
kraft pulp	4°C;20kHz; 5,30,60,120 and 240 min	Li 2011
MCC and flax fiber	ultrasonic cleaner, 150W, 30 min	Qua 2011
MCC	80W; 38kHz; 50mg/L	Aliyu 2000
kraft pulp	68-170 kHz;1000W;25°C; 1% w/v; ultrasonic probe; 5,10,15,20,25 min; ultrasonic bath (40kHz; 5,10,15,20,30,60 min)	Mishra 2012
regenerated CF (avicel)	1-4% w/w;1500W; 30 min	Wang 2009
bamboo, wheat straw, softwood	0.05% w/w, 20-25 kHz; 30min;1200w	Chen 2011

Figure 2.5 Masuko Sangyo Supermasscolloider (MKCA6-2) (Masuko 2015)

Figure 2.6 Microfluidics fluidizer (Microcorp 2015).

THE FREQUENCY RANGES OF SOUND

Human hearing	16Hz - 18kHz
Conventional power ultrasound	20kHz - 100kHz
Extended range for sonochemistry	20kHz - 2MHz
Diagnostic ultrasound	5MHz - 10MHz
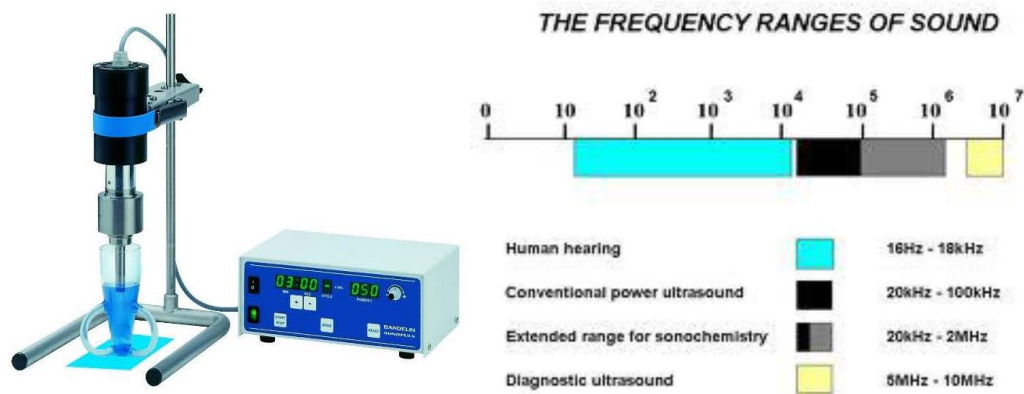
Figure 2.7 Bandelin Sonopuls HD 2070 Ultrasonic Homogenizer (Bandelin 2015)

MFCs have been used as a thickening agent in the food and cosmetics industries. The MFC particles are considered to contain multiple elementary fibrils each consisting of 36 cellulose chains arranged in the Iβ crystal structure, have a high aspect ratio (10–100 nm wide, 0.5–10's mm in length), are ~100% cellulose, and contain both amorphous and crystalline regions (Moon *et al.* 2011). Detailed structure of microfibrillated cellulose schematized in Figure 2.8.
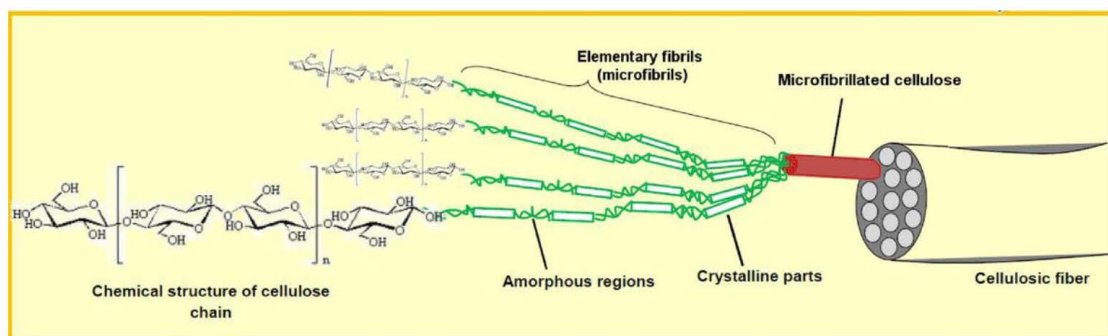
Figure 2.8   Fibre structure with emphasis on the cellulose micro fibrils (Lavoine, *et al.*2012.).

2.2 Edible and biodegradable coatings and films, process parameters and their mechanism

Films are generally defined as stand-alone thin layers of materials. They usually consist of polymers able to provide mechanical strength to the stand-alone thin structure (Han 2005). Edible coatings are thin layers of edible material applied to the product

surface in addition to or as a replacement for natural protective waxy coatings and to protect foods against moisture/gas transfer and solute movement. They are applied directly on the food surface by dipping, spraying, or brushing to create a modified atmosphere. Because they would be consumed, the material used for the preparation of edible films and coatings should be generally regarded as safe (GRAS) approved by FDA and must conform to the regulations that apply to the food product concerned. An ideal coating is defined as one that can extend storage life of fresh fruits and vegetables without causing anaerobiosis and reduces decay without affecting their quality.

Edible coating technology is a promising method to preserve the quality of fresh fruits and vegetables. Research and development efforts are leading to an improvement of the functional characteristics of the coatings, which depends on the properties of the fruit to be preserved or enhanced (Dhall 2012). An edible film is essentially a dried and extensively interacting polymer network of a three-dimensional gel structure. Various biopolymers can be mixed together to form a film with unique properties that combine the most desirable attributes of each component, e.g. presented in Table 2.3 (Han 2005).

Table 2.3 Materials used in edible films and coatings (Han 2005).

film-forming materials	proteins	Collagen, gelatin, casein, whey protein, corn zein, wheat gluten, soy protein, egg white protein, fish miyofibrillar protein, sorghum protein, pea protein, rice bran protein, cottonseed protein, peanut protein, keratin.
	lipids	Waxes (beeswax, paraffin, carnauba wax, candelilla wax, rice bran wax), resins (shellac, terpene), acetoglycerides
	polysaccharides	Starch, modified starch, modified cellulose (carboxyl methyl cellulose, methyl cellulose, hydroxyl propyl cellulose, hydroxyl propyl methyl cellulose)
plasticizers	Glycerin, propylene glycol, sorbitol, sucrose, polyethylene glycol, corn syrup, water	
functional additives	Antioxidants, antimicrobials, nutrients, nutraceuticals, pharmaceuticals, flavors, colours	
other additives	Emulsifiers (lecithin, Tweens, Spans), lipid emulsions (edible waxes, fatty acids)	

Film formation from polymeric solutions is a relatively straight forward process since the polymer is in the dissolved state. The sprayed droplets spread onto the substrate surface and, as the solvent evaporate, the polymer chains interpenetrate, going through a gel state then forming the film with further drying. Polymer chain

interpenetration occurs at a specific concentration which is the reciprocal of the intrinsic viscosity of the solution. The intrinsic viscosity is the increase in relative viscosity caused by the dissolved polymer and thus is an indication of the hydrodynamic interaction between the polymer and the solvent. Random coil structure of the polymer chains is generally thought to improve adhesion of the resultant film to the substrate, as more of the polymer is exposed to and interacts with the substrate surface. Solvent evaporation rate directly effect film formation ability, interms of surface attachability, high/low drying rate may give damage on polymer network, then may form unwanted structures and might prevent ideal film formation on surface; spray drying or spreading on the surface (orange peel effect), see Fig. 2.9 (Felton 2013).
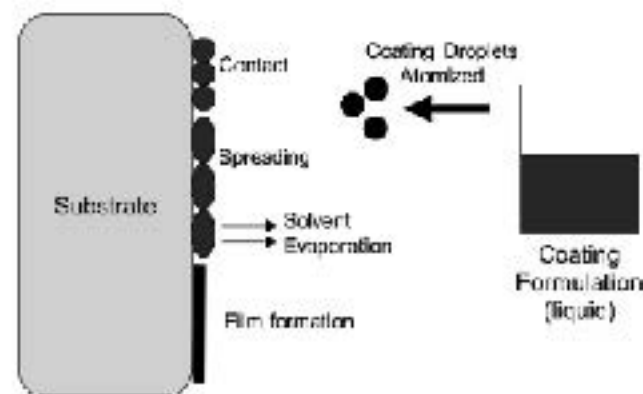
Figure 2.9 Overview of the film formation process (Felton 2013)

In film coating processes, several surface tensions are involved, including liquid–air, solid–liquid, and solid–air interfaces. Spreading of the polymer-containing liquid droplets can be described as surface wetting or the replacement of a solid–air interface with a solid–liquid interface. The process is dependent on the ability of the atomized droplets to wet the substrate (wetting power) and the ability of the substrate to be wetted by the droplets. Thus 'wetting' is influenced by not only the properties of the solution but also the characteristics of the solid substrate. There are three types of wetting processes: adhesion, where the liquid–air interface disappears; spreading, where a liquid–air interface forms; and immersion, where there is no change in the liquid–air interface.

All types of wetting involve solid–air interfaces being replaced by solid–liquid interfaces. Variables that influence wetting are related to substrate formulation (such as surface roughness, porosity, hydrophobicity), coating formulation (for example, viscosity), and processing conditions (including droplet momentum, atomizing air

pressure, distance between the spray gun and substrate, and the rate of solvent evaporation).

In contrast to aqueous polymeric dispersions, viscosity is a key variable in coating operations involving solutions. As the concentration of the polymer is increased, solution viscosity increases. Also molecular weight of the polymer, directly affect viscosity values. Higher solution viscosities require more energy to atomize the solution (Felton 2013)

The discrete polymer spheres must coalesce and the polymer chains interpenetrate to form a continuous film and thus are considered more complex. Initially, the polymer spheres closely pack together after application to the substrate due to water evaporation. Next, the polymer spheres deform to fill in the void spaces left by the evaporating water. With continued drying, the polymer spheres flow together and the polymer chains interpenetrate to form the film, a process referred to as coalescence.

Driving force for particle deformation has been attributed to the viscous flow of the polymer resulting from shearing stresses caused by polymer-air surface tension. In contrast, Brown (Brown, 1956) proposed a capillarity theory, where the driving force for the particle deformation is the air–water interfacial surface tension in the interstitial regions.

In contrast to polymer solutions, dispersed polymer systems require the polymer spheres to deform and fuse together to form the film. Thus, these systems exhibit a minimum film forming temperature (MFFT). Below this temperature, a polymeric dispersion form an opaque, discontinuous material upon solvent evaporation, whereas a clear continuous film could formed at temperatures above the MFFT. Drying at temperatures above the MFFT provides sufficient capillary force for coalescence to occur. In contrast, polymer solutions do not exhibit a MFFT and form a film at room temperature. The MFFT is dependent on the polymer, polymer sphere diameter, and the coating formulation. For example, plasticizers in coating formulations soften the polymer spheres to allow for coalescence at lower temperatures. Both plasticizer type and plasticizer concentration have been shown to influence minimum film forming temperatures. For some systems, the polymer spheres are so soft that the MFFT is below room temperature. Knowledge of the MFFT is critical in developing a coating process or casting a free film, as processing temperatures must exceed the MFFT to form a film.

Rapid drying rates are generally considered desirable but may have adverse effects on the resulting film. A rapid loss of water, for example, may not allow for the development of the capillary pressure necessary and thus inhibit deformation and coalescence.

Excess drying can also prevent the droplets from spreading across the substrate during the coating process. In addition to temperature, the rate of drying is also dependent on the relative humidity of the environment.

High humidity conditions have been shown to facilitate coalescence as adequate capillary pressure is attained and also increase polymer chain inter-diffusion. In addition, water itself can function as a plasticizing agent to soften the polymer spheres and allow for viscous flow and polymer chain interpenetration.

Controlling both temperature and relative humidity during coating processes is ideal and may require humidification or dehumidification of the drying air. Using dispersions with lower solids content (less than 15%, w/w) has also been suggested as a way to ensure higher local humidity during coating.

While coalescence may occur relatively quickly at processing temperatures above the MFFT, many polymers require a sub-sequent post-coating drying step, often referred to as 'curing' in the pharmaceutical literature. Exposing coated substrates to elevated temperatures immediately after the coating process has been shown to potentially change the structure of the film. Such post-coating curing can significantly influence the mechanical properties of free films, film-tablet adhesion, and the dissolution profiles of coated substrates. Thus it is critical to coalescence a film completely, as incomplete or partial coalescence can lead to changes in polymer properties over time, which can be especially problematic for modified release systems. Curing can be accomplished by placing the coated substrates in an oven set to a specific temperature after application of the coating dispersion (static curing) or allowing the product to remain moving within the heated coating equipment(dynamic curing) (Muschert et al., 2011).

The inclusion of plasticizers in film coating formulations is critical when working with brittle polymers. Plasticizers reduce the intermolecular forces between the polymer chains and reduce internal stresses within a film. Plasticizers soften the polymer spheres to facilitate coalescence to be effective, the plasticizer must be compatible with the polymer.

One method to predict plasticizer-polymer compatibility is by comparing solubility parameters, with materials of similar values likely to be compatible. For softening of the polymer spheres in an aqueous dispersion, the plasticizer must partition into the polymer phase.

For water soluble plasticizers, uptake into the polymer spheres has been shown to occur relatively quickly whereas longer equilibration times are required for water insoluble plasticizers.

Sufficient mixing time to allow for plasticizer partitioning into the polymer phase prior to initiation of coating is critical, as insufficient mixing can lead to nonhomogeneous distribution of the plasticizer which could adversely affect the coalescence process (Felton 2013).

Gas barriers of packaging materials become essential when the gas composition inside the package has to be kept constant or free from oxygen. Many polysaccharides (natural polymeric carbohydrates) are known to be good oxygen barriers, explained by their hydrogen-bonded network which leads to small free volume that makes the oxygen transmission low (Miller and Krochta 1997).

Hemicelluloses are known to be good oxygen barriers. Film formation applications were conducted with mannan type hemicelluloses, which have resistance to oxygen diffusion (Edlund et al. 2010). The barrier and mechanical properties of cellulose-based films are dependent on the molecular weight of cellulose, higher the molecular weight better are the properties.

Many cellulose derivatives possess excellent film-forming properties, but they are simply too expensive for bulk use. Research is required to develop efficient and cost effective processing technologies for the production of cellulose derivatives (Dhall 2012).

In food products, not only microbiological stability plays an indispensable role in its quality, but also sensory aspects are essential to ensure that the application of emerging technologies such as edible films and coatings become successful. Some researchers have proved the effectiveness of edible films and coatings on the control of browning processes and polyphenol oxidase activity (Falguera et al. 2011).

Oxygen permeability data for a number of bio-based polymers as well as more traditional packaging materials are compared in a previous study (Hansen and Plackett 2008). Comparing the oxygen barrier properties of materials derived from hemicellulose with the other materials, the former are seen to be very promising as new materials in

the field. Films from amylose and amylopectin obtained from starch have good barrier properties with permeability values in the same range as the studied hemicellulose films (i.e., 7 and 14 cm^3 μm m^{-2} d^{-1} kPa^{-1}, respectively).

Chitosan, poly(vinyl alcohol) PVOH, and ethylene vinyl alcohol (EVOH) films have excellent oxygen barrier properties with values below 0.5 cm3 μm m^{-2} d^{-1} kPa^{-1} in all cases, which was matched by the xylan film produced. Comparable but slightly higher oxygen permeability was found for an O-acetylgalactoglucomannan (AcGGM) film as well as for blend films of AcGGM with CMC and alginate (with and without grafted styrene). Research in the area of oxygen barrier materials from hemicellulose is ongoing and seems to hold great promise for future practical applications (Hansen and Plackett 2008).

Since hemicelluloses are hydrophilic in nature and films produced from these materials are generally hygroscopic, resulting in poor properties in environments with high humidity. The use of a plasticizer is often necessary to ensure flexibility and the most commonly used for hemicellulose films are sorbitol, glycerol and xylitol (Hansen and Plackett 2008).

Cellulose is hydrophilic but insoluble in water because of strong intermolecular hydrogen bonds. Recently, the role of hydrogen bonding in the solubility and insolubility properties of cellulose has been challenged. It is believed that the properties of cellulose are also significantly influenced by hydrophobic interactions, and the surface of crystalline cellulose has both hydrophobic and hydrophilic planes. As a result of this amphiphilic character, it is not surprising to see that crystalline cellulose is capable of forming stable emulsions if they are dispersed well.

Earlier studies have found colloidal microcrystalline cellulose (MCC) can stabilize oil-in-water emulsions and water-in oil-in water (w/o/w) multiple emulsions by forming a network around the emulsified oils. The function of MCC is to orient at the oil-in-water interface thus providing a mechanical barrier to droplet coalescence, whereas the sodium carboxymethylcellulose functions as a dispersing and protective colloid for the MCC. Pictures for microfibrillated cellulose solution, gel and films were shown in Figure 2.10.

Figure 2.10 Microfibrillated cellulose solution, gel and films (Innventia, Tappi, Melodea 2015)

Recent studies have demonstrated that cellulose nanocrystals, without any dispersing agent, can also effectively stabilize oil-in-water. The amphiphilic character of cellulose nanocrystals resides in the crystal organization at the elementary brick level, and their emulsion stabilization mechanism is Pickering stabilization. In Pickering stabilization, nano/micro-particles are absorbed at the oil-water interface and protect emulsion droplets against flocculation and coalescence by a steric barrier. Both oil-in-water and water-in-oil emulsions can be formed depending on the particle wettability. (X. Jia 2015)
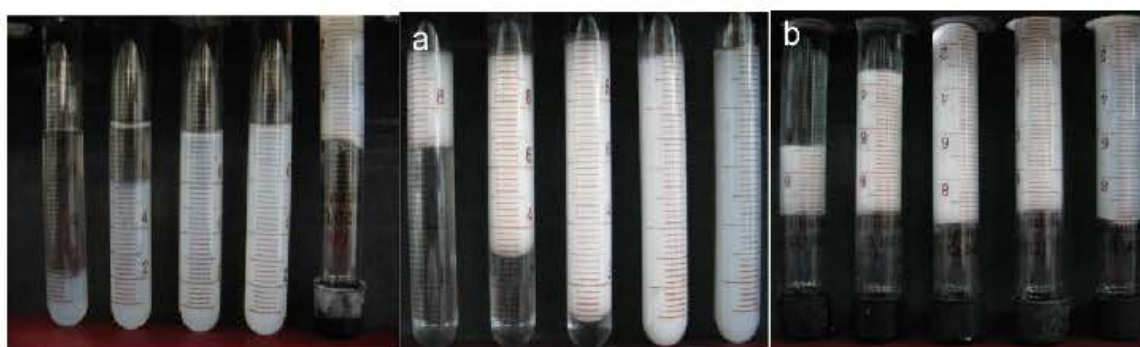
Figure 2.11 Dispersion states of amorphous cellulose as a function of cellulose concentration (X. Jia 2015)

Effects of amorphous cellulose concentration on the stability of oil-in-water emulsions (a- 1 day of storage; b -7 days of storage) were shown in Figure 2.11 above.

From left to right, the concentrations of cellulose are 0.07, 0.28, 0.56, 0.83 and 1.10%, respectively. Amorphous cellulose prepared by an inexpensive solvent, phosphoric acid, can effectively stabilize oil-in-water emulsions at a concentration less than 1% through combined Pickering and network stabilization mechanisms. The resulting emulsions are shear-thinning with typical gel characteristics and can be described as emulsions with attractive interactions (X. Jia 2015)

2.3 Film characterization techniques

There are some main parameters applied in researches conducted in area of film production studies. Briefly these parameters and their measurement tools were summarized in Table 2.4.

Mechanical characteristics of a film sample are very critical in terms of producing film in big scale or handling it through food packaging easily. There are a few parameters considered when mechanical properties of a film sample were measured. One of them is stress which defined as "*force per unit area*". Tensile stress - *stress able to lengthen film* – that acts normal to the stressed area. Tensile Modulus is a term showing stiffness of an elastic material. Elongation or compression of an object could be predicted with tensile modulus if stress is less than the yield strength value. Elasticity is a physical property of a material where the material returns to its original shape after being deformed. High elasticity and high modulus are both desirable for film materials (Engineering toolbox, 2015).

MIR spectra contain information about the complete chemical composition and physical state of the material under analysis. Therefore, high number of data is generated (Downey 1998). Attenuated total reflection (ATR) sample accessories have greatly eased the analysis of solids, liquids, semisolids, and thin films. ATR equipment was also critical for this study, since FTIR spectrum data of film samples at any thickness value gave very noisy peaks those were unable match with peaks corresponding to predefined chemical structures/bonds.

Multivariate data analysis was required to extract the relevant information from these spectra. Multivariate data analysis was also benefited in order to extract data from XRD spectra and thermal diagrams of tested powder and film samples. Score plots were

drawn with the most meaningful two principal components selected. Score plot shows the possible presence of outliers, groups, similarities and other patterns in the data and how the modeled observations in X space are situated with respect to each other (Umetrics-AB 2013).

Table 2.4 Some basic characterization techniques currently applied in film materials

Instrument Used	Measured Parameter	Target
FTIR/ FTIR-ATR	Middle Infrared Absorption spectrum	Differentiating chemical structure through chemical bonds
XRD	Sharp peaks from diffractogram	presence/absence of sharp peaks give idea about crystalline/ amorphous structure of sample
SEM	Image	Surface properties, crosssectional area properties
SEM-EDX	Molecular compound profile	Chemical residue check (residues from solvents, treatments etc.)
AFM	Image	Surface properties, topography
PCM	Size distrubution	size of microfibrils , emulsion droplets
A_w tester	Water activity	
Texturometer	Mechanical characteristics	Determination of elasticity, tensile strength
Water Vapor transmission tester	Water Vapour transmission rate	Water vapour resistance and permeability
Gas transmission tester	O_2, CO_2, N_2 transmission rate	Gas permeability
TGA, DSC	T_g, T_m, degradation temperature	T_g and T_m is useful in scale-up studies, with extruder or blown film extrusion or simply for thermal sealing application
Conductivitymeter	conductivity	MFFT
Colorimeter	Colour, light transmission	Vegetable and film colour
Refractometer	Refractive index	solubility, dispersibility, concentration
Spectrophotometer	light transmission, opacity	solubility, dispersibility, concentration
Micrometer	Thickness	used in tensile strength, oxygen and water vapour permeability calculations
Stereozoom Microscobe	Image	Surface properties
Analytical Balance, Desiccator, Incubator	Weight gain, weight loss	Change in the moisture of film during storage; moisture content determination

In AFM analyses; height signals (z piezo voltage signal) are the only signals with meaningful z scale with those topographical measurements could be made. The shape of the sample could be visualized by amplitude signal (error signal).

Heterogeneity of the sample could be analysed by phase image. It is important to collect all images in the same direction, i.e. all in forward or backward (Eaton and West 2011).

Permeation is the mass transfer phenomenon that occurs when a molecule passes through a material or membrane from high to low concentration (Han 2005). Material's barrier properties can be determined *via* their gas transmission rate (GTR) values. Materials that transfer maximum 10 ml gas on 1 m^2 surface per day are generally considered as highly barrier, upper limits for medium and low barrier materials are 1000 ml/m^2/day and 10 000 ml/m^2/day (Abdellatief and Welt 2012).

Table 2.5 Oxygen and water vapour transmission rates of selected packaging materials for fresh produce (Jongen 2005)

Packaging film (25 μm)	OTR (cm³/m²*day*atm)	Relative OP	WVTR (g/m²*day)	Relative WVTR
Al	<0.1	Barrier <50	<0.1	Barrier, <10
EVOH	0.2-1.6		24-120	Variable
PVdC	0.8-9.2		0.3-32	Barrier, <10
MXDE	2.4		25	Semi-barrier, 10-30
PET	50-100	Semi-barrier 50-200	20-30	Semi-barrier, 10-30
PA6	80		200	Very high 200-300
PETG	100		60	Medium 30-100
MOPP	100-200		1.5-3.0	Barrier, <10
PVC	2000-5000	Medium, 200-5000	200	Very high 200-300
OPP	2000-2500		7	Barrier, <10
HDPE	2100		6-8	Barrier, <10
PS	2500-5000		110-160	High, 100-200
OPS	2500-5000		170	High, 100-200
PP	3000-3700		10-12	Semi-barrier, 10-30
PC	4300		180	Very high 100-200
LDPE	7100	High 5000-10000	16-24	Semi-barrier, 10-30
PVC	5000-10000		200	Very high 200-300
EVA	12000	Very high 10000-15000	110-160	Very high 100-200
MP	>15000	Extremely high, >15000	Variable	Extremely high, >300
MPOR	>15000		Variable	Extremely high, >300

Gas transmission properties of some selected polymer films were listed in Table 2.5; synthetic polymers were grouped as barrier/ semi-barrier/ highly permeable according to their permeability values. Additionally in Table 2.6, comparison of

cellulose based films with some frequently used polymer films in terms of permeability, mechanical characteristics and expected production costs were mentioned.

Table 2.6 Comparative properties of Bio-derived polymers with PE and PS
(Petersen et. al 1999)

Polymer	Moisture Permeability	Oxygen Permeability	Mechanical properties	Expected Price (ECU/kg)
cellulose / cellophane	high -medium	high	good	1.5-3
cellulose acetate	moderate	high	moderate	3-5
starch / PVA	high	low	good	2-4
proteins	high -medium	low	moderate	1-8
Polyhydroxy alcanoates	low	low	good	10-12
polylactate	moderate	high-moderate	good	2-4
LDPE	low	high	moderate-good	0.7-2
PS	high	high	poor-moderate	1-2

CHAPTER 3

FRESH CUT PRODUCE

Fruits and vegetables are living tissues; they continue respiration after harvesting and during storage. In order to extend shelf life freshcut fruits and vegetables, controlling respiration activity is necessary. Processing fruit and vegetables into fresh cut form, wound their tissue. Wounded tissues are more prone to softening, discolouration, or dying (Lin and Zhao 2007).

There are some critical quality parameters (visual, textural, aromatic, nutritive and microbial) that affect market value of fresh cut fruit and vegetables (Table 3.1). Plant variety, stage of maturity or ripening, conditions before and after harvesting cause variations in quality characteristics (Lin and Zhao 2007).

Vegetables and fruits are highly perishable as they contain 80–90% water by weight. If they are left without cuticle, the water quickly begins to evaporate, resulting in poor product shelf life. Major losses in quality and quantity of fresh fruits and vegetables occur between harvest and consumption. When the fruit is harvested, there is a change of the gaseous balance between the consumption of oxygen and the production of carbon dioxide (Dhall 2012).

Table 3.1 Major quality attributes of fresh fruits and vegetables (Lin and Zhao 2007).

Quality Factor	Primary Concern
Appearance (visual)	Size, shape and form, colour: intensity, uniformity, gloss, defects
Texture (mouth-feel)	Firmness/softness, crispness, juiciness, toughness (fibrousnesses)
Flavour (taste, aroma)	Sweetness, acidity, astringency, bitterness, volatile compounds
Nutritional value	Vitamins, minerals
Safety	Toxic substances, chemical contaminants, microbial contamination

Browning is the result of a chain of reactions that very often occurs in fruit and vegetables. The first step of that process takes place in the vacuole and it is the deamination of the amino acid phenylalanine by PAL. The product of that reaction is the cinnamic acid which is hydroxylated into various phenolic compounds. When O_2 is

present, the polyphenoloxidase located in the cytoplasm (plastids) oxidises the compounds to o-quinones, which polymerise into brown compounds (Ahvenainen 2003).

Rapid browning at cut surfaces of fresh fruit and vegetables occurs due to oxidation of phenolics and enzymes involved (polyphenol oxidase and peroxidase) in fruits and vegetables. Traditional solutions to browning are to inhibit enzymatic activity, to remove enzyme, or using inhibitors i.e. Cu^{2+} or O_2 (Niranjan and Harsa 2013).

Most browning reactions are promoted by oxygen; therefore avoiding oxygen in the food environment can slow down deterioration of the product. This can be achieved by using a packaging material with low oxygen permeability. Such packaging can be combined with a mild pre-treatment in order to provide a minimally processed food with a high quality and which has a relatively long shelf life. Cutting operation decreases shelf life of fruit and vegetables significantly, due to increased surface area, formation of injured tissues compared to whole product (Niranjan and Harsa 2013).

3.1 Artichoke

Artichokes are widely consumed vegetables origined from Mediterranean Region. Artichoke has rich polyphenol content. Hepatoprotective effect, cholesterol biosynthesis inhibitory, diuretic, anti-inflammatory and antimicrobial activities are frequently claimed functional properties of artichoke supported with previous *in vivo* and *in vitro* studies (Cabezas-Serrano et al. 2009). Artichokes exhibit a high antioxidant capacity, reaching the fourth place when the antioxidant content is expressed in terms of the serving size. The content of phenolics varies among different cultivars, age, generation of the plant, growing conditions, harvest, post-harvest and storage conditions, and the technological procedures used (Lutz et al. 2011).

The artichoke is classified as *Cynara scolymus*. It grows wild in the south of Europe and is also cultivated in the United States. The leaves proceed from the base of the stem and are long and somewhat spiny (Sleuth 2012). According to literature, artichoke stalk contains proximately 9.76 ash; 29.2 % lignin; 52.1 % hemicellulose; 16.1 % cellulose and 2.6 % extractives in dry basis. Edible part of artichoke is only artichoke heart, the remained parts (stems, leaves, and stalk) are considered as waste.

Waste part of artichoke constitutes 80% of globe artichoke. Utilizing inedible parts for the extraction of nutraceuticals (i.e. phenolics, inulin, and dietary fiber) might add value to artichoke product (V. Lattanzio et al. 2009). In Turkey, artichoke is cultivated in Mediterranean, Aegean, Marmara regions. With a production value of 35000 metric tons, Turkey ranks 12th in the world and 4th in Europe.

There is various artichoke varieties planted in Turkey, in Figure 3.1 photographs of Bayrampaşa, Şimşek, Sakız and Şebnem were given. Dimensional characteristics of artichokes differ among varieties or parts of the plant, average size values were shown in Table 3.2. The flower head was separated into 'petals'/bracts (~50% of the harvested flower head), 'choke' (~3%), receptacle (~20%) and stem (~25%). The bracts were further divided into 4 groups to reflect their apparent stage of maturity in the flower. Division, on the basis of colour, was brown (external), green, yellow and white (adjacent the choke) (Femenia *et al.* 1998).

Figure 3.1   Artichoke varieties from Turkey, Bayrampaşa, Şimşek, Sakız and Şebnem, from left to right (Sevinç Başay and Tokuşoğlu 2013)

Table 3.2 Lowest/ highest dimension and weight values among different artichoke varieties (Sevinç Başay and Tokuşoğlu 2013)

Values	Stem			Head		
	Weight (g)	Width (cm)	Height (cm)	Weight (g)	Width (cm)	Height (cm)
lowest	277.06	10.48	8.88	72.75	8.26	3.43
highest	432.52	12.69	11.72	118.29	9.88	4.10

The leaves proceed from the base of the stem and are long and somewhat spiny (Sleuth 2012). According to literature, artichoke stalk contains proximately 4.1 % (m/m) moisture; 9.76 ash (dry basis); 29.2 % lignin; 52.1 % hemicellulose; 16.1 % cellulose and 2.6 % extractives. Also, general polysaccharide composition of artichokes was presented in Table 3.3 below.

Table 3.3 General polysaccharide composition of artichokes (Alcohol insoluble
residues (AIRs), non-starch polysaccharides (NSP))
(Femenia et al. 1998)

parts of artichoke	NSP (g/kg FW)		(NSP %)			Soluble NSP (%)	
	fibre	AIR	cellulose	hemicellulose	pectic polysaccharide	fibre	AIR
receptacle	32.2	36	25.4	17.8	56.9	25.7	---
stem	36.6	38.7	35.7	15.1	49.2	11.3	7.1

Edible part of artichoke- *artichoke heart*- constitutes only 20%, remained parts (stems, leaves, and stalk) are considered as waste. Utilizing inedible parts for the extraction of nutraceuticals (i.e. phenolics, inulin, and dietary fiber) might add value to artichoke product (V. Lattanzio et al. 2009). In Turkey, artichoke is cultivated in Mediterranean, Aegean, Marmara regions. With a production value of 35,000 metric tons, Turkey ranks 12th in the world and 4th in Europe.

Many fruits and vegetables become brown or discoloured after mechanical or physiological injury suffered during harvesting or storage, and this reactivity raises an important economic question in the post-harvest physiology of plant commodities. During the processing and storage of fruits and vegetables the need to prevent colour changes or browning is considered to be a matter of great importance from the point of view of consumer acceptability and palatability as well as retention of the original quality of the food.

Discolouration is caused by the oxidation of certain phenolic compounds catalysed by specific enzymes and it is generally agreed that polyphenol oxidase (PPO) is the enzyme system mainly responsible for browning. When the cellular compartmentalization is disrupted, plant phenols are involved in both enzymic and nonenzymic browning reactions. In the former case the oxidation of phenolic compounds is catalysed by a PPO activity and the quinones formed can take part in secondary reactions bringing about the formation of more intensely coloured secondary products. In the latter case the common cause of darkening is attributable to the interactions between phenolics and heavy metals, especially iron. It is generally accepted that a dark coloured complex of ferric iron and an orthodihydric phenol is responsible for discolouration. It has been suggested that the phenol involved is chlorogenic acid (5-O-caffeoylquinic acid) and that disruption of the cells during processing and/or storage allows the organic ligand to chelate the iron. Since the metal is originally present in the reduced state, a colourless complex is first formed which,

upon exposure to oxygen, is oxidized to yield a coloured compound. Changes in the concentration of phenolic substrates during development and ripening do not run parallel to the changes in the actual browning. Therefore, it is clear that factors other than the amount of phenols alone are responsible for the intensity of browning. The in-situ enzyme activity can be considered an even more important factor contributing to browning than the concentration of phenolic substrates, but PPO activity does not change in a parallel way to the browning reaction (Lattanzio 1994).

Rich phenolic and polysaccharide content of artichoke brings browning phenomena into act. Since, consumers prefer to purchase mostly fresh cut form (artichoke heart), colour deteriorations easily happen. Rate of browning in different parts of artichoke varies. Poly phenol oxidase (PPO) activity and chlorogenic acid content fluctuation among treated and non-treated artichokes by time were illustrated in Figure 3.2.

Chlorogenic acid in tissues of artichokes (a)   PPO activity in artichoke heads (at 4 °C) (b)

PPO activity in injured artichokes (c)   PPO activity in tissues of artichokes (d)
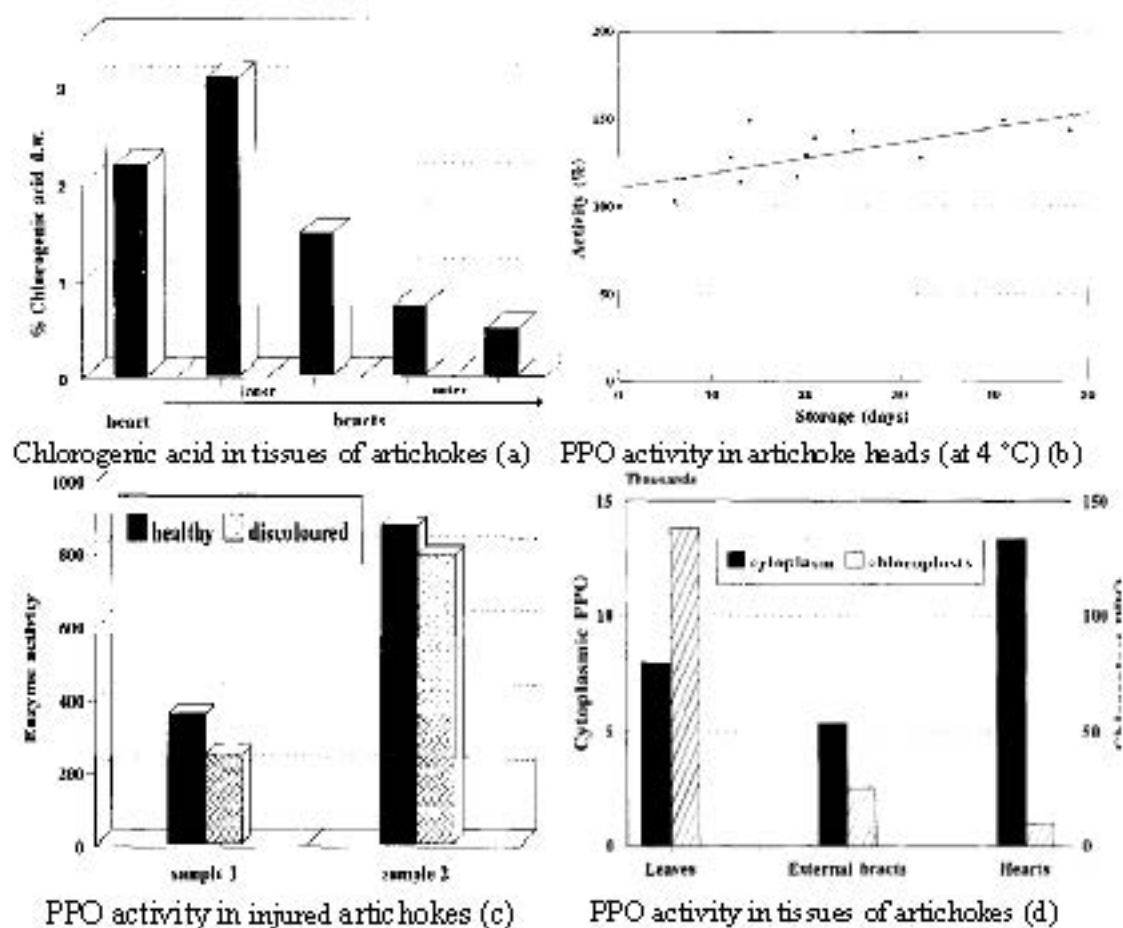
Figure 3.2 Browning in different parts of artichoke during storage due to enzymatic activity, mechanical damage (Lattanzio *et al*. 1994)

Fig. 3.2-(a) shows that chlorogenic acid content may be inversely related to the whole plant or tissue development: the arrow on the x-axis in the figure indicates the ageing of plant tissues, inner bracts being younger than outer ones. These phenolics are good substrates for both enzymic and non-enzymic reactions.

Ideally, it would be desirable to compare samples where the differences in the intensity of blackening. Because of the localization of the blackening at the level of inner bracts, changes in chemical parameters between inner and outer bracts and between browned and healthy tissues of the same bract were observed.

Although iron could be directly involved in the formation of the coloured pigments, its concentration is of lesser importance than other factors in determining the distribution of blackening on individual heads, since it is almost constant in the different bracts.

On the other hand, chlorogenic acid content (Fig. 3.2-(a)) rapidly decreases from the inner to the outer bracts. It has been shown that exposure of artichoke heads to low non-freezing temperature can stimulate phenolic metabolism.

29

Low-temperature storage leads to a rise in caffeoylquinic acid derivatives, particularly chlorogenic acid, involving a cold-induced stimulation of PAL activity. Figure 3.2-(b) shows changes in PPO activity during the storage at 4°C: the trend observed is a gradual increase in PPO activity, but this increase is not so relevant from a statistical viewpoint. This small activation of PPO could be induced by ageing phenomena in the tissues and/or by stress conditions during storage, which result in increased levels of enzyme, apparently due to release from membranes. These data show that enzyme activity and the amount of phenolic substrates do not change together.

Phenolics which act as substrates for PPO are either sequestered in special cells, or in the vacuole, away from the enzyme. The optimum pH of artichoke PPO usually lies between 5.0 and 8.0 for the different substrates, indicating that it is present in a cell compartment separated from the rather acid cell vacuole. Thus, it seems that PPO is not involved in the oxidation of the bulk of phenolics present in non-mechanically damaged tissues. It is known that phenols with two free o-hydroxy groups give coloured complexes at pH 6.0-6.5 (the physiological pH of artichoke head tissues ranges between 6.0 and 6.2).

Under these conditions chlorogenic acid and 1,5-O-dicaffeoylquinic acid form dark-coloured complexes with Fe^{3+}. It was observed that in the absence of oxygen these phenolics form colourless complexes with Fe^{2+}. After exposure to air the complexed Fe^{2+} was quickly oxidized to Fe^{3+} to give coloured compounds.

Citric acid produced a 100% reduction in colour when an iron citric acid ratio of 1:10 was used and the solution pH was kept unchanged. In mechanically damaged tissues the enzyme activity is not so different from healthy tissues: a small decrease could possibly be due to the inhibitory effect of the reaction products (Fig. 3.2-(c)).

As far as the subcellular localization of PPO (Fig. 3.2-(d)) is concerned, in all tissues analysed the enzyme activity was found mainly in the cytoplasm. In the internal tissues of artichoke heads, where the browning phenomena are localized, the cytoplasmic activity was about 1400 times higher than the chloroplast activity which, in turn, was very low.

Phenolics, PPO, PAL and iron play important roles in blackening reactions. Amongst phenols, chlorogenic acid, the best substrate of artichoke PPO, 13-O-dicaffeoylquinic acid and 3,5-O-dicaffeoylquinic acid, ligands for iron together with chlorogenic acid, being generally the most representative artichoke phenolics, must be

considered. Suggesting a mechanism of browning reaction in non-mechanically damaged tissues presented in Fig. 3.3.

Cold Storage
↓
PAL
Phenolics
PPO

Fe(III)/Fe(II)   Quinones

Phenolics-Fe(II) Complexes

Phenolics-Fe(III) Complexes
↓
BROWNING
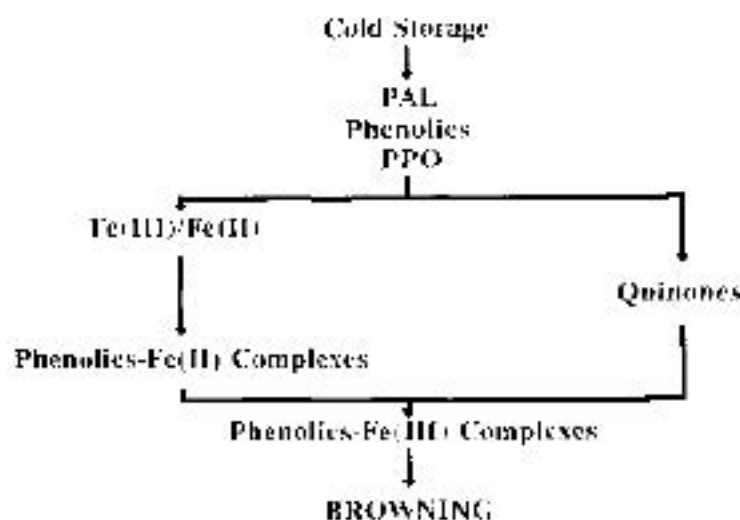
Figure 3.3 Browning phenomena in artichoke (Lattanzio et al. 1994)

During cold storage of artichoke heads, low-temperature induction of PAL activity caused a biosynthetic increase of phenolics, especially chlorogenic acid. On the other hand, PPO activity did not change significantly during the storage period. The increased content of phenolics provided an adequate substrate for the browning phenomena. Results lead to a proposed mechanism of browning phenomena in cold-stored, non-mechanically damaged, artichoke heads (Lattanzio 1994). Browning of artichoke may arise from enzymatic or non-enzymatic reaction. Chemical basis for browning of artichoke was schematized in Figure 3.3.

3.2 Packaging applications for fresh cut produce

Bio-based packaging materials are generally obtained from agroindustrial wastes. Although biodegradable and renewable films are more expensive than the petrochemical films, they have the advantage being as biopolymers. Among the biopolymers, films made from starch are the most developed.

Interest in the application of edible coatings to fruits and vegetables has increased because they can be used to maintain fresh quality by controlling oxygen and carbon dioxide exchange between the product and the ambient atmosphere and by

31

providing microbial stability for the product by incorporating antimicrobial agents. Both functional approaches reduce the vulnerability of the product to microbial decay (Jongen 2005).

High quality and microbial safety of fruits and vegetables have become increasingly important with the increased consumption of fruits and vegetables. Growth of microorganisms on the surfaces of fruits and vegetables can result in production of unwanted appearance/odors, and invasion of the interior of fruits and vegetables, accelerating further decay. Spoilage of fruits and vegetables results in large economic loss. It has been estimated that 25–80% of harvested fresh fruits and vegetables are lost due to spoilage. There is also potential for the growth of human pathogens that can cause human disease. These microorganisms usually come from mishandling and crosscontamination (Jongen 2005).

Cellulose, starch and chitosan have been used to form edible films/coatings on foods to provide an oxygen or lipid barrier and to improve appearance, texture and handling (Jongen 2005).

Edible polymers make good O_2, aroma and lipid barrier films at low to intermediate RH, but their barrier properties decrease as the RH increases. The optimum RH for the storage of fresh fruits and vegetables varies from product to product. Generally, levels of 85–95% represent a compromise between preventing excessive weight loss while providing some control of microbial spoilage.

Thus, edible polymer materials and coating thicknesses that provide desirable barrier properties at high RH must be selected. In addition, the RH must be controlled within a reasonable range (Jongen 2005). Respiration rates of fruit or vegetables are inversely proportional to achievable shelf life and higher respiration rates are associated with shorter shelf life (Jongen 2005).

Treatment with reducing/acidifying/chelating agents and calcium solutions reduce/prevent browning in fresh cut produce. Dehydration is another unwanted alteration that negatively affects consumer preferability in case of artichoke. Storage temperature, RH %, and air stream within package, affect dehydration rate. The weight loss is a natural consequence of the catabolism of horticultural products, catalysed by enzymes and accelerated by cutting and slicing. The decrease in weight may be attributed to respiration and other senescence-related metabolic processes during storage. Pretreatment methods for artichoke before packaging to overcome the browning problems are presented in Table 3.4.

Table 3.4 An overview of the pre-treatment methods for fresh cut artichokes (AA: ascorbic acid; CA: citric acid; PA: phosphoric acid; CD: cyclodextrin; Cys: cysteine)

Treatment	Conditions	Effectivenes	Source
AA	10 (mol/m³)	+	Ghidelli 2013
CA	10;20;50 (mol/m³)	-	
PA	10;25;50 (mol/m³)	-	
CaCl₃	10;25;50 (mol/m³)	-	
CD	10;50 (mol/m³)	-	
Cys	50 (mol/m³)	+	
NaOCl	100ppm	+	Ricci 2013
NaCl	0.50; 1%	+	Amodio 2011
AA	0.50; 1%	+	
AA	1 ; 2 %	-	
CA	1%	+	
CA	2%	-	
Cys	0.25%	-	
Cys	0.50%; 0.50% at pH = 3 and 1%	+	
EtOH	0.50; 1%	+	
AA + CA+ Cys	1% + 1% + 0.5%	-	

The physical damage or wounding caused by peeling increases respiration rate in short time, lowering initial respiration rate help extending shelf life of fresh cut vegetables. Calcium ion is known to inhibit respiratory activity and ethylene production (Qi 2011).

According to previous studies in literature, sodium alginate coated and $CaCl_2$ treated fresh-cut Madrigal artichokes packed in biodegradable polyester film guarantee a shelf life of 3 days at 4°C, which compared to the control sample packed in the same film, corresponds to an increase in the shelf life value of 200%. A shelf life of about 3 days seems to be enough for produce distribution to the local markets. In addition, the developed packaging strategy is characterized by a low environmental impact that could increase its potential industrial application (Qi 2011).

With the exception of macroperforated PVC, where the atmosphere within the packages had a composition very similar to the ambient air, the atmosphere within the rest of packages changed during the first hours, reaching a constant content of oxygen in the first 24 h. The CO_2 content within the packages reached equilibrium after 24 h in no perforated PVC and P-Plus 210 films, whereas P-Plus 160 film reached an equilibrium modified atmosphere on day 3. For P-Plus 120 film, the rapid decrease in the oxygen levels together with the high levels of CO_2 reached in the first 24–48 h led to the

establishment of an anaerobic metabolism in the vegetable that caused an increase in the levels of CO_2, reaching a peak on day 6 (31.7%).

The respiratory activity showed by artichoke, even at storage temperatures of 4°C, means that the different permeability of the films used caused differences in the composition of the atmosphere inside the packages after reaching equilibrium. The different atmospheres obtained, together with the differences in the permeability to the water vapor, also had a significant influence on the visual quality (Gimenez 2003).

There are various studies on application of biodegradable films for packaging fresh cut produce in literature. Results of Pitak and Rakshit's showed the positive effect of banana flour-chitosan composite films on shelf life of fresh cut vegetables (Pitak and Rakshit 2011). Sangsuwan *et al.* claimed positive effect of methlycellulose-chitosan blend films on shelf life of fresh cut cantaloupe and pineapple during storage at 10°C in their study (Sangsuwan et al. 2008).

There are very interesting researches on application of biodegradable and edible film production from fruit purees. Sothornvit and Rodsamran studied production of biodegradable films from mango puree, and produced films were applied on freshcut mango fruit in comparison with cellophane bags / no packaging. Results showed that there is a significant positive effect of packaging *-whether with cellophane or mango puree film-* on shelf life of fresh cut mangoes (Sothornvit and Rodsamran 2008). Azeredo et al. studied nanoreinforced (*via* cellulose whiskers) alginate-acerola puree films for extending shelf life of acerola fruits, and presented promising results on related area (Azeredo et al. 2012).

CHAPTER 4

MATERIALS AND METHODS

Artichoke was the main raw material used through the study in formation of film forming materials. Artichoke wastes were collected from local artichoke producers in spring season. Calcium carbonate, sulphuric acid, glycerol, sorbitol, sodium carboxyl methyl cellulose (MW 250,000), xylan from beech wood, monochloroacetic acid, isopropanol, methanol were purchased from Sigma-Aldrich (Germany). Sodium hydroxide was obtained from Pancreac (Spain). Ethanol, citric acid, sodium metabisulphite, cysteine, stearic acid, ascorbic acid were purchased from Tekkim (Turkey). Hydrogen peroxide, tween 80, glucano-δ-lactone were bought from Merck (Germany).

In this part, methodology for raw material treatment, mechanical treatment of cellulose fibers, characteristics of artichoke by-products, production and optimization of films, characterization of films, and treatment trials for globe artichoke, packaging and coating trials with films produced were presented. The experimental layout is schematically summarized in Figure 4.1.
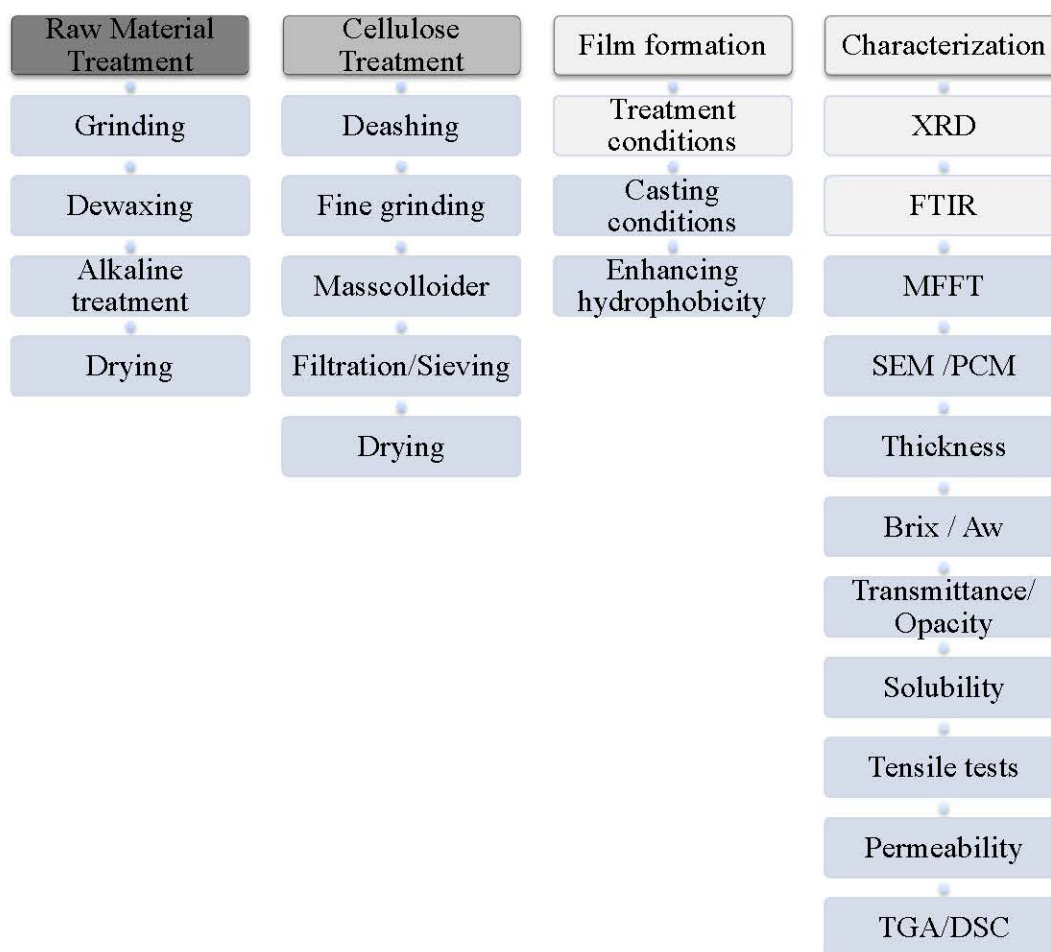
Figure 4.1 Overall procedure of methodology

4.1 Raw material treatment

Artichoke leaves were separated from stalk and left drying in oven at 50°C for 48 hours as seen in Figure 4.2. Dried artichoke leaves were grinded with a grain mill. Grinded samples sieved, and artichoke leaf powder was obtained with ~0.5 mm size (average). Powder was eliminated from its pigments and waxes *via* hot ethanol extraction (Soxhelet method). The dewaxed sample was dried overnight at 50°C. From lignocellulosic raw material, cellulose fibers were separated with alkaline-peroxide method (Sun *et al.*, 2000). Dewaxed powder was treated with mild peroxide-alkaline solution (2% H_2O_2 v/v in DW, pH = 11, 1/10 solid/liquid ratio) at 50°C for 16 hours in order to separate cellulose from lignin and hemicellulose (Fang *et al.* 1999; Peng *et al.* 2012; Sun *et al.* 2000). Treatment with ethanol separated hemicellulose from lignin.

Lignin remains in liquid phase while hemicellulose stays in precipitate form. The hemicelluloses were obtained as pellet form after filtration. They were washed with ethanol and air dried at 50°C overnight. Remaining solution was stored in refrigerator and used later as lignin fraction. Separated fractions such as wax and hemicellulose were also kept to be used to enhance the film forming material.

Figure 4.2 Drying artichoke leaves at 40°C for 24 h in fanned oven

4.2 Treatment of cellulose fibers

Sodium carboxyl methylcellulose was synthesized from cellulose fibers that were previously obtained from artichoke wastes. Obtained cellulose fibers were treated with monochloroacetic acid and isopropanol and finally washed with methanol and dried in an oven. Synthesized carboxyl methylcellulose (NCMC) was primarily dissolved in distilled water by heat stirring; remained undissolved parts were separated *via* centrifuge and precipitated as gel. Additionally, soluble parts were extracted with freeze drying technique. Initially, excess amount of NCMC put in distilled water in order to reach maximum soluble amount and then insoluble part separated carefully with simple filtration technique (NCU2). Remained clear solution was dried in a lyophilizator (NCF1/A1). The dried insoluble Synthesized CMC fraction redissolved in

distilled water and then insoluble part (NCUU1) separated using a coarse filtration paper secondarily then dried in an oven, and supernatant solution again dried in a lyophilizator (NCF2, A2). It was tried to differentiate NCMC from cellulose, artichoke leaf and Na-CMC (Sigma-Aldrich) using various characterization techniques. See Figure 4.3 below.

			Lyophilization of soluble part	Product: NCF1/A1
		Dissolution in dw	Filtration of insoluble part	Product: NCU2
	Product: NCMC			Dissolution of NCU2 in dw
Isopropanol-methanol-monochloro acetic acid treatment			Filtration of undissolved part	Lyophilization of dissolved part
Cellulose fiber from artichoke			Product: NCUU1	Product: NCF2/A2
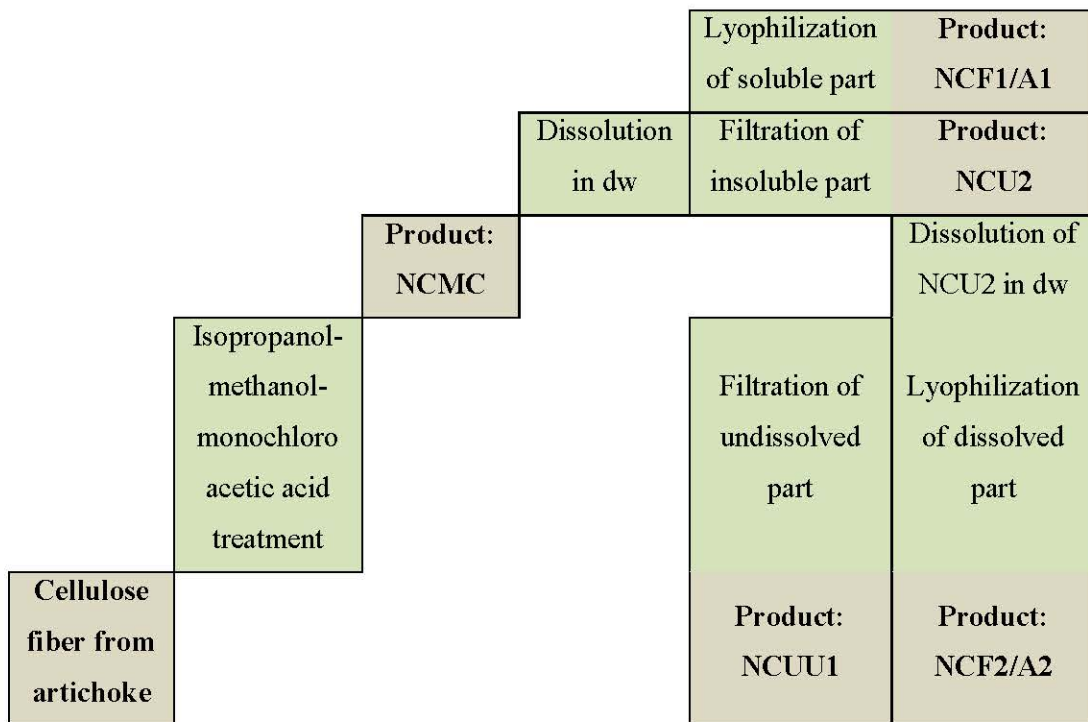
Figure 4.3 Treatment of cellulose fiber from artichoke leaves for synthesizing NCMC and different fractions to be used in film formation

Overall production procedures of MFC and films and their characterizations were given in Figure 4.1 above. Micro-fibrillated cellulose was produced from the cellulose fibers; that were extracted from the agro-industrial wastes. Firstly, it was planned to test effect of plain supermasscolloider treatment. Additionally, samples were treated with microfluidics fluidizer in order to obtain micro-fibrillated cellulose. Figure 4.4 shows the images of these equipments. After obtaining micro fibrillated cellulose, crystalline and polymeric structure properties of cellulose micro-fibrils were observed.

Figure 4.4 Images from Spray drier, Supermasscolloider and Homogenizer Treatments

Filtrated and dried cellulose fibers were grinded iteratively. Half of the grinded cellulose fibers were directly treated for fibrillation, while other part used after deashing process. Ashes and other impurities removed from cellulose fibers with glucano-δ-lactone treatment as mentioned at US Patent-2825646 (Wayman *et. al.* 1958).

Cellulose fibers *at 1; 2.46; 2.65; 3 % (w/v)* concentrations were suspended in distilled water. These suspensions were fed into a Supermasscolloider (Masuko MKCA6-2, Japan) *via* adjusting spaces between toothed wheels starting from 300 μm to -150 μm. Cellulose pulp was fed through the grinder 3, 4, 5 and 7 times and grind size was reduced *via* observing flow rate through process.

The same process was also applied to artichoke leaf powder at 15 % (w/v) concentration again in distilled water. This method was adapted from related sources in the literature (Abdul Khalil, *et al.* 2014; Iwamoto, *et al.*2007; Lavoine, *et al.*2012; Uetani, *et al.* 2011). A little portion of CLP-1 sample was taken and filtrated from a stainless steel having 212 μm pore size. Produced samples were coded according to preparation/process conditions (Table 4.1).

Table 4.1 Microfibrillated cellulose samples produced from different raw material concentrations with two different methods

Raw material (RM)	Treatment method(s)	MFC fraction (code)
1 %(w/v) Cellulose fiber suspension	Grinded with supermasscolloider	CLP-1
2.46 %(w/v) Cellulose fiber		CLP-2
2.65 %(w/v)Deashed cellulose fiber suspension		DCLP-2
3 %(w/v) Cellulose fiber suspension		CLP-3
15 %(w/v) Artichoke leaf powder suspension		ALP-15
Filtrated CLP-1 particle size ≤ 212 μm	Microfluidized with Homogenizer	MCLP-3

4.3 Production of films: Screening and optimization

In order to produce films with desirable properties with minimum cost, many film casting trials were conducted. At first trials for film formation were applied only with extracted components from artichoke wastes. At second step addition of various plasticizers, crosslinking agents, emulsifiers and oils were studied. Then effect of casting conditions and amount of materials used in film formation were screened in detail to determine the optimum conditions. Finally films were formed at optimized conditions and compositions and then characterized for their physicochemical properties. Evaluations of films were done with some of the selected experiments; these experiments were called as responses.

Films were prepared and their preparation conditions (treatments, compositions) were listed in Table 4.2. Film formation properties of micro fibrils were roughly determined at different dilution ratios with and without plasticizing additives. (Film trial tests were also benefited in order to have an idea about dissolution properties of produced micro fibrils.) Films were produced from MFC samples both from freeze dried powder and pulp form. Films were produced with solution casting method. In Figure 2.7 picture of ultrasonic homogenizer used in the study were shown. Films prepared and their preparation conditions (drying temperature-time, compositions) were listed in Table 4.2.

Table 4.2 Factors and responses of screening tests

FILM FORMING CONDITIONS		
Operating Conditions	Dehydration Media (Oven, Environmental chamber) Temperature (25°C; 30°C; 35°C; 40°C; 45°C; 60°C;100°C) Relative humidity (40%, 50%) Duration (2 h; 24 h; 48 h; 72h) pH of the film solution (5; 7; 8.6; 11) Concentration of polymers/additives (%) [w/w or v/v] Treatments (heat; ultrasonic / mechanical homogenization)	
FILM FORMING MATERIALS		
Commercial polymers	Na-CMC (MW: 250,000 or 700,000); Xylan from beechwood; corn starch; methylcellulose; whey protein isolate; Micro granular cellulose (Aldrich)	
Polymers from artichoke waste	Hemicellulose, lignin-hemicellulose and lignin-hemicellulose-wax fractions, cellulose fibers (from ethanol-alkaline peroxide treatment) dewaxed artichoke leaf Synthesized CMC (produced *via* different alkaline treatments, 10-50 %) artichoke stalk juice Micro fibrillated cellulose, CMC, Wax	
Solvents	Dw; Alkaline DW; dw+etoh; LH Fraction; Ultrapure water, ethanol-water, lignin solution, lignin-hemicellulose-wax solution	
Dilution Ratio	LHW(1/1; ½; ¼;1/6; 1/8;1/10); LH (4; 2;1; ½; 1/4)	
Additives	Sorbitol; Sunflower oil; Beeswax, Stearic Acid, Citric acid, Lactic Acid, Glycerol, PEG 400, Tween 80	
FILM FORMATION PARAMETERS		
State of Desiccation	Fully dried, semi-dried, sticky wet	
Light Transmission Property	Bright, Semi-opaque, opaque	
Elasticity and Toughness	Strong, elastic, brittle	
Colour Intensity	Dark, light, colourless	

As seen from Table 4.2, film formation properties of micro fibrils were roughly determined at different dilution ratios with and without plasticizing additives.
Both freeze dried powder and pulp forms of MFC samples were used to produce films by using solvent casting method.

Emulsion films were prepared by using Bandelin HD 2070 Ultrasonic Homogenizer. In emulsion formation low power values (from 20% to max 40%) were applied for 1 to 4 min. For sono chemical grinding of cellulose microfibers, higher power values (from 60% to max 90%) were applied for 1 to 4 min.

Excess heat treatment applied to film solutions at 100°C oven for 2 h, and then semi-dried samples were taken to desiccator (25°C / 30% RH) and held for 24 h.

Different concentrations of MFC, wax, GLY, StA, Tw80 were studied. Also, effects of NCMC or Na-CMC addition to the roughness of emulsion films were investigated.

Experimental design was developed for testing different alternatives for our raw materials (extracts). Factors were selected as; plasticizer, raw material source, solvent

type, pH of the solvent. Film forming properties of these different combinations were evaluated roughly and these evaluations were determined as the response of the design. Fractions obtained in alkaline treatment; namely, dried hemicellulose extract, lignin-hemicellulose fraction, were mixed with a plasticizer (glycerol or sorbitol) or carboxyl methyl cellulose. The mixtures were poured into plastic Petri dishes. Films were dehydrated at 40°C for 20 hours.

Film production was conducted *via* solvent casting method as mentioned previously. Effect of drying conditions (temperature, relative humidity) was investigated in an environmental chamber unit. Screening tests was applied in order to optimize composition of films in case of some critical parameters; gas permeability, elasticity, thermal behaviour (have effect on tensile properties).

4.4 Characterization of artichoke by products and film samples

Bond structure of raw materials, cellulose fibers, micro-fibrillated cellulose, films and all of the additives used in film formation; were estimated through FTIR analyses.

Glass transition temperature, melting temperature and thermal degradation behaviour were determined by using DSC and TGA equipment.

Smoothness/roughness of the film surfaces were observed before application of AFM analyses in order to study surface properties.

Size distributions of micro fibrils were investigated firstly *via* phase contrast microscope (Inverted Phase Contrast Microscope, Olympus CKX-41).

Later, SEM analyses were done in order to evaluate morphology, homogeneity of the films and to measure their thickness.

Also, gas permeability and elasticity of film samples were tested with the procedure mentioned below.

Samples from supermasscolloider/homogenizer were both directly used or diluted with DW. Evaluations of PCM images were made *via* DP2-BSW software in order to roughly determine size distribution profile. Size distribution was also further examined by using Zeta-sizer (Malvern Instruments, 3000 HSA).

Before characterization analyses, samples were dehydrated *via* 3 different methods; oven drying, lyophilisation, spray drying. Dehydration conditions were selected according to previous studies from literature (Peng & Gardner, *et al.* 2012; Peng & Han, *et al.*2012), as given in Table 4.3. Dehydration conditions of MFC were selected as (-) 51°C, 0.04 mbar vacuum.

Table 4.3 Dehydration conditions of MFC

Method	Instrument	Conditions
Oven drying	Memmert Ine-500 Incubator	45°C / 48 h
Lyophilisation	Labconco-Freezone18 freeze dryer	-51°C ; 0.04 mbar vacuum
Spray drying	Buchi mini spray drier B-290	T_{inlet}:175°C;T_{oulet}:101°C; 0.15L/h

4.4.1 Measurement of thickness

Thicknesses of films are important in calculating WVP values and it is useful maintaining unity among different samples in solubility and dispersibility tests. Thickness of films was measured with a digital micro meter (0.01 mm precision). Photographs of all samples were taken in close-up mode with a 20mp camera (Samsung KZoom, Korea).

4.4.2 Determination of minimum film forming temperature

Conductivity based method was adapted from US patent (Pashley et al. 2001). Prepared film solutions were heated from 5°C to 65°C and conductivity values (mS/cm) of film solutions were measured as temperature increased. MFFT values were determined for carboxyl methylcellulose, micro fibrillated cellulose, lignin-hemicellulose and lignin-hemicellulose-wax solutions. In equation (4.1), MFFT calculation was shown where d^2K second derivative of conductivity value, dT^2 second derivative of temperature value.

$$MFFT = (+/-) \, d^2K/dT^2 \qquad (4.1)$$

4.4.3 Water activity and brix value of powdered samples, film samples and solutions

In colour and a_w analyses both bright (br) and rough (ro) side of films was measured separately in order to observe differences. Water activity (A_w) of the films tested with Rotronic water activity tester (USA).

Brix of prepared film samples were observed with RE50 refractometer (Mettler Toledo, USA). Refractive index (nD) measures velocity of light through sample solution compared velocity of light in vacuum. Light travels more slowly in a medium than in a vacuum. nD increases with density, higher density provides more viscous film solution.

$$n_D = v_{vacuum}/v_{medium} \tag{4.2}$$

Cellulose does not melt, it stay solid even if it is hot stirred. Cellulose fiber has a density value of ~1.53 g/cm^3. Its density differs from 1.49 to 1.6 g/cm_3 whether it is in amorphous or crystal form. Amorphous form is preferable in film formation applications. Brix gives idea practically for cellulose microfiber solutions coming from various pre-treatment methods such as supermasscolloider, ultrasonic homogenizer.

In order to evaluate brix and aw data statistically ANOVA was applied.

4.4.4 Determination of solubility and dispersibilty

Hydrophilicity/hydrophobicity of produced film samples were observed through dispersibility, solubility tests. For testing dispersibility of different film samples, films were cut into pieces having same dimension (2cm X 2cm). Samples were put into wells and 1 ml UPW were added onto them (t=0). Samples were held at 50°C ovens for 5 minutes, and then liquid part was taken and analysed for their brix%. Then semi dispersed film samples put to 60°C ovens for dehydration. Photographs of each step were taken and recorded.

In testing solubility of film samples, firstly effect of pH on solubility of film was tested for neutral and alkaline medium. Then effect of wax addition and emulsifiers on solubility was observed. For solubility test, films were cut into pieces having same dimension (1cm X 1cm). Samples were put into wells and 2 ml liquid were added onto them. Wells were held at 25°C and shake (300 rpm) for maintaining solubility. Solubility test for mfc pulp precipitate film, again conducted in an incubator shaker, at 300 rpm, under alkaline (pH=11) and neutral (pH=7) conditions at 25°C. At different time intervals, liquid part of samples were taken and put to Eppendorf tubes, then centrifuged at 5000 rpm for 3min. Brix measurements or absorbance readings were conducted to supernatant. Centrifugation was not applied to liquid samples for dispersibility test, and brix values were quantified directly by Refractometer measurements.

4.4.5 Opacity and transmittance properties

In colour and a_w analyses both bright (br) and rough (ro) side of films was measured separately in order to observe differences. Colour of film samples, powdered samples and treated artichokes were measured with Konica Minolta Chroma meter (CR-400, USA). Formulas and parameters used in colour measurements explained detailed in Table 4.4. Colour properties of some artichoke by products (leaf powder, dewaxed leaf powder, freeze-dried MFC, NCMC) and Na-CMC were observed in a clean glass Petri dish under daylight. Colours of dried artichoke samples were also measured and results were compared within each other. For observing colour of treated artichokes L*, a*, b* parameters were measured and hue angle, Chroma city, browning index values were calculated in order to detect differences correctly. Film samples' colours measured with a clean polystyrene Petri dish, while colour of artichoke and powdered samples were measured in clean glass Petri dishes. In colour analyses, all measurements for the samples in same batch were made at similar hours of the day, in all measurements lights were closed and measurement was applied under day light.

Microscopic images of dried film samples were observed both with inverted and optic microscopes. Since films transmit light partially, PCM gave more valuable images.

Table 4.4 Colour parameters (Meaning & Calculations)

Parameters	Meaning	Formula	Used in
L*	lightness (0:black;100:white)	$\Delta L^* = L^*_{standard} - L^*_{sample}$	Film + artichoke
-a*	Greenness	$\Delta a^* = a^*_{standard} - a^*_{sample}$	
+a*	Redness		
-b*	Blueness	$\Delta b^* = b^*_{standard} - b^*_{sample}$	
+b*	Yellowness		
ΔE	Total colour difference	$\Delta E = [(\Delta L^*)^2 + (\Delta a^*)^2 + (\Delta b^*)^2]^{1/2}$	
Chroma	saturation value of a colour	$= [(a^*)^2 + (b^*)^2]^{1/2}$	
Hue angle	perception of colour by eye	$= Arc\ tan\ (b^*/a^*)$	
WI	whiteness index	$= 100 - [(\Delta L^*)^2 + (\Delta a^*)^2 + (\Delta b^*)^2]^{1/2}$	film
BI	Browning index $a^*_t, L^*_t\ \&\ b^*_t$; colour values at each storage period a^*_0: initial colour	$x = \dfrac{a^*_t + 1.75 L^*_t}{5.645 L^*_t + a^*_0 - 3.012 b^*_t}$ $BI = \dfrac{100(x - 0.31)}{0.17}$	artichoke

[Yoshida 2014; McHugh 1993; Pereda 2014; Valenzula 2013; Cefola 2012]

4.4.6 Morphology, size evaluation and surface properties

Morphology of dehydrated micro fibrils, cellulose fibers was examined by SEM (FEI QUANTA 250 FEG). Samples were coated with gold-palladium (100-200 Å thickness) prior to imaging to eliminate charge effect (Emitech K550X). ETD detector was used and 100x, 500x, 1000x, 2500x, 25000x, 50000x magnifications were applied during SEM analysis. Thickness and microstructures of surfaces and cross section of films (esp. porosity and smoothness) were examined using Scanning Electron Microscopy (SEM).

Surface porosity of some selected films was imaged in Stereo Zoom microscope with 10 fold magnification under light.

Droplet size in emulsion films were measured with inverted phase contrast microscope (Olympus CX41; USA). Again fibre size of cellulose microfiber pulps, films solutions from MCF and FDMCF samples were measured with the same device.

Micro fibril samples were dehydrated as very thin layers for the AFM analysis. Micro fluidized micro-fibril samples were also analysed with AFM (Digital

Instruments-MMSPM Nano scope IV) in order to have a more precise idea about infrastructure of micro fibrils. Instrument was worked in tapping mode and results were evaluated by using Nano scope Software.

4.4.7 Determination of bond structure

Produced and dehydrated micro fibrils were tested by using FTIR (Digilab FTS 3000 Mx) in order to compare their structures with cellulose and cellulose fibers extracted from artichoke leaves. Samples were prepared *via* the standard KBr pellet technique and scanned at room temperature under vacuum from 4000 to 400 cm^{-1} wavelength with a resolution of 2 cm^{-1}. The spectrometer was equipped with a DTGS-TEC detector. For all the spectra, the baseline correction and normalization (with respect to the most intense band) were carried out. Absorbance peaks were evaluated with ACDLABS 6.0 software (Canada).

FTIR-ATR instrument was equipped with a horizontal ATR sampling accessory (ZnSe crystal) and a deuterated tri-glycine sulphate (DTGS) detector were used for analyses of film solutions and film components in liquid state. ZnSe crystal was used to determine the spectra of film solution at a resolution of 4 cm^{-1}. DTGS detector measurements were in the range of 64 scans in average at the wave number range of 4000-650 cm^{-1}. ZnSe crystal was cleaned with hexane in between runs.

4.4.8 Determination of crystal structure

Crystalline-amorphous structure distribution of cellulose fibers, micro-fibrillated cellulose, artichoke leaf fibers were determined with XRD. All samples were loaded to instrument in powder form. Intensities of 2θ values from 5° to 60° were monitored with 0.02 step size (50 second per step).

4.4.9 Thermal characterization

Artichoke by products in powder form was also tested for their thermal characteristics with TGA and DSC techniques. DSC were applied in order to determine glass transition (T_g) and melting (T_m) temperatures. In DSC analyses, samples were heated under nitrogen flow, at a heating rate of 10°C / min, from 20°C to 500°C. In TGA method samples were heated with 10°C/min heating rate from 50 to 500°C temperature and degradation percent of samples were observed.

4.4.10 Mechanical characteristics

Mechanical properties of film samples were tested using a TA-XT texture analyzer (equipped with a 5kgf load cell, in tensile mode, testing speed 10 mm/min) using the method stated in ASTM-D882. Samples tested having 10 mm width and 70 mm length, conditioned at 25°C / 50% RH / 48 h pre-analyses. Main parameters mesured frequently in tensile testing of film materials are stress, strain and young modulus. Calculation equations for those parameters were tabulated in Eq. 4.3, 4.4, 4.5 below.

$$\text{Strain } (\varepsilon) = \frac{\text{elongation of the material (dL)}}{\text{length of the material (L)}} = \frac{m}{m} \qquad (4.3)$$

$$\text{Stress } (\sigma) = \frac{\text{force (F)}}{\text{area of object (A)}} = \frac{N}{m^2} \qquad (4.4)$$

$$\text{Young's modulus (E)} = \frac{\text{stress}}{\text{strain}} = \frac{F/A}{dL/L} = (N/m^2) \qquad (4.5)$$

The thickness of the test pieces was measured at 5-10 points with μm precision micrometer and an average thickness was calculated. At least six films were tested and the average was reported.

4.4.11 Water vapor transmission rate

A modified ASTM (1995) method E96 was used to measure water vapour transmission rate (WVTR) of the samples. The films without any defects firstly put into Schott bottles containing ultrapure water (assay cup) sealed with plastic ring and lid (0.0854865 m^2 film area). For blank trial, bottles closed with classical lid. In order to maintain the gradient of RH $\approx 30\%$ throughout the film, these cells were placed inside 30 cm ϕ desiccator containing dry silica gel at the test temperature of 25°C. Picture of test conditions and equipment used were given in Fig 4.5 below. Then the cells were weighed at 12 h intervals over seven days period. Changes in the weight of cells were recorded (at 0.0001 g sensitivity) and result data were plotted as a function of time. Eq (4.6) were used to evaluate and calculate WVTR of films. The slope of the plot divided by the effective film area to obtain WVTR:

$$WVTR = slope\ /film\ area = \Delta W\ /\ (\Delta T\ {}^*A) \qquad (4.6)$$

Where ΔW= weight change in solvent/sorbent (g), A = area of the exposed film surface (m^2), ΔT = incubation period (day)

Figure 4.5 WVTR testing apparatus (cells, desiccator and oven)

Additionally effect of method was searched moisture transfer rate of selected film sample. Sample was coded with "$_{Wgainmthd}$" as subscript (and the sample with ordinary method was coded as"$_{Wlossmthd}$"). For the weight gain method all conditions were similar except dry $CaCl_2$ was used within tubes (A = 0.025434 m^2) in 30 cm ϕ desiccator with saturated NaCl solution (75% RH).

4.4.12 Oxygen transmission rate

Gas permeability tests conducted using Lyssy L100-5000 Manometric Gas Permeability Tester for determination of O_2 transmission rate of films at 23°C / 0% RH conditions *via* the method stated in ASTM-D1434.

4.5 Fresh cut treatment and packaging trials

4.5.1 Treatment experiments for globe artichoke

Freezed globe artichoke samples were thawed in distilled water, 1% citric acid, 1% Ascorbic acid, 1% Sodium MetaBiSulphite and 0.5% Cysteine solutions and stored at 5°C for two days in treatment solution. During storage colour of artichoke samples were observed as mentioned in section 4.4.6. Then excess liquid were drained with a filter paper, artichokes were dehydrated slowly at 35°C in presence of $CaCl_2$ (as desiccant) in incubating oven.

4.5.2 Packaging and coating experiments

Firstly, artichoke stalks were coated under nitrogen within a glove box cabin. Dip coating was applied for 2 times with 3 % Na-CMC solution. Stalks were stored in room conditions and effects of coatings were observed.

Packaging trials were done 2 % CMC + 0.6 % GLY films with the thermal sealer. Before packaging samples were dipped into 1 % CA solution. Parallel to packaged films, control samples (with and without CA treatment) were held at the same conditions in order to detect differences. During packaging trials artichoke stalks stored at room temperature for 7 days; while fresh and freeze thawed artichoke heart stored at 4°C for 7 days. Packaging trials were done with a manual thermal sealer, as seen in Figure 4.6. Artichokes were stored in 4°C Nüve incubators for 7 days; each day observed visually pictures were taken.

Figure 4.6 Thermal Sealer; Vacuum Packaging Machine

4.6 Statistical analyses and data evaluation

For determination of optimum film formation conditions and compositions screening tests were applied initially. For film composition determination screening tests were conducted initially, than optimization tests were carried out for selection of best compostion ratios and preparation conditions. Results were evaluated with ANOVA in Design Expert software. To get evaluation abaout data general factorial design tests were conducted for each analysis with different parameters. In ANOVA there are 3 main parameters those were benefited in determination of optimum conditions; p-value, desirability, R^2. Desirability and similarity of samples were determined for detection of best condition and looking for significant differences between two different samples in sequence. Desirability values were determined *via* predefined target response values with different importance ratios for that selected analysed samples. Similarity ratios were determined *via* comparison of Prob > [t] values of samples individually.

Results of selected film samples were characterized and characterization data for raw materials, extracts, film samples and solutions were evaluated with PCA in Simca software. In PCA main evaluation principle is based on Q^2 and R^2 parameters, in terms of selected model for predefined conditions (Erikkson et al. 2013). PCA gives an overview of the information in a data table, shows how the observations are related and if there are any deviating observations or groups of observations in the data. PCA describes the correlation structure in X. R^2 is a measure of fit, i.e. how well the model fits the data. Q^2 tells you how well the model predicts the variable (Umetrics-AB 2013). PCA analyses especially used for discrimination of different samples from their spectrum data *via* usage of FTIR, XRD instruments. Dataset of FTIR-ATR spectra, XRD and thermal diagrams were clustered by means of Hierarchical Clustering Analysis (HCA) in order to evaluate results in a meaningful relation. The result of HCA was shown by means of dendrogram plots.

CHAPTER 5

RESULTS & DISCUSSION

In order to obtain an ideal film to handle in fresh cut packaging products, some targets that have been predefined at the outset of the study. First, the polymer used in film formation should be able to form a whole rough structure that do not dispersed or degraded easily when peeled from Petri dish or stored at room conditions for at least one month. Film product should have appropriate stress resistance and elasticity letting packaging application with or without vacuum. Also film should have preferable colour and visual appearance in order to not to effect consumer acceptance negatively. Film should resist to moist conditions, should not be easily dispersed even when exposure directly to water vapor in fact to water itself (in advance). In another term final product should be hydrophobic as well as it would produce from agricultural wastes without any synthetic additives or chemical treatment application. Therefore, 3 of these targets were actually maintained with the use of extracts obtained from artichoke wastes, many composition alternatives were studied preliminary with screening tests. Trials to increase hydrophobicity of the film products were also presented in this section.

5.1. Preparation of film forming materials from artichoke leaves

Preparations of film forming materials were carried out using artichoke leaves as raw material. Initially artichoke leaves were grinded with a lab scale grinder. Grinded samples sieved, if there are significant differences in particle sizes and artichoke leaf powder was obtained with ~0.5 mm size (average). Next, approximately 16% of the dry matter was removed as wax or other alcohol soluble compounds in Soxhelet extractor *via* hot ethanol extraction.

The main components of the films were lignin, hemicellulose, cellulose and wax fractions by hot ethanol and mild alkaline extraction methods as described in Chapter 4.

Each obtained fractions were characterized as pure forms and/or in different mixture combinations.

Besides carboxymethylcellulose (NCMC) was chemically synthesized from cellulose fraction obtained, pictures of Na-CMC (NCMC) synthesized from produced cellulose fibers, could be seen in Figure 5.1.
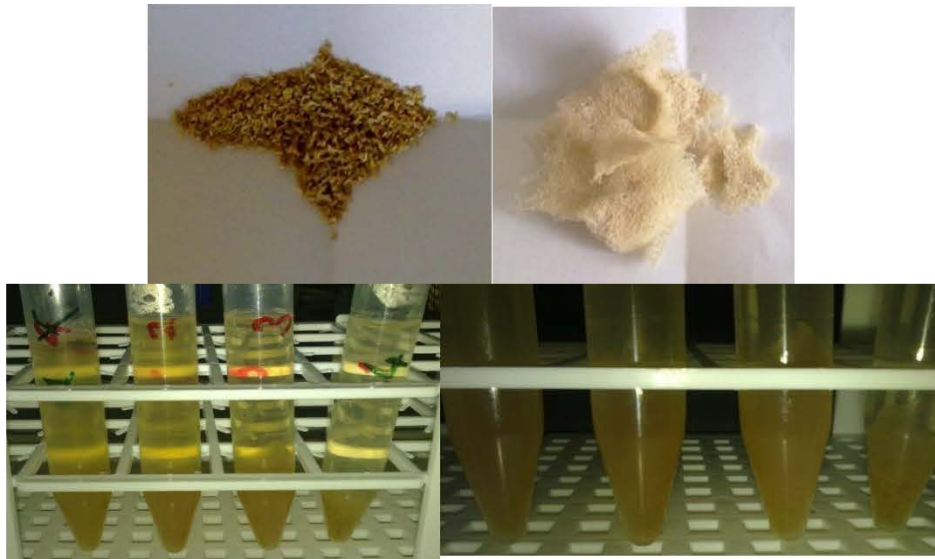
Figure 5.1 NCMC synthesized from artichoke wastes; before and after dehydration

Microfibrillated cellulose were also obtained from cellulose fraction using mechanical homogenizer, supermasscolloider. Pictures of cellulose microfibrils produced could be seen from Figure 5.2. As seen, microfibrillated cellulose samples obtained from the homogenizer were having a pulpy and homogenous structure at first sight. But after a while thin liquid layer (1-2 % of the total pulp volume) was observed, remaining part was still stable, homogenous and pulpy.
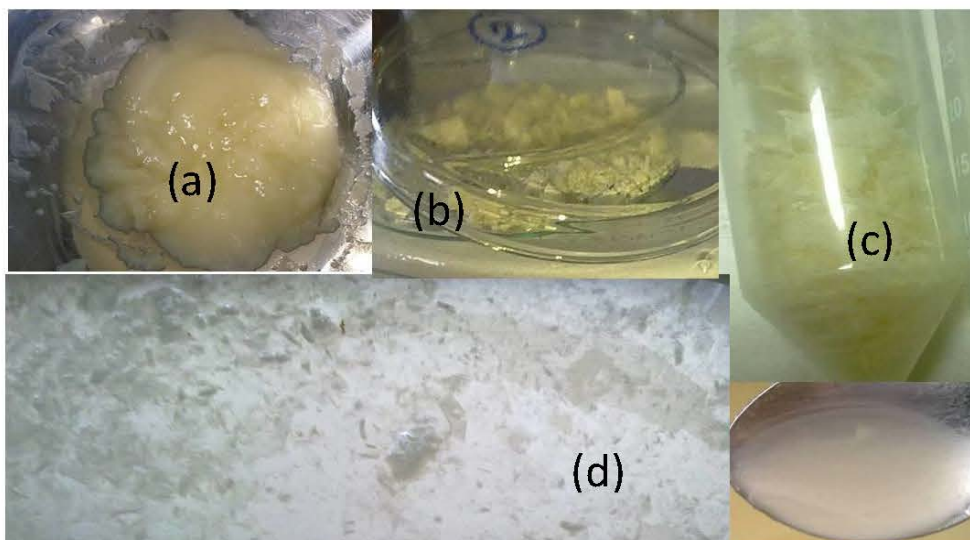
Figure 5.2   Images of microfibrillated cellulose pulp (a), ovendried micro fibrillated cellulose pulp (b), freezedried microfibrillated cellulose pulp(c), microfluidized microfibrillated cellulose pulp(d)

These by products analyzed for determining some pysicochemical and morphological characteristics using FTIR, TGA, PCM, and SEM, etc. instruments, in order to determine film forming ability and/or to compare their structures, before and after film formation.

Results of chromatography analyses showed that 52.17 ±1.81 g cellulose and 22.12 ± 0.00 g hemicellulose could be obtained from 100g dried and grinded artichoke residues. Using the original (unmodified) alkaline extraction method around 50% of the raw material was removed as the solid residue after alkaline peroxide treatment; while the maximum hemicellulose fraction yield was 9.14% (w/w). The alkaline treatment method exerts a drawback since extraction yields of pure hemicellulose obtained in low amounts.

5.2. Preparation of packaging films

A wide range of literature survey was conducted for the usage of hemicellulose, lignin, and cellulose in packaging materials. According to the data obtained, an experimental design was developed to verify different alternatives of the raw materials (the extracts were mentioned in Chapter 4, Section 4.1. and 4.2) produced.
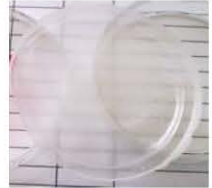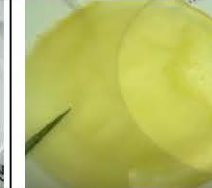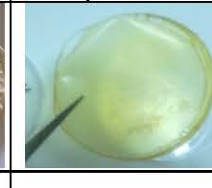
Factors were selected as; plasticizer, raw material source, solvent type, pH of the solvent. Film forming properties of these different combinations were evaluated roughly

and these evaluations were determined as the response of the design. Factors and responses of screening tests were summarized in Table 4.2. Various composition combinations were tried in order to determine the optimum conditions.

First attempts were done to develop hemicellulose films from the extracts of artichoke wastes. Hemicellulose films were brittle and dark coloured. Besides no positive effect were proven as to contribute on the gas barrier property of the films with HMC addition.

LHW fractions were resulted in elastic/opaque films having very high gas permeance property. Fractions obtained in alkaline treatment; namely, dried hemicellulose extract, lignin-hemicellulose fraction, were mixed with a plasticizer (glycerol or sorbitol) or carboxyl methyl cellulose. The mixtures were poured into plastic Petri dishes. Films were dehydrated at 40°C for 20 hours. Some of the successful films produced were summarized in Table 5.1.

Table 5.1 Some of the Successful Films Produced

Picture				
Composition (w/v)	CMC + GLY + StA + Tw80	CMC + GLY	CMC + GLY + SFO + Tw80	CMC in ¼ diluted LHW solution
Properties	Strong, elastic, semi-opaque	Strong, elastic, transparent	Strong, elastic, semi-opaque	Semi strong, elastic, opaque, yellow
Picture				
Composition (w/v)	HMC + CMC + GLY	GLY + SFO + Tw80 + CA - cmc	NCMC + GLY	Lignin – hmc - CMC
Properties	Semi strong, semi elastic, dark	Strong, elastic, semi-opaque	weak, elastic, opaque, nor homogenous	

The films with Na-CMC gave good results in terms of gas barrier properties, plasticizers were also added to these films. Firstly, GLY was incorporated and CMC films with GLY were brittle. It was decided that applicable concentrations of GLY were

not appropriate to obtain elastic films with CMC; the films were easily dispersed even in low amounts of DW. When sorbitol was also tried as plasticizer, films with obtained extracts were not given satisfactory results unlikely with trials of CMC and GLY. Na-CMC either alone or in combination with different fractions of alkaline peroxide treatment yielded acceptable films.

Properties of MFC films were compared with previous film samples those prepared with other artichoke waste by products such as hemicellulose, lignin and carboxyl methylcellulose. In some cases, addition of wax solution (in ethanol) was considered for obtaining an artichoke sourced plasticizer. Producing highly hydrophobic and natural films is an important target for benefiting packaging materials in storing fresh cut vegetables securely. Since it is not possible to form a hydrophobic film from cellulose micro fibrils, addition of StA, PEG 400, artichoke wax, GLY (with Tw80 combination) were studied.

Emulsion films were developed in order to solve dispersibility problem. Thus, incorporation of SFO or StA trials was carried out. Results in terms of homogeneity and dispersibility were not good enough for real time applications on fresh-cut fruits and vegetable samples. In preparation of emulsion films Ultrasonic Homogenizer was benefited for reduction in size of droplets and for maintaining homogeneity through film solutions.

Films from NCMC were prepared with solvent casting method. 3 g NCMC were put into 100 ml hot water in order to dissolve. Films were casted in three ways;
- without separation of undissolved part (1st)
- only dissolved (upper phase) was used as film solution (2nd)
- undissolved part was separated *via* a cheese cloth(3rd)

Best films were obtained with the second method, while the films produced with 2nd method were not reproducible within each other (At the same preparation conditions; properties of films were not similar; it might be arised from instable physicochemical characteristics of NCMC). For the third method, films produced were too thin due to the high decrease in concentration after filtration.

In order to be able to handle CMC during film applications, soluble fraction of NCMC preparate were obtained with filtration and lyophilization. NCMC films from NCF were insufficient to form film structure. Products obtained were sticky, weak and very difficult to handle (even at high concentrations up to 15 % w/v) in film applications; this was attributed to variable properties (e.g. molecular weight, viscosity)

of NCMC than expected. Also there could be reproducibility problem for NCMC film casting.

Lignin/hemicellulose fraction, obtained after the alkaline peroxide treatment of the dewaxed raw material, was also concentrated by rotary evaporator. The films obtained using concentrated form, mainly composed of soluble lignin and hemicellulose, were yielded with uniform, opaque and elastic films. The mixture of lignin/hemicellulose was found desirable; presence of lignin improved the elasticity of the films. Therefore, it is thought not to separate hemicellulose from lignin fraction by further purification. Thus, the steps of precipitation of lignin by lowering pH and precipitation of hemicellulose by addition of alcohol could be omitted.

Among the combinations tested for film casting, the mixture of two fold concentrated liquid lignin/hemicellulose fraction and Na-CMC (2% (w/v)) formed an elastic film, which was promising to be used in packaging applications. This film and all the other films produced further characterized as was presented in Section 5.3.

Different treatment applications and casting conditions were reported in the literature to produce stabile micro fibrillated cellulose films. Rastogi *et* al. 2014, described short term heat treatment of film solution in oven at 100°C for 2 hours. Different casting conditions were studied with or without controlled relative humidity, (Aulin *et al.* 2010; Shankar *et al.* 2015) prefer low temperatures (23 or 25 °C). In this study also medium temperature condition (40, 45, and 60 °C) were applied.

Conditions applied listed previously in Table 4.2 in section 4.3. (Products obtained with excess heat treatment (100°C/ 2h) could not peel from Petri dishes in whole form, so it was decided heat treatment would not applicable for that kind of film products.

In order to have an idea on effect of heat application on physical properties of micro fibrillated cellulose, solubility test were conducted, for results were shown in section 5.3.3. Film formation potential of cellulose pulps were tested *via* preparation of aqueous solutions with products either from directly masscolloider/homogenizer or from dehydrated products obtained from oven dryer/lyophilizator. Films prepared only from MFC, may lead handling problems on packaging applications since they are having elasticity problems. In order to overcome the brittleness of the films, GLY was applied and these films had improved tensile properties.

Besides, emulsion type films were prepared by the addition of fatty acids and emulsifying agents into film forming solution. Emulsion was stabilized by IKA Ultraturrax homogenizer. All of the films were prepared after casted onto 5cm or 9cm φ Petri dishes and dehydrated in a simple oven at 40-50°C under not controlled humidity conditions. Before and during packaging trials environmental chamber are planned to be used as dehydration media, if possible. Pictures of the developed films and their compositions of films are presented in Table 5.1, above.

In order to obtain hydrophobic films, emulsion formation was tried with addition of wax from artichoke, stearic acid and glycerol. Tw80 was used as a surfactant. Ultrasonic homogenization was also used in formation of stabilized emulsion form.

5.3 Characterization of artichoke by-products and film samples

In order to evaluate characteristics of artichoke by products pysicachemical test methods were benefited. Mainly; film forming ability & hydrophilicity of film materials, mechanical & thermal & permeability properties of films, bond & crystalline structure of artichoke by products, size and morphology of microfibrils and finally packaging ability of produced films was investigated.

5.3.1 Minimum film forming temperature values of raw materials

Minimum film forming temperatures were determined in order to optimize casting conditions of films produced and since there were no information for that kind of film forming materials in literature. 1st and 2nd derivatives conductivity values were taken against temperature. 2nd derivative values of conductivity were plotted against temperature and the maximum value in graph gives MFFT values for that solution. Results were summarized in Table 5.2 below. Regularity of casting temperatures were proved *via* MFFT values.

Table 5.2 MFFT values calculated for frequently used film forming solutions

composition/treatment	mfft (°C)
Sonicated 1 % mfc sol'n	18.00
Sonicated 1.5 % mfc sol'n	20.75
2 times conc. lignin-hmc-wax sol'n	48.15
lignin-hmc sol'n	23.85
2 % na-cmc sol'n	11.05

5.3.2 Brix and Aw values of films and film solutions

A_w is a critical factor in food deterioration. For the films produced a_w values are also critical for respiration rate of packaged vegetable and also directly effective on mechanical properties of films (*especially elasticity values*).

Thickness values of some of film samples were shown in Tables D.1 and D.2. The difference between film samples at various compostions and casting volumes were found siginificant due to evaluation data from ANOVA.

Brix values for standard compounds were measured in solution form and presented in Table 5.3. Also, brix values for aqueous solution of artichoke by-products were measured and recorded, shown in Table 5.4. Brix values of different film solutions were presented in Table 5.5, for having more valuable conclusion on dispersibility and solubility test results. Brix values for film solutions were found significantly different. This information is valuable for dissolution tests since the significancy of difference needed in order to be able to use refractive index data to evaluate solubility of film samples. Results were aligned according to the aveg brix% values from low to high.

Table 5.3 Brix values of standard solutions

Brix%	n	aveg	±	stddev
ph=7 upw	2	0	±	0
dw	2	0	±	2.45E-05
ph=11 dw	2	0.06	±	0
cellulose	2	0.3	±	0
ph=12 upw	2	0.31	±	0
microgranulated cellulose	2	0.31	±	0
hot stirred cmc hot mw 250.000	2	0.98	±	0.000215
cold stirred cmc cold mw 250.000	2	1.04	±	3.36E-05
cold stirred cmc cold mw 700.000	2	1.27	±	0.012569
hot stirred cmc mw 700.000	2	1.33	±	7.44E-09
cmc 1.5%	2	1.46	±	6.88E-05
cmc-2%	2	2.09	±	0
1.6% cmc solution	2	2.64	±	0
3 % cmc	2	3.4	±	0.00014
sunflower oil	2	23.39	±	0
tween 80	2	72.53	±	8.78E-05
glycerol	2	72.93	±	0.001021

Table 5.4 Brix values for aqueous solutions of artichoke by products

Brix%	n	aveg	±	stddev
mortared mfc-40 times diluted	2	0.02	±	0
mfc-40 times diluted	2	0.04	±	0
mfc-20 times diluted	2	0.08	±	0
mortared mfc-20 times diluted	2	0.11	±	0
mfc-10 times diluted	2	0.11	±	0
mortared mfc-10 times diluted	2	0.21	±	0
microfluidized cellulose fiber	2	0.38	±	0
8 times diluted mfc	2	1.17	±	0
1/2 diluted lhw	3	1.2	±	0.003994
6 times diluted mfc	2	1.45	±	0
mfc	2	1.57	±	0
4 times diluted mfc	2	1.61	±	0
mortared mfc	2	1.83	±	0
2 times diluted mfc	2	1.93	±	0
1/4 diluted lhw	2	1.94	±	0.001741
ncmc	4	2.115	±	0.248261
freeze dried ncmc solution	4	2.71	±	0.1501
artlp solution	4	14.74	±	4.165594

Table 5.5 Brix values of film solutions

Brix%	n	aveg	±	stddev
mfc-wax-tw80-sta	4	1.44	±	0.005753
cellulose-peg400	2	1.47	±	0
mfc-cmc-sta-gly	12	1.99	±	0.288522
1 (lhw)	2	2.03	±	0.000174
ncmc +gly	10	2.1	±	0.402299
mfc2-ncmc-sta-gly-tw80	6	2.16	±	0.003222
mfc-chi-cmc-gly-wax	12	2.22	±	0.353412
mfc-ncmc-sta-gly-tw80	4	2.31	±	0.006602
cmc-2% + gly-0.5%	4	2.32	±	0.000125
filtrated ncmc solution	2	2.42	±	0.1352
mfc-chi-ncmc-gly-wax	10	2.47	±	0.010412
mfc-peg400-ncmc-gly	6	2.47	±	0.000638
mfc-cmc-sta-gly-tw80	10	2.58	±	0.005337
homogenized ncmc -gly	2	2.6	±	0
mfc -cmc- gly-sta	4	2.75	±	1.48E-05
cmc + gly + tw80	2	2.87	±	9.20E-05
mfc-chi-ncmc-gly	6	2.95	±	0.000338
cmc + gly	3	3.04	±	2.96E-31
mfc-chi-cmc-gly	4	3.07	±	0.000291
cmc 1.5% in 1/4 diluted and centrifuged lhw	2	3.08	±	3.12E-05
cmc-lignin-tw80-mfc-gly-wax	4	3.2	±	7.73E-06
mfc2-peg400-ncmc-gly	4	3.22	±	0.000131
emulsion film cmc-gly-sta	6	3.33	±	0.148217
3 % cmc in 1/4 diluted lhw	2	3.95	±	0.003401
mfc-cmc-sta-gly-wax	8	4.02	±	0.002623
cmc 1.5% in 1/2 diluted and centrifuged lhw	2	4.54	±	0.006324
3 % cmc in 1/2 diluted lhw	2	5.91	±	0.000875
freeze dried ncmc solution with gly	2	6.28	±	0
ncmc + lignin	2	7.42	±	0

A_w of film samples were found generally below 0.5 and in some films even below 0.4. Rough and bright sides of films differ in water activity values. Since microbial deterioration could rarely be observed below 0.6 a_w values, it could be stated that presence of films would not have contribution on microbial growth. It is difficult to draw a conclusion that films prevent deterioration of fresh-cut by looking at present findings. Addition of artichoke wax fraction into films should be considered from this aspect, since wax fraction of artichoke might contain antioxidant/antimicrobial components originated from artichoke.

Effect of film type or composition on a_w value was found significant (p-value < 0.05). F-value of 321.99 and adeq precision value of 54.943 for the model implies the indirect relation between film types and a_w values of films (probability of noise for the model, 0.01%). Also model has an acceptable R^2 value as 0.9966.

Table 5.6 Desirability evaluation of film samples according to a_w values

film type	a_w	Desirability
MFc-Cmc-Peg400-1% Wax	*0.3645*	*0.944*
MFc-Cmc-Peg400	0.3715	0.891
MFc-Cmc-peg400-3% Wax	0.388	0.767
MFc-Cmc-Peg400-4% Wax	0.396	0.707
MFc-Cmc-Peg400-5% Wax	0.4005	0.673
MFc-Cmc-Peg400-2% Wax	0.403	0.654
Wax sprayed mfc	0.4295	0.455
Mfc-wax	0.449	0.308
Mfc 1%	0.4525	0.282
Mfc 1.5 %	0.4615	0.214
MFc-Cmc-Gly-Tw80-Sta	0.463	0.203
Cmc-Gly sonicated	0.4675	0.169

In desirability evaluation with ANOVA data of film samples in terms of a_w values, target a_w value was set as minimum as possible. In Table 5.4, desirability evaluation for film samples in terms of a_w values presented. "Mfc-cmc-peg400" containing films generally evaluated as most desirable films since they have lowest a_w values.

On another experiment set again a_w values of films were measured and compared via ANOVA. In this term, additionally effect of film surface was observed. Effect of film type or composition on a_w value was significant and effect of surface type on a_w was also significant (p-value < 0.05). F-value of 899.87 and adeq precision value of 129.224 for the model implies the indirect relation between film composition or surface types and a_w values of films (probability of noise for the model, 0.01%). The interaction term (combined effect of film compostion and surface) was significant, too. Model had an acceptable R-Squared value as 0.9988.

Table 5.7 Desirability evaluation of film samples according to a_w values

film type	surface	a_w	Desirability
mfc pulp precipitate	ro	0.3925	0.996
mfc pulp precipitate	br	0.3955	0.971
artlp	br	0.455	0.471
mfc-cmc-sta-gly-wax2	ro	0.4645	0.391
mfc-cmc-sta-gly-wax2	br	0.466	0.378
2% ncmc	br	0.4665	0.374
2% ncmc	ro	0.468	0.361
mfc	ro	0.469	0.353
artlp	ro	0.4705	0.340
mfc + gly	ro	0.473	0.319
mfc-cmc-sta-gly-wax	br	0.476	0.294
6% ncmc	br	0.4765	0.290
mfc-cmc-sta-gly-wax	ro	0.4765	0.290
4% ncmc	br	0.478	0.277
6% ncmc	ro	0.478	0.277
4% ncmc	ro	0.4785	0.273
mfc-cmc-sta-gly	br	0.479	0.269
mfc-cmc-sta-gly	ro	0.4815	0.248
mfc + gly	br	0.4825	0.239
mfc	br	0.485	0.218
cmc-lignin-tw80-mfc-gly-wax	ro	0.508	0.025

In desirability evaluation for a_w values of different film samples again target value was set as minimum. Desirability values of different surfaces for same films were also listed in Table 5.5 above. Rough side of mfc pulp precipitate film was determined as most desirable film since it has lowest a_w value. In some films bright side gave lower a_w values while in some others rough side of films gave lower a_w values.

5.3.3 Solubility and dispersibility properties of films

Solubility is a concern giving idea about hydrophobicity of a film sample, lower aqueous solubility shows that film is highly hydrophobic. In this study, solubility values tried to be determined with the help of brix or absorbance values measured when film sample put in aqueous solution and held at prodefined constant conditions (stirring rate: 300rpm orbital shaker; mfc: 1.5% m/v; cmc: 1 %m/v; dissolution media: pH=7 upw).

Refractive index or absorbance reading values gives idea about solubility of carbohydrate based molecules within film sample. Higher nD or absorbance values shows film sample is more soluble in UPW and means film pretend to be hydrophilic.

In Figure 5.3 pictures taken from experimental setup used in dispersibility and solubility tests were presented. In the first row of Figure 5.3; pictures taken at three different time intervals were shown (t=0, t=5 min and dried form of semi-dispersed film samples) in dispersibility test.

t=0; dispersibility; P& PW t=5min; dispersibility; P& PW dried; dispersibility; P& PW

Solubility test t=0 emulsion film t=120min
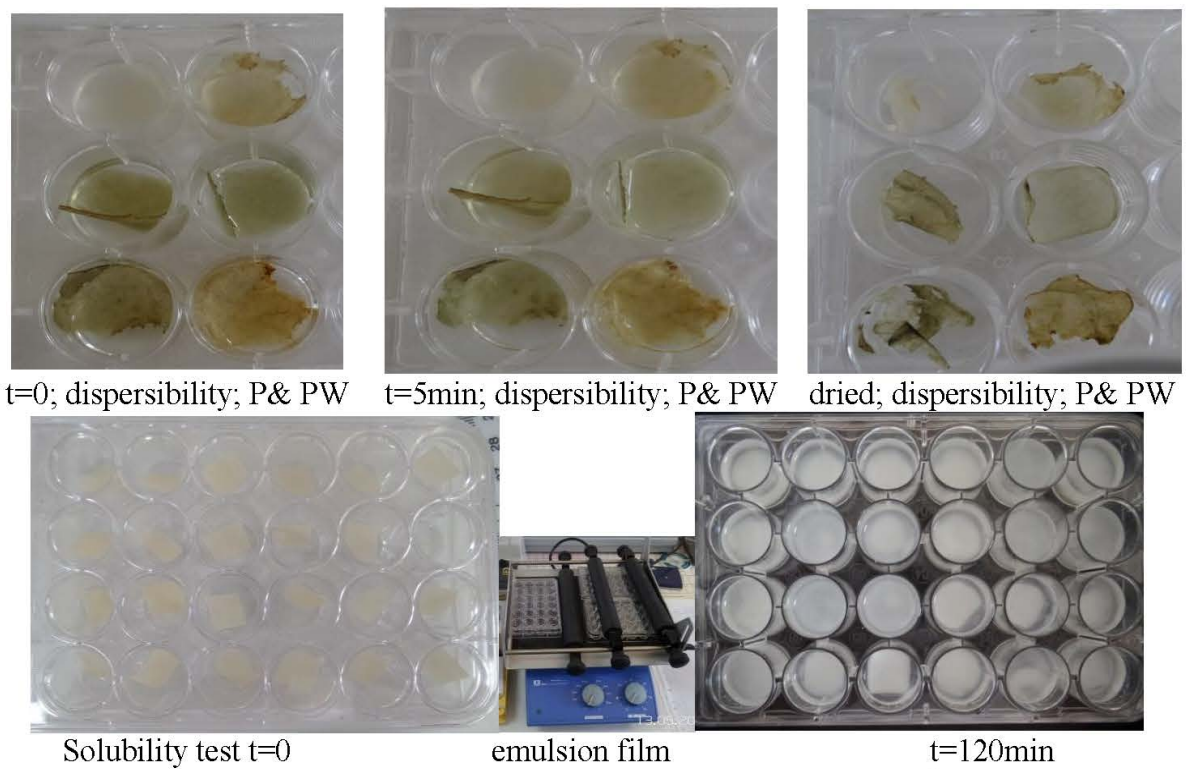
Figure 5.3 Pictures from solubility and dispersibility tests[1]

---

[1] PW: MFC- cmc-gly-peg400film; PW1: PW+ 1% wax; PW2: PW+ 2% wax; PW3: PW+ 3% wax; PW4: PW+ 4% wax; PW5: PW+ 5% wax
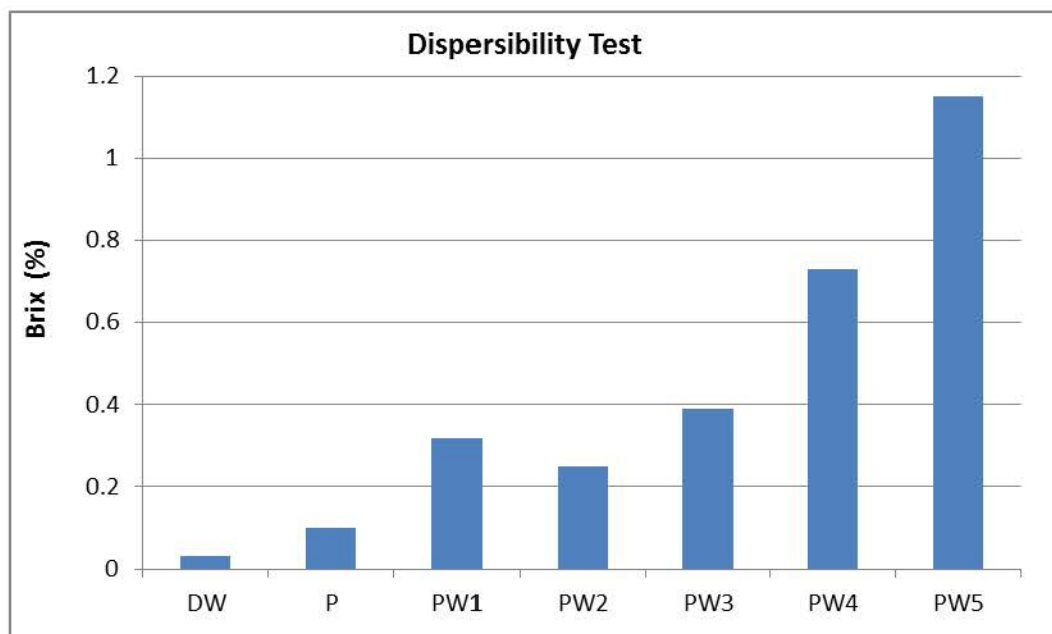
Figure 5.4 Dispersibility test (n=1)

In Figure 5.4 graphical illustration of brix data from dispersibility test was shown. The increasing trend in the brix values of PW3, PW4 and PW5 samples could be attributed to excessively high wax concentrations (up to 5%), since green colour of artichoke wax interferes with nD value. Thus, not only the increasing concentrations of carbohydrate solution but also increase in green colour of wax solution resulted with high Brix values.

Therefore, lower wax concentrations, in the form of liquid wax solution, were found to be more applicable into the film solutions; or efficient usage may be reconsidered from the dispersibility and solubility results together. Also, another method for quantification of solubility data may also be evaluated. Thickness of film samples used insolubility tests were shown in Table D.1, thickness data important in terms of providing more standardized data in analyses.

Figure 5.5 shows solubility test results considering effect of gly, peg400, gly-peg400 addition to mfc-cmc film with and without sonication treatment in solution form. As seen from plot most desirable solubility values (lowest abs/w readings) was obtained with sample 111S (mfc-cmc-gly-peg400-sonicated).
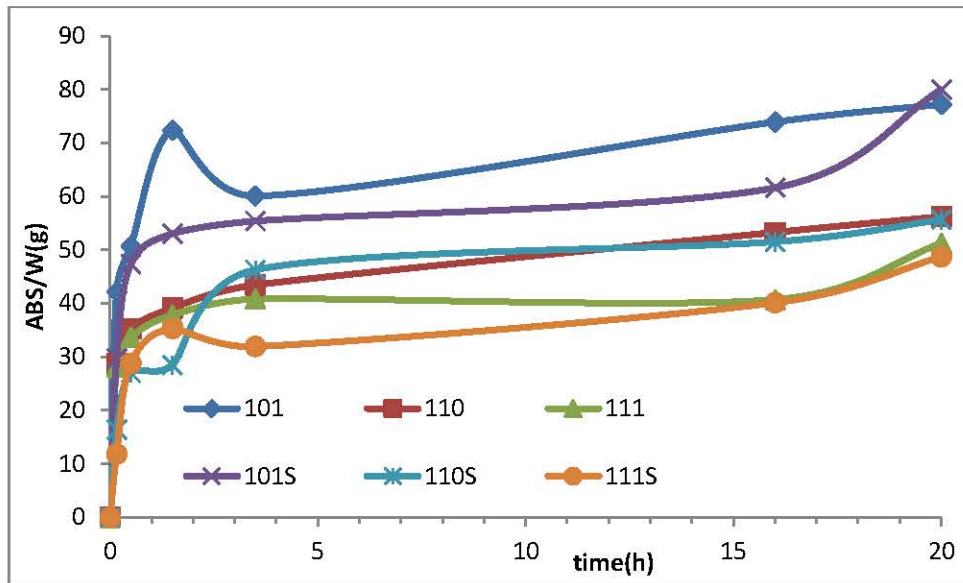
Figure 5.5 Absorbance/weight values for microfibrillated cellulose films with and without sonication (S) [101:mfc-peg400;110:mfc-gly;111:mfc-peg400-gly]

In Figure 5.6, solubility results for mfc pulp precipitate films those were tested in neutraline and alkaline media were presented. Alkaline media were tested in case film samples might be more easily dispersed (since Na-cmc used in this study was easily soluble in pH=11 usually). But statistical evaluation of dissolution data did not show any significant differences in terms of pH of the media tested.
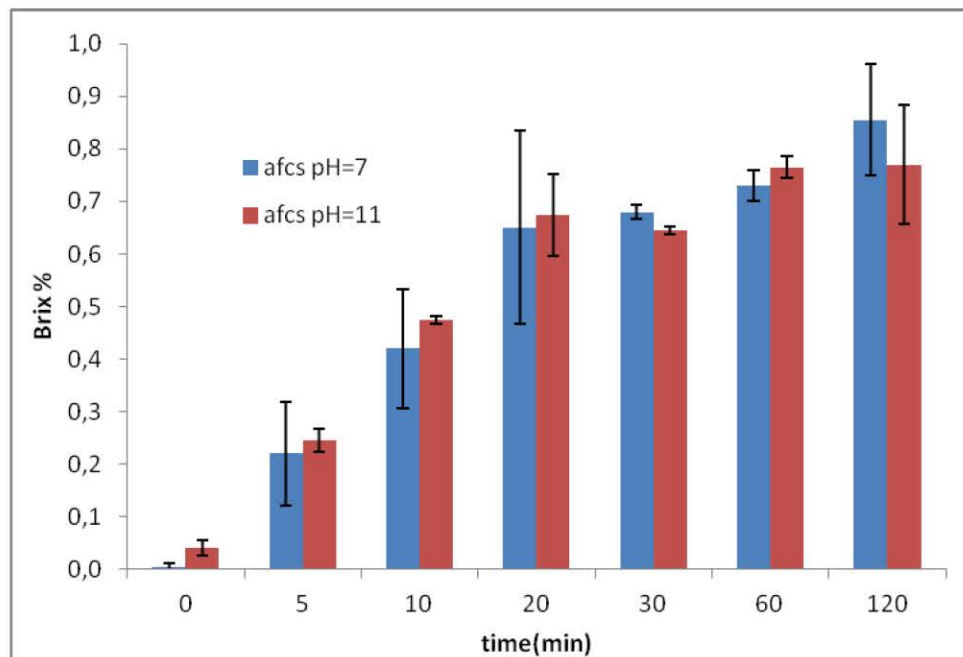
Figure 5.6 Solubility of MFC pulp precipitate film in Alkaline& Neutral Medium (n=2)
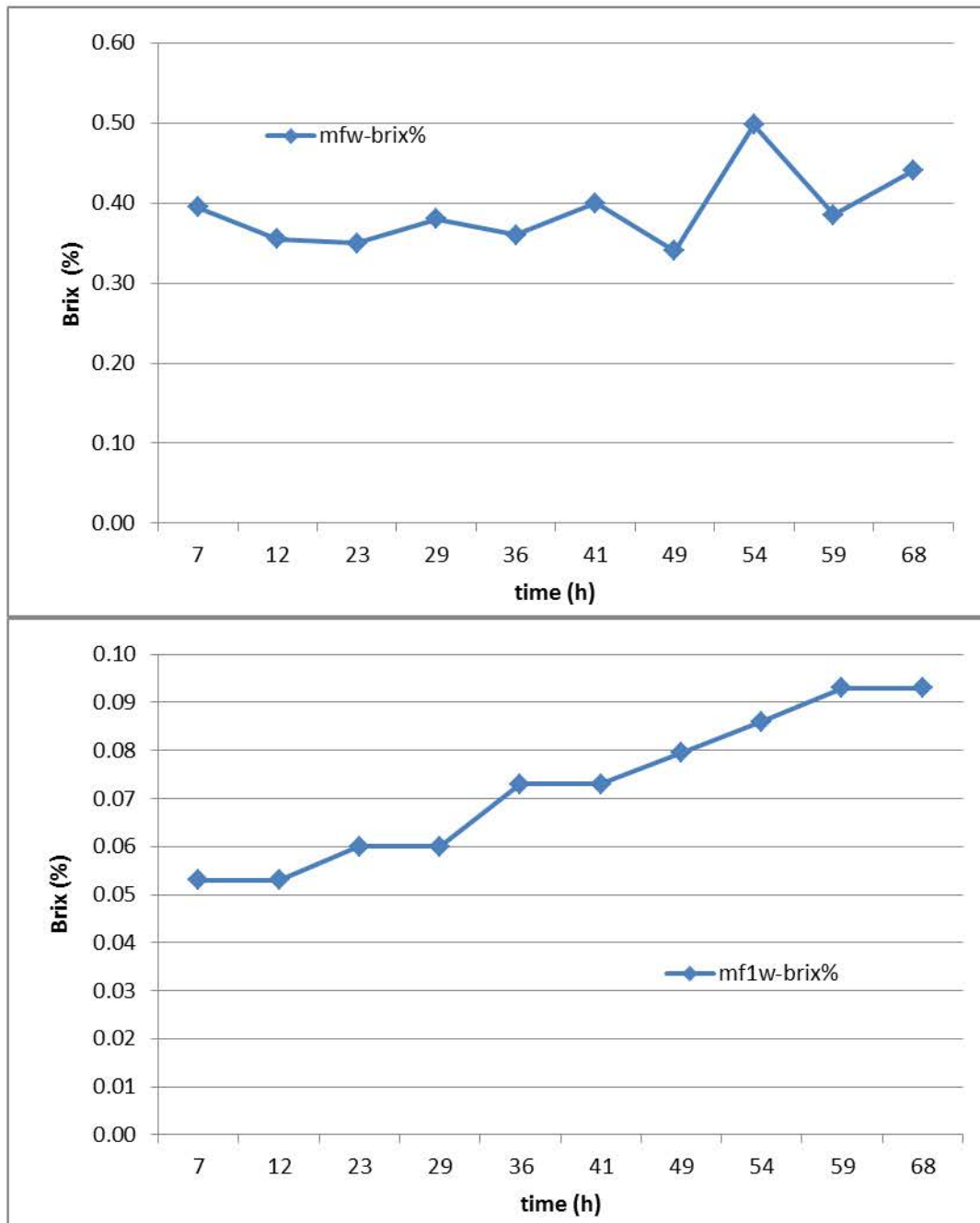
Figure 5.7 Solubility of MFC films with wax addition [mfw: casted with wax; mf1w: wax sprayed on film] (n=2)

In Figure 5.7 solubility results of wax sprayed mfc (soaked in wax) and mfc-wax (wax directly added to film solution) film samples were presented. From the figures it can be clearly observed that, addition of wax directly increases range of brix values regardless of time intervals (from 0-0.1% to 0-0.6%) instead of soaking them to wax solution. When results compared with solubility data of 1% mfc film sample (neither soaked in wax solution, nor wax was added to film solution; again having same FDMFC concentration), it may be concluded that soaking to wax solution decreases solubility of

MFC films, since range of brix results lowered (from 0-0.14 to 0-0.1). This finding should be evaluated more detailed and soaking conditions (time, concentration and maybe temperature) should be regulated to have best results.

In Figure 5.8 solubility results for mfc 1% (w/v) and sonicated cmc-gly film samples were presented. From the figures it can be clearly observed that, addition of CMC, directly increases range of brix values regardless of tested time intervals (from 0-0.14% to 0-0.7%).
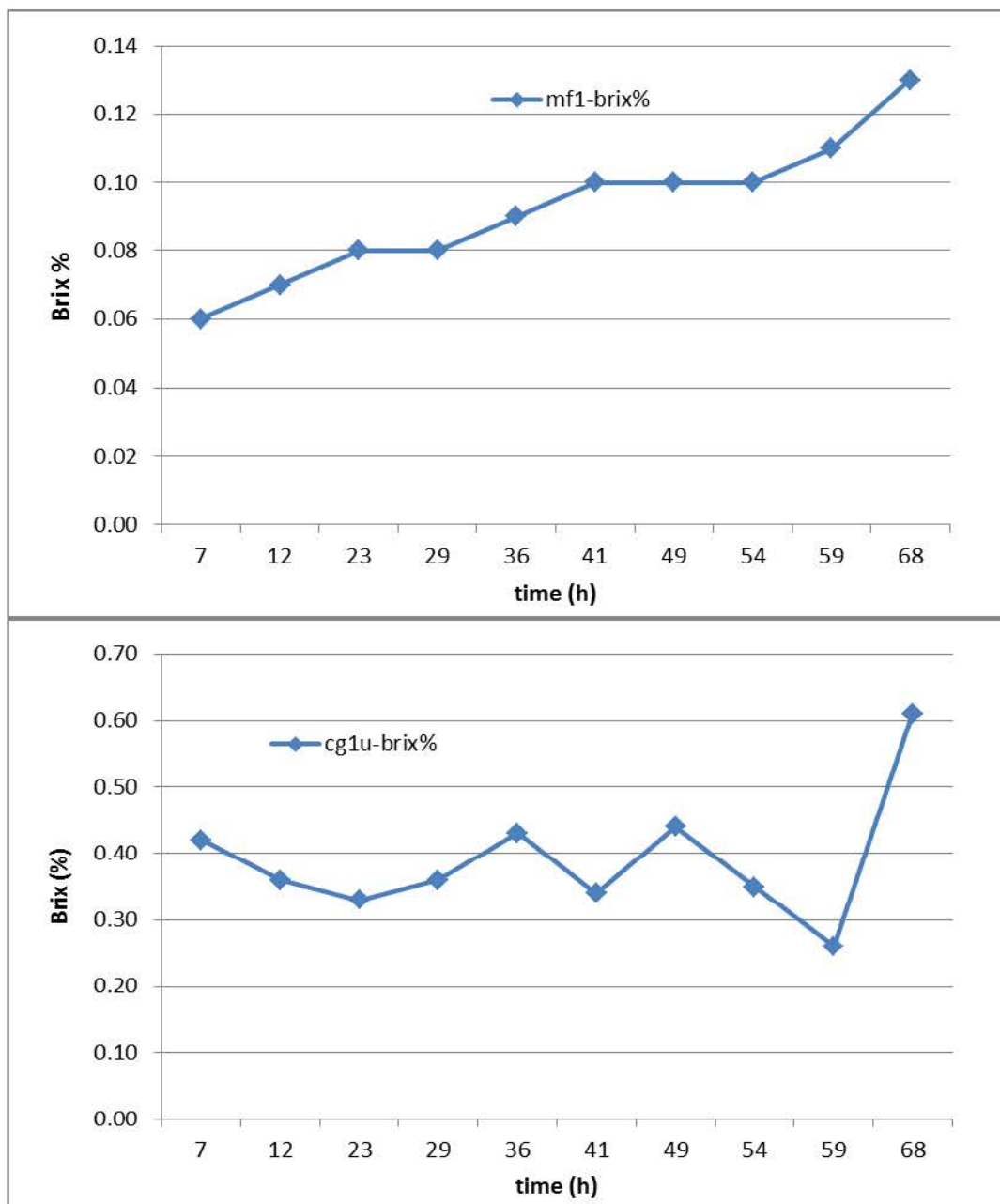
Figure 5.8 Solubility of MFC films w [cg1u] and w.o CMC [mf1] (n=2)

In Figure 5.9 solubility data of emulsion film with StA + CMC and without wax (mfc-cmc-gly-sta film) was presented. Addition of StA does not decrease solubility of that film, when compared with data of cmc-gly sonicated film; since ranges increased to 0-1.2% (it was 0.7 % at 68th min).
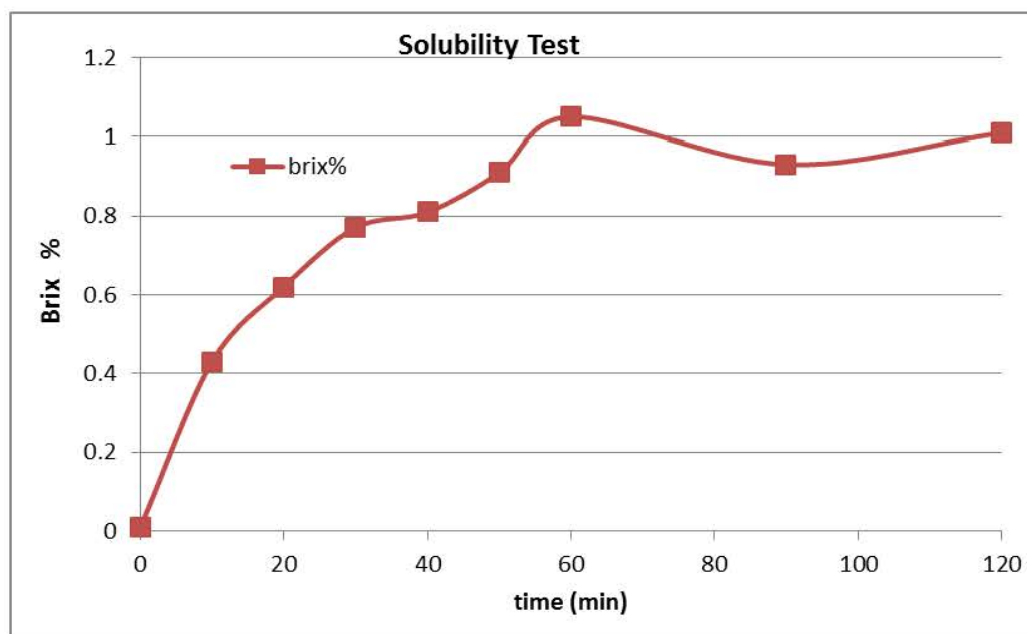
Figure 5.9 Solubility of emulsion films w StA (n=3)

Statistical evaluation of solubility data were done *via* Design Expert Software (with general factorial design and Anova). Pre-defined constant conditions were stirring rate: 300rpm orbital shaker; mfc: 1.5% m/v; dissolution media: pH=7 upw. In order to ignore experimental errors absorbance values of film samples were individually divided by their measured initial weight values. Factors tested in analyses were dissolution temperature (5, 30°C); CMC concentration of film (0, 1 % w/v); Gly concentration of film (0, 0.7, 1 % w/v); Peg400 concentration of film (0, 0.66 % w/v); and wax concentration of film (0, 3 spray); $CaCO_3$ concentration (0, 0.1, 0.15, 0.2, 0.3, 2.5 % w/v); and dissolution time period (0.5, 1, 1.5, 2, 2.5, 15.5 hours). Addition of GLY, cmc, peg400, wax, $CaCO_3$ and their concentration used were found significantly effective on film's solubility (p value < 0.05). Effects of tested dissolution temperatures were not statistically significant. Also there were not any significant differences between time intervals tested for dissolution. Effect of different compounds used with combinations (interaction effect) was found significant in terms of dissolution; i.e. effect of gly concentration with combination of temperature factor (interaction effect of

gly + temperature) was found significant in terms of dissolution. According to results of dissolution test and ANOVA analyses of data, highest $CaCO_3$ concentration, and lowest GLY concentration gave best result. But in terms of elasticity and visual properties of film samples $CaCO_3$ and GLY concentrations were set as 0.2 % w/v and 0.7 % w/v in order to be used in characterization tests. According to the evaluation results of desirability analyses, most preferable film samples were having lowest gly, highest peg400, highest wax and lowest Cmc concentrations. But sample having 0.7% gly, 0.66% peg400, 1% cmc (w/v) and 3 spray wax were selected when other factors like mechanical or gas barrier properties were considered.

5.3.4 Opacity and transmittance properties of films and artichoke by-products

Colour property of film samples produced is important when considering consumer acceptability of packaged final product. Also, colour of artichoke by-products produced throughout extraction steps was also important since they indirectly affect colour of film materials. Results of colour measurements were presented for comparison within each other in Table 5.8.

Table 5.8 Colours of Powdered Samples

Sample name	n	L *	a*	b*	Hue Angle	Chroma
Dewaxed Artichoke Leaf Powder	5	64.18± 0.3428	3.27 ± 0.0541	18.13± 0.1625	1.39± 0.0024	18.43± 0.1654
Artichoke Leaf Powder	5	59.23±0. 4191	2.3±0.16 76	16.79±0. 142	1.43±0.0099	16.95±0.1414
Freeze dried microfibrillated cellulose (deashed)	5	79.89±0. 7458	-1.9 ± 0.0635	10.66±0. 3828	-1.39± 0.0070	10.83±0.3804
Newly synthesized CMC	4	55.85±0. 6363	5.67±0.3 002	20.63±0. 5644	1.3± 0.0095	21.4±0.6054
Na-CMC (from Aldrich)	4	92.28±0. 0668	-1.47± 0.0645	6.29± 0.1711	-1.34±0.0050	6.46±0.1800

By looking to L* values of samples effect of different treatment steps on colour of artichoke by-products could be observed. For example, effect of dewaxing on lightness and greenness of artichoke leaf powders by looking at L*, b* values. Also lightness and yellowness value of MFC samples and how MFC sample's colour is close to white could be observed

from presented data. Also colour index of CMC and NCMC could be compared *via* L*, a*, b*, Hue angle and Chroma and was the colour difference between Na-CMC and CMC synthesized from artichoke leaves (NCMC) significant.

Colour of various dried film samples were observed with CIELAB parameters, both from rough and bright sides of film samples in order to draw a conclusion about transmittance property of film samples. Hue angle values of film samples were calculated, results were presented in Tables E.1, E.2, E.3. Also whiteness index and chromacity values were calculated and presented in Appendix E.

Effect of film composition and film surface on colour properties was studied. Measurement parameters were L*, a*, b*, C* values. Measured data were also analysed statistically with ANOVA. Most desirable film samples were also extracted in terms of colour and opacity properties from the data obtained in ANOVA.

Each of measured L*, a*, b*, C* values for film samples were found significantly different (p value < 0.05). The models that were constituted with ANOVA data of general factorial design developed for each colour parameter of different film materials were evaluated significant due to their F-values. F-values for each colour parameter (L*, a*, b*, C*) were 65.06, 390.37, 298.92, 289.10 in turn. R-Squared values for the models were acceptable at least having value of 0.97.

In desirability evaluation target values have selected for colour attributes of film samples. For L* and C* values highest values set as most desirable and then for a* and b* values "0" value were set as most desirable result in determination of most prefarable film sample. In Tables 5.9 and 5.10, desirability values for film samples (films were grouped into simple and mix according to the number of the components they contain; simple films contain aqueous solution of one or two compounds while mix films could contain aqueous solution or emulsion of many) in terms of colour properties (average of L*, a*, b*, C* parameters) were aligned.

Table 5.9 Desirability list in terms of colour of simple films

Surface	Type	L*	a*	b*	C*	Desirability
br	mfc	52.23	-0.68	8.43	8.14	0.56
br	artlp	66.54	2.08	13.61	13.77	0.56
br	mfc 1%	50.54	-0.47	5.22	5.24	0.55
br	diluted mfc	48.95	-0.10	3.81	3.82	0.54
ro	mfc	45.89	-0.76	6.88	7.34	0.52
ro	diluted mfc	48.99	-0.54	3.87	3.91	0.51
ro	mfc 1%	48.87	-0.47	3.57	3.62	0.51
br	mfc-gly	41.48	1.15	12.11	12.18	0.50
ro	mfc-gly	37.09	0.42	7.83	7.82	0.50
br	cmc-gly sonicated	48.52	-0.30	2.18	2.20	0.47
br	mfc pulp precipitate	37.64	-0.32	4.70	4.72	0.46
br	wax sprayed mfc	60.07	-1.62	10.39	10.52	0.44
ro	diluted mfc + gly	45.42	-0.72	2.39	2.50	0.43
br	diluted mfc + gly	42.73	-0.29	1.65	1.68	0.41
ro	wax sprayed mfc	63.99	-1.77	9.78	9.94	0.40
ro	mfc pulp precipitate	35.50	-0.35	2.88	2.90	0.40
ro	artlp	54.61	3.67	14.83	15.28	0.40
ro	cmc-gly sonicated	44.70	-0.21	1.25	1.27	0.39
br	mfc pulp supernatant	33.46	-0.12	1.67	1.67	0.35
ro	mfc pulp supernatant	29.98	-0.27	1.51	1.54	0.29

Table 5.10 Desirability list in terms of colour of mix films

Surface	Type	L*	a*	b*	C*	Desirability
br	mfc-cmc-sta-gly-wax	44.35	-0.02	3.68	3.68	0.52
br	mfc-cmc-sta-gly-wax	44.68	0.10	3.54	3.54	0.51
br	mfc2-cmc-sta-gly-tw80 (diluted)	38.53	-0.27	6.64	6.38	0.49
br	mfc-cmc-peg400-5% wax	42.71	0.02	3.125	3.13	0.49
ro	mfc-cmc-peg400-5% wax	42.14	-0.03	3.18	3.18	0.48
ro	mfc2-cmc-sta-gly-tw80	36.03	0.01	12.27	12.32	0.48
br	mfc-cmc-gly-peg400-wax –(40ml)	44.55	-1.09	6.40	6.21	0.46
br	mfc-cmc-peg400-1% wax	43.45	-0.03	2.09	2.09	0.45
br	diluted mfc-cmc-chi-gly-peg400	41.07	-0.65	3.83	3.57	0.44
br	mfc-cmc-sta-gly-tw80 -(40 ml)	41.63	-0.94	3.88	4.26	0.44
br	diluted mfc-cmc-chi-gly-peg400-wax	40.28	-0.76	4.32	4.04	0.44
br	mfc-cmc-chi-gly-peg400	43.47	-1.36	8.11	8.76	0.44
br	mfc-cmc-sta-gly-tw80 -(30 ml)	41.24	-1.00	4.94	4.74	0.43
br	mfc-cmc-peg400	49.27	-0.09	1.39	1.39	0.43
br	mfc-cmc-peg400-4% wax	42.25	-0.39	2.22	2.26	0.43
ro	mfc-cmc-peg400-4% wax	41.88	-0.38	2.27	2.30	0.43
br	mfc-cmc-peg400-2% wax	41.76	-0.37	2.26	2.29	0.43
ro	mfc-cmc-peg400-3% wax	41.72	-0.60	2.47	2.54	0.42
ro	mfc-cmc-sta-gly-wax	41.67	0.01	1.75	1.75	0.42
ro	mfc2-cmc-sta-gly-tw80 (diluted)	34.00	-0.33	4.12	4.30	0.42
ro	mfc-cmc-sta-gly-wax	40.69	0.06	1.81	1.81	0.42
br	mfc-cmc-gly-peg400-wax -(30 ml)	43.54	-1.28	5.38	5.02	0.42
br	mfc-cmc-sta-gly-tw80 (diluted)	41.37	-0.49	2.45	2.27	0.42
br	mfc-cmc-peg400-3% wax	41.74	-0.52	2.04	2.11	0.41
ro	mfc-cmc-peg400-2% wax	39.84	-0.28	1.88	1.90	0.40
ro	mfc-cmc-sta-gly-tw80 -(30 ml)	35.71	-0.75	3.22	3.64	0.40
ro	mfc-cmc-peg400-1% wax	39.17	0.03	1.52	1.52	0.39
ro	mfc-cmc-gly-peg400-wax -(30 ml)	39.68	-1.36	4.76	5.12	0.39
ro	mfc-cmc-sta-gly-tw80 (40 ml)	37.51	-1.09	2.85	3.67	0.39
ro	mfc-cmc-gly-peg400-wax -(40 ml)	38.16	-1.17	4.45	3.88	0.38
br	diluted mfc-cmc-gly-peg400-wax	35.98	-0.39	1.62	1.57	0.35
ro	mfc-cmc-chi-gly-peg400	37.20	-1.53	5.32	5.37	0.34
ro	mfc-cmc-sta-gly-tw80 (diluted)	36.33	-0.18	1.14	1.16	0.34
br	mfc2-cmc-sta-gly-tw80	41.64	0.72	16.68	16.72	0.33
ro	diluted mfc-cmc-chi-gly-peg400-wax	31.38	-0.18	1.09	1.27	0.30
ro	mfc-cmc-peg400	42.54	0.17	0.46	0.49	0.29
ro	diluted mfc-cmc-chi-gly-peg400	32.11	-0.24	1.01	0.98	0.28
ro	diluted mfc-cmc-gly-peg400-wax	32.24	0.02	0.29	0.32	0.20
br	cmc-gly-tw80-sta	33.62	0.27	-0.20	0.27	0.15
ro	cmc-gly-tw80-sta	32.69	-0.10	-0.29	0.44	0.15

5.3.5 Size distribution and morphology

In order to evaluate the size distribution profile roughly, samples were directly taken to the PCM and tried to have images proving existence of micro fibrils at different focusing lenses and magnifications. There were clear and detectable fibril like structures in most of the samples, but for a quantitative evaluation about dimensions of fibrils, dilutions were needed prior to imaging. In Figures 5.10, 5.11, 5.12 interior structure of cellulose pulps treated with supermasscolloider are presented.

Pulp, supernatant of pulp and precipitate of pulp phases of MFC fibers' dimension data was presented in Table 5.11. Smallest dimension data were observed in supernatant phase (which was fully soluble in water) of MFC pulp obtained.

There were detailed findings about size distributions of cellulose microfibers obtained from supermasscolloider treatment in Tables 5.11 and 5.12. That's why in this study only 3 different phases of MFC fibers' dimension data was presented. Precipitation was applied during thawing of freezed MFC and 3 parts obtained from this application; one part taken without precipitation operation (pulp), one part-supernatant of the MFC and the other-precipitate of mfc pulp. Their dimensions were presented in Table 5.11, while their pictures taken by PCM were presented in Figures 5.10, 5.11, 5.12. Dimension calculations were done with the help of DPW2 software of PCM.

Table 5.11 Average dimensions of cellulose microfiber pulps (μm)

Sample name	Width (μm)	n	Height (μm)	n
Mfc pulp supernatant	4.85 ±2.7301	126	65.26 ±63.1974	113
Mfc pulp precipitate	19.3 ±11.7602	339	165.08 ±115.7324	225
Mfc pulp	15.57 ±6.5182	72	146.86 ±87.9269	60

In Figures 5.10, 5.11, 5.12 interior structures of MFC samples were shown at different magnification ratios. Size calculations for microfibrils within solution were applied at 40x magnification. Colour of MFC solutions are generally creamy bright yellow, due to different magnification ratios the colour of filter used change background image of the sample, that's why colour of different samples varies.

CL-10x	CL3-10x	CL3-D-10x

CL1-4D-10x	CL1-4D-4x	CL1-40x

CL2-10x	CL2-4TD-10x	CL2-4D-40x
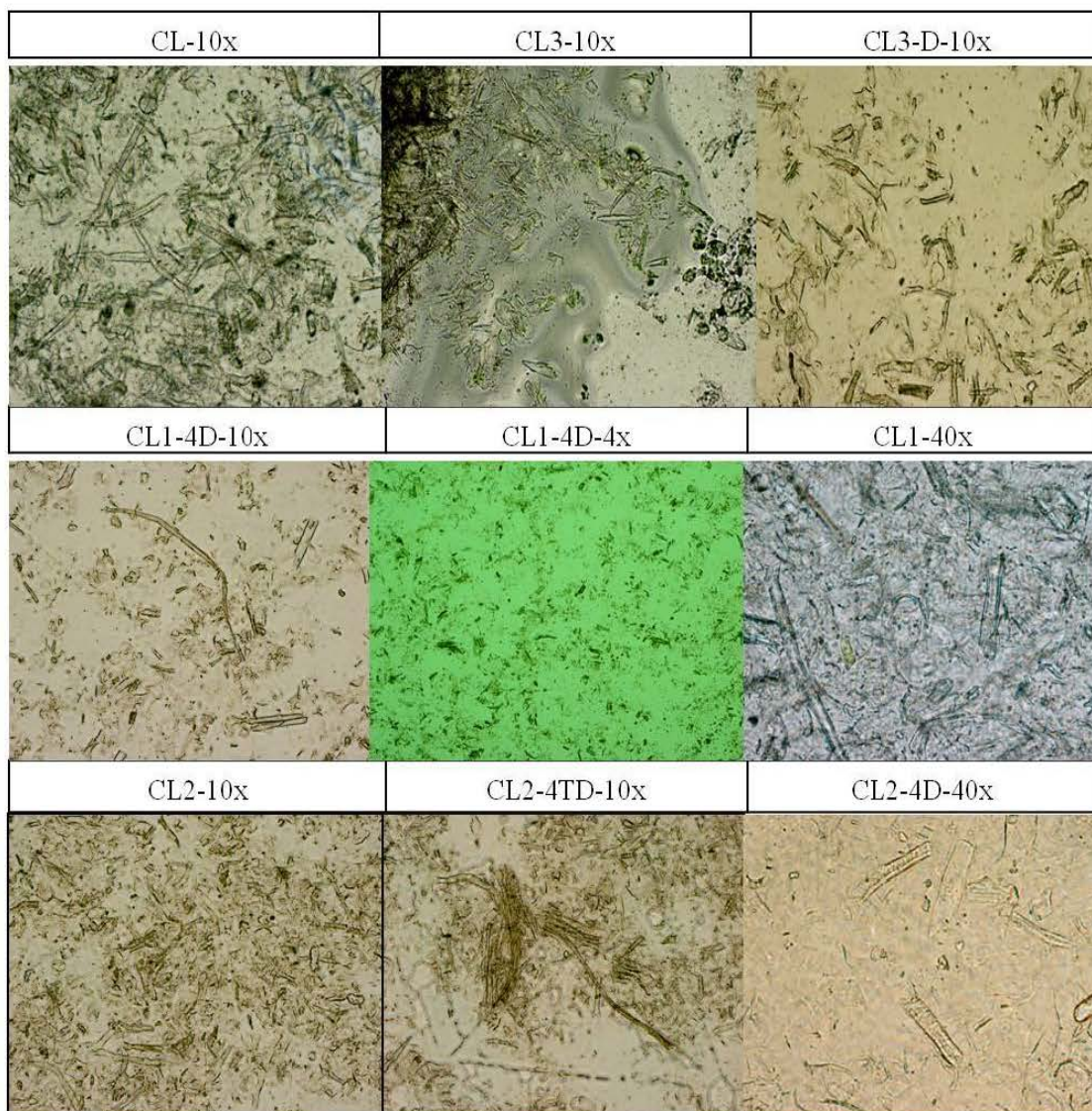
Figure 5.10 PCM images for microfibrillated cellulose samples for 4x, 10x, 40x magnifications[2]

Also interior morphology of ALP-15 and MCLP-3 samples were tried to be investigated by PCM, too. Fibril like structures were observed in ALP-15, but fibrils in MCLP-3 sample could not be clearly detected by PCM even at 40x or 100x magnifications.

---

[2] CL, CL3: cellulose microfibril pulp;CL2: deashed cellulose microfibril pulp;4D, 4TD:4 times diluted

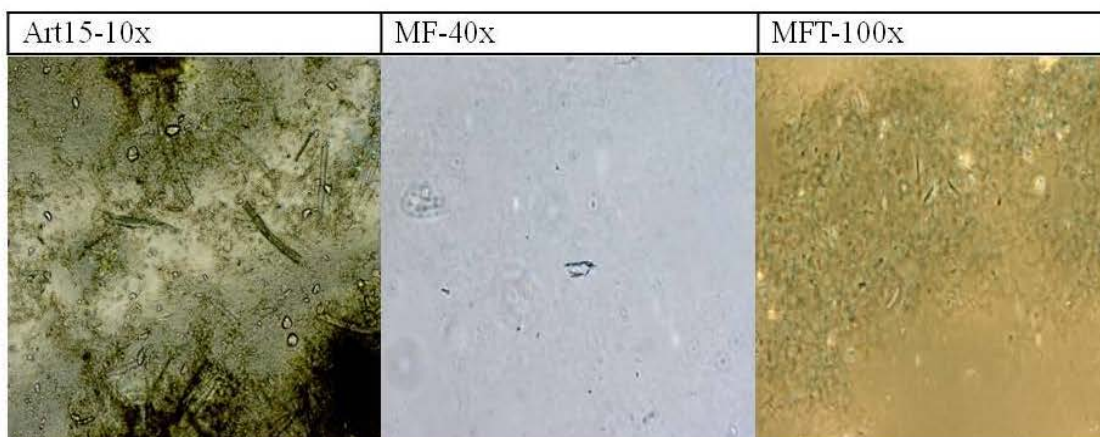| Art15-10x	MF-40x	MFT-100x

Figure 5.11 PCM images of 10x magnified artichoke leaf microfibril, 40x and 100x magnified microfluidized cellulose microfibril solution from left to right

4 T.D. microfibrillated cellulose pulp 20X magnified	4 T.D. microfibrillated cellulose pulp precipitate 10X magnified
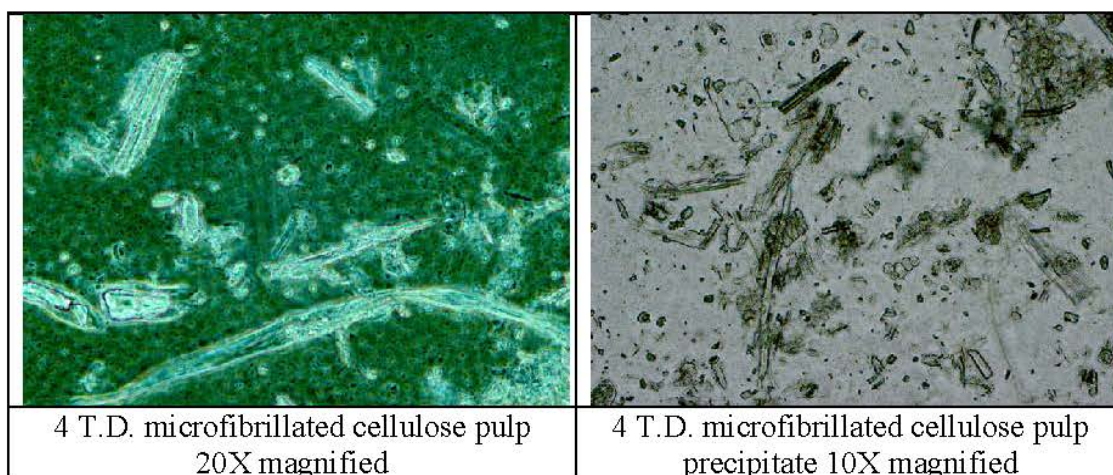
Figure 5.12 Microscopic images of cellulose microfibers

In order to evaluate infrastructure of samples before any dehydration treatment applications, Zeta sizer instrument was tried to be used. Trials with Zeta sizer did not give accurate information in the case of most of the samples, but the data of MCLP-3 sample was shared since there was not a better indicator in terms of liquid/not treated form of MCLP-3, results presented in Figure 5.13.
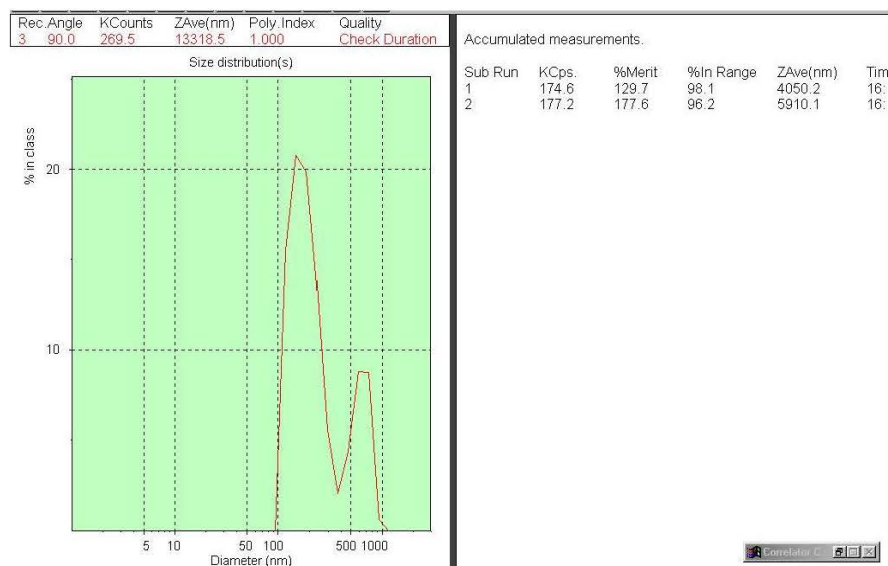
Figure 5.13 Size Determination of microfluidized cellulose microfibril with Zeta-sizer

Films produced were characterized in different means and properties. In Figure 5.14 10X and 20X magnified images of mfc film was presented, that were taken by PCM. There were pictures taken by optic microscope, too. Since films were semitransparent, data was too bright to be able to present.

| Microfibrillated cellulose 10x magnified | Microfibrillated cellulose 20x magnified |
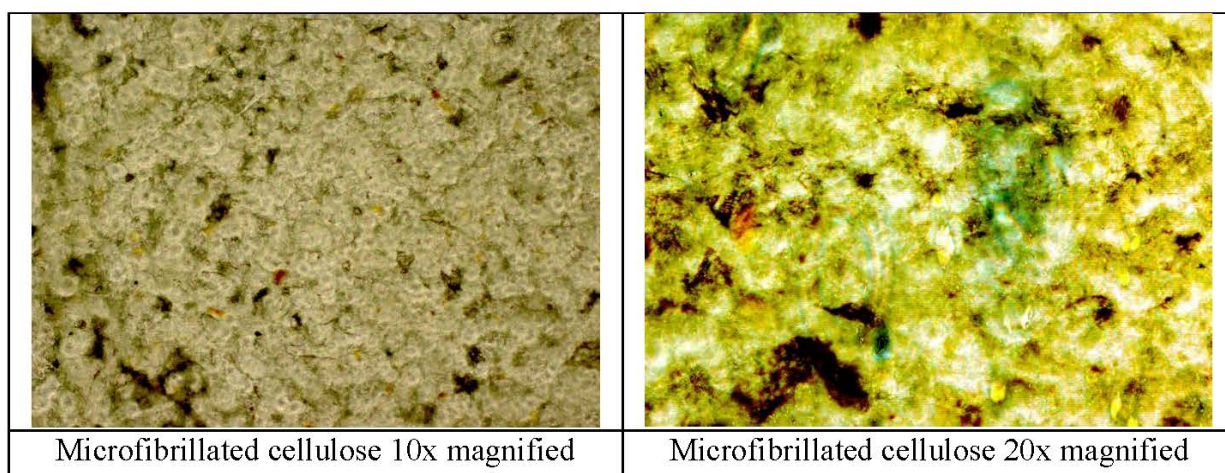
Figure 5.14 Microscopic images of dry micro fibrillated cellulose films

Table 5.12 Size distribution of emulsion droplets of films (average values)

Code	avg ± stddev (µm)	n	Code	avg ± stddev (µm)	n
Mfc pulp supernatant film	2.68 ±0.93	81	MFC film	59.76 ± 28.87	29
Mfc pulp supernatant film	1.67 ± 0.75	14	MFC film	55.33 ± 26.07	51
Mfc pulp precipitate film	7.27 ±5.77	45	Emulsion mfc film	4.03 ± 3.92	38
MFC film	4.5 ± 1.82	78	Cmc-gly-sonicated-10 times diluted	2.5 ± 0.97	14

Again PCM images were taken from film solutions in order to be able to detect and quantitate emulsion formation in film solutions. In some of the films solution micro sized emulsion droplet were observed. Droplet size measurement was done with DP2BSW software and results for some of the films were presented in Table 5.12. Results presented in Table 5.12 give information about dimension of cellulose microfibrils in film solution (after mixed with other film additives and treated with related methods i.e. sonication) different from Table 5.11.

PCM images of film solutions at different magnification ratios and with different light filters (causing colour variations in images) were presented in Figure 5.15 below.

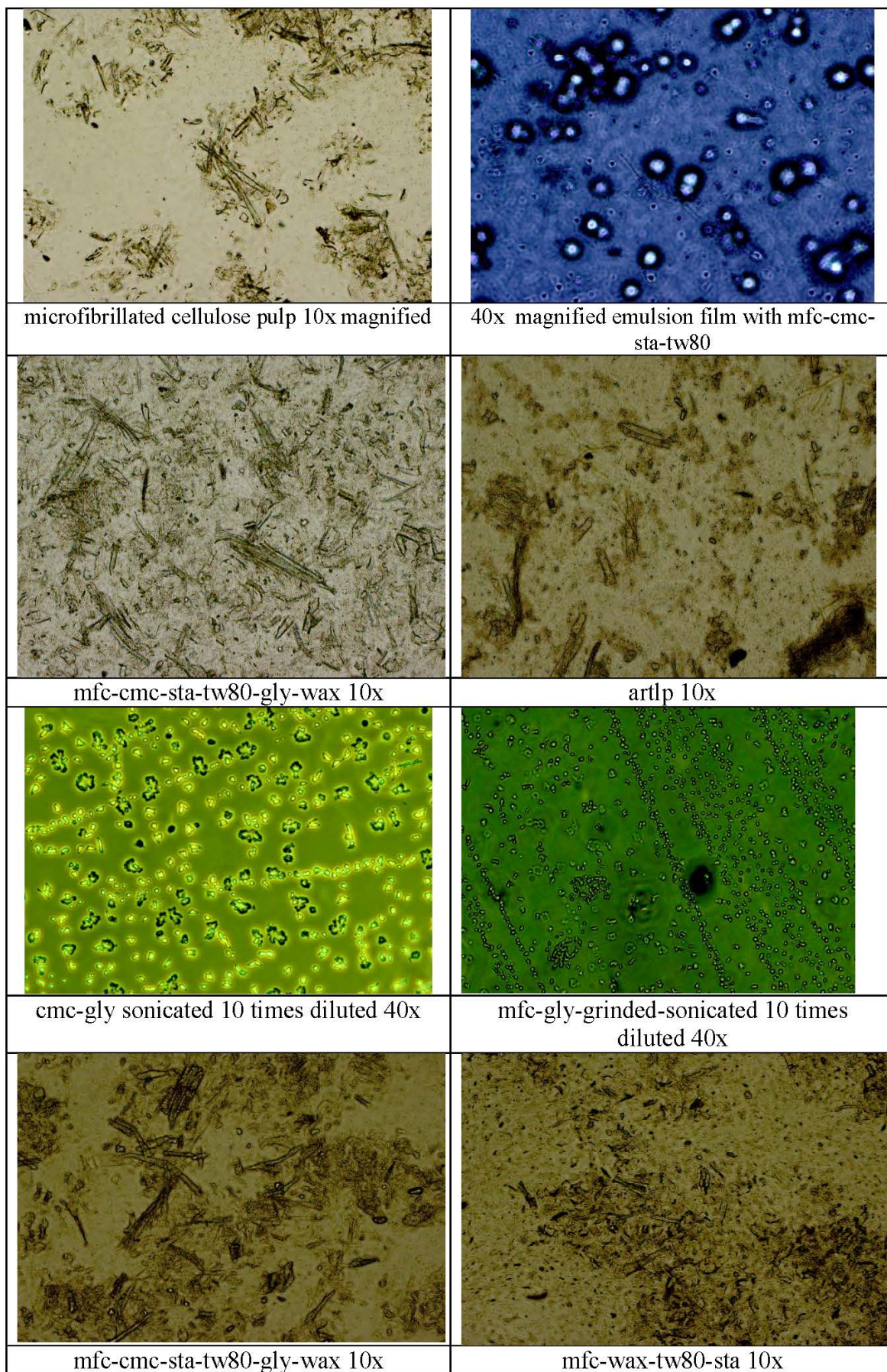|	
microfibrillated cellulose pulp 10x magnified	40x magnified emulsion film with mfc-cmc-sta-tw80
mfc-cmc-sta-tw80-gly-wax 10x	artlp 10x
cmc-gly sonicated 10 times diluted 40x	mfc-gly-grinded-sonicated 10 times diluted 40x
mfc-cmc-sta-tw80-gly-wax 10x	mfc-wax-tw80-sta 10x

Figure 5.15 Microscopic images of film solutions at 4X, 10X, 40X magnifications

Morphology of extracted cellulose fiber was investigated in advance with SEM at 100x and 1000x magnifications, (Figure 5.16). Electron microscope images were especially taken in order to observe effect of supermasscolloider/homogenizer treatments on fiber's morphology clearly. Both of the information from previous sources or previous film formation trials in this study, no successive result was present showing film forming ability of cellulose in DW or ETOH. By fine grinding operations, it was tried to modify suspended structure of cellulose in DW into a promising hydro gel/ homogenous pulp form. Film trials conducted under controlled conditions and vacuum packaging applications with fresh cut vegetables could give clearer and more precise evaluation for a successful fibrillation application.

In SEM images of cellulose fibers, no micro fibril like structure was observed neither 100x nor 1000x magnifications as can be seen in Figure 5.16.
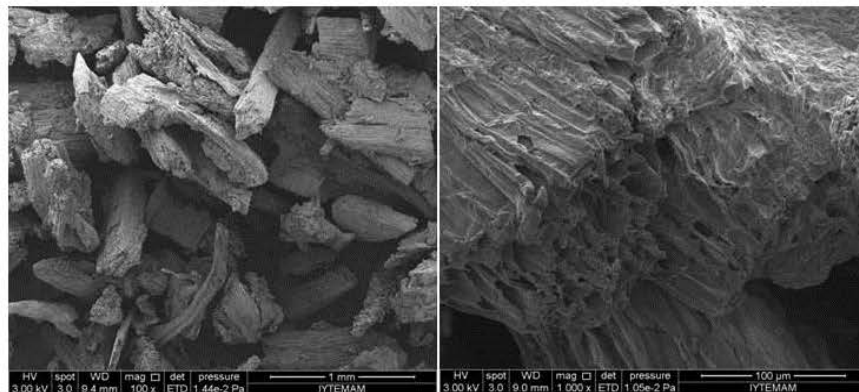

Figure 5.16 SEM image of cellulose fiber, 100x and 1000x respectively.

For determination of nano dimensioned fibrils, samples were tested with SEM and AFM instruments. Since these instruments do not let to examine the liquid samples, different dehydration methods were tried in sequence (Table 4.3) in order to get more precise data considering size and morphology.

Initially, samples were dehydrated simply in an incubator and taken for analyses. But results showed that, oven drying was not an ideal technique, since slow evaporation during dehydration process could let a significant agglomeration of micro fibrils. Thus, freeze drying technique was also applied. From the SEM images of lyophilized samples, it could be possible to observe micro fibrils in some parts of samples and their dimensions could be fortunately calculated (Table 5.13).

In Figure 5.17 morphology of spraydried and freezedried microfibrillated cellulose samples were presented to be compared.
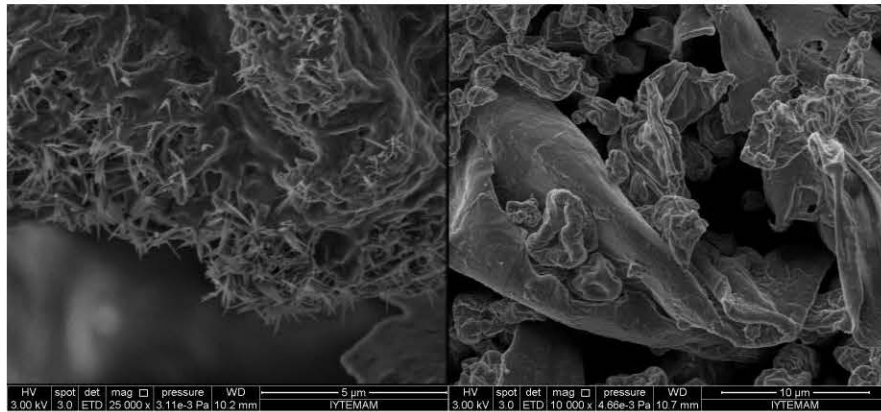
Figure 5.17 SEM images of dry cellulose micro fibrils: freeze dried (left) 25000x magnified and spray dried (right) 10000x magnified

Predicted homogenous fibrillated structure could not be observed since then. Therefore spray drying technique was also carried out as an alternative method. Samples prepared with different methods were illustrated in Table 4.3 and also equipment used was shown in Chapter 4 and Figure 4.4. In Figures 5.18 and 5.19 below, SEM images of cellulose microfibrils were shown. Fibrils could be detected from their thin, long, rodlike structure from magnifications applied at 500 x, 1000x, 2500x, 5000x, 10.000x, 25.000x, 50.000x magnifications.
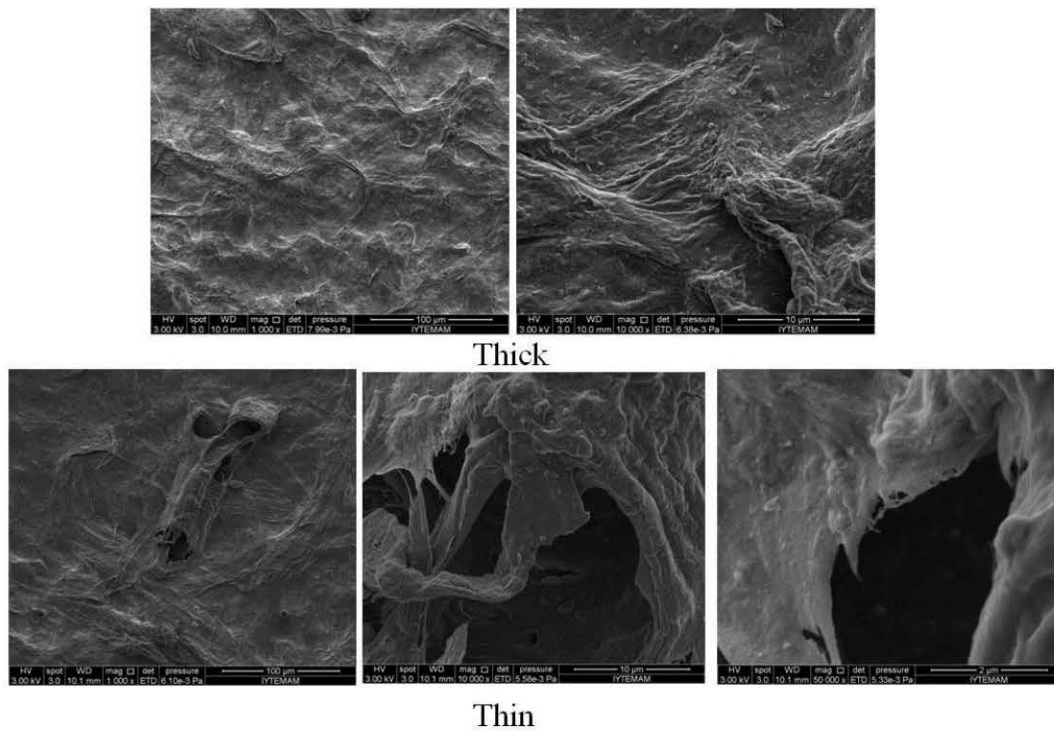

Thick

Thin

Figure 5.18 SEM images of dry cellulose micro fibrils
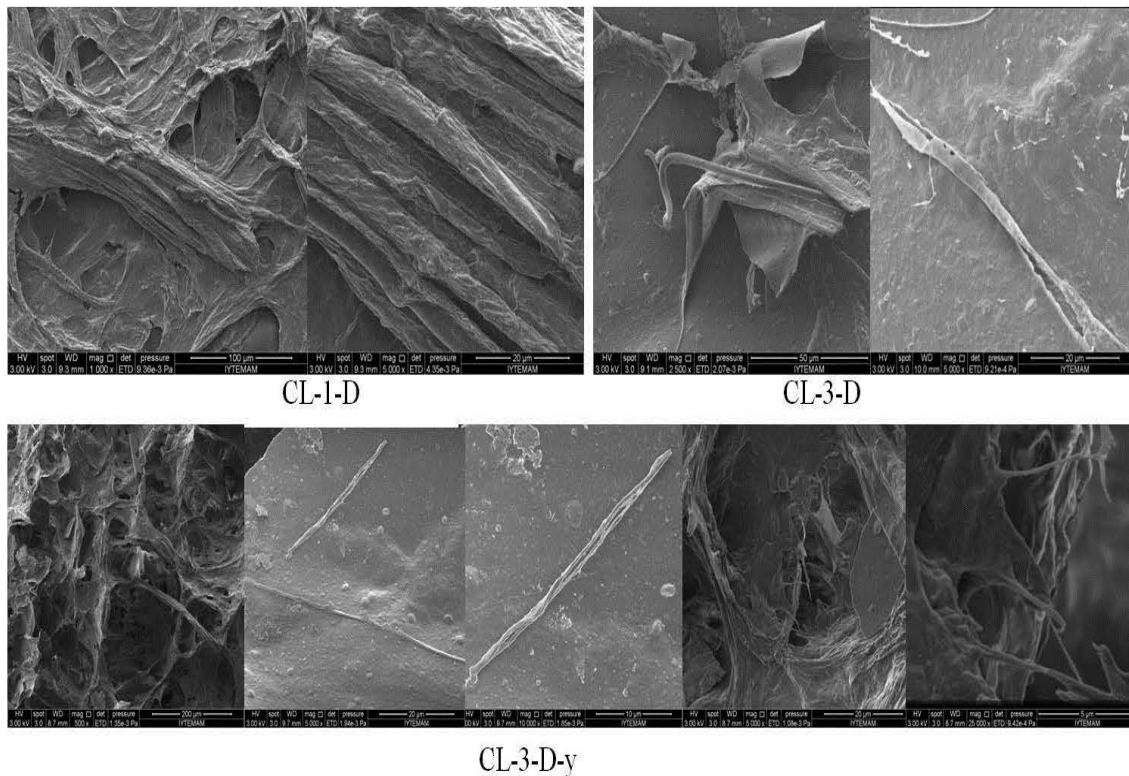
CL-1-D   CL-3-D

CL-3-D-y

Figure 5.19 SEM images of of 3 times diluted microfibrillated cellulose samples, sample in 2nd lyophilized

Dimensions of cellulose micro fibrils were measured with DP2-BSW software. Results do not present 100% accurate dimensions and do not present total distribution profile of fibril dimensions. Calculations could be done online, since measurements were taken manually by operator from the monitor screen attached to the microscope.

Also, dimension of micro fibrils were calculated rather sensitive *via* software of SEM again while images were taken, but there might be operational mistakes in this method, too. Table 5.13 shows the statistical evaluation of measured fibril dimensions. AVG values were calculated for two different dimensions separately, but there were still very high variations even within different parts of the samples.

In Table 5.13 'min' and 'max' value terms were the measured minimum fiber length and the measured maximum fiber length, respectively by PCM. Only for one dimension expressed as width (W, μm) or length (L, μm). 'AVG' values give average of measured fiber lengths/widths separately, while 'STDDEV' values give measured maximum difference from AVG value for that sample.

Table 5.13 Size distributions of micro fibrils; calculated with the results of PCM & SEM[3]

	MF		MFT 2		ART 15		CL1	
	L (μm)	W(μm)	L (μm)	W (μm)	L (μm)	W (μm)	L (μm)	W (μm)
AVG	14.09	6.16	5.14	1.04	137.46	13.35	297.69	21.63
STDDEV	7.43	3.45	1.89	0.47	61.42	4.71	133.51	8.14
max	21.52	9.98	8.78	1.78	208.11	21.59	546.66	45.19
min	6.66	1.11	2.77	0.53	48.48	7.67	100.34	7.56

	CL 3		CL3 D		CL1		CL1 2TD	
	L (μm)	W (μm)	L (μm)	W (μm)	L (μm)	W (μm)	L (μm)	W (μm)
AVG	121.15	13.31	135.24	18.35	93.51	12.23	82.90	11.90
STDDEV	51.57	5.09	66.67	6.67	56.14	2.01	31.24	2.13
max	191.39	22.13	305.43	35.88	206.13	15.49	131.47	15.25
min	59.45	3.78	51.18	9.73	29.25	8.87	46.24	8.24

	CL1 4TD		CL2		CL2 2TD		CL2 4TD	
	L (μm)	W (μm)	L (μm)	W (μm)	L (μm)	W (μm)	L (μm)	W (μm)
AVG	100.60	12.09	75.70	13.82	110.25	13.35	179.74	14.40
STDDEV	129.41	5.24	34.33	3.54	65.05	4.45	166.67	4.08
max	781.66	26.44	121.53	19.92	297.69	21.49	635.32	23.77
min	30.47	5.84	33.86	8.93	33.29	4.83	33.71	6.15

	CL3D-y-SEM	
	L (μm)	W (μm)
AVG	3.96	0.60
STDDEV	0.74	0.75
max	4.68	2.26
min	2.94	0.16

Figure 5.20 shows the Stereo Zoom images of the films. Front sides of films were observed as rough and uniform, while back sides of films (in contact with the Petri dish) were smooth, clear and bright.
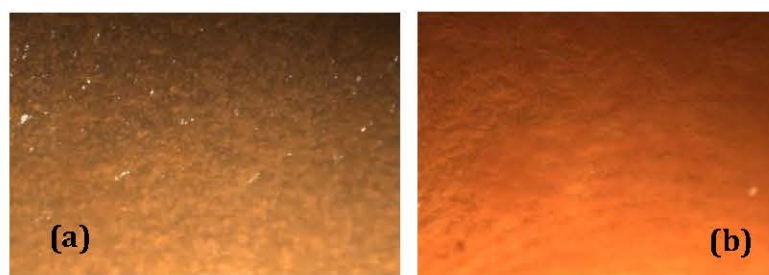

Figure 5.20 Stereo Zoom Microscope Images front side (a); and reverse side of film (b)

---

[3] MF: microfluidized microfibrillated cellulose; ART: artichoke leaf micropowder; CL,CL1,CL3: microfibrillated cellulose; CL2:deashed microfibrillated cellulose; D:1 times diluted; 2TD: 2 times diluted; 4TD:4 times diluted; CL3D-y-SEM: image taken by SEM 3 times diluted cellulose microfiber

As seen from the SEM images presented in Figures 5.21, 5.22, 5.23, in general films had uniform, homogeneous and smooth structure. But in some parts of films, formation of crystal substructure was observed; results of XRD analyses support this case, too, that is shown in Figure 5.33.
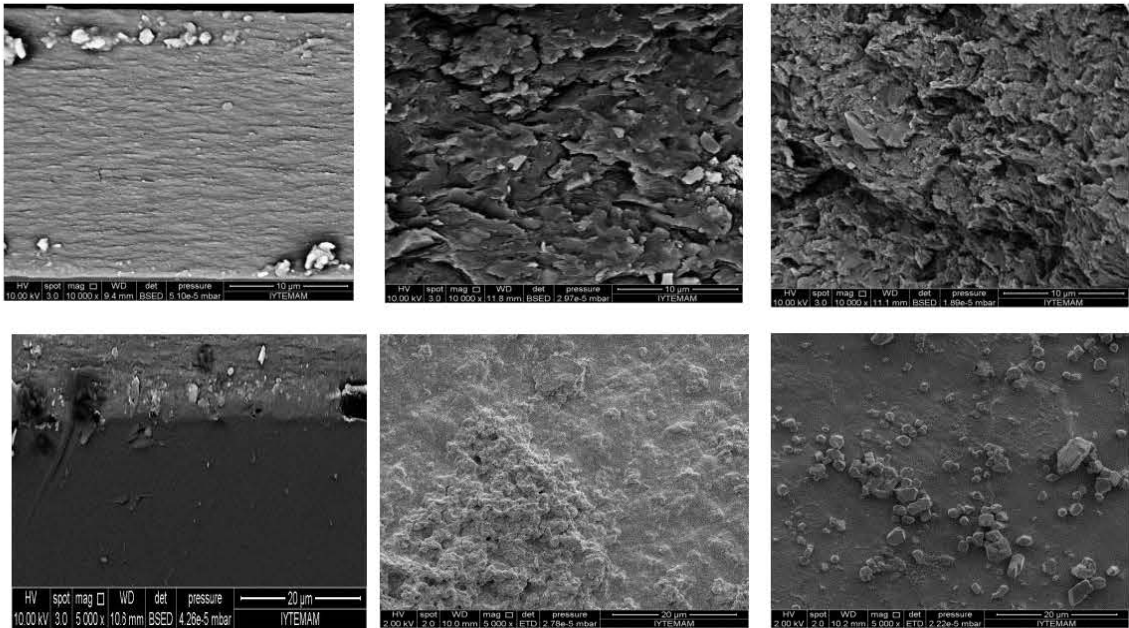

Figure 5.21 Surface and cross section images of MFC films with SEM imaging

In Figures 5.22 and 5.23 surface (at 1000x magnification) and cross section area (at 250x magnification) images of selected film samples were shown. In Figure 5.22 samples shown were mfc-cmc-sta-gly-tw80-wax, mfc-cmc-gly-chi-peg400, and mfc-cmc-gly-peg400-wax in Figure 5.23 samples shown were mfc-ncmc-gly-peg400-wax, mfc2-cmc-sta-gly-tw80-wax, mfc-cmc-gly-peg400-wax, mfc-cmc-gly-chi-peg400-wax (from top row to bottom). The first columns cross section images and in second column surface images were presented.

In cross section images of film samples dense and uniform structure were observed. And in surface of film samples any hole was not observed, but surfaces of films were wavy (not absolutely smooth).
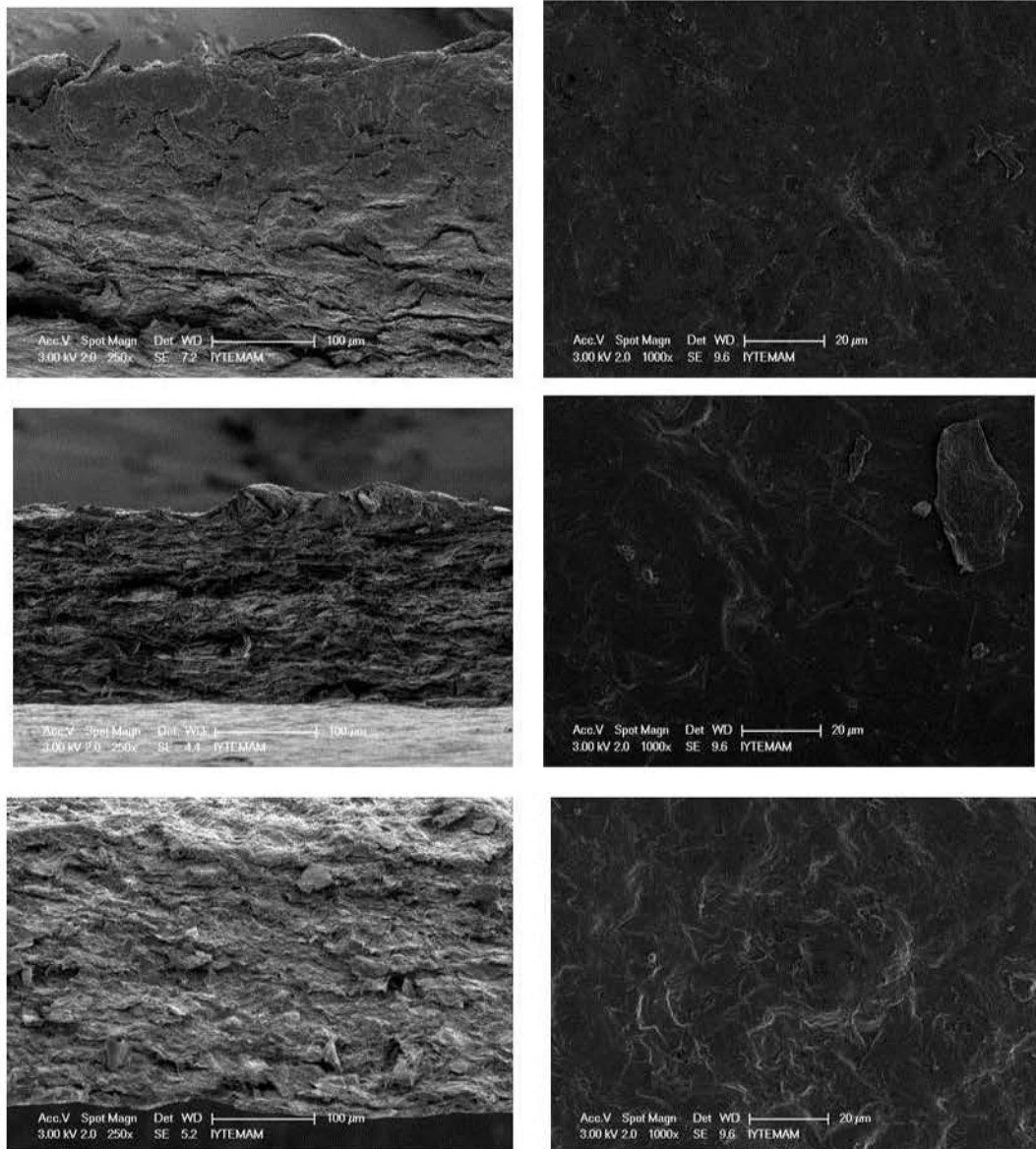
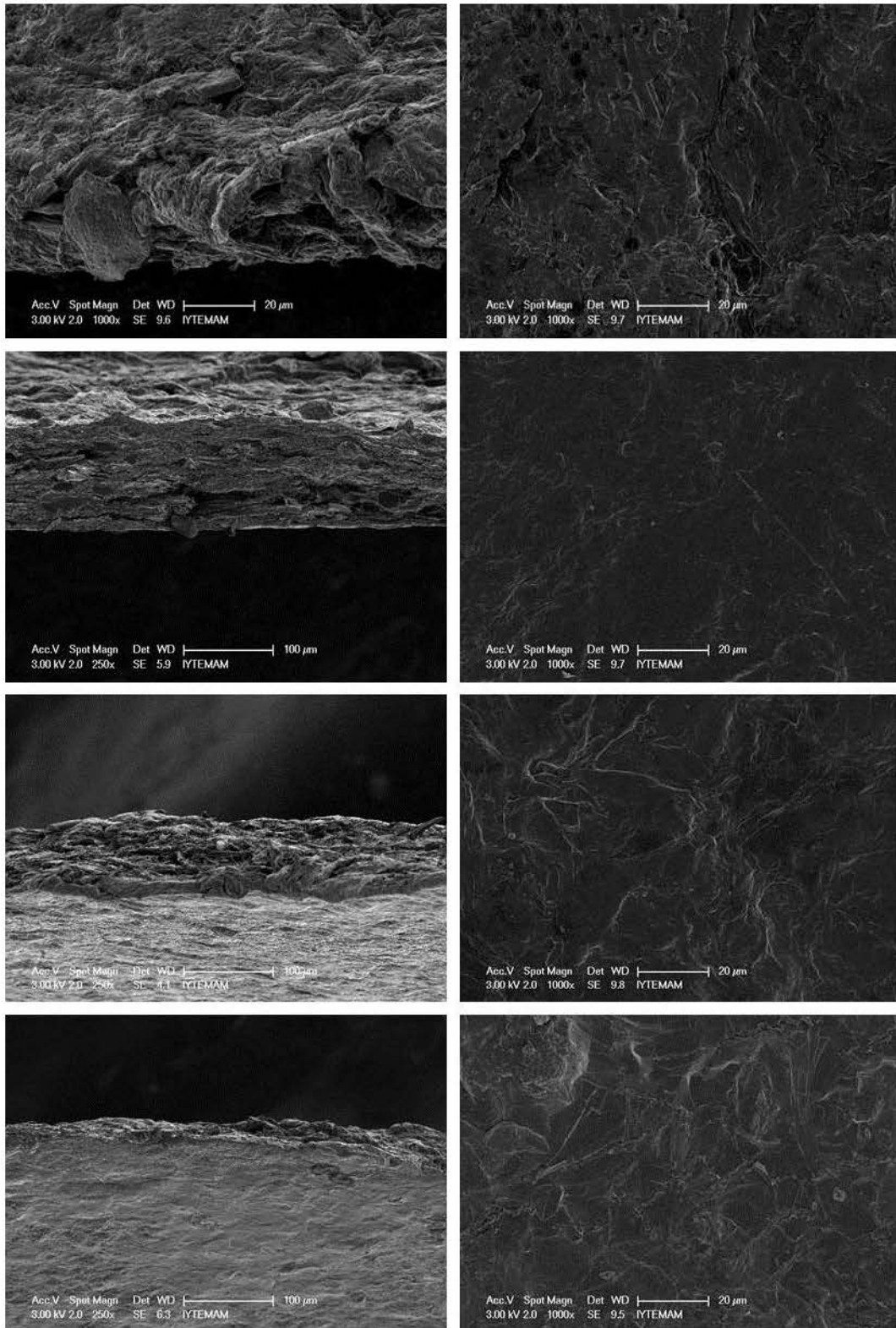Figure 5.22 Surface and cross section images of MFC films with SEM imaging

Figure 5.23 Surface and cross section images of MFC films with SEM imaging

In each of AFM images, shown in Figures 5.24 and 5.25; 1st column gave information about the height distribution within the sample surface (taken from $25\mu m^2$ surface area); 2nd column gave data about distribution of different phases and 3rd column give information about amplitude data of sample.

First column of AFM images give idea about surface smoothness of film samples by presenting average height differences from baseline of that surface. In Figure 5.24 average height of wavy structure on film surface was calculated as 500nm for both 2 times diluted/not diluted MFT films. In Figure 5.25 average height of wavy structure on film surface was calculated as 200 nm for both not diluted/2 times diluted/3 times diluted MFT films.

Samples look homogenous according to phase images and the amplitude signals did not enough to give a quantitative idea about the shapes of the samples. But in comparison, shapes of each sample look similar from their amplitude images.
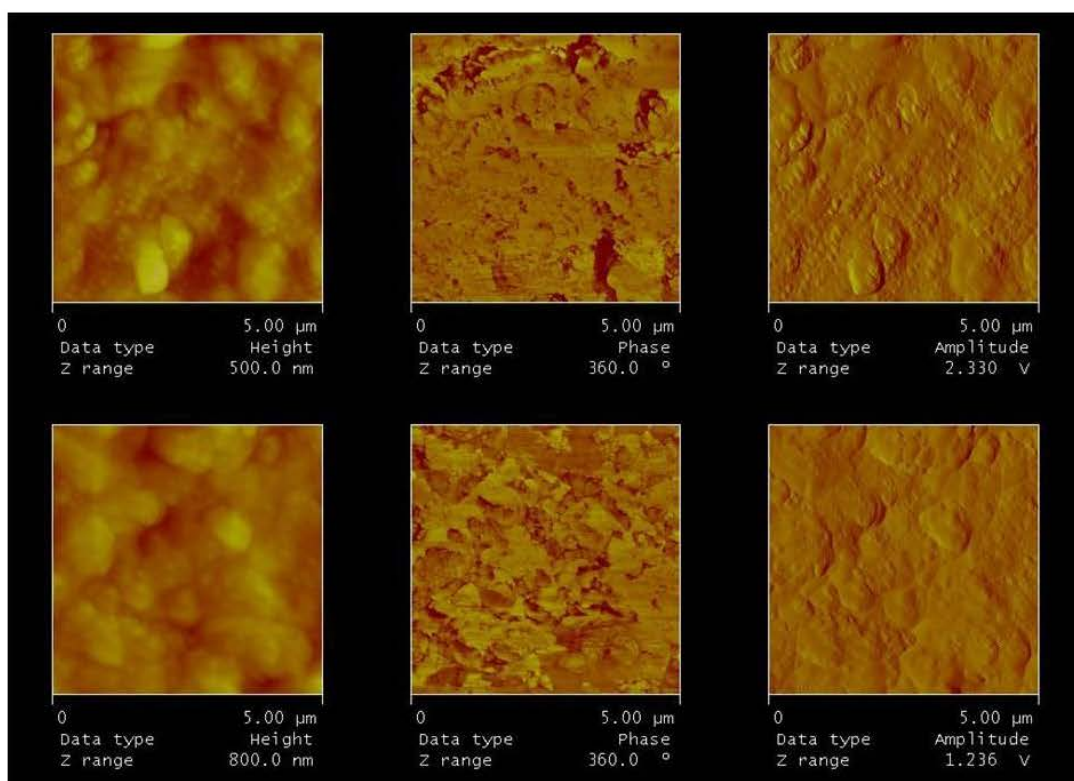

Figure 5.24 AFM images of 2 times diluted (1st row/above) and not diluted microfluidized cellulose microfibril films
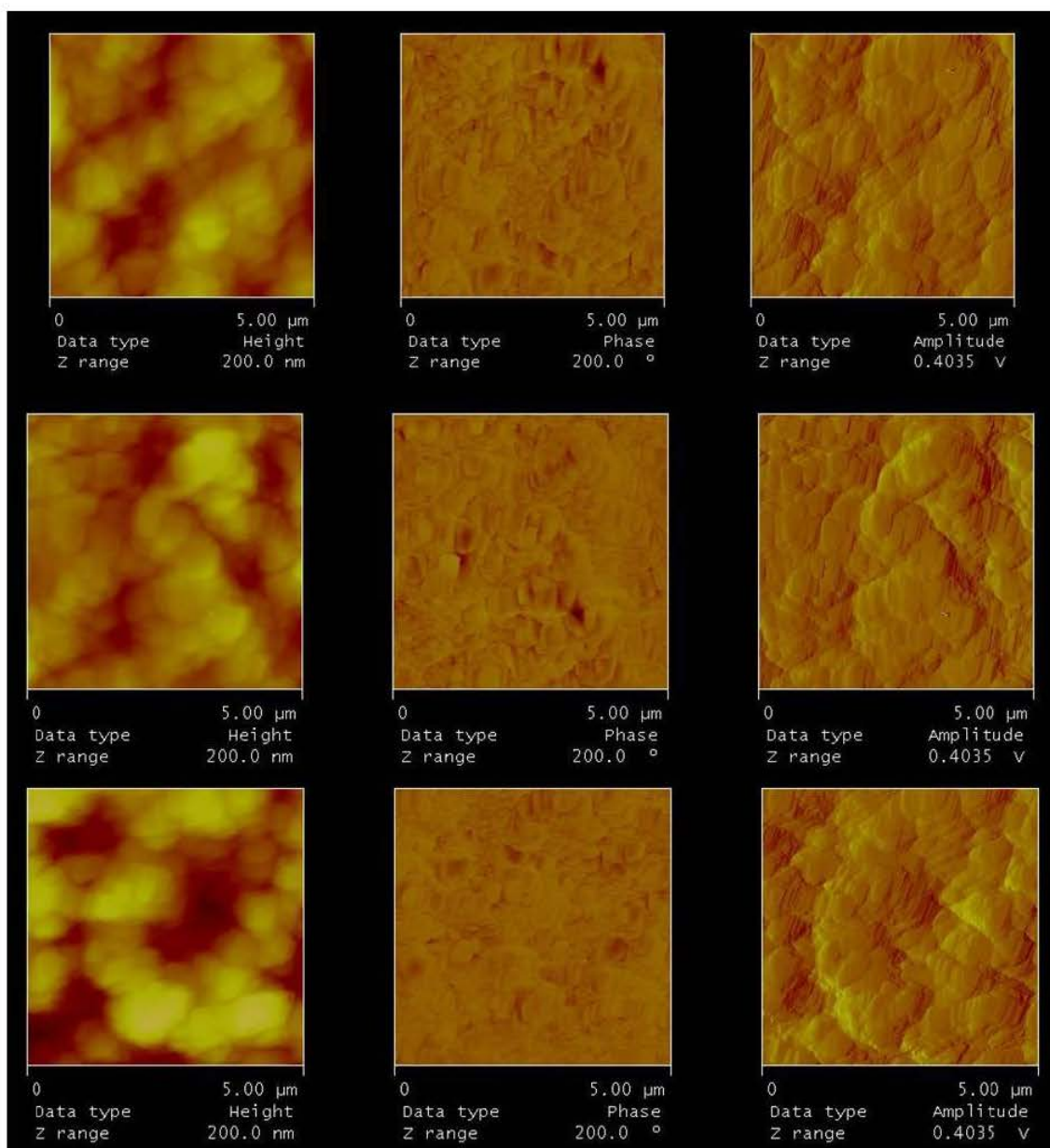
Figure 5.25 AFM images of cellulose microfibril (1st row/above), 2 and 3 times diluted in 2nd and 3rd rows

5.3.6 Determination of bond structure

Alkaline treated artichoke leaves were dehydrated and obtained CF structure was tested in FTIR by comparing spectra of CF with cellulose standard (micro granular, Sigma C-6413). Results prove similarity of extracted cellulose fibers with cellulose standard, structural similarities/differences was discussed in this section; FTIR diagrams of powdered samples were given in Figure 5.26 and 5.28. Results were evaluated with PCA-X model; differences could be detected from Figures 5.27 and 5.29 for score plot

from PCA. Effect of deashing step on purity of cellulose was found to be positive, but there was not any evidence about its significance and also its necessity for the final product evaluation in this thesis which should be considered in detail.

FTIR spectra of samples could be examined; similarity ratios of each different compound could be easily observed in Figure 5.26; Cellulose fiber (a), Artichoke leaf (b), synthesized CMC (c), freeze dried + synthesized CMC (d), freeze dried + synthesized CMC 2ndary batch (e), New CMC Un Dissolved (NCU2) (f), New CMC Un dissolved (NCU2) 2ndary batch (g).
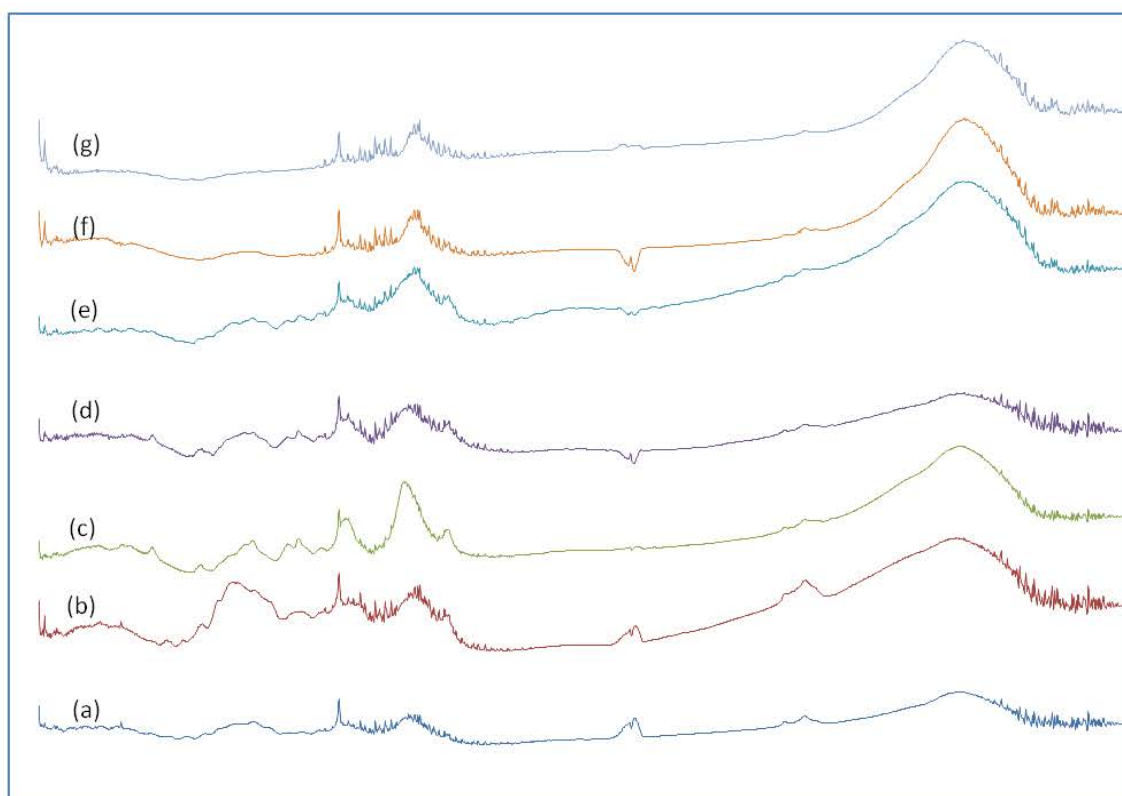
Figure 5.26 FTIR Spectra of Cellulose and Cellulose Derivatives.

Degree of substitution of a polymer is the (average) number of substituent groups attached per base/monomeric unit, and mainly used in cellulose chemistry (Kroschwitz 2004). DS shows yield effectiveness of synthesis reaction from cellulose fibre to NCMC. Degree of substitution values (DS) for synthesized CMC samples and related fractions were calculated from the FTIR data with the help of formula stated in Eq. 3.1 below. Results of calculations were presented in Table 5.14.

$$DS_{Rel} = A_{1606} / A_{2927} \qquad DS_{Abs} = 0.4523 * DS_{Rel} \qquad (3.1)$$

Table 5.14 Degree of substitution values for synthesized CMC samples and related fractions

| Sample	CL2	LF2	NC2	NCF1	NCF2	NCU2	NCUU1
content	Cellulose fiber	artichoke leaf	synthesized CMC	freeze dried + synthesized CMC	freeze dried + synthesized CMC 2nd batch	New CMC Un Dissolved	New CMC Un dissolved 2ndary batch
DS abs	0.4510	0.4156	**0.5574**	**0.4891**	**0.4375**	0.4538	0.4187
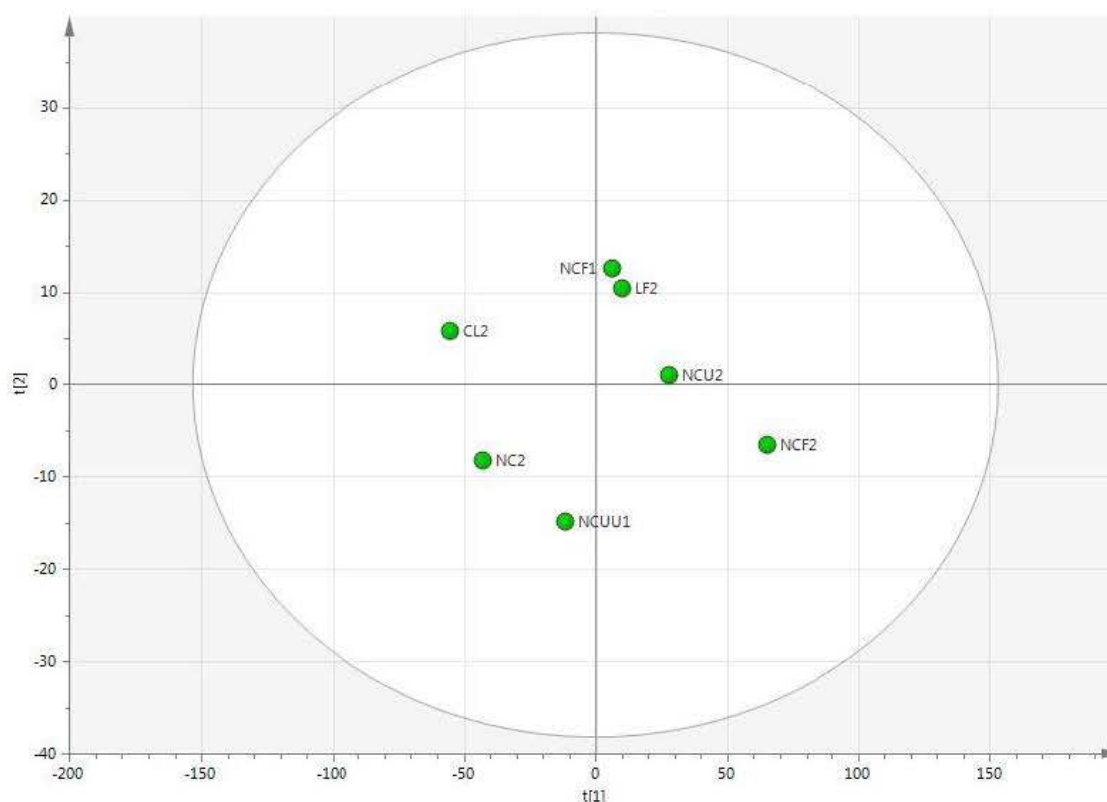
Figure 5.27 Score plot from PCA for FTIR data for cellulose derivatives

Result data of PCA were clustered in order to differentiate cellulose derivative products clearly and visibly. Differentiation was meanigful, i.e. NCF2 sample was definetely different from all samples tested in overall. While samples CL2 and NC2 show similar bond structure. LF2 and NF2 show similar chemical structure showing ineffective synthesis/extraction process.

In Figure 5.28, starting from the 2nd line in the spectra, the effect of purification/separation steps on characteristic peaks of cellulose; 6th line (CPF, most purified one, final product) gave most similar spectrum with CLS (3rd line).

Figure 5.28 Comparison of FTIR spectra of GDL, ARTLP, CLS, CF, DCF, and CPF
(Starting from below line to the above)[4]

Additionally, results evaluated with PCA and differences among samples could be observed from score plots in Figures 5.27 and 5.29.
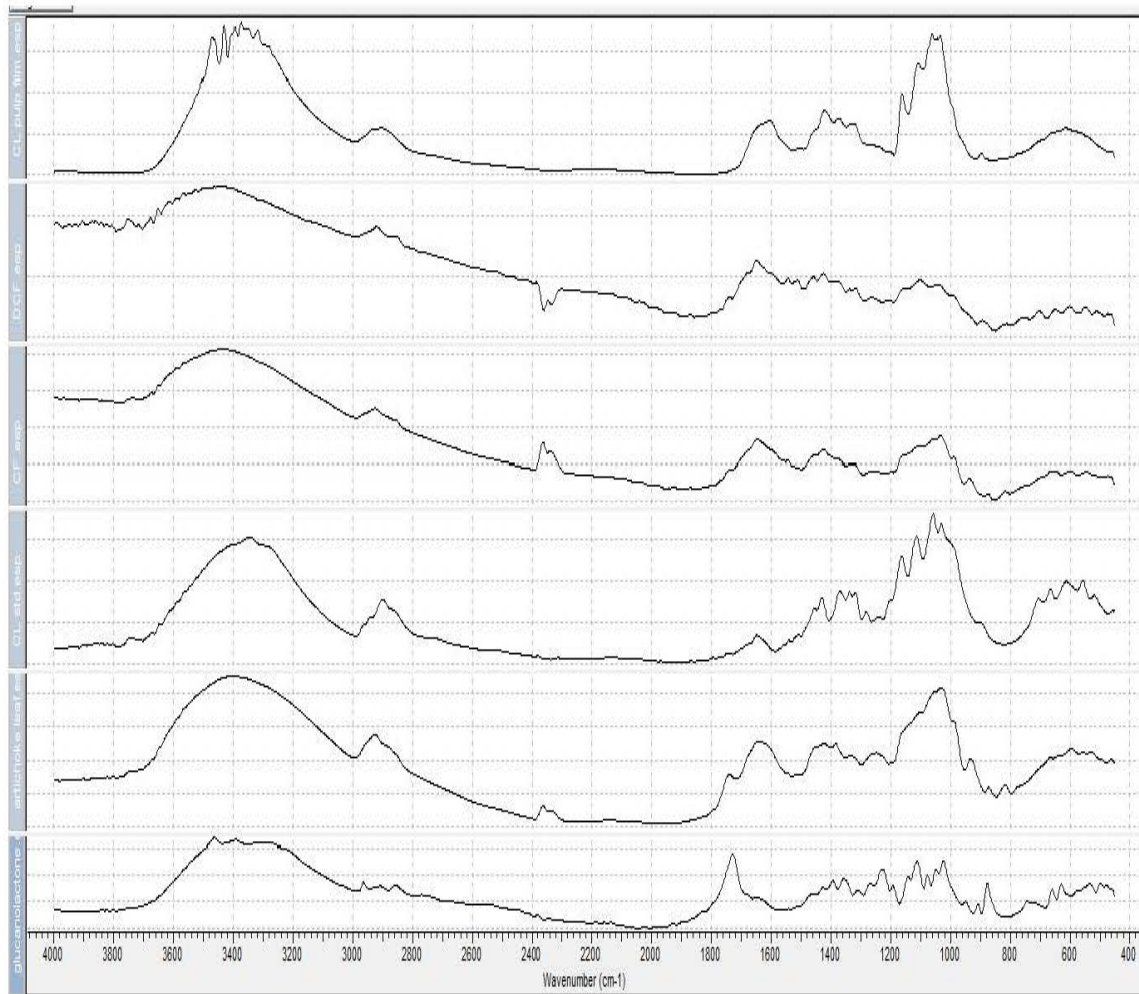
In drawal of score plot from PCA data, 1st and 2nd principal components (t[1] and t[2]) were selected since their Eigen values are bigger than 1, and they gave most meaningful presentation for result data. The score t1 (first component) explains the largest variation of the X space, followed by t2 etc. Hence the scatter plot of t1 vs t2 is a window in the X space, displaying how the observations are situated with respect to each other (Umetrics-AB 2013).

In HCA, result product is a dendrogram that represents the relationships of similarity among a group of entities. The height of the vertical lines indicates the degree of difference between branches. The longer the line means the greater the difference. The horizontal orientation of dendrograms is irrelevant (Drout and Smith 2012).

---

[4] GDL; glucano delta lactone, ARTLP; artichoke leaf micro powder, CLS; micro granular cellulose (cellulose standard), CF; cellulose fibril, DCF; deashed cellulose fibril, and CPF; cellulose pulp film
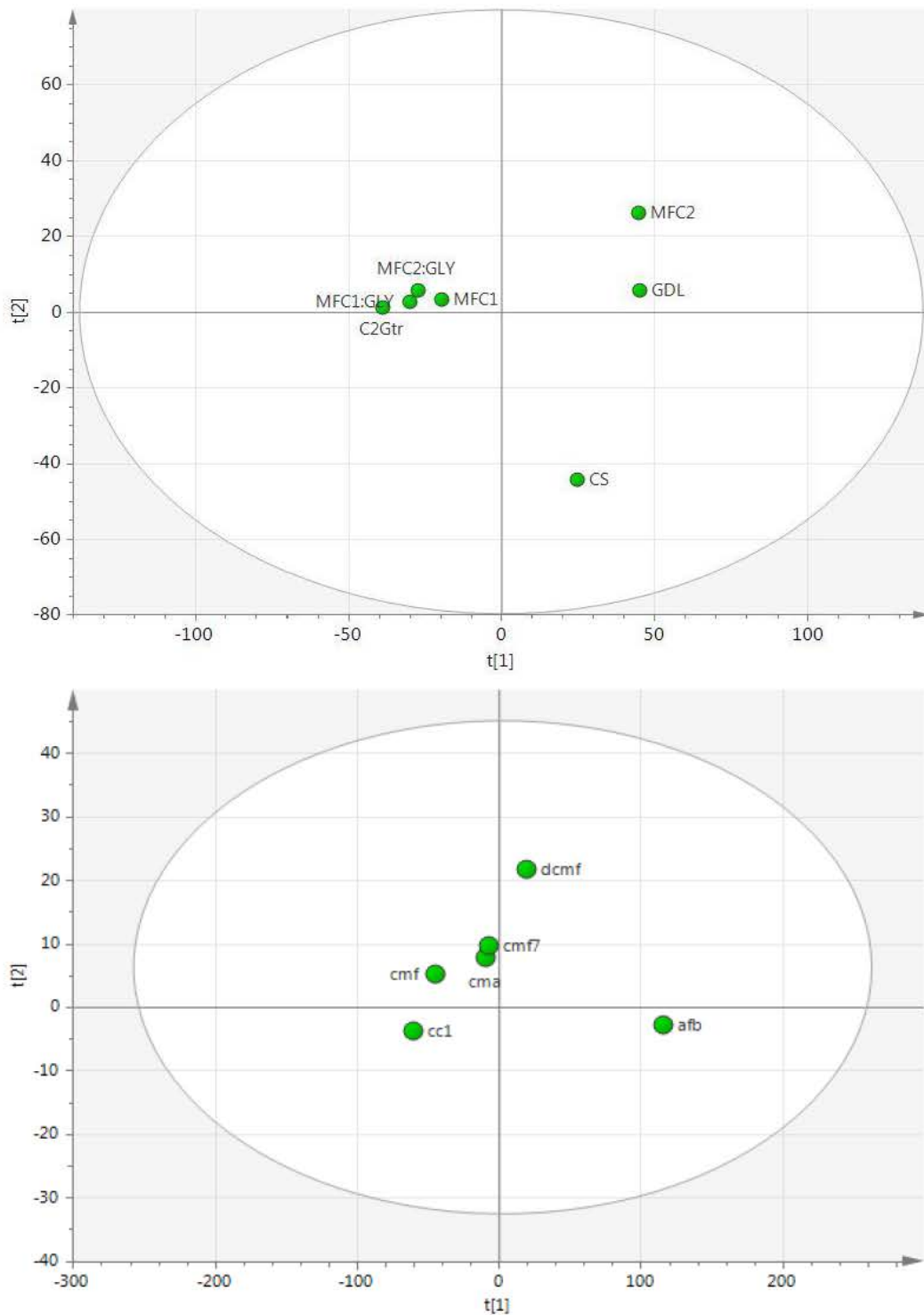
Figure 5.29 Score plot from PCA for FTIR data for powdered products[5]

Samples MFC1 and MFC2 was not totally similar in terms of their bond structures, while interestingly films casted from these products via addition of gly showed near completely similar bond structure as measured in FTIR spectra.

---

[5]Cmf/cmf7: cellulose microfibrils, dcmf: deashed cellulose microfibril; afb: artichoke leaf; cc1: cellulose fibril, cma: granulated micro cellulose, CS: cellulose standard, c2gtr: deashed cellulose fiber, mfc1/mfc2: microfibril cellulose; mfc+gly: film sample, gdl: glucanodeltalactone.

Additionally, interior chemical bonds of afb was found significantly different from the other powdered samples (i.e. microgranular cellulose) and products (i.e. microfibrillated cellulose).

Since usage of standard FTIR instrument was not applicable enough to differentiate film samples produced, FTIR-ATR was applied to film samples, seperately components used in film formation in liquid form. There were 32 different samples tested (observations), that's why grouping samples tested was necessary in order to understand and present the results clearly. Samples were grouped as adsorbent, extract, standards, control films, emulsion films, and films with chitosan. Samples were both evaluated seperately and as in groups.

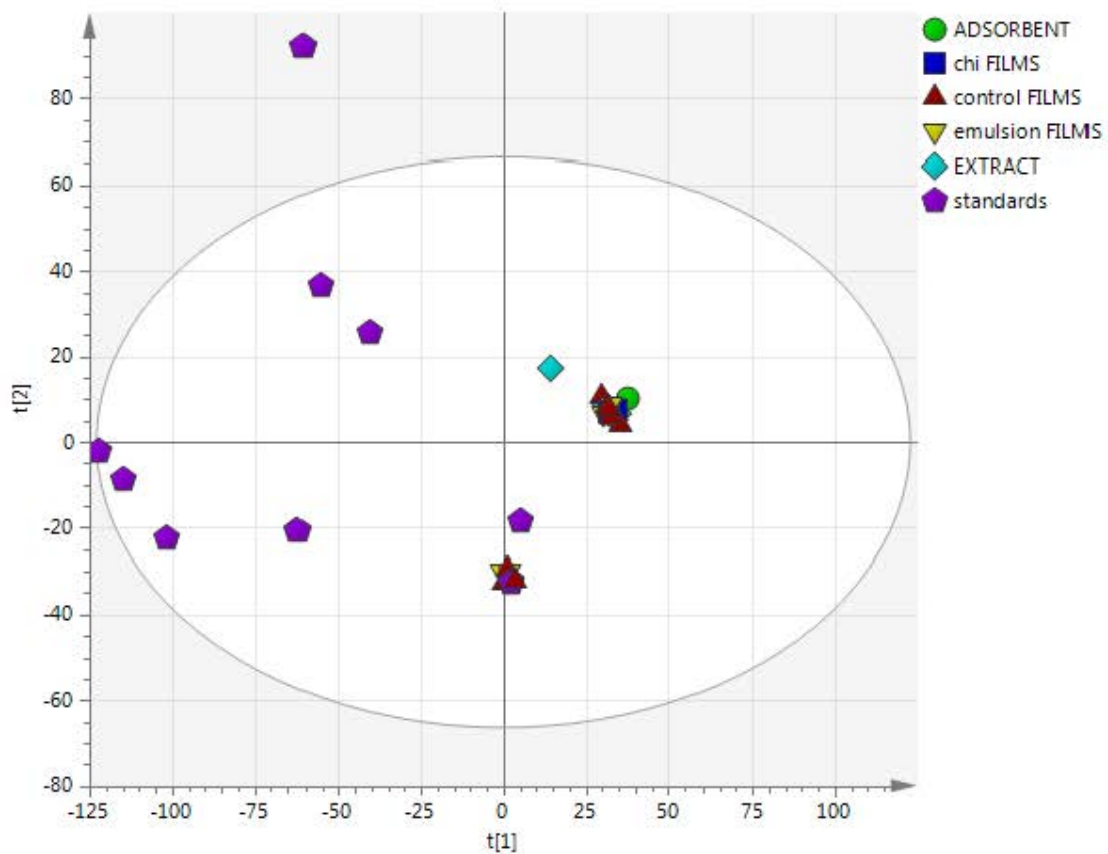Figure 5.30 Score plot from PCA of FTIR-ATR data for film samples and film components in solution form

Detailed diagrams of samples were illustrated in Figure B.1 in Appendix B. For further examination, Table B.1 (for ATR-FTIR peak assignments of artichoke fiber) and Table A.1 (for characteristic FTIR peaks assignments and their assignments to related bond type for cellulose) could be seen in Appendix A. and B.

ftir atr.M1 (PCA-X) Hierarchical Clustering t[1 2 3 4 5 6 7]

Legend:
- ADSORBENT (green)
- chi FILMS (blue)
- control FILMS (dark red)
- emulsion FILMS (yellow)
- EXTRACT (cyan)
- standards (purple)

Calculated with single linkage and sorted by size.

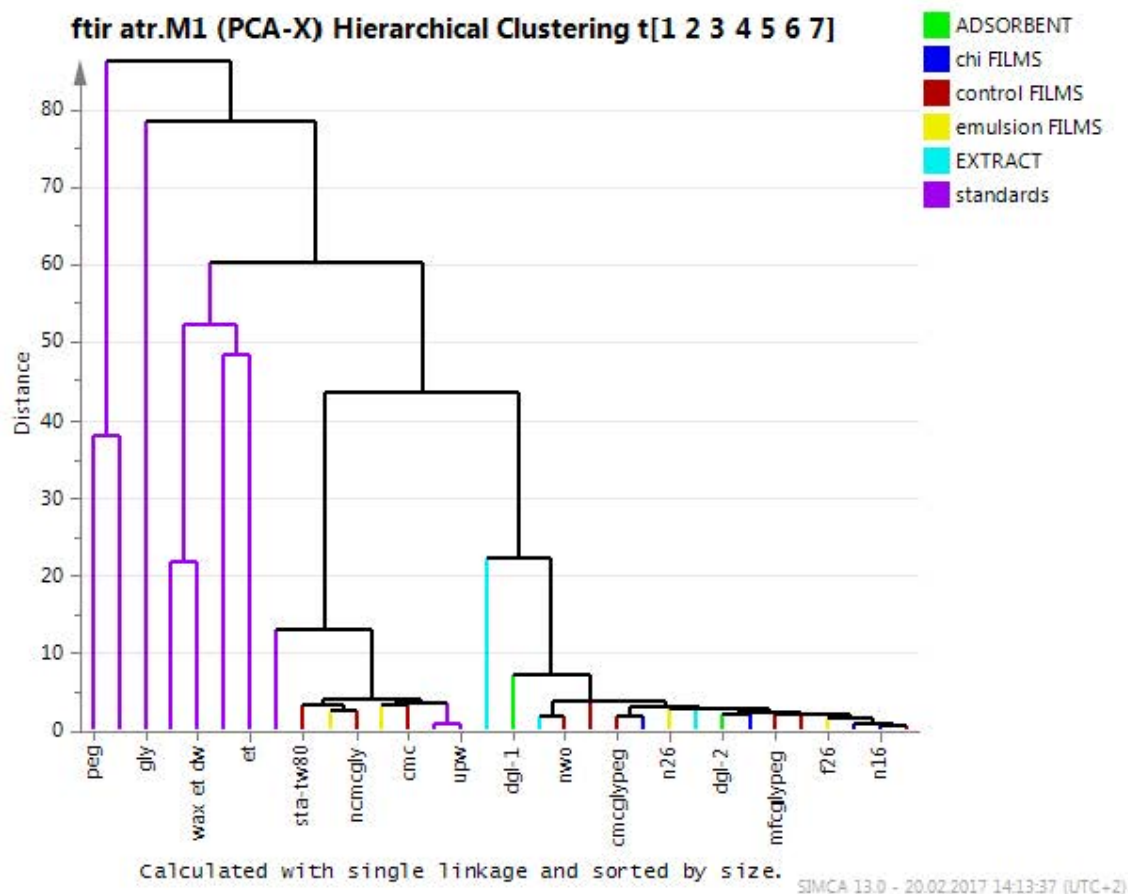SIMCA 13.0 - 20.02.2017 14:13:37 (UTC+2)

Figure 5.31 Dendrogram for HCA of FTIR-ATR data for film samples and film components in solution form

From Figure 5.31 (clustering analysis), it could be concluded that plain standards tested showed completely different pattern from all other film samples and extracts in their ATR spectra. The standards were also significantly different from eachother as expected. Peaks of wax samples for either extracted in EtOH or DW: EtOH gave almost identical character, this means there is no positive or negative effect of DW usage in extraction fraction. Chemical structure of lignin molecule is completely different from rest of the compounds. Chitosan films prepared without acetic acid addition were very similar with diluted aqueous solutions since solubility of chitosan in DW is very very low. Lignin and the phase seperated in deashing operation was also found similar. In overall all film samples show similar bond structures except emulsion films prepared with StA. Similar pattern in their bond structure means they have similar chemical structure.

5.3.7 Determination of crystal structure

In Figure 5.32 X-ray diffraction peaks for CMC and NCMC samples were compared in first plot, in general crystallinity patterns of CMC and NCMC were found similar. In second plot a more sensitive diagram (by decreasing time/step during measurement to detect sharp peaks more accurately) for NCMC were shown.
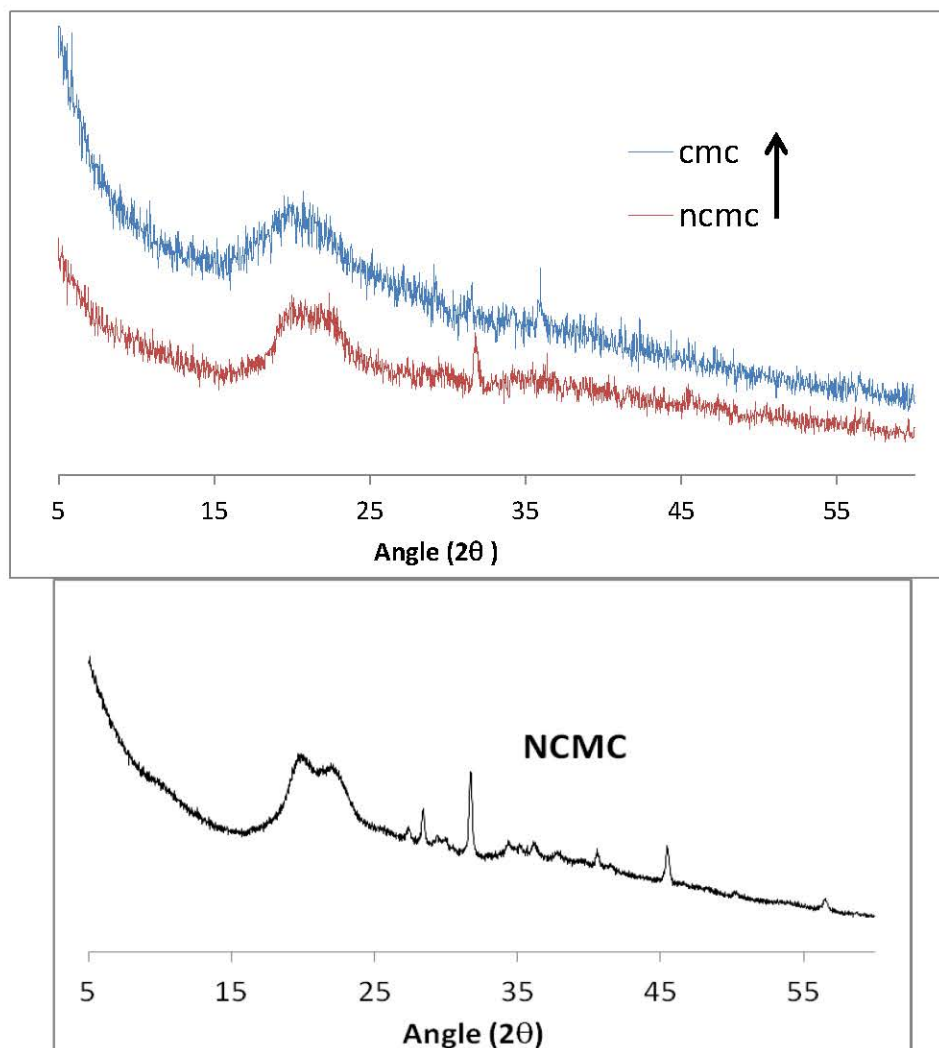
Figure 5.32 XRD plot for Na-CMC; New CMC; New CMC-P

Results of X-ray diffraction analyses for cellulose fiber, microfibrils and artichoke microfibrils were presented in Figure 5.33 below. From plot similar points and differences in crystalline structure of powders produced from artichoke wastes with mass colloider, freeze drying, oven drying treatments.
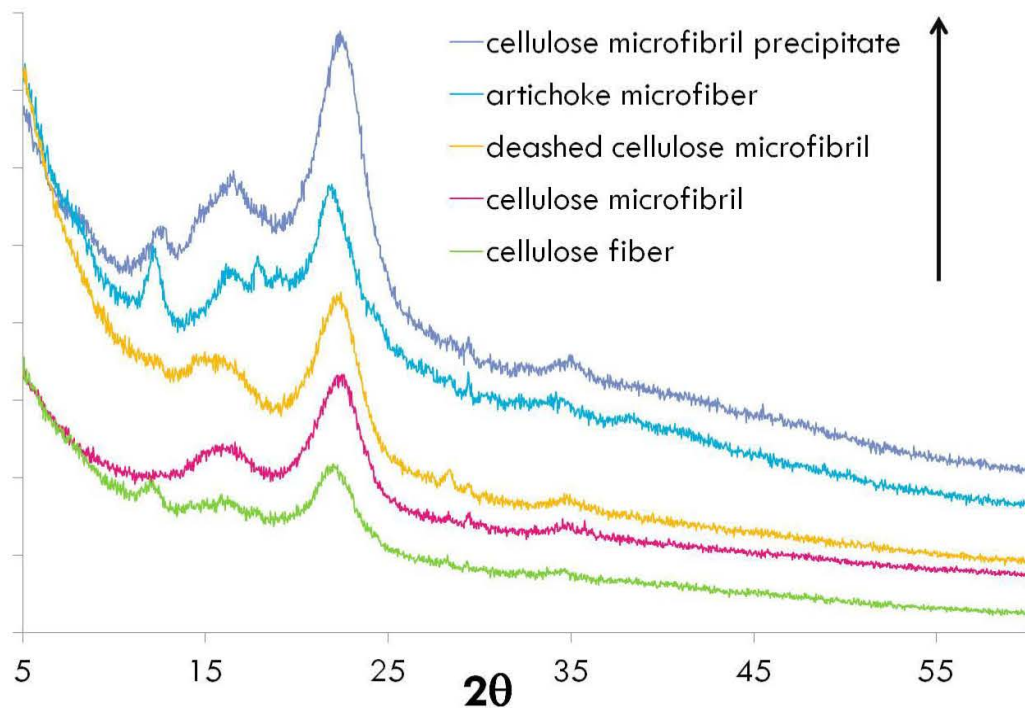
Figure 5.33 XRD diagrams for cellulose micro fibril precipitate, artichoke micro fiber, deashed cellulose micro fibril, cellulose micro fibril, cellulose fiber (from upper to lower)
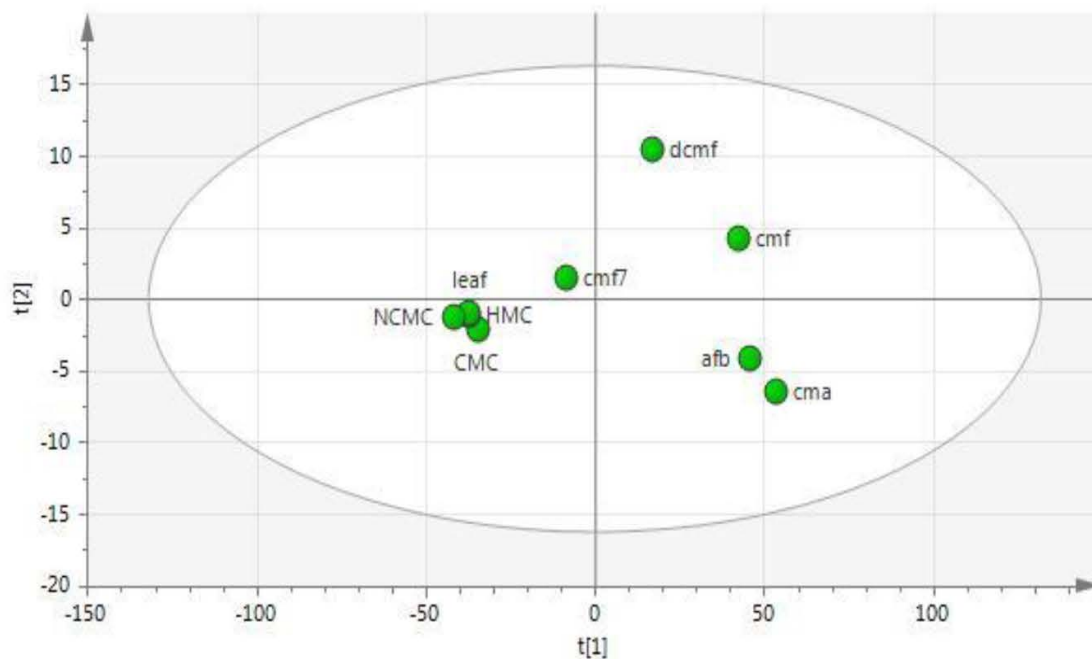
Figure 5.34 Score plot for PCA model of XRD results of powdered products[6]

---

[6] Cmf/cmf7: cellulose microfibrils, dcmf: deashed cellulose microfibril; afb: artichoke leaf; cc1: cellulose fibril, cma:granulated micro cellulose, CS: cellulose standard, c2gtr: deashed cellulose fiber, mfc1/mfc2: microfibril cellulose; mfc+gly: film sample, gdl: glucanodeltalactone.

Principal components were having Eigen value bigger than 1, so model developed was substantive for discrimination of samples about crystalline structure differences. In order to analyse similarity within samples HCA was applied. Results of HCA was gave idea for comparison of different powdered and film samples. For powdered products; crystalline structure of deashed cellulose microfibril completely differs from NCMC, HMC and afb. While crystalline pattern of microfibrillated cellulose samples were similar in between, and ncmc/ cmc samples were not found typically similar. For film samples; crystallinity behaviour of plain mfc film was completely different from all other samples. While films prepared with NCMC (instead of CMC) gave similar pattern within eachother. Addition of both StA or chitosan into film solution, affected on the same way and decreased crystallinity ratio and put these type of film samples into similar crsytalline behaviour. Results of PCA analyses were shown in figures 5.34 and 5.36, also xrd specta were shown in figures 5.33 and 5.35.
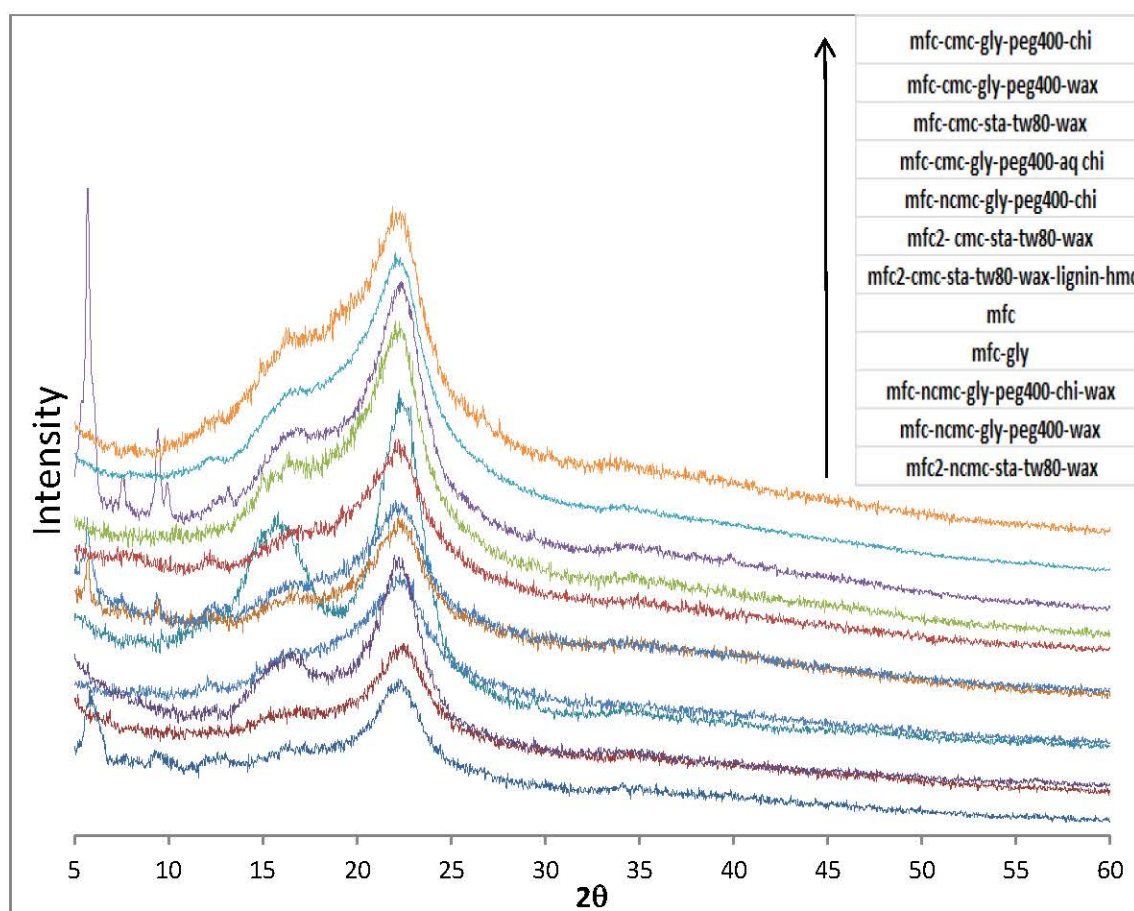
Figure 5.35 XRD Plots of film samples
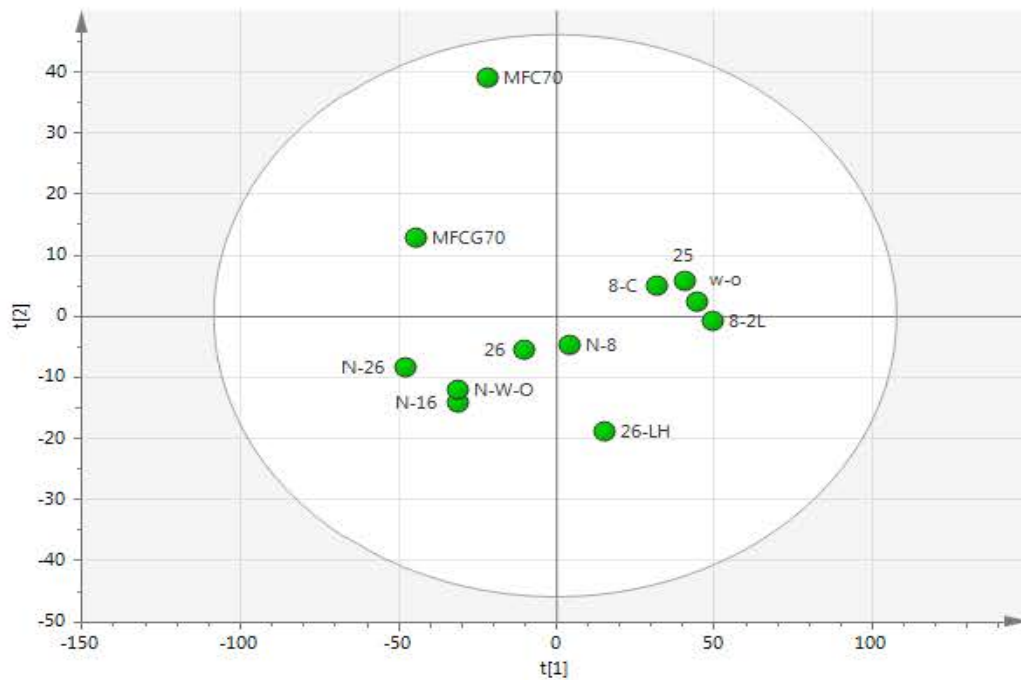
Figure 5.36 PCA analyses of XRD diagrams of film samples[7]

5.3.8 Thermal characterization

Results of thermal data were processed in order to obtain dTg and DTA data. Peaks for melting and glass transition states and decomposition were extracted from Dtg data. Thermal data for cellulose and artichoke leaf powder (AFB) powders were presented in Figure 5.37. In afb sample has two melting peaks at 247.67°C and 322.13°C due to its complex content while cellulose sample has a melting peak at 311.73°C. degradation temperatures for afb and cellulose powders were determined as 452.45°C and 441.61°C. Thermal properties for freeze dried and spray dried microfibrillated cellulose samples were presented in Figures 5.38 and 5.39.

---

[7] 25:mfc-cmc-sta-tw80-wax; MFC70: mfc; MFCG70:mfc-gly;W-O: mfc-cmc-gly-peg400-wax; 8-2L: mfc-cmc-gly-peg400-chi; 8-C: mfc-cmc-gly-peg400-aq chi; 26: mfc2- cmc-sta-tw80-wax; 26-LH: mfc2-cmc-sta-tw80-wax-lignin-hmc; N-8: mfc-ncmc-gly-peg400-chi; N-16: mfc-ncmc-gly-peg400-chi-wax; N-26: mfc2-ncmc-sta-tw80-wax; N-W-O: mfc-ncmc-gly-peg400-wax
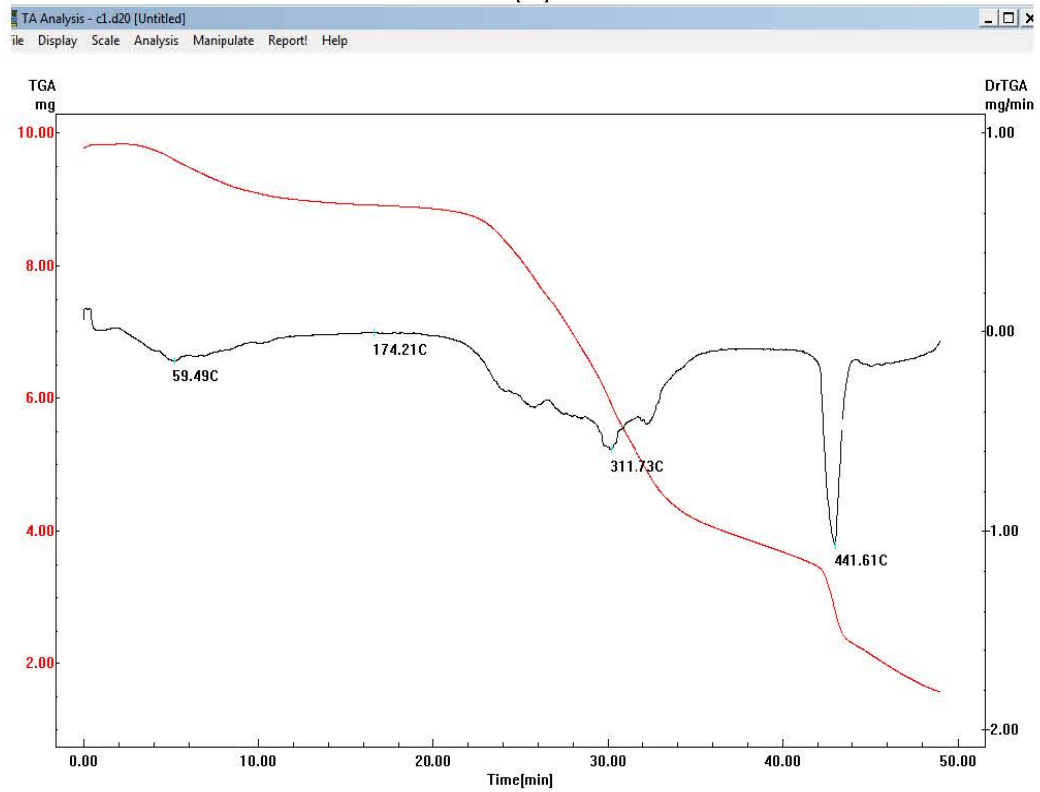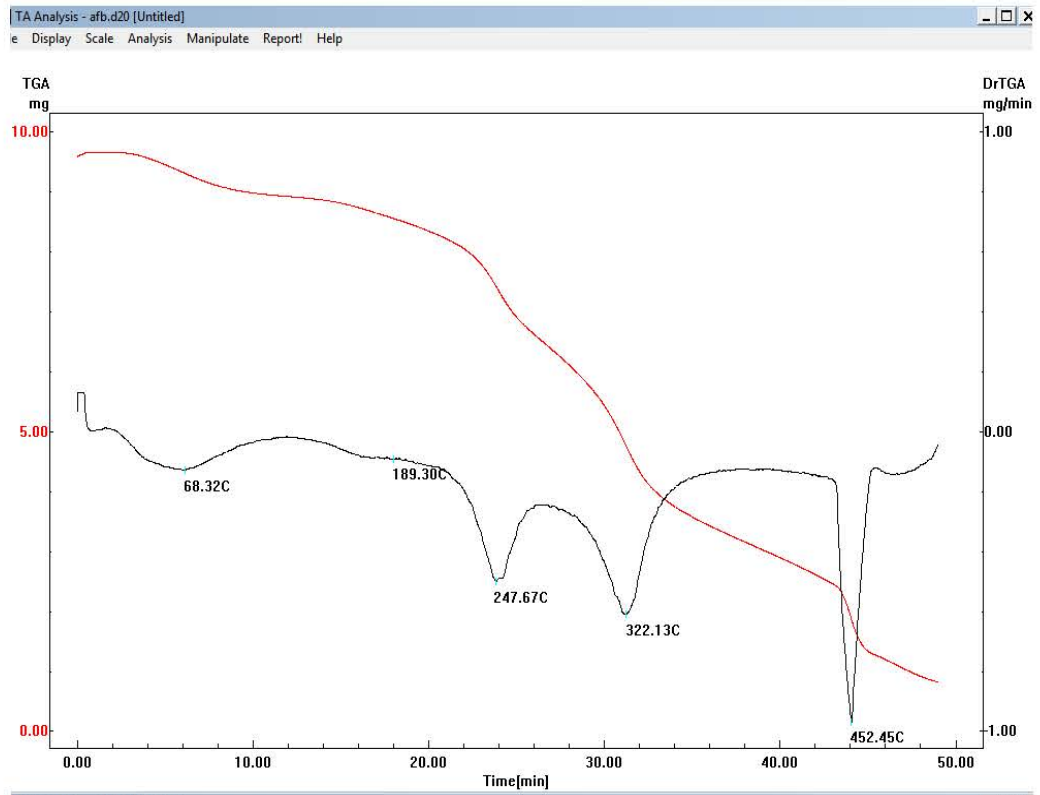
Figure 5.37 TGA-dtg diagrams for cellulose and AFB
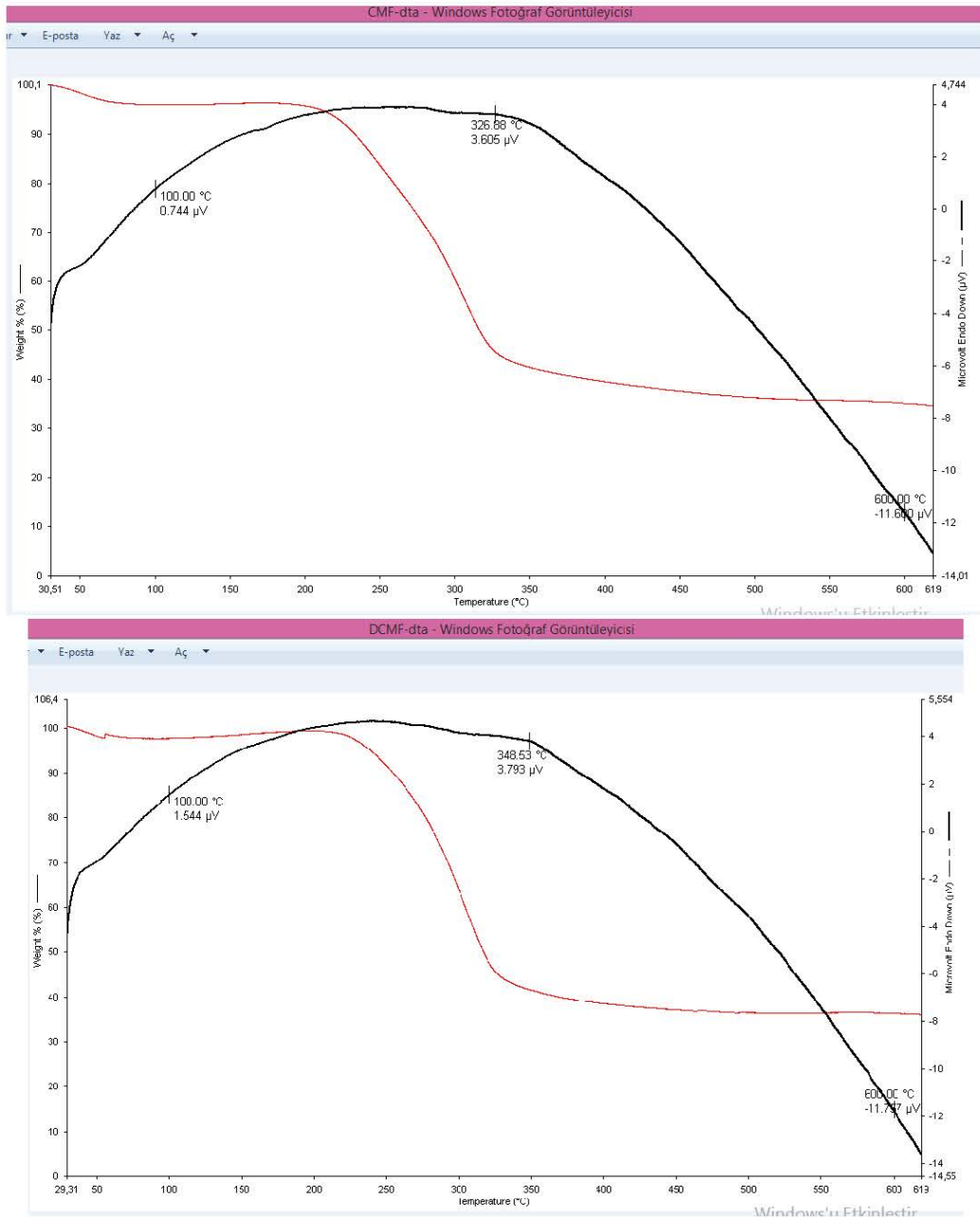
Figure 5.38 TGA-DTA diagrams for CMF, DCMF
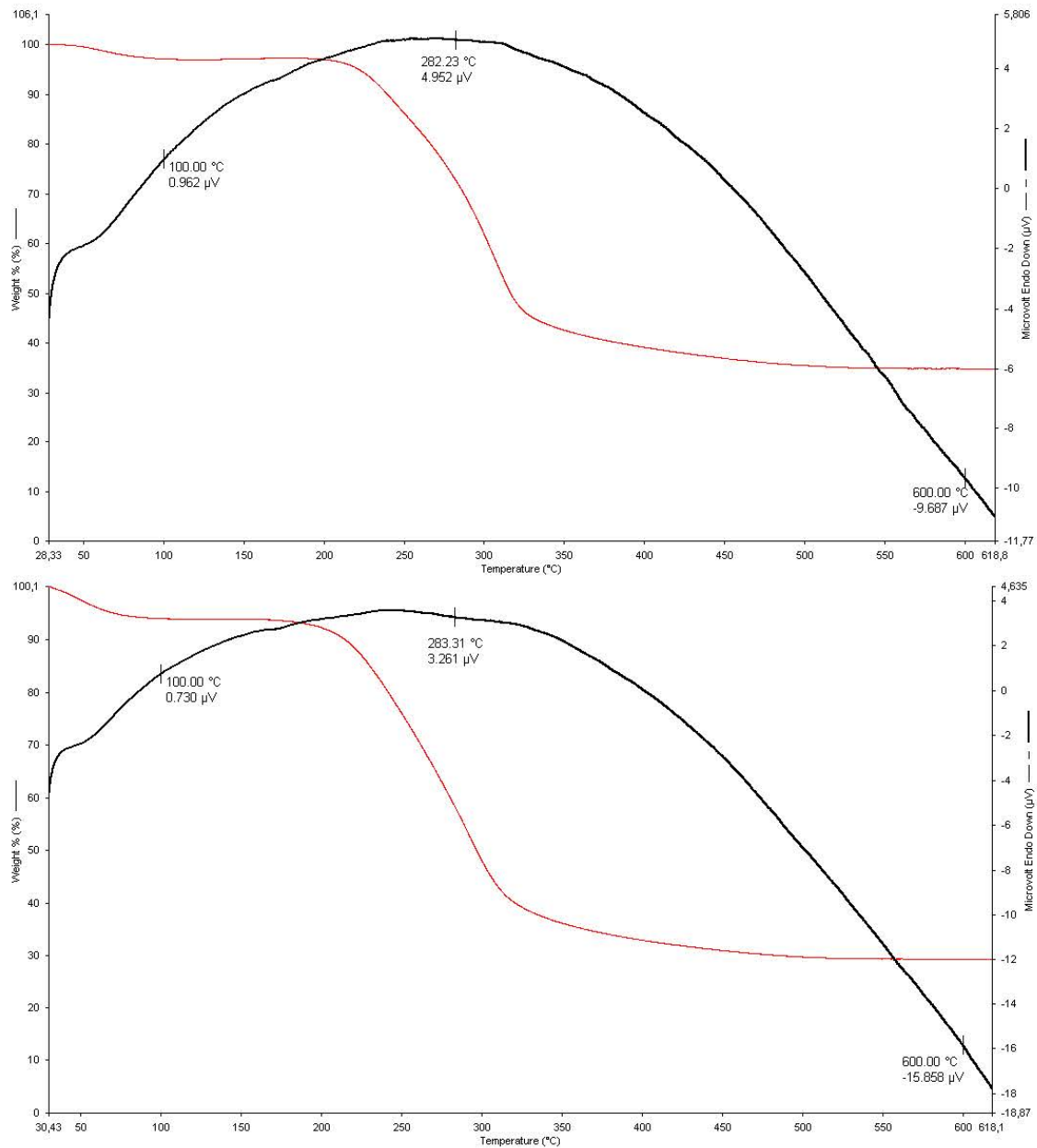
Figure 5.39 TGA-DTA diagrams for CLP1SPC, CLP1SP

From results of PCA, thermal behaviour of afb and cf were discriminated as different from other powdered samples tested (especially based on different forms of microfibrillated cellulose). Effect of microfibril formation was found helpful in enhancement of thermal stability, but this process was not enough to obtain sealeble films via usage of MFC, since melting patterns of films formed with mfc were not applicable in lab scale thermal sealers. Presence of lignin significantly affects thermal behaviour of films on undesirable way. There was no significant evidence on effect of chitosan or stearic acid addition on thermal property of films. In figure 5.40 and 5.41

detailed distrubution of samples tested through the study were schematized via score plots of principal components. As in former PCA results presented for FTIR and XRD, Eigen values were bigger than 1 for the principal components of the model developed.
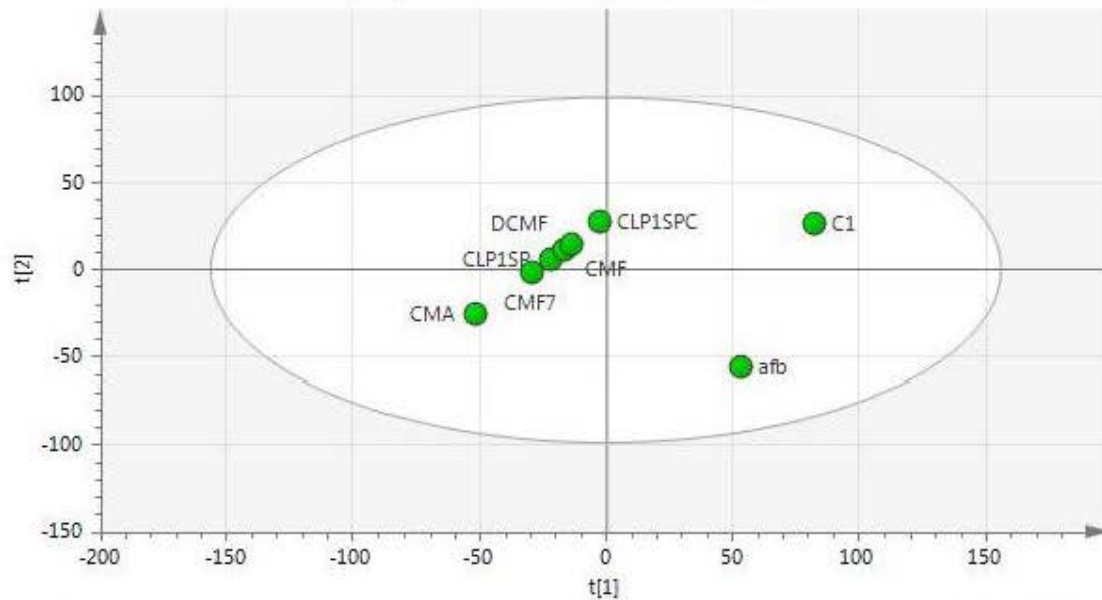
Figure 5.40 PCA for TGA results of powdered samples[8]

Results of thermo gravimetric analyses showed that at a temperature range of 200-240 °C, thermal sealing might be maintained conveniently for the extract films. But mfc films were not conveniently sealed at any temperature tested. Examine tables C 1-5 in Appendix C.

---

[8] CLP1SP/ CLP1SPC: spraydried cellulose microfibril, Cmf/cmf7: cellulose microfibrils, dcmf: deashed cellulose microfibril; afb: artichoke leaf, cc1: cellulose fibril, cma: granulated micro cellulose, CS: cellulose standard, c2gtr: deashed cellulose fiber, mfc1/mfc2: microfibril cellulose; mfc+gly: film sample, gdl: glucanodeltalactone.
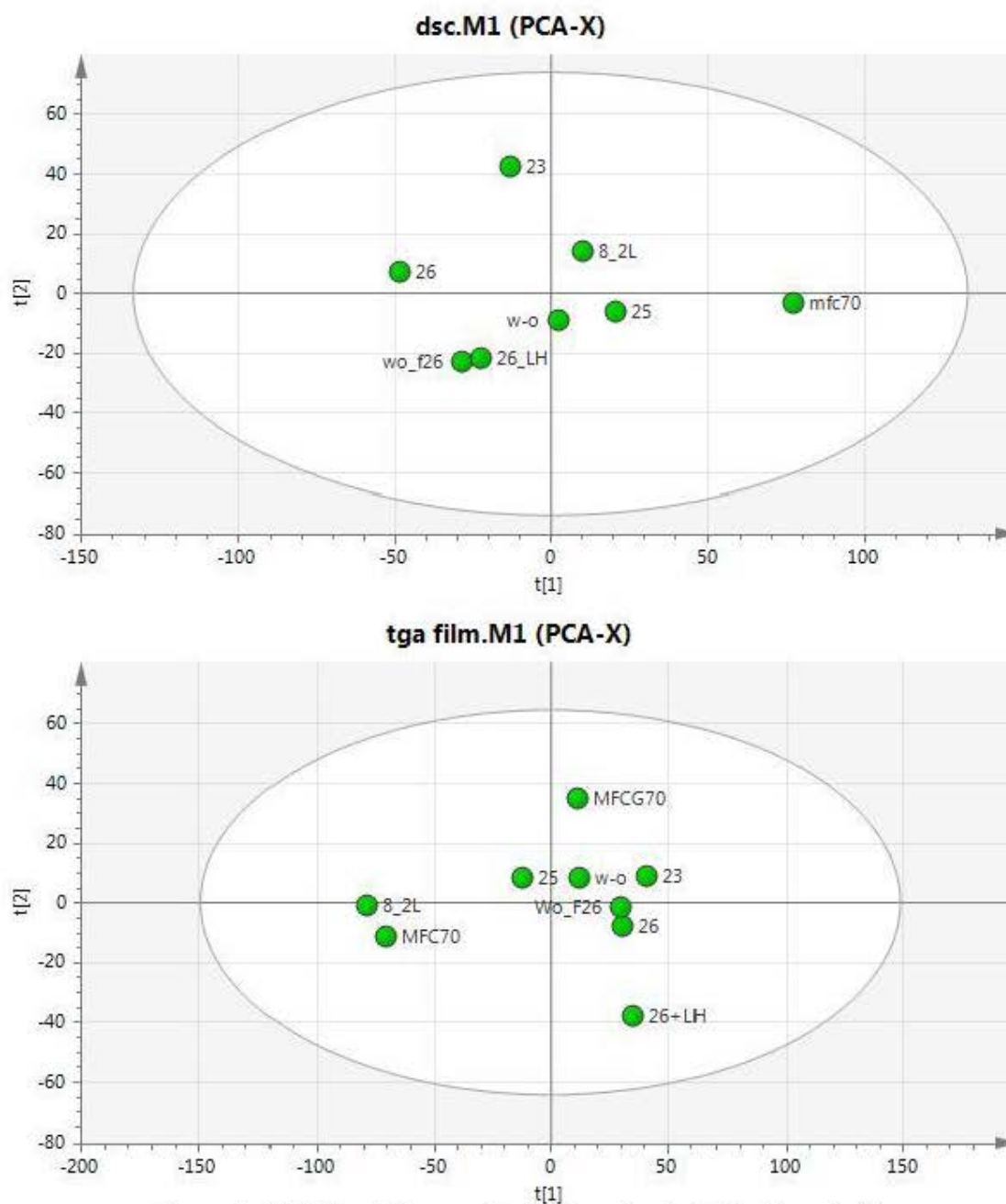
Figure 5.41 PCA of Thermal Data for selected Film Samples[9]

[9] 25:mfc-cmc-sta-tw80-wax; MFC70: mfc; MFCG70:mfc-gly;W-O: mfc-cmc-gly-peg400-wax; 8-2L: mfc-cmc-gly-peg400-chi; 8-C: mfc-cmc-gly-peg400-aq chi; 26: mfc2- cmc-sta-tw80-wax; 26-LH: mfc2-cmc-sta-tw80-wax-lignin-hmc; N-8: mfc-ncmc-gly-peg400-chi; N-16: mfc-ncmc-gly-peg400-chi-wax; N-26: mfc2-ncmc-sta-tw80-wax; N-W-O: mfc-ncmc-gly-peg400-wax

5.3.9 Mechanical properties of films

Addition of lignin and / or glycerol was proved to have an ability to increase elasticity of films, while presence of HMC increased the fragility of films. Besides, addition of CMC had improved tensile strength and toughness of films. The films produced with the addition of CMC had more uniform and dense microstructures. In this study mechanical characteristics of prepared films were mainly introduced by the CMC component incorporation.

In screening tests for determination of best compositions mechanical characteristics were used as evaluation tool. In screening different film samples due to their mechanical properties general factorial design and ANOVA was applied. Difference of mechanical characteristics due to MFC, GLY, STA, CMC, NCMC, Wax, beewax, $CaCO_3$, HMC, and SRB content was observed. The differences between tested film samples were found statistically significant (p-value < 0.05). *F and R^2 values* for each mechanical term were listed below.

Force (30.16 and *0.795)*   *Strain (14.24* and *0.6467)*

*Stress (23.84* and *0.7540)*   *Strength (43.81* and *0.8492)*

The results of screening tests were also used in comparison of CMC films with NCMC films for their mechanical characteristics, again with ANOVA technique. The differences between tested film samples were found statistically significant (p-value < 0.05). *F and R^2 values* for each mechanical term were listed below.

*Force (*151.81 and 0.9574*)*   *Strain (*41.18 and 0.8592*)*

*Stress (*173.56 and 0.9626*)*   *Strength (*159.38 and 0.9594*)*

Desirability of film samples from screening tests was determined according to their mechanical properties *via* ANOVA data. In calculation of desirability values strain and strength terms were selected as most critical parameters while force and stress results considered in secondary importance. Comparison was between selected films prepared with NCMC and CMC. The compostion of those films were predetermined in screening tests, evaluation and selection of film composition and/or casting conditions

were exracted from previous results on solubility and mechanical characteristics of films. Results for desirability analyses were presented in Table 5.15. According to average of results, desirability analysis was conducted. Most desirable film sample was determined as "CMC-CHI-MFC-GLY-PEG400" film. There were no siginificant differences between the tensile properties of the film samples casted with CMC or NCMC, but there were synergistic or antagonistic effect of additives used in film formation on tensile properties of films. There were no positive effect of HMC addition on development of tensile strength and elasticity. Results of screening test and comparison test was summarized in Table 5.15.

Table 5.15 Desirability values for film samples according to mechanical properties (Screening and comparison tests)

Film composition	Force (kg)	Strain (%)	Stress (MPa)	Strength (kg/mm)	Desirability
Cmc-Chi-Mfc-Gly-Peg400	5.27	11.71	27.24	0.53	0.75
Ncmc-Chi-Mfc-Gly-Peg400	5.37	11.62	25.11	0.54	0.74
Cmc-Mfc-Gly-Tw80-Sta-Wax	4.55	13.28	18.59	0.45	0.68
Cmc-Mfc2-Gly-Tw80-Sta-Wax	4.74	9.67	23.26	0.47	0.62
Cmc-Chi-Mfc-Gly-Peg400-Wax	4.06	9.39	27.104	0.41	0.59
Mfc- Gly- Sta-Cmc	4.53	11.88	29.64	0.45	0.47
Ncmc-Gly	2.04	16.56	39.95	0.26	0.39
Mfc	3.71	7.065	20.45	0.46	0.35
Ncmc-Mfc2-Gly-Peg400-Wax	2.02	5.67	11.95	0.21	0.24
Ncmc-Mfc-Gly-Tw80-Sta-Wax	1.4	6.86	6.96	0.14	0.19
Cmc-Gly-Sta	0.9	14.03	16.24	0.11	0.19
Mfc-Gly- Sta- Wax- Beewax	1.204	8.56	9.86	0.13	0.16
Mfc- Gly	0.97	8.71	9.024	0.13	0.15
Ncmc-Mfc-Gly-Peg400-Wax	0.84	6.04	4.11	0.08	0.1
Mfc- Gly- 0.15% w/v CaCO$_3$-Cmc	0.73	6.74	5.733	0.08	0.096
Mfc- Gly- 0.2 % w/v CaCO$_3$-Cmc	0.56	5.44	3.298	0.059	0.059
Hmc-Cmc-Gly	0.34	26.4	7.142	0.011	0.055
Ncmc-Chi-Mfc-Gly-Peg400-Wax	0.6	4.18	2.78	0.06	0.04
Hmc-Cmc-Srb	0.93	2.46	17.4	0.009	0.037

With selected film samples an optimization study was carried out according to their mechanical properties in order to compare effect of casting volume (indirectly film thickness) and film composition on preferability of those films. Four different compositions and three different casting volumes were applied in tests. Results for mechanical analyses for optimization trials were shown in Table 5.16 below, results

presented in form of AVG±STDDEV. In first column of the table 5.16, detailed information about film composition and casting volume were stated.

Table 5.16 Optimization study (effect of film thickness on tensile properties)

Samples	Force (kg)	Strain (%)	Stress (MPa)	Strength (kg/mm)
Mfc-cmc-gly-peg400-chi-20ml	1.62 ± 0.17	7.68 ± 1.31	6.56 ± 1.04	0.16 ± 0.03
Mfc-cmc-gly-peg400-chi -30ml	1.95 ± 0.18	9.51 ± 2.7	6.38 ± 0.6	0.2 ± 0.02
Mfc-cmc-gly-peg400-chi-40ml	2.62 ± 0.58	10.37 ± 2.76	7.44 ± 1.67	0.33 ± 0.07
Mfc-cmc-gly-peg400-chi-wax-20ml	0.78± 0.1	8.17 ± 1.71	3.16 ± 0.44	0.078 ± 0.01
Mfc-cmc-gly-peg400-chi-wax-30ml	1.03 ± 0.14	8.77 ± 1.14	3.39 ± 0.48	0.1 ± 0.01
Mfc-cmc-gly-peg400-chi-wax-40ml	1.28 ± 0.21	9.51 ± 1.17	3.42 ± 0.52	0.13 ± 0.02
Mfc-cmc-sta-gly-tw80-wax-20ml	1.25±0.32	15.42±3.31	11.15±2.88	0.13±0.03
Mfc-cmc-sta-gly-tw80-wax-30ml	3.92±1.74	9.93±3.05	32.6±14.72	0.48±0.22
Mfc-cmc-sta-gly-tw80-wax-40ml	5.17±1.54	6.03±3.26	30.35±10.67	0.65±0.19
Mfc-cmc-gly-peg400-wax-20ml	1.07±0.29	11.24± 2.2	10.54±2.84	0.11 ± 0.03
Mfc-cmc-gly-peg400-wax-30ml	1.2±0.25	12.9±3.37	9.45±2.12	0.12± 0.03
Mfc-cmc-gly-peg400-wax-40ml	1.34± 0.53	10.03±6.42	8.74±3.47	0.13±0.05

Strength values of films were found strongly related with composition and thickness values of film samples. The interaction effect of these factors was also found significant. The Model F-value of 54.56 implies the model is significant (probability of noise is 0.01%). Composition, thickness, and their interaction are significant model terms (p-value < 0.05). R-Squared value of the model is 0.90912.

Stress values of films were found strongly related with composition and thickness values of film samples. The interaction effect of these factors was also found significant. The Model F-value of 43.17 implies the model is significant (probability of noise is 0.01%). Composition, thickness, and their interaction are significant model terms (p-value < 0.05). The "R-Squared" of 0.887823 fitting good for that model.

Strain values of films were found strongly related with composition values of film samples. But effect of thickness values on strain were found in significant.The

interaction effect of these factors was found significant. The Model F-value of 6.05 implies the model is significant (probability of noise is 0.01%). B, AB are significant model terms (p-value < 0.05), while effect of thickness on strain value is not significant. R-square value of the model is 0.525982.

Force values of films were found strongly related with composition and thickness values of film samples. The interaction effect of these factors was also found significant. The Model F-value of 51.17 implies the model is significant (probability of noise 0.01%). Composition, thickness, and their interaction are significant model terms (p-value < 0.05). R-Squared value of the model is 0.90368. Mechanical properties of films studied for optimization for effect of compostion and thickness were aligned according to their desirability.

Addition of chitosan or wax into "Mfc-cmc-gly-peg400" film did not have a significant effect of tensile property of film. Usage of peg400 component was decreased the maximum force applied for tearing the film product, results were comparable from Tables 5.15 and 5.17.

Table 5.17 Desirability values for film samples according to mechanical properties (Optimization test)

Film Type	Force (kg)	Strain (%)	Stress (MPa)	Strength (kg/mm)	Desirability
Mfc-cmc-sta-gly-tw80-wax-40ml	6.83	8.82	42.32	0.85	0.57
Mfc-cmc-sta-gly-tw80-wax-30ml	4.32	11.33	36.94	0.52	0.48
Mfc-cmc-gly-peg400-chi-40ml	2.88	11.28	8.15	0.36	0.23
Mfc-cmc-gly-peg400-wax-40ml	1.81	13.22	11.85	0.18	0.19
Mfc-cmc-sta-gly-tw80-wax-20ml	1.38	16.65	12.28	0.14	0.16
Mfc-cmc-gly-peg400-chi-30ml	2.04	10.46	6.64	0.20	0.15
Mfc-cmc-gly-peg400-wax-30ml	1.30	14.19	10.43	0.13	0.13
Mfc-cmc-gly-peg400-chi-20ml	1.65	7.97	6.91	0.16	0.11
Mfc-cmc-gly-peg400-wax-20ml	1.17	10.20	11.44	0.12	0.10
Mfc-cmc-gly-peg400-chi-wax-40ml	1.38	9.77	3.63	0.14	0.06
Mfc-cmc-gly-peg400-chi-wax-30ml	1.09	8.73	3.58	0.11	0.04
Mfc-cmc-gly-peg400-chi-wax-20ml	0.85	8.45	3.38	0.08	0.02

In sample "Mfc-cmc-sta-gly-tw80-wax" there were no significant difference on tensile properties of thickest and medium thick films, while strength of thinnest film was significantly and unexpectedly low. For other film samples effect of thickness on strength values were directly proportional.

5.3.10 WVTR test

WVTR values were calculated from the formula tabulated in eq. 4.6 in section 4.4.12. Average results with their standard deviations were presented in Table 5.18. Results of WVTR analyses were also evaluated statistically with ANOVA. F-value of 45.44 implies the model was found significant (with 0.01% mistake ratio). Effect of film composition on WVTR values of samples are significant according to p-value of the model tested. Results of ANOVA were summarized in Table 5.19 below.

Table 5.18   WVTR values (g/day*cm^2) of some selected films (n=3)

WVTR (g/day*cm^2)			
Sample	avg	±	stdev
Control- (bottle lid)	0.000	±	0.0002
sonicated mfc	0.075	±	0.0058
MFC	0.051	±	0.0113
MFC-gly	0.050	±	0.0104
sonic cmc-gly-sta-tw80 w_{gain}	0.014	±	0.0048
sonic cmc-gly-sta-tw80 w_{loss}	0.046	±	0.0096
0.15%CaCO$_3$+mfc	0.067	±	0.0048
0.2%CaCO$_3$+mfc	0.079	±	0.0048
Mfc-cmc-gly-peg400-wax	0.051	±	0.0122
Mfc2-cmc-gly-peg400-wax	0.045	±	0.0027
Mfc2-cmc-gly-sta-wax-tw80	0.045	±	0.0018
Mfc2-cmc-gly-sta-wax-tw80-lignin-hmc	0.011	±	0.0006
cmc-chi-mfc-gly-peg400	0.039	±	0.0053
cmc-aq chi-mfc-gly-peg400	0.072	±	0.0117
cmc-chi-mfc-gly-peg400-lignin	0.006	±	0.0003
Cmc-chi-mfc-gly-peg400-wax	0.038	±	0.0083
cmc-aq chi-mfc-gly-peg400-wax	0.073	±	0.0050
Ncmc-mfc-gly-peg400-wax	0.069	±	0.0147
Mfc-ncmc-sta-gly-tw80	0.064	±	0.0043
Mfc2-ncmc-sta-gly-tw80	0.067	±	0.0110
ncmc-chi-mfc-gly-peg400	0.053	±	0.0110
ncmc-chi-mfc-gly-peg400-wax	0.051	±	0.0100
Mfc-cmc-sta-gly-tw80	0.048	±	0.0124

Usage of lignin or hmc instead of wax or chitosan was found helpful for development of water vapor resistance, while all of the components stated were thereotically useful for increasing hydrophobicity.

Table 5.19 Analysis of variance table for WVTR results of film samples

Source	SS	df	MS	F Value	p-value	
Model	0.054	22	0.0025	45.44	< 0.0001	significant
A-film	0.054	22	0.0025	45.44	< 0.0001	
Pure Error	0.0062	115	$5.38E^{-05}$			
Cor Total	0.06	137				

The "Pred R-Squared" of 0.8514 is in reasonable agreement with the "Adj R-Squared" of 0.8771 and R-Squared of 0.89683. Adeq Precision value "24.668" indicates the model can be used to navigate the design space. Film samples were evaluated for their desirability in terms of WVTR characteristics, values closer to 1 gives most desirable sample while values closer to 0 gives least desirable film sample, (Table 5.20). According to results of desirability test applied with ANOVA data, most preferable film in terms of WVTR properties was determined as "cmc-chi-mfc-gly-peg400-lignin" film.

Table 5.20 Desirability of different film samples according to their WVTR values

Film	Desirability	Film	Desirability	Film	Desirability
cmc-chi-mfc-gly-peg400-lignin	**0.996**	Mfc2-cmc-gly-sta-tw80	0.460	Mfc2-ncmc-gly-sta-tw80	0.237
Mfc2-cmc-gly-sta-tw80-lignin-hmc	0.930	mfc	0.446	0.15%$CaCO_3$+mfc	0.210
sonic cmc-gly-sta-tw80 w_{gain}	0.867	ncmc-chi-mfc-gly-peg400-wax	0.441	Mfc-cmc-gly-peg400-aq chi	0.167
Mfc-cmc-gly-peg400-chi-wax	0.624	Mfc-cmc-gly-peg400	0.438	cmc-chi-mfc-gly-peg400-wax	0.123
Mfc-cmc-gly-peg400-chi	0.611	ncmc-chi-mfc-gly-peg400	0.423	sonic mfc (111S)	0.105
Mfc2-cmc-gly-peg400	0.495	Ncmc-mfc-gly-peg400-wax	0.357	0.2%$CaCO_3$+mfc	0.062
sonic cmc-gly-sta-tw80 w_{loss}	0.487	Mfc-gly	0.255		
Mfc-cmc-sta-gly-tw80	0.464	Mfc-ncmc-gly-sta-tw80	0.243		

5.3.11 OTR test

Film's barrier properties were determined *via* their gas transmission rate values. CO_2 transmission rate of Na-CMC-(lignin +hemicellulose) fraction film was measured

as 68 ml/m^2 day, while O_2 transmission rate was measured as 77 ml/m^2 day. In order to determine effect of different factors (type and concentration of film forming material or plasticizer); oxygen transfer rates were observed, and given in Table 5.21 below.

Table 5.21 Oxygen Transfer Rates [(OTR); (ml/m2*day) (23°C / 0% RH)] of selected films with different contents

Films	OTR	Films	OTR
cmc	9.08	cmc+2.8% (w/v) hmc	11.44
cmc+2% (w/v) xylan	12.75	cmc+(lignin+hmc) fraction	43
cmc+2% (w/v) hmc	12.28	cmc+lignin+1% (w/v) hmc + wax	30.51
cmc+1.5% (w/v) hmc	9.4	cmc+(lignin+hmc+wax) fraction	19.11
mfc + 0.15%caco3	-	sonicated mfc + gly	1920
mfc + 0.2%caco3	-	sonicated mfc +cmc (45°c)	-
mfc	-	ncmc-mfc-gly-peg400-wax	171.02
Mfc-chi-cmc-gly-peg400	1310	Mfc-cmc-gly-peg400-wax	847
Mfc-ncmc-sta-gly-tw80	262	Mfc-cmc-sta-gly-tw80	151.75
Mfc-cmc-sta-gly-tw80	720	Mfc-cmc-gly-peg400-wax	2060

Products were prepared in order to measure their oxygen transmission rates in appropriate conditions. Since there were surface problems (surface were not flat enough to apply vacuum during analyses) in MFC and MFC + CaCO$_3$ films, measured results could not be presented. Also for sonicated MFC+CMC film, interferences were happened with the instrument while having measurements, this case were suspected since analysis could not equilibrated for a long period of time (may be sample bonds oxygen within its structure). OTR values of MFC + GLY films were calculated as 1920 ml/m^2*day, which was an average permeability value neither low nor high, but not much preferable for the target product.

5.4. Fresh cut treatment and packaging trials

Colour changes of freezed globe artichoke was observed while thawing within different antioxidant solutions (with ascorbic acid, citric acid, cysteine, sodium metabisulphide solutions and distilled water as control) and drying it in mild conditions (35°C) in presence of a desiccant for accelerating drying rate. Results were illustrated in Figure 5.42 to observe change in L*, a*, b* values by time separately. First 4 results

(from t=0.5 h to t=41.5 h) considers colour information of thawing artichoke, while last data (t= 105.5 h) present colours of dried artichoke samples. Also, numerical results for colour variations due to different type of treatments during thawing and drying were presented in Tables F.1 and F.2 by means of L*, a*, b*, ΔL*, hue angle and chromacity parameters, also browning index of final products were calculated to observe differences. According to results presented in figures and tables most applicable antioxidant solution and its concentration were determined as 1 % w/v citric acid, while results of ascorbic acid treatment gave lowest browning index values. Additionally in Figure 5.43, images for freeze thawed artichokes - *treated with different antioxidant solutions and DW for control* - at 30 min and 105 h time periods were shown.
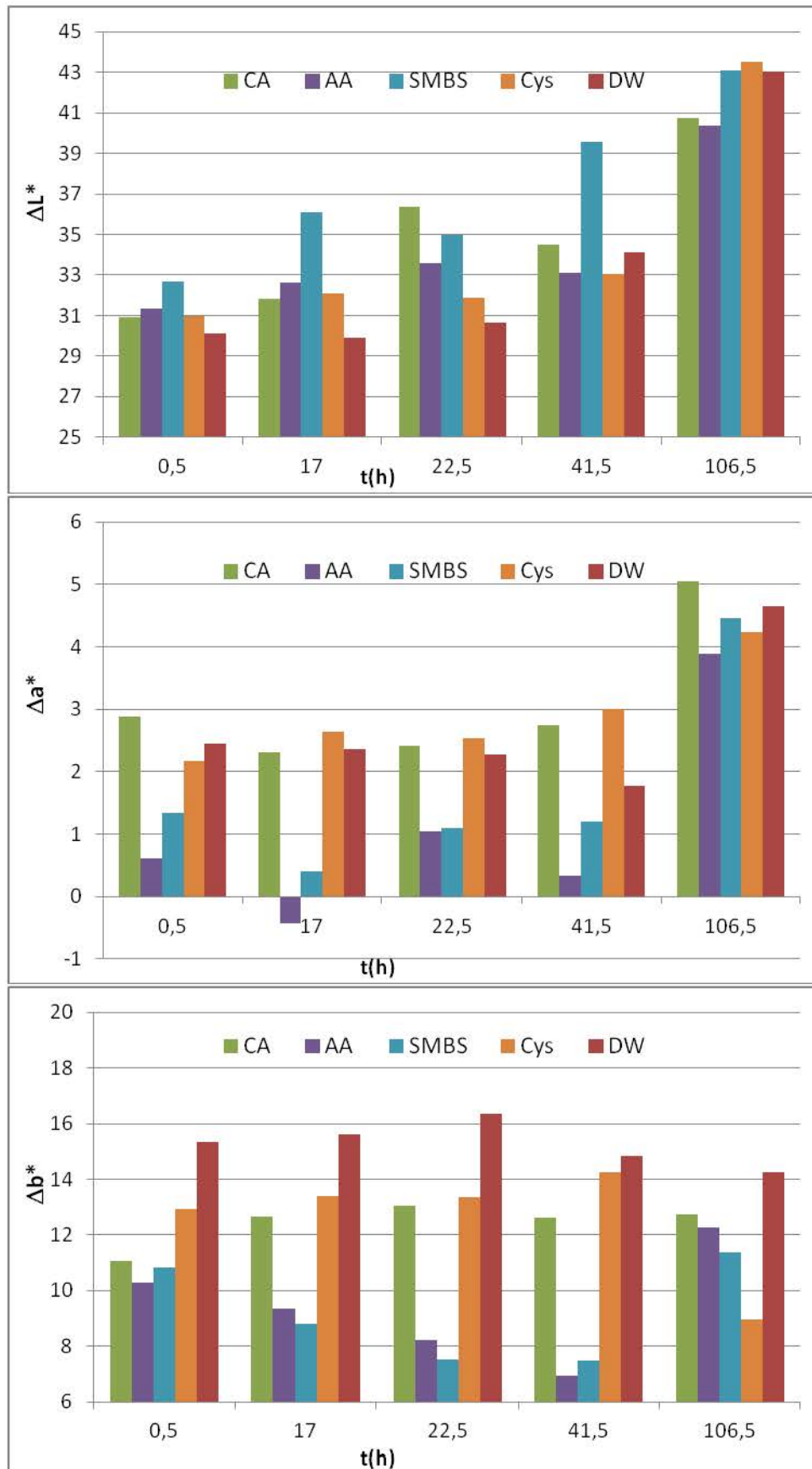
Figure 5.42 Differential L*, a*, b* values of freeze thaw artichokes among different treatment methods

113

Control t=30min	control t=105h
1% CA t=30min	1% CA t=105h
1% AA t=30min	1% AA t=105h
0.5% Cys t=30min	0.5% Cys t=105h
1% SMBS t=30min	1% SMBS t=105h

Figure 5.43 Pictures from artichoke treatment trial

5.4.1 Packaging experiments

Packaging trials were done with 2 % CMC + 0.6 % GLY films using a thermal sealer. Before packaging artichoke samples (heart or stalk) were dipped into 1 % CA solution. Parallel to packaged films, control samples (with and without CA treatment) were held under same conditions in order to detect the difference. There were no detectable differences within colour of samples. During packaging trials; artichoke stalks were stored at room temperature for 7 days; while fresh and freeze thawed artichoke hearts were stored at 4°C for 7 days. Packaging t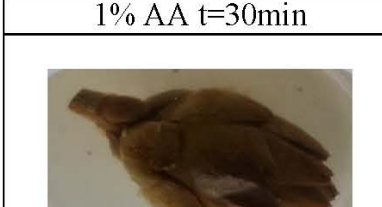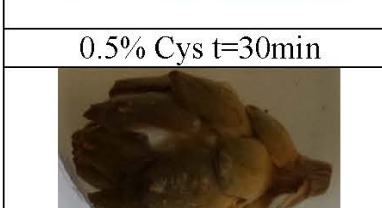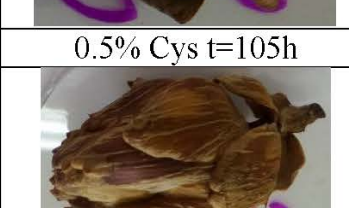rials were done with a manual thermal sealer; these were presented in section 4.5.2 Figure 4.6. Artichokes were stored at 4°C Nüve incubators for 7 days; each day observed visually pictures were taken.

In Figure 5.44, images for packaging trials with CMC-GLY films of fresh artichoke stalks with and without citric acid treatment before and after storage period were shown. No significant effect on preventing browning reaction was observed in packed stalks.

Figure 5.44 Packaging trial of artichoke stalks with and without citric acid treatment

In Figure 5.45, images for fresh cut artichoke heart packed with CA-CMC-GLY; CMC-GLY; CMC-GLY-STA-Tw80-CA films and treated with CA solution pre-

packaging were shown. First line shows images initial and second line from final conditions. In all samples effect of packing on browning were negative.

Figure 5.45 Packaging Trial with Fresh Artichoke Heart

In Figure 5.46, images for fresh cut artichoke heart packed with CA-CMC-GLY; CMC-sorbitol-CA; CMC-GLY-STA-Tw80-CA films were shown. First line shows images initial and second line from final conditions. No significant effect of packaging on prevention of browning was observed.

Figure 5.46 Packaging Trial with Freeze-Thawed Artichoke Hearts

In Figure 5.47, images for fresh cut artichoke heart packed with CMC-GLY-STA-Tw80 film and treated with CA solution pre-packaging were shown. First three images show initial and last two images show final conditions.

Figure 5.47 Packaging Trial with Freeze-Thawed Artichoke Hearts (Soaked in CA solution)

In Figure 5.48, images for fresh cut artichoke heart packed with two layers of CMC-GLY-STA-Tw80 film and treated with CA solution pre-packaging were shown. First three images show initial and last two images show final conditions. Effect of second layer on browning was found positive, prevents browning.

Figure 5.48 Packaging Trial with Freeze-Thawed Artichoke Hearts (soaked in CA solution) with two layers of packaging material

In Figure 5.49, images for fresh cut artichoke heart packed with NCMC-GLY film and treated with CA solution pre-packaging were shown. First image show initial and last two images show final conditions.

Figure 5.49 Packaging Trial with Synthesized CMC[10]

---

[10] Packaging trials were applied with apple samples, since there were not artichoke samples at that time films were casted from NCMC.

CHAPTER 6

CONCLUSIONS

Biodegradable packaging film materials with high barrier (water vapour, gas, moisture etc.) properties are in demand in food industry especially for fresh-cut fruits&vegetables. The aim of this thesis was to utilize artichoke by-products for biodegradable packaging materials in order to preserve fresh-cut artichokes. Thus, the extraction process -with minimum additive- was designed, cellulosic film materials obtained *via* green methods were successfully used to cast the packaging films.

Therefore, in the thesis 2 different approaches were used. The first one was to extract lignocellulosic biomass in different fractions by using mild chemical treatment. Carboxymethyl cellulose was also produced from cellulose fractions. Second was to produce MFC directly by mechanical methods. The later approach can be considered as an environmentally friendly process. Supermasscolloider technique was enough to obtain cellulose in micro fibrillated form with almost 100% extraction yield.

Various combinations of polysaccharide based extract fractions, CMC and MFC at different concentrations were used to prepare the films. Most important challenge for the films was moisture resistance and also prevention of oxygen transfer; since the film interact with fresh-cut surfaces subjected to respiration and moisture lost. Promising results were obtained for different preparates with acceptable properties which were able to meet the expectations for a biodegradable film. The main properties of these film forming materials were summarized in Table 6.1.

As seen from the table 6.1, hemicellulose films were poor in hydrophobicity and sealibility with low barrier properties. Hemicellulosic films were improved with lignin and wax combinations LWH films were very elastic with a good strength and sealability properties. But still hydrophilicity was a problem that cause low moisture resistance and barrier properties. Lignin fractions were found to be essential to enhance the elasticity.

Table 6.1 General Comparison of Films Produced[11]

PROPERTIES OF FILMS							
MAIN POLYMER SOURCE	Elasticity	Gas Barrier Property	Strength	Visual Acceptability	Homogeneity / Reproducibility	Resistance to DW	Sealability
Hemicellulose	2	1	2	1	3	1	1
Na-CMC	2	4	4	4	4	1	3
NCMC	2	4	2	3	1	1	3
LHW	4	1	3	3	3	1	3
CMC Emulsion films	3	3	3	4	3	3	4
MFC Films	2	3	2	4	4	2	1
MFC+CMC Emulsion Films	4	3	4	4	4	3	1
Chi+MFC+CMC films	4	3	4	4	2	4	1

Oxygen permeability properties were improved both in hemicellulosic and CMC films. Some additives such as stearic acid, chitosan and wax were needed to increase the hydrophobicity of films in order to prevent film surfaces from moisture loss.

CMC films emulsified with stearic acid gained elasticity, hydrophobicity, and sealability. CMC films combined with MFC were much more flexible with high mechanical strength and visual properties, but the sealability properties were not good. Chitosan addition into the film combinations improved the hydrophobicity.

Film characteristics were determined by using different physicochemical and morphological methods. Results of FTIR analyses proved that, extraction of cellulose from artichoke leaves were successfully conducted. Comparison of FTIR diagram of MFC films gave comparable and similar pattern with FTIR diagram for cellophane presented in literature (Shimadzu-Corporation 2006). With the help of FTIR data DS values were calculated for different fractions of synthesized CMC (NCMC). When results compared with Na-CMC (Sigma Aldrich) sample, synthesize of NCMC was proved. But, some physicochemical properties of NCMC that affecting its aqueous solubility made it difficult usage of NCMC in film formation. Results of PCM analyses

---

[11] Comparisons were made relatively within all films produced, and subjectively without any quantitative experiments (except gas barrier and elasticity properties). Score values for evaluations: 1-Bad/not enough; 2-might be developed/need to be studied; 3-Promising but not enough; 4-Good; NS: not studied yet

showed the existence of cellulose microfibrils; it was evident that their original structure and dimensions were protected before and after dehydration, within solution or powdered form, or in film solution form. Particle sizes of the micro fibrils those calculated *via* SEM & PCM results were found averagely 50-200 μm in length and 5-30 μm in width. Most of the films prepared had smooth surfaces and, homogenous and dense structure. Addition of wax into the formulations decreased the thermal stability of the films while presence of MFC increased. Thermal analyses proved sealability of films obtained by extracted fractions from artichoke at 200-250°C temperature intervals. But, presence of MFC in films hindered the heat sealing ability.

It can be concluded that, different films were successfully prepared from polysaccharide based extracts. Barrier properties and mechanical strength were found to be high in case of CMC and MFC based films. Impact of MFC on these properties was very positive while negative effects were observed on the sealability of the films. In order to achieve a successful packaging for fresh-cut produce, sealability of the films is thought to be important. Therefore, in the light of findings in this thesis, MFC film properties should be improved for large-scale processes to extend the shelf life of the fresh-cut.

In this thesis; apart from the MFC based films, other films from polysaccharide materials showed acceptable properties. There have been research on bio-based packaging films present in the literature, but moisture resistant and stable films have not been prepared yet as far as current knowledge. Therefore, the challenge was to produce hydrophobic and strong films without addition of petroleum derived raw materials.

REFERENCES

Abdellatief A., Welt B.A. 2012. Comparison of New Dynamic Accumulation Method for Measuring Oxygen Transmission Rate of Packaging against the Steady-State Method Described by ASTM D3985. Packaging Technology and Science.

Abdul Khalil H. P. S., Davoudpour Y., Islam M. N., Mustapha A., Sudesh K., Dungani R., Jawaid M. 2014. Production and modification of nanofibrillated cellulose using various mechanical processes: A review. Carbohydrate Polymers 99: 649-665.

Adler E. 1977. Lignin chemistry—past, present and future. Wood Science and Technology 11 (3): 169-218.

Ahvenainen R. 2003. Novel food packaging techniques: CRC Press. http://books.google.com.tr/books?id=rI7b34Pwjv8C

Albertsson A.C., Edlund U., Varma I. K. 2011. Synthesis, Chemistry and Properties of Hemicelluloses. In Biopolymers – New Materials for Sustainable Films and Coatings, 133-150. John Wiley & Sons, Ltd.

Aliyu M. Hepher M.J. 2000. Effects of ultrasound energy on degradation of cellulose material. Ultrasonics Sonochemistry 7 (4): 265-268.

Amodio M.L., Cabezas-Serrano A.B., Peri G., Colelli G. 2011. Post-cutting quality changes of fresh-cut artichokes treated with different anti-browning agents as evaluated by image analysis. Postharvest Biology and Technology 62 (2): 213-220.

Ankerfors M. 2012. Microfibrillated cellulose: Energy-efficient preparation techniques and key properties. Department of Fibre and Polymer Technology, KTH Royal Institute of Technology, Stockholm, Sweden.

Anon 2013-H. "Hemicellulose," Wikipedia, The Free Encyclopedia 2012a [cited November 25 2013]. Available from http://en.wikipedia.org/w/index.php?title=Hemicellulose&oldid=576073622

Anon 2013-L. "Lignin," Wikipedia, The Free Encyclopedia 2012b [cited November 25 2013]. Available from http://en.wikipedia.org/w/index.php?title=Lignin&oldid=580140045

Aulin C., Gällstedt M., Lindström T. 2010. Oxygen and oil barrier properties of microfibrillated cellulose films and coatings. Cellulose 17 (3) : 559-74.

Azeredo H.M.C., Miranda K.W.E., Rosa M.F., Nascimento D.M. De Moura M.R. 2012. Edible films from alginate-acerola puree reinforced with cellulose whiskers. LWT - Food Science and Technology 46 (1): 294-97.

Bandelin 2015, http://bandelin.com/produkte/ultrasonic_homogenizers/sonopuls-hd-2070-und-hd-2200/?lang=en , Accessed on April 2015.

Başay S., Tokuşoğlu Ö. 2013. The proximate composition and quality characteristics in artichoke (cynara scolymus l.) varieties developed with clonal selection. Journal of Food, Agriculture & Environment 11 (1): 584-87.

Cabezas-Serrano A.B., Amodio M. L., Cornacchia R., Rinaldi R., Colelli G.. 2009. Screening quality and browning susceptibility of five artichoke cultivars for fresh-cut processing. Journal of the Science of Food and Agriculture. 89 (15): 2588-2594.

Cefola M., D'Antuono I., Pace B., Calabrese N., Carito A., Linsalata V., Cardinali A., 2012 Biochemical relationships and browning index for assessing the storage suitability of artichoke genotypes. Food Research International. 48 (2): 397-403.

Chakraborty A., Mohini S., Kortschot M. 2005. Cellulose microfibrils: A novel method of preparation using high shear refining and cryocrushing. In Holzforschung.

Chen W., Yu H., Liu Y. 2011. Preparation of millimeter-long cellulose i nanofibers with diameters of 30–80 nm from bamboo fibers. Carbohydrate Polymers 86 (2): 453-461.

Del Nobile M.A., Conte A., Scrocco C., Laverse J., Brescia I., Conversa G., Elia A. 2009. New packaging strategies to preserve fresh-cut artichoke quality during refrigerated storage. Innovative Food Science & Emerging Technologies 10 (1): 128-133.

Dhall R.K. 2012. Advances in edible coatings for fresh fruits and vegetables: A review. Critical Reviews in Food Science and Nutrition 53 (5): 435-50.

Downey G. 1998. Food and food ingredient authentication by mid-infrared spectroscopy and chemometrics. Trends in Analytical Chemistry 17 (7): 418-24.

Downey G., McIntyre P., Davies A.N. 2003. Geographic classification of extra virgin olive oils from the eastern Mediterranean by chemometric analysis of visible and near-infrared spectroscopic data. Applied Spectroscopy 57:158-163.

Drout M., Smith L. 2012. How to read a dendrogram. http://wheatoncollege.edu/lexomics/files/2012/08/How-to-Read-a-Dendrogram-Web-Ready.pdf, Wheaton College, National Endowment for the Humanities, Accessed on January 2017.

Eaton P., West P. 2011. Atomic Force Microscopy, Oxford University Press, New York, USA.

Edlund U., Zhu Ryberg Y., Albertsson A. C. 2010. Barrier Films from Renewable Forestry Waste. Biomacromolecules 11 (9): 2532-2538.

Engineering toolbox, 2015. Accessed on 18.12.2015, http://www.engineeringtoolbox.com/young-modulus-d_417.html

Eriksson L., Byrne T., Johansson E., Trygg J., Vikström C. 2013. Multi- and megavariate data analysis basic principles and applications: MKS Umetrics.

Falguera V., Quintero J. P., Jiménez A., Muñoz J. A., Ibarz A. 2011. Edible films and coatings: Structures, active functions and trends in their use. Trends in Food Science & Technology. 22 (6): 292-303.

Fang J.M., Sun R.C., Salisbury D., Fowler P., Tomkinson J. 1999. Comparative study of hemicelluloses from wheat straw by alkaline and hydrogen peroxide extractions. Polymer Degradation and Stability 66 (3): 423-432.

Felton L.A. 2013. Mechanisms of polymeric film formation. International Journal of Pharmaceutics 457: 423-427.

Femenia J. A., Robertson K.W., Waldron R., Selvendran R. 1998. Cauliflower (*Brassica oleracea L*), globe artichoke (*Cynara scolymus*) and chicory witloof (*Cichorium intybus*) processing by-products as sources of dietary fibre. Journal of the Science of Food and Agriculture. 77 (4): 511-518.

Ferracane R., Pellegrini N., Visconti A., Graziani G., Chiavaro E., Miglio C., Fogliano V. 2008. Effects of different cooking methods on antioxidant profile, antioxidant capacity, and physical characteristics of artichoke. J Agric Food Chem 56 (18): 8601-8608.

Fiore V., Valenza A., Di Bella G. 2011. Artichoke (*Cynara cardunculus L.*) Fibres as potential reinforcement of composite structures. Composites Science and Technology 71 (8): 1138-1144.

Ghidelli C., Mateos M., Rojas-Argudo C., Pérez-Gago M. B. 2013. Antibrowning effect of antioxidants on extract, precipitate, and fresh-cut tissue of artichokes. LWT - Food Science and Technology 51 (2): 462-468.

Giménez M., Olarte C., Sanz S., Lomas C., Echávarri J.F., Ayala F. 2003. Relation between spoilage and microbiological quality in minimally processed artichoke packaged with different films. Food Microbiology 20 (2): 231-242.

Goksu E.I., Karamanlioglu M., Bakir U., Yilmaz L., Yilmazer U. 2007. Production and Characterization of Films from Cotton Stalk Xylan. Journal of Agricultural and Food Chemistry 55 (26): 10685-10691.

Han, J.H. 2005. Innovations in food packaging: Elsevier Science. http://books.google.com.tr/books?id=MbVtx091tCUC

Hansen N.M.L., Plackett D. 2008. Sustainable Films and Coatings from Hemicelluloses: A Review. Biomacromolecules 9 (6): 1493-1505.

Harsa H.S., Buyukkileci O.B., Niranjan K., Samli M. 2013. Low environmental impact polysaccharide based packaging solutions for fresh cut fruits and vegetables Istanbul: Izmir Institute of Technology & University of Reading. Project Meeting Report.

Heinze T., Barsett H., Ebringerova A., Harding S. E., Heinze T. 2005. Polysaccharides I: Structure, Characterisation and Use: Springer Verlag, 1120 U.S. Highway 22 East, Bridgewater, NJ, 08807.

Ghosh A.K., Bandyopadhyay P. 2012. Polysaccharide-protein interactions and their relevance in food colloids. The complex world of polysaccharides. Intech Publishing, Crotia.

Innventia 2015, http://www.innventia.com/en/Our-Expertise/New-materials/Barriers-and-films/, Accessed on June 2015.

Iwamoto S., Nakagaito A. N., Yano H. 2007. Nano-fibrillation of pulp fibers for the processing of transparent nanocomposites. Applied Physics A: Materials Science and Processing 89 (2): 461-466.

Jia R.X., Shen W., Xie M., Abid M., Jabbar S., Wang P., Zeng X., Wu T. 2015. Stabilizing oil-in-water emulsion with amorphous cellulose. Food Hydrocolloids 43: 275-282.

Jongen W. 2005. Improving the Safety of Fresh Fruit and Vegetables. CRC, Woodhead Publ. Ltd., Cambridge, UK. 639 pp

Kroschwitz J.I. 2004. Encyclopedia of polymer science and technology: J. Wiley & sons. https://books.google.com.tr/books?id=8iZaAAAAYAAJ

Laaman T.R. 2011. Hydrocolloids in food processing: Wiley. http://books.google.com.tr/books?id=skliBKgnVMgC

Lattanzio V., Cardinali A., Venere D.D., Linsalata V., Palmieri S. 1994. Browning phenomena in stored artichoke (*Cynara scolymus l.*) heads: Enzymic or chemical reactions? Food Chemistry 50 (1): 1-7.

Lattanzio V., Kroon P. A., Linsalata V., Cardinali A. 2009. Globe artichoke: A functional food and source of nutraceutical ingredients. Journal of Functional Foods 1 (2): 131-144.

Lavoine N., Desloges I., Dufresne A., Bras J. 2012. Microfibrillated cellulose - Its barrier properties and applications in cellulosic materials: A review. Carbohydrate Polymers 90 (2): 735-764.

Lee D.S., Yam K.L., Piergiovanni L. 2008. Food packaging science and technology: CRC Press. https://books.google.com.tr/books?id=jmPNBQAAQBAJ

Li Q., Renneckar S. 2009. Molecularly thin nanoparticles from cellulose: Isolation of sub-microfibrillar structures. Cellulose 16 (6): 1025-1032.

Li Q., Renneckar S. 2011. Supramolecular structure characterization of molecularly thin cellulose nanoparticles. Biomacromolecules 12 (3): 650-659.

Lin D., Zhao Y. 2007. Innovations in the development and application of edible coatings for fresh and minimally processed fruits and vegetables. Comprehensive Reviews in Food Science and Food Safety 6 (3): 60-75.

Lutz M., Henríquez C., Escobar M. 2011. Chemical composition and antioxidant properties of mature and baby artichokes (*Cynara scolymus l.*), raw and cooked. Journal of Food Composition and Analysis 24 (1): 49-54.

Masuko 2015, http://www.masuko.com/English/product/Masscolloder6-2.html, Accessed on June 2015.

Mazeau K. 2015. The hygroscopic power of amorphous cellulose: A modeling study. Carbohydrate Polymers 117: 585–591.

Mchugh T.H., Avena-Bustillos R., Krochta J.M. 1993. Hydrophilic Edible Films: Modified Procedure for Water Vapor Permeability and Explanation of Thickness Effects. Journal of Food Science 58: 899–903.

Melodea 2015, http://www.melodea.eu/Default.asp?PageId=104256 , Accessed on June 2015.

Menon V., Rao M. 2012. Trends in bioconversion of lignocellulose: Biofuels, platform chemicals & biorefinery concept. Progress in Energy and Combustion Science. 38 (4): 522-550.

Microcorp 2015, http://www.microfluidicscorp.com/microfluidizers/lab-machines/m-110p/ Accessed on June 2015.

Miller K. S., Krochta J. M. 1997. Oxygen and aroma barrier properties of edible films: A review. Trends in Food Science and Technology. 8 (7): 228-237.

Mishra S.P., Manent A.-S., Chabot B., Daneault C. 2011. Production of nanocellulose from native cellulose – various options utilizing ultrasound. Vol. 7

Moon R.J., Martini A., Nairn J., Simonsen J., Youngblood J. 2011. Cellulose nanomaterials review: structure, properties and nanocomposites. Chemical Society Reviews 40 (7): 3941-3994.

Moura M.R., Avena-Bustillos R.J., McHugh T.H., Wood D.F., Otoni C.G., Mattoso L.H.C. 2011. Miniaturization of cellulose fibers and effect of addition on the mechanical and barrier properties of hydroxypropyl methylcellulose films, J. Food Eng. 104: 154-160.

Nature 2015, http://www.nature.com/articles/srep17703 , Accessed on June 2015.

Niranjan K., Harsa H.S. 2013. Low environmental impact polysaccharide based packaging solutions for fresh cut fruits and vegetables. Izmir. Project Meeting Report.

Pascall M.A, Lin S.J. 2013. The Application of Edible Polymeric Films and Coatings in the Food Industry. J Food Process Technol. 4: e116.

Pashley R.M., Karaman M.E., Ninham B.W. 2001. Method and apparatus for the measurement of film formation temperature of a latex, Patent, US 6275049 B1.

Peng F., Peng P., Xu F., Sun R.-C. 2012. Fractional purification and bioconversion of hemicelluloses. Biotechnology Advances 30 (4): 879-903.

Peng, Y., Gardner D. J., Han Y. 2012. Drying cellulose nanofibrils: In search of a suitable method. Cellulose 19 (1): 91-102.

Peng Y., Han Y., Gardner D. J. 2012. Spray-drying cellulose nanofibrils: Effect of drying process parameters on particle morphology and size distribution. Wood and Fiber Science 44 (4): 448-461.

Pereda A.D., Aranguren M. I., Marcovich N.E. 2014. Polyelectrolyte films based on chitosan/ olive oil and reinforced with cellulose nanocrystals, Carbohydrate Polymers 101: 1018-1026.

Petersen K., Vaeggemose Nielsen P., Bertelsen G., Lawther M., Olsen M.B., Nilsson N.H., Mortensen G. 1999. Potential of biobased materials for food packaging. Trends in Food Science and Technology 10 (2): 52-68.

Phan T.D., Debeaufort F., Luu D., Voilley A. 2005. Functional Properties of Edible Agar-Based and Starch-Based Films for Food Quality Preservation. Journal of Agricultural and Food Chemistry 53 (4): 973-981.

Pitak N., Rakshit S.K. 2011. Physical and antimicrobial properties of banana flour/chitosan biodegradable and self sealing films used for preserving fresh-cut vegetables. LWT - Food Science and Technology 44 (10): 2310-15.

Qi H., Hu W., Jiang A., Tian M., Li Y. 2011. Extending shelf-life of Fresh-cut 'Fuji' apples with chitosan-coatings. Innovative Food Science & Emerging Technologies 12 (1): 62-66.

Qua, E.H., Hornsby P.R., Sharma H.S.S., Lyons G. 2011. Preparation and characterisation of cellulose nanofibres. Journal of Materials Science 46 (18): 6029-6045.

Rastogi V., Stanssens D., Samyn P. 2014. Mechanism for tuning the hydrophobicity of microfibrillated cellulose films by controlled thermal release of encapsulated wax. Materials 7 (11): 7196.

Rein D. M., Cohen Y. 2012. Cellulose as a novel amphiphilic coating for oil-in-water and water-in-oil dispersions. Journal of Colloid and Interface Science 386: 456-63.

Ricci I., Amodio M.L., Colelli G. 2013. Influence of pre-cutting operations on quality of fresh-cut artichokes (*Cynara scolymus l.*): Effect of harvest dates. Postharvest Biology and Technology 83 (0): 90-96.

Robertson, G.L. 2005. Food packaging: Principles and practice, second edition: Taylor & Francis. https://books.google.com.tr/books?id=NFRR6GayR74C

Sangsuwan J., Rattanapanone N., Rachtanapun P. 2008. Effect of chitosan/methyl cellulose films on microbial and quality characteristics of fresh-cut cantaloupe and pineapple. Postharvest Biology and Technology 49 (3): 403-410.

Sárossy Z., Tenkanen M., Pitkänen L., Bjerre A.-B., Plackett D. 2013. Extraction and chemical characterization of rye arabinoxylan and the effect of β-glucan on the mechanical and barrier properties of cast arabinoxylan films. Food Hydrocolloids 30 (1): 206-16.

Shimadzu-Corporation. 2006. IR Solution FTIR control software, Ver.1.30. Spectra Library of IR Solution Software.

Shankar S., Reddy J.P., Rhim J.-W., Kim H.-Y. 2015. Preparation, characterization, and antimicrobial activity of chitin nanofibrils reinforced carrageenan nanocomposite films. Carbohydrate Polymers 117: 468-475.

Sleuth, Gourmet. 2012. Accessed on May 2013.Available from http://www.gourmetsleuth.com/articles/detail/artichokes.

Sluiter B., Hames R., Ruiz C., Scarlata J., Sluiter D., Templeton, Crocker D. 2011. Determination of Structural Carbohydrates and Lignin in Biomass. In NREL Laboratory Analytical Procedures. Colourado: National Renewable Energy Laboratory.

Sothornvit R., Rodsamran P. 2008. Effect of a mango film on quality of whole and minimally processed mangoes. Postharvest Biology and Technology 47 (3): 407-415.

Sun J., Tomkinson Y., Wang X., Xiao B. 2000. Physico-chemical and structural characterization of hemicelluloses from wheat straw by alkaline peroxide extraction. Polymer 41 (7): 2647-2656.

Tappi 2015, http://www.tappi.org/content/events/10nano/papers/25.2.pdf. Accessed on May 2015.

Todaro A., Peluso O., Catalano A.E., Mauromicale G., Spagna G. 2010. Polyphenol oxidase activity from three sicilian artichoke [*Cynara cardunculus L. Var. scolymus L. (Fiori)*] cultivars: studies and technological application on minimally processed production. J Agric Food Chem. 58 (3): 1714-1718.

Uetani K., Yano H. 2011. Nanofibrillation of wood pulp using a high-speed blender. Biomacromolecules 12 (2): 348-353.

Umetrics-AB. 2013. Principal component analysis and hierarchical cluster analysis. http://www.umetrics.com/ https://mksdataanalytics.com/. Help topics for Simca-Version 13.0.3.0. Accessed on January 2017.

Wang S., Cheng Q. 2009. A novel process to isolate fibrils from cellulose fibers by high-intensity ultra-sonication, part 1: Process optimization. Journal of Applied Polymer Science 113 (2): 1270-75.

Wayman M., Holkestad H.P., Rupert P. 1958. Reducing the ash content of cellulose. US Patent-2825646. Columbia Cellulose Company Ltd., British Columbia, Canada.

Yoshida C., Maciel V., Mendonça M., Franco T. 2014. Chitosan Biobased and Intelligent films: Monitoring pH variations, LWT - Food Science and Technology, 55 (1): 83-89

APPENDIXES

In this section, preliminary data for the characterization of film forming materials and films were presented. Figures and tables include data obtained from FTIR/FTIR-ATR Spectra, colour, opacity, thermal analyses, and film thickness measurements. Figures and Tables shown separately in different sections for each analysis type. FTIR results were shown in Appendix A, while FTIR-ATR results shown in Appendix B. Result data for thermal analyses (detailed peaks extracted from plots) in Appendix C. Thickness of some selected films were presented in Appendix D. Opacity values for films and colour variations in artichokes were presented in Appendix E. and F.

APPENDIX A. FTIR Spectra for cellulose derivatives

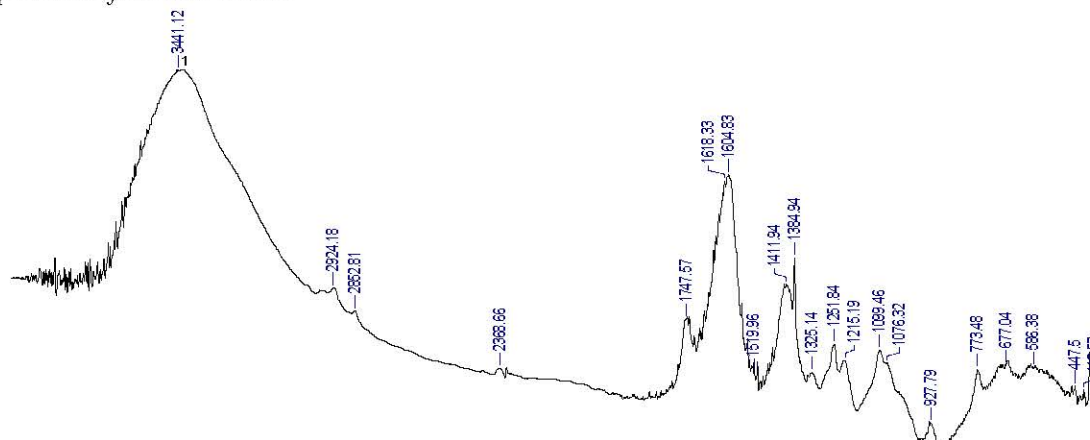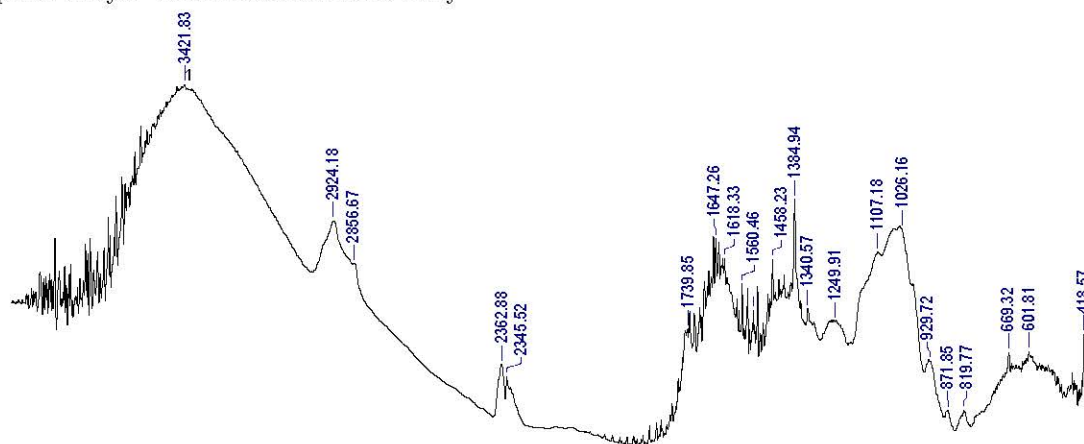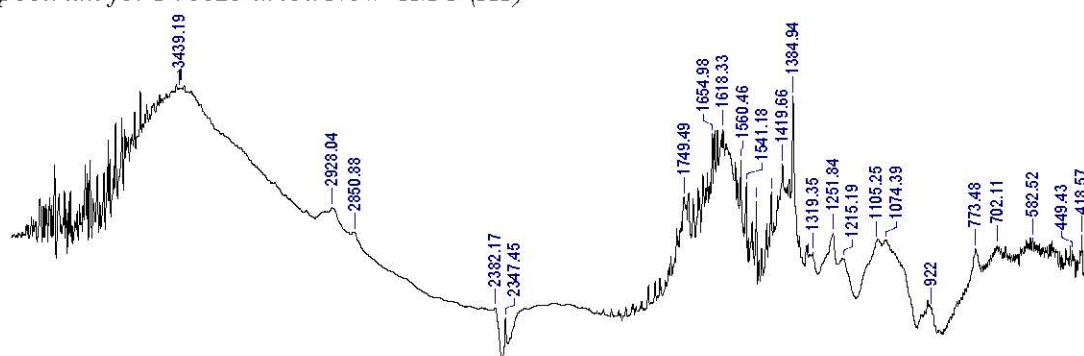*Spectrum for Cellulose*
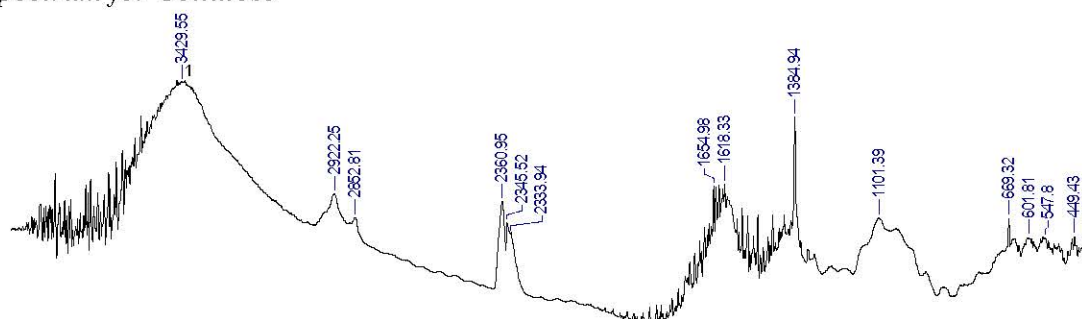
Spectrum for New CMC

Figure A. 1 FTIR peaks for powdered products from artichoke

Spectrum for Grinded Artichoke Leaf

Spectrum for Freeze dried New CMC (A1)
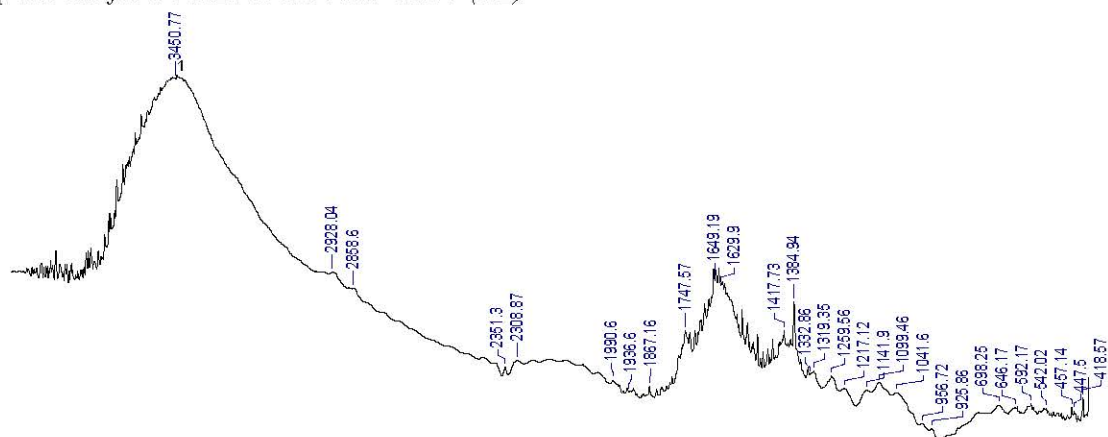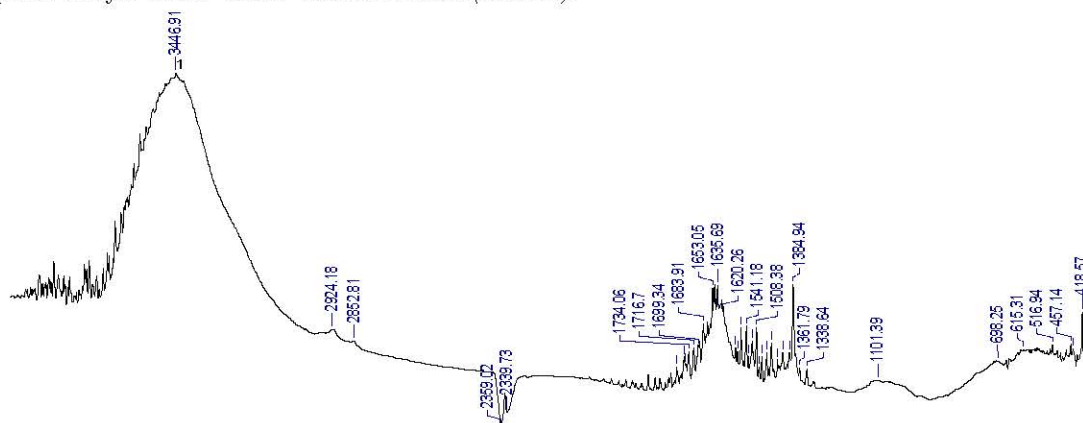
Spectrum for Freeze dried New CMC (A2)

Figure A. 1 (Continued)

(Continued on next page)

Spectrum for New CMC Un dissolved (NCU2)

Spectrum for New CMC Un dissolved (NCUU1)
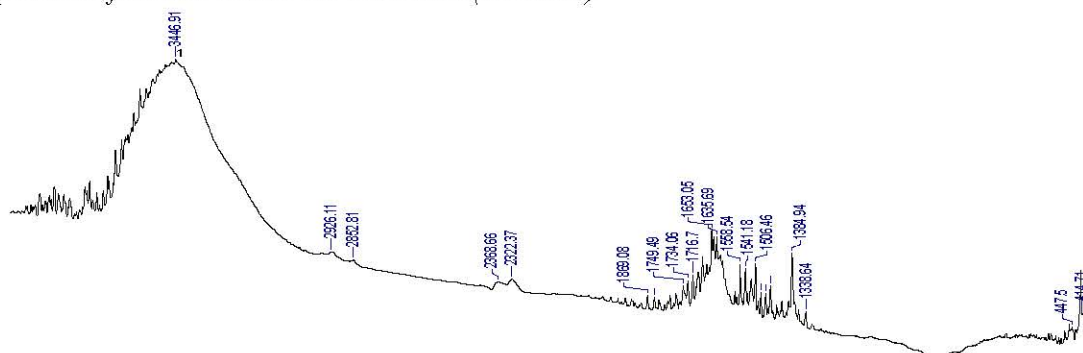
Figure A. 1   (Continued)

Table A. 1   FTIR Peaks Assignments for Cellulose Molecule

Peaks (cm⁻¹)	Assignments	Peaks (cm⁻¹)	Assignments
3422	OH stretching	1321	OH in plane bending
2896	CH stretching	1164	C-C ring breath
1644	H_2O bending	1111	C-O-C symmetry
1447	CH_2 bending	1055	C-O-C asymmetry
1375	CH & C-O bonds	897	β-glycosidase linkage

APPENDIX B. FTIR-ATR Peaks

Detailed diagrams for film forming components separately and together as in the film solution form were presented in Figure B.1.

Sample no.1 (wax in Et-OH : DW)

Sample no.2 (wax in Et-OH)

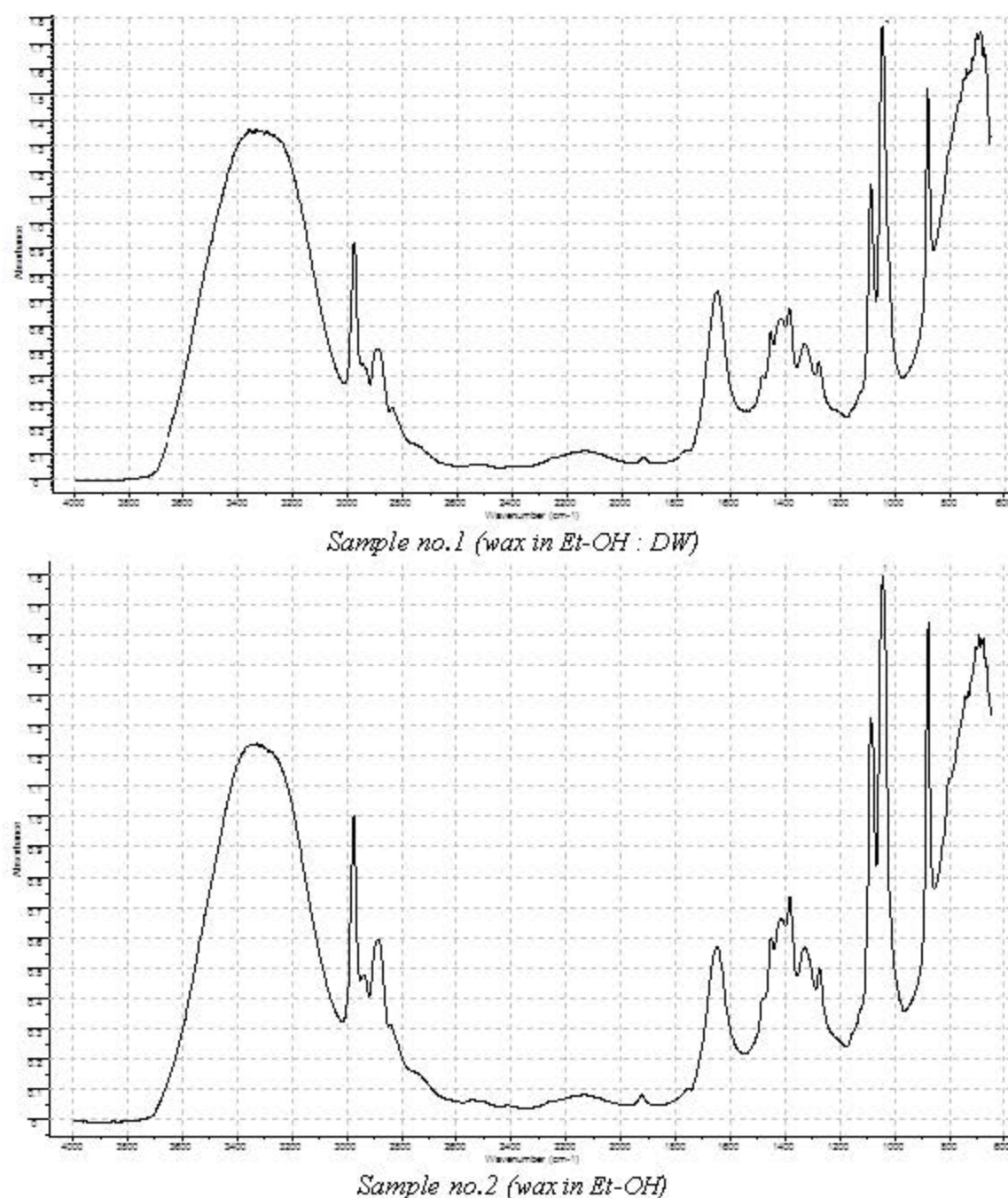Figure B. 1   FTIR ATR diagrams for films and film component solutions

(Continued on next page)
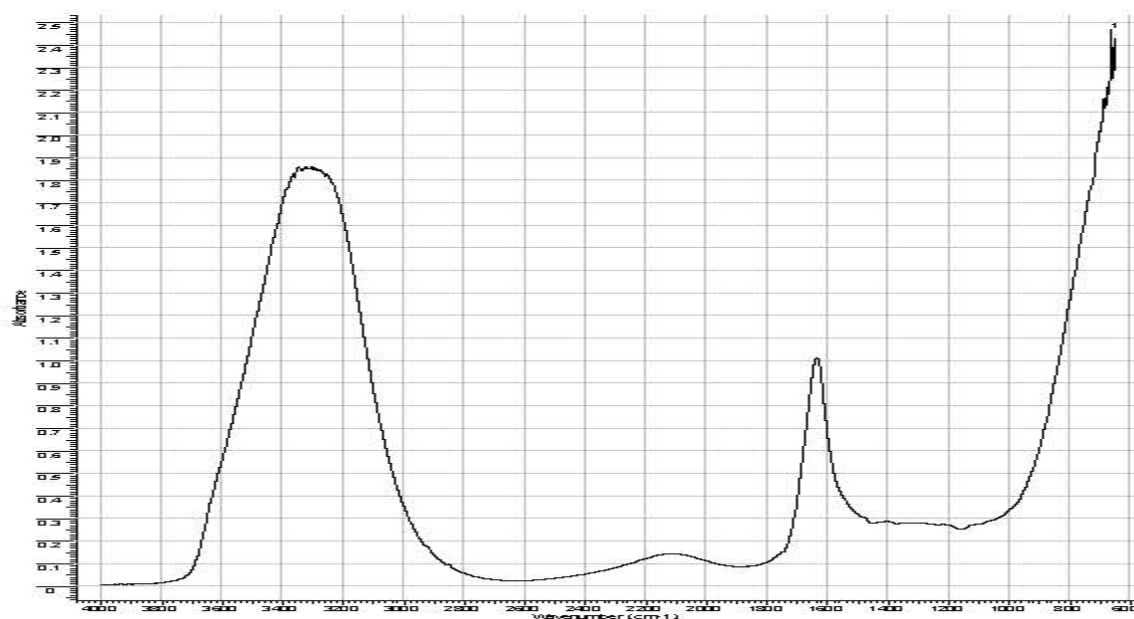
Sample no.3 (0.38% St-A : 0.4% Tw80 solution pH=11 UPW)
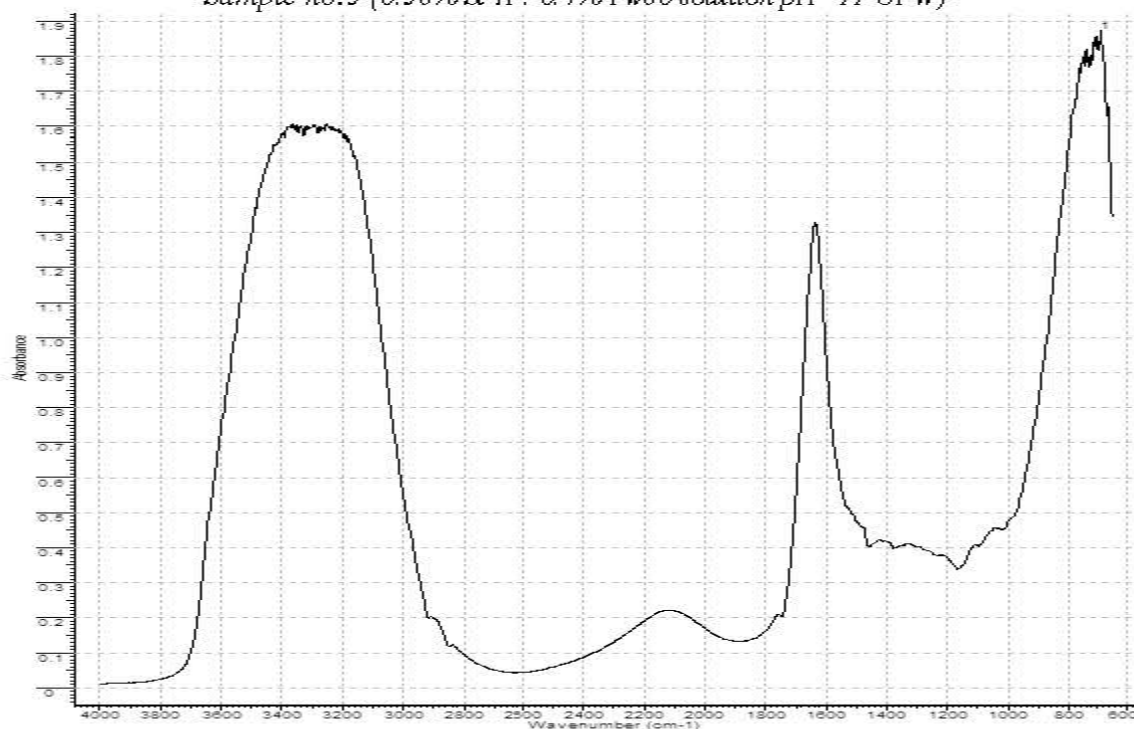
Sample no.4 (1% Na-CMC + 0.7 % GLY + 0.66% PEG 400 solution)

Figure B. 1   (Continued)

(Continued on next page)
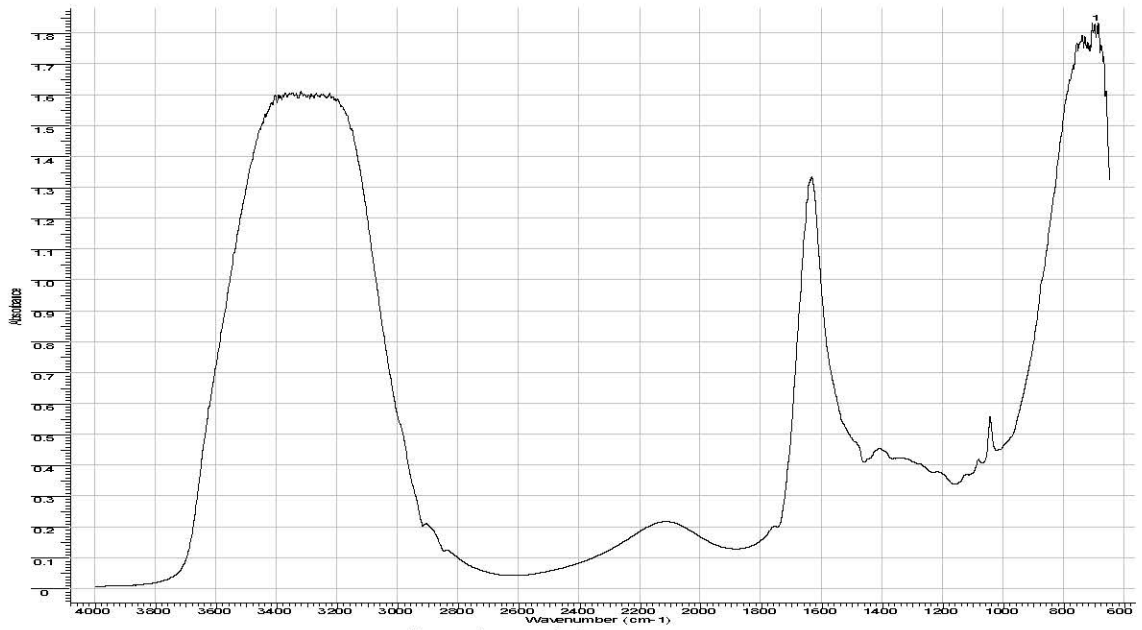
Sample no.5 (LH Fraction)
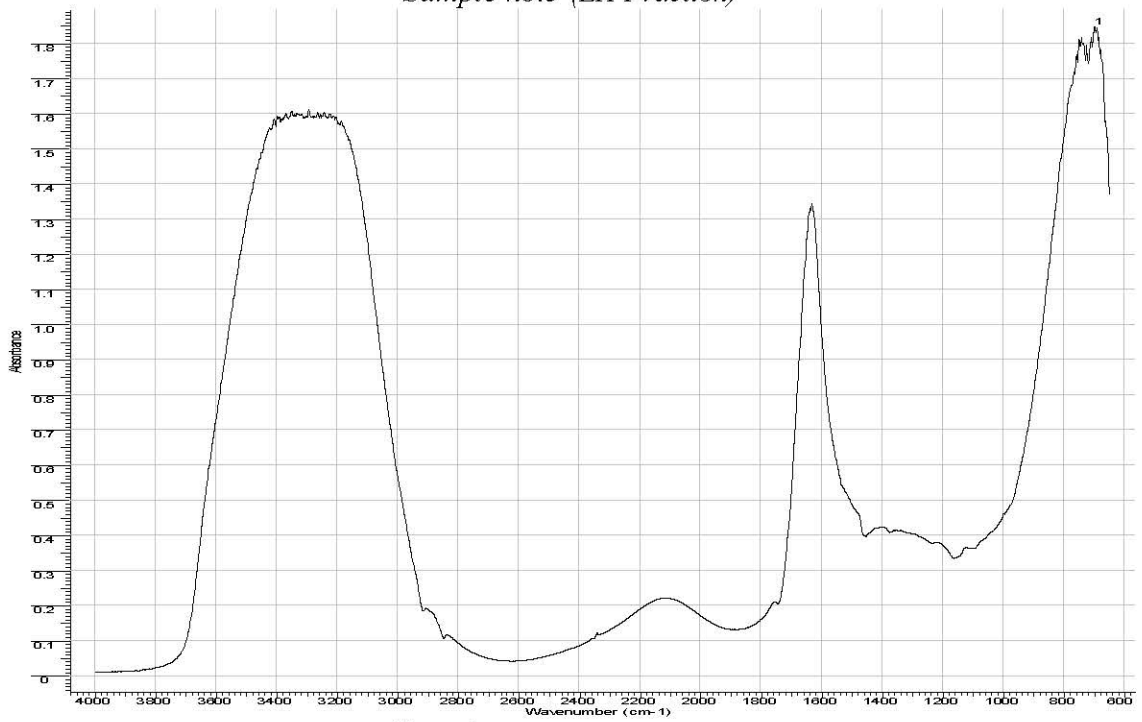
Sample no.6 (LHW Fraction)

Figure B. 1   (Continued)

(Continued on next page)
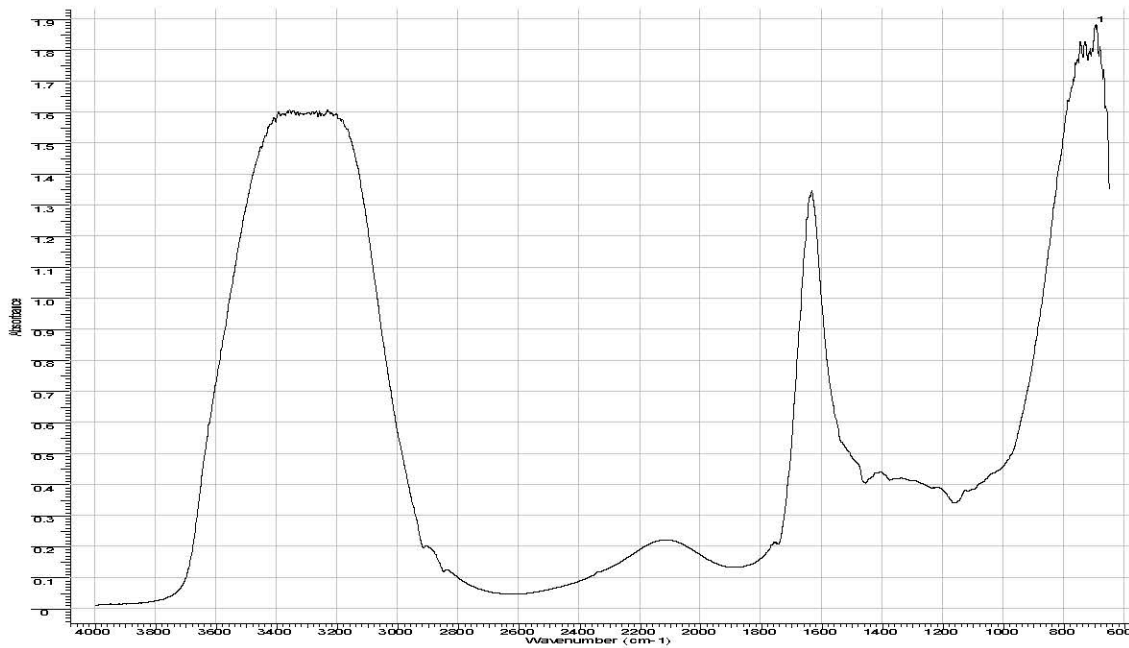
Sample no.7 (γ-GL 1ˢᵗ phase adsorption solution)
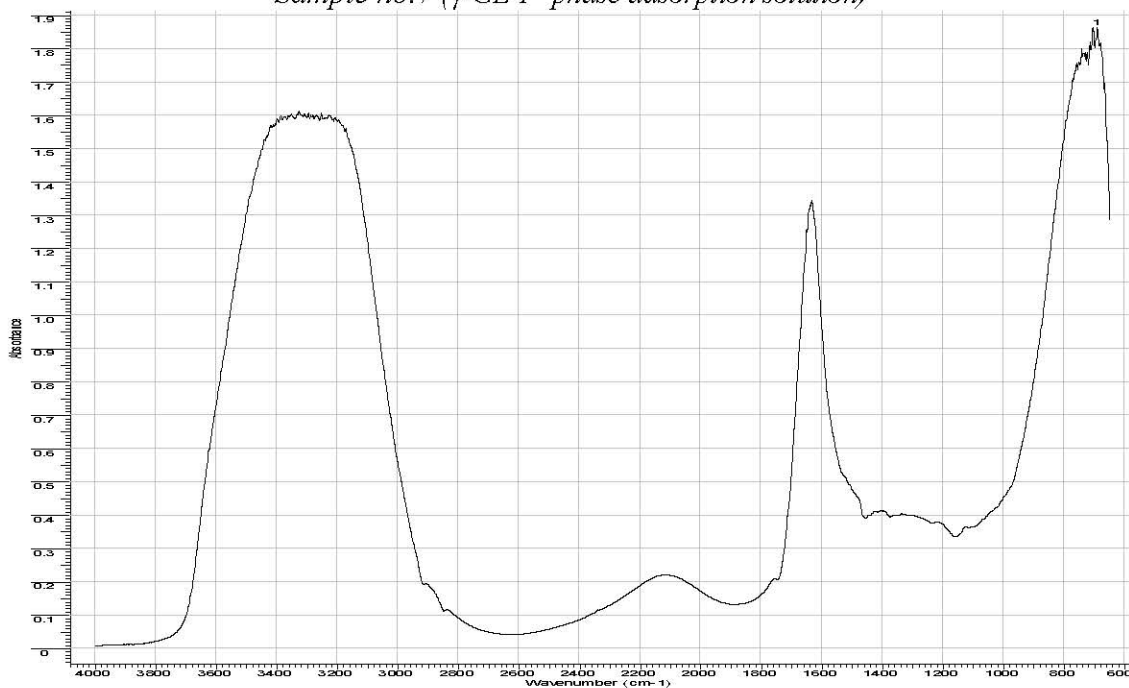
Sample no.8 (γ-GL 2ⁿᵈ phase adsorption solution)

Figure B. 1   (Continued)

(Continued on next page)
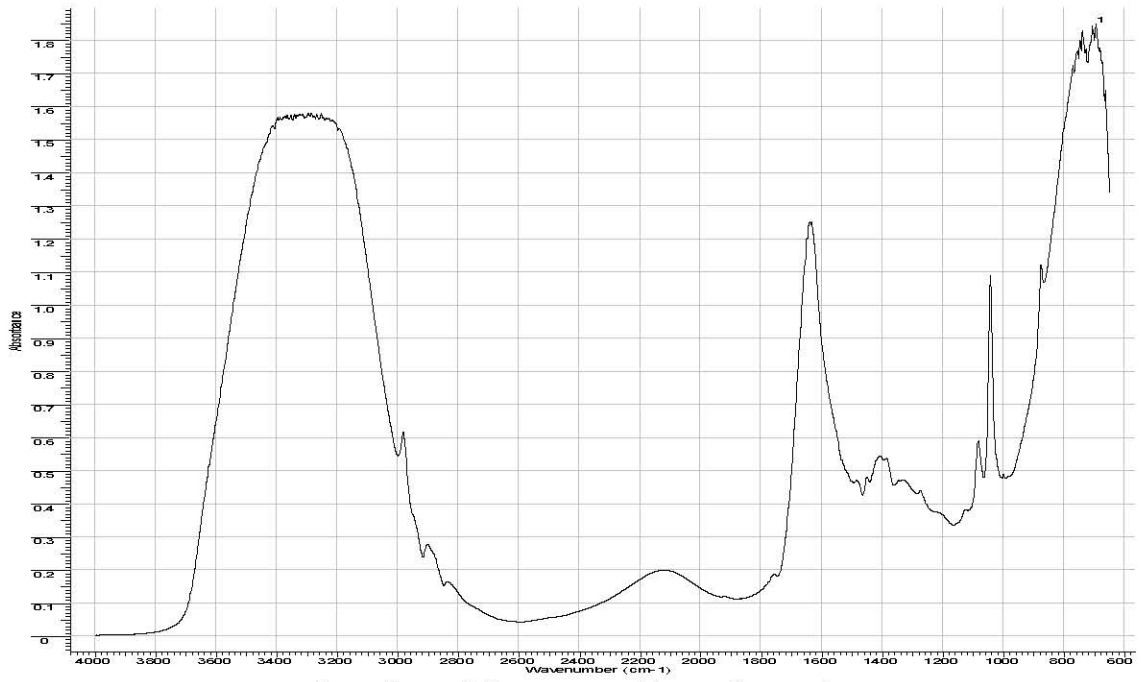
Sample no.9 (concentrated lignin fraction)
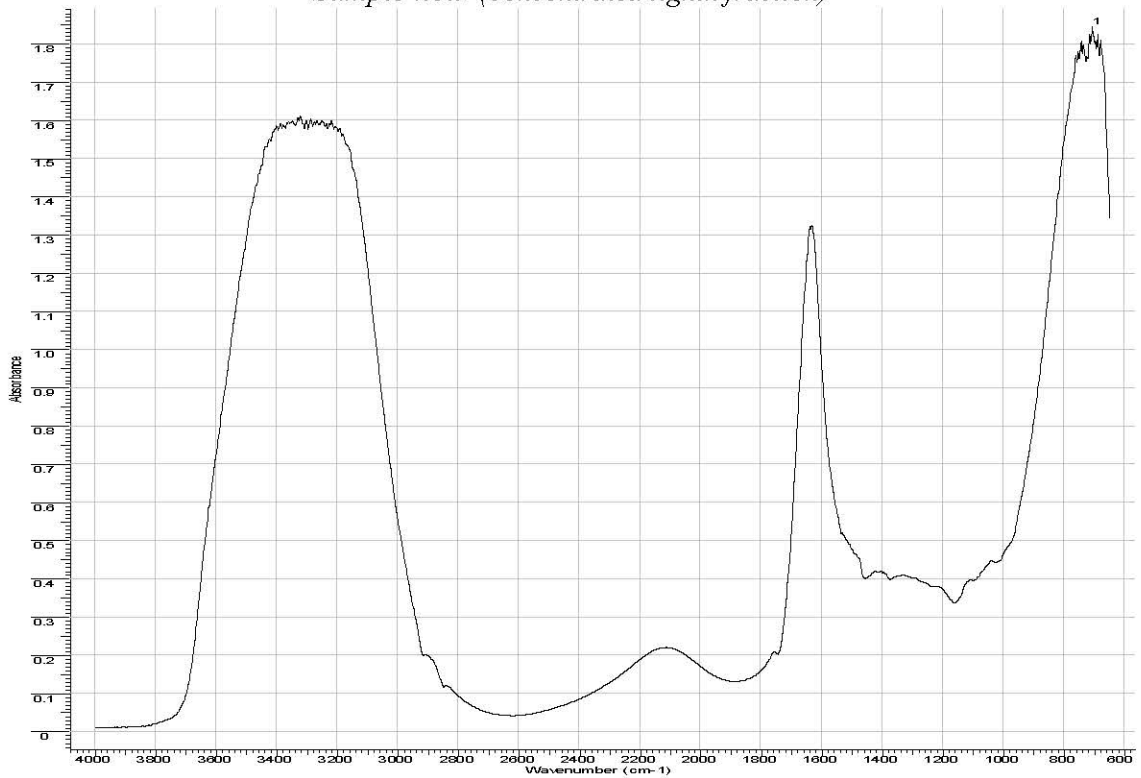
Sample no.10 (mfc-ncmc-gly-peg400-chi solution)

Figure B. 1   (Continued)

(Continued on next page)
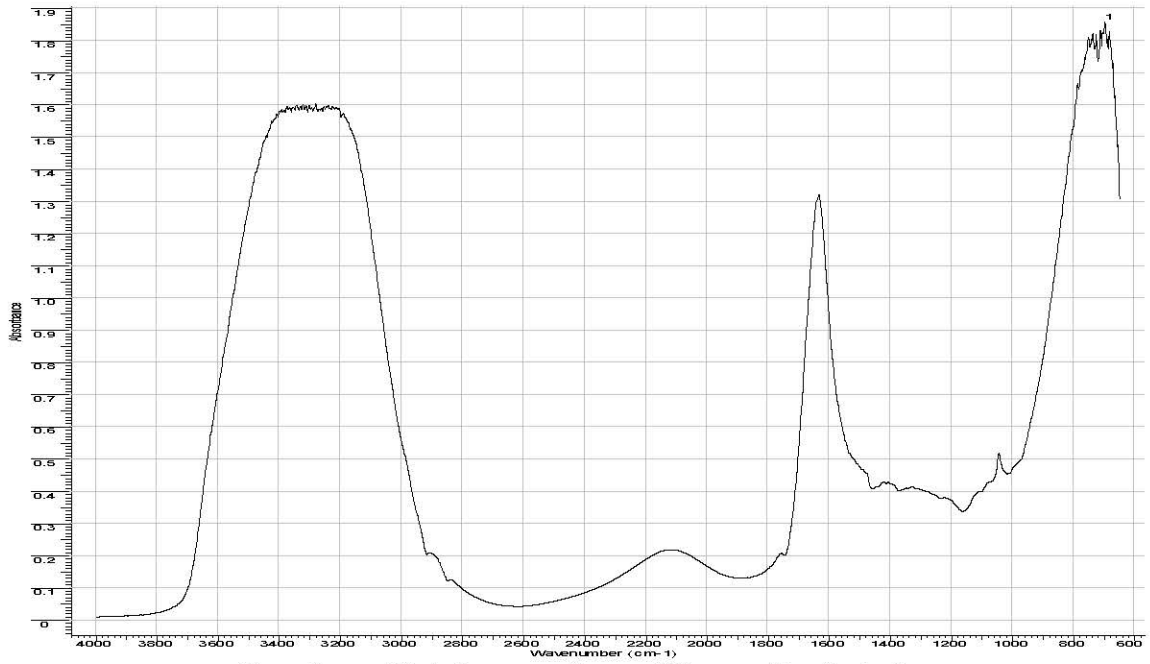
Sample no.11 (mfc-ncmc-gly-peg400-wax-chi solution)
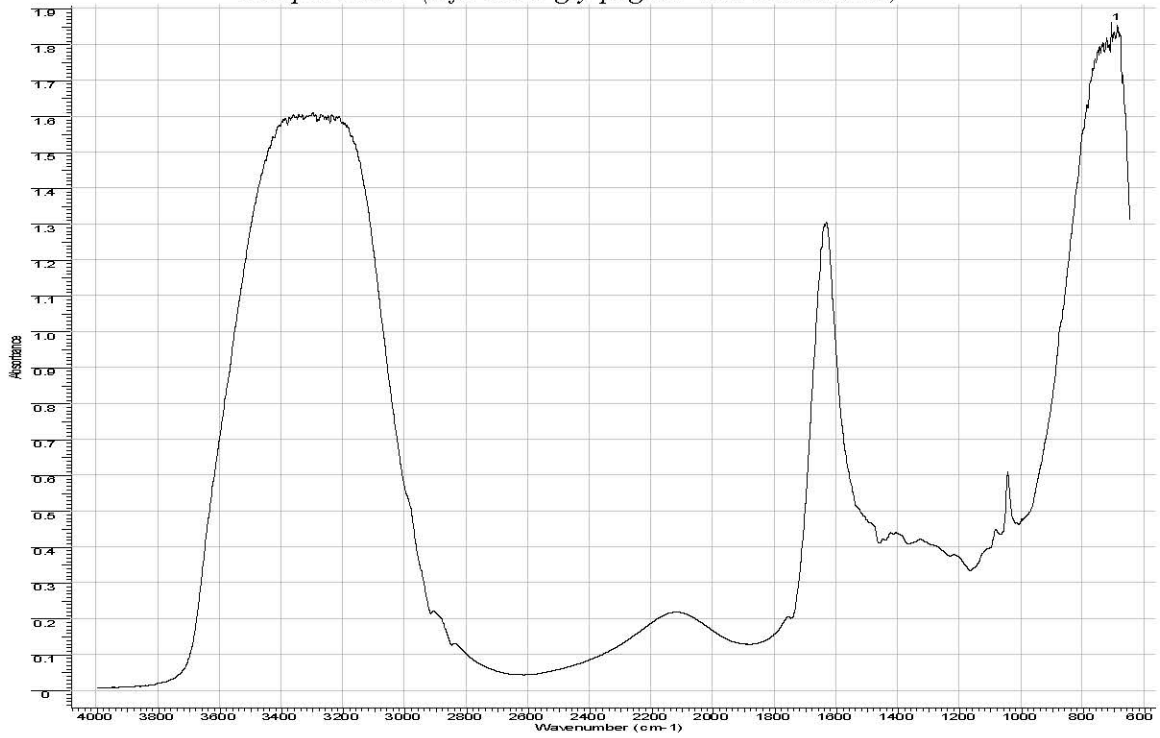
Sample no.12 (mfc-ncmc-gly-peg400 solution)

Figure B. 1 (Continued)

(Continued on next page)
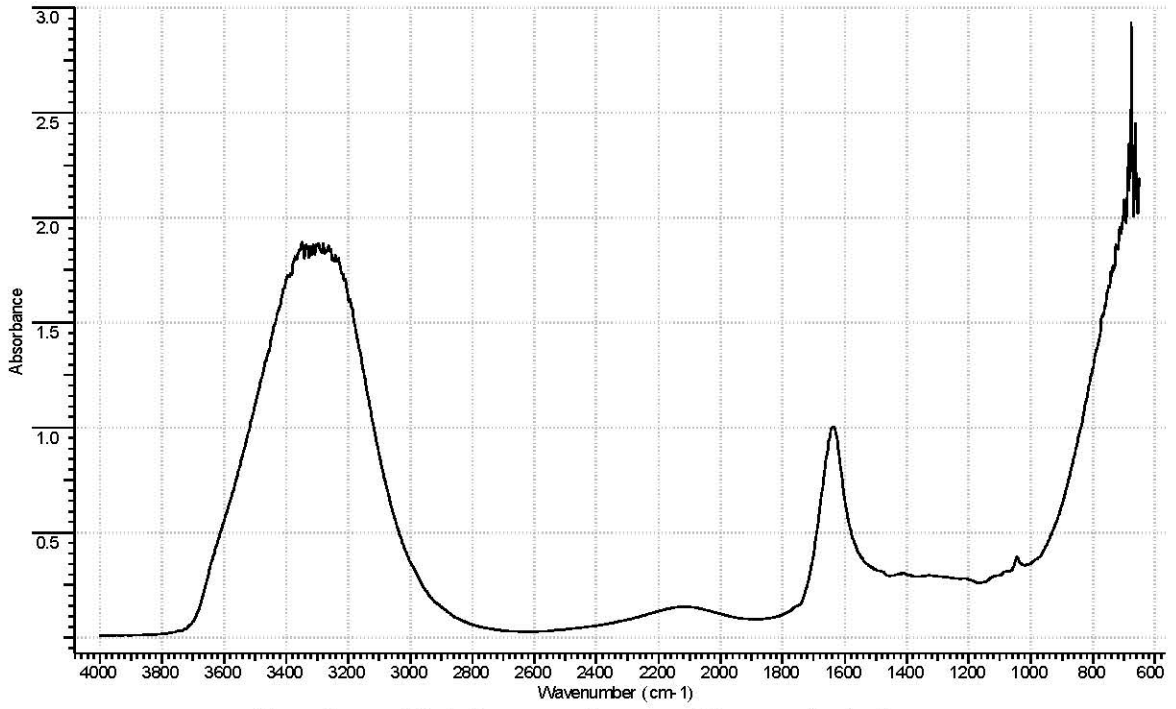
Sample no.13 (mfc-ncmc-gly-sta-tw80-wax solution)
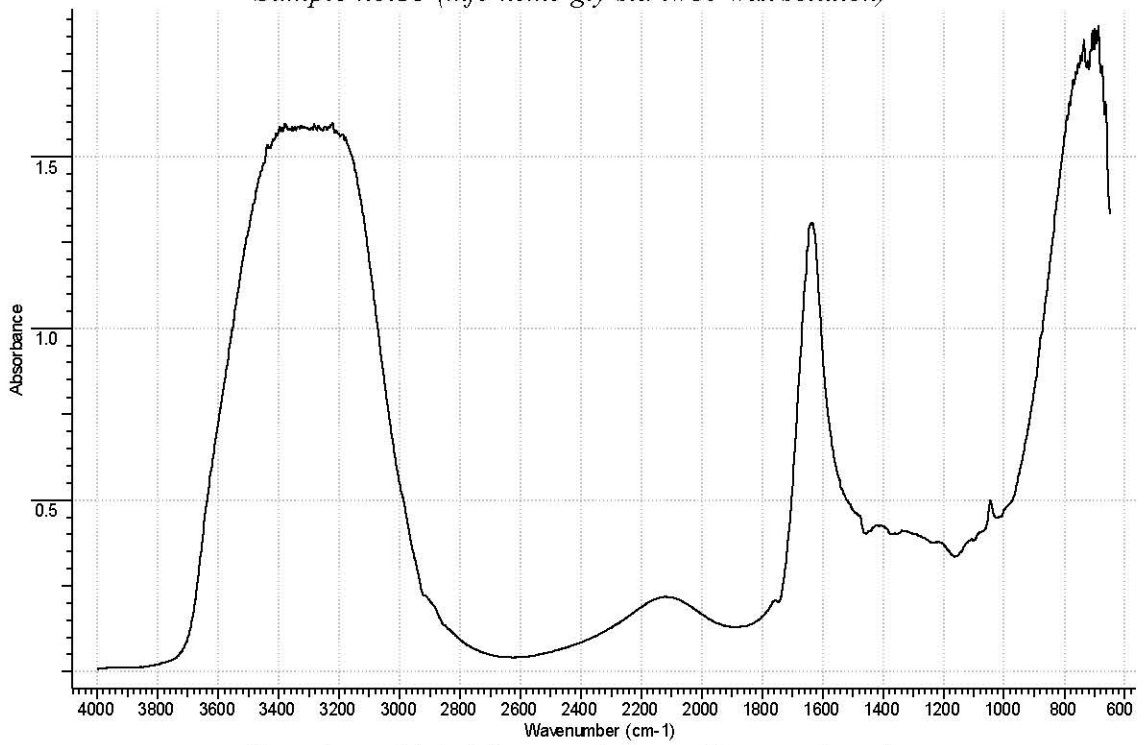
Sample no.14 (mfc2-ncmc-gly-sta-tw80-wax solution)

Figure B. 1   (Continued)

(Continued on next page)
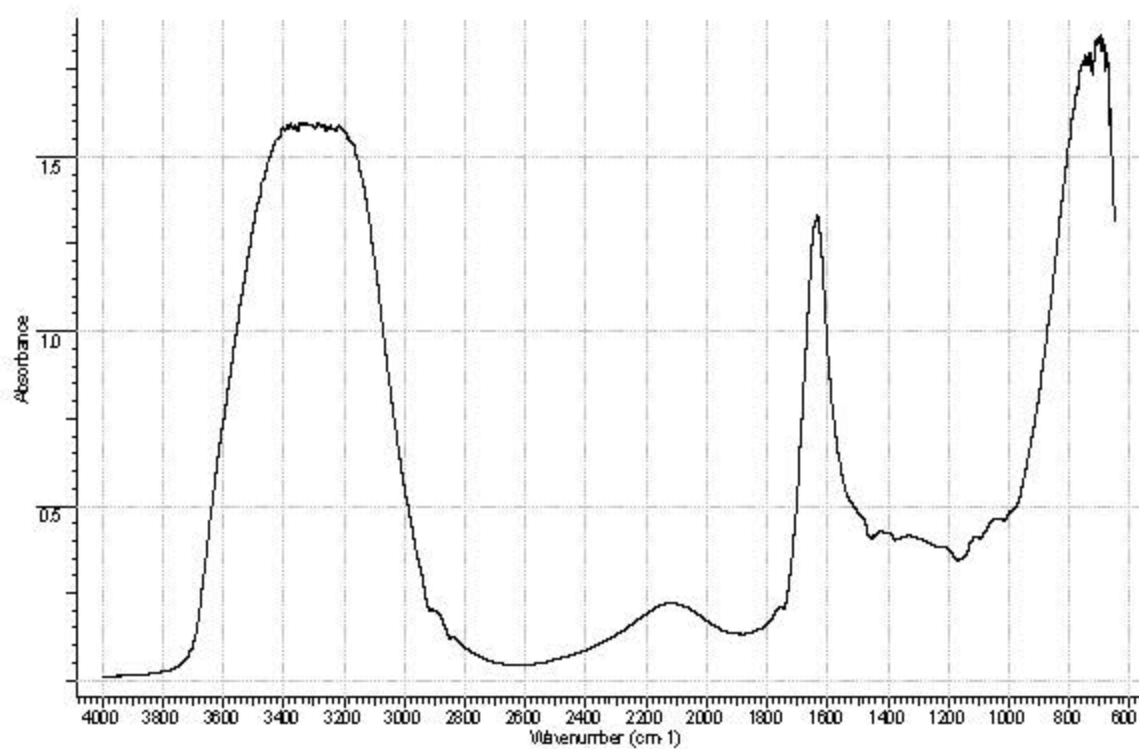
Sample no.15 (mfc-cmc-gly-peg400-aq chi solution)
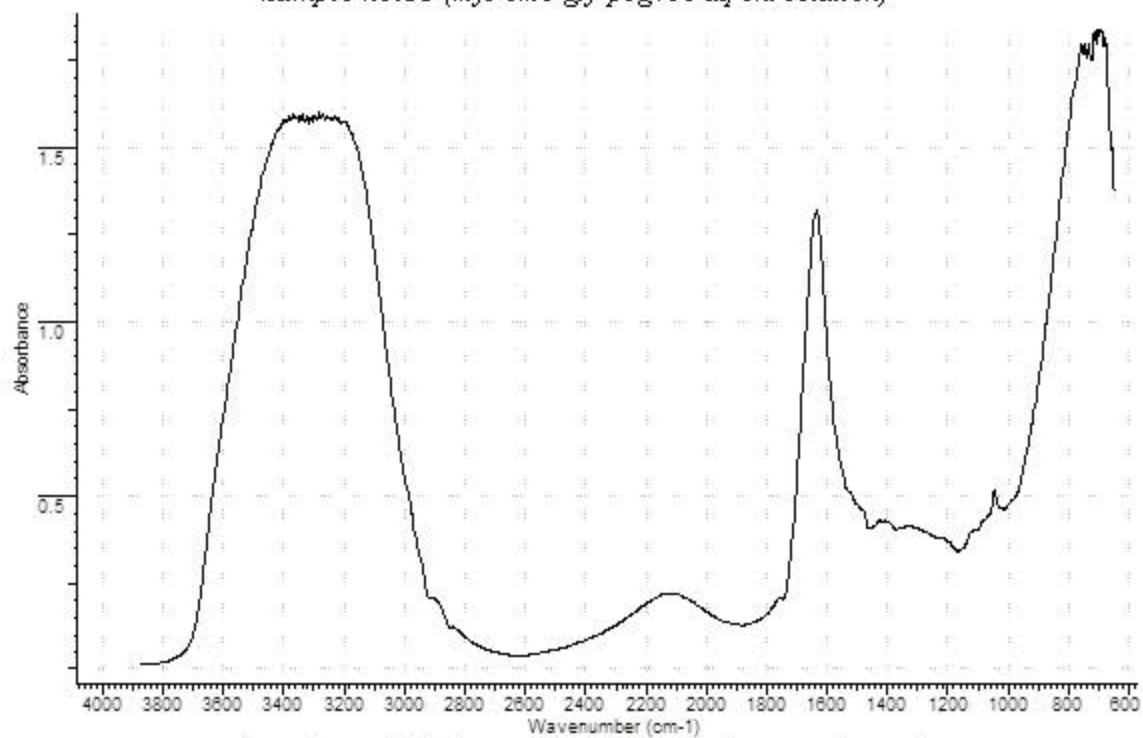
Sample no.16 (mfc-cmc-gly-peg400-aq chi-wax solution)

Figure B. 1   (Continued)

(Continued on next page)
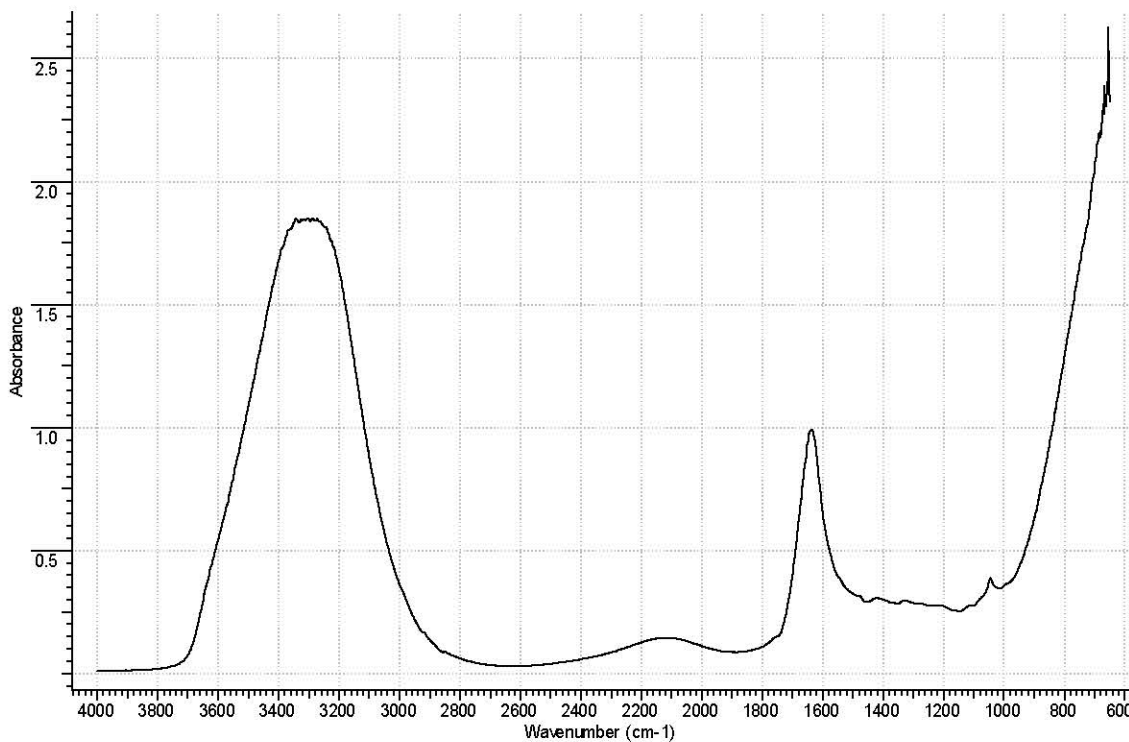
Sample no.17 (mfc-cmc-gly-sta-tw80-wax solution)
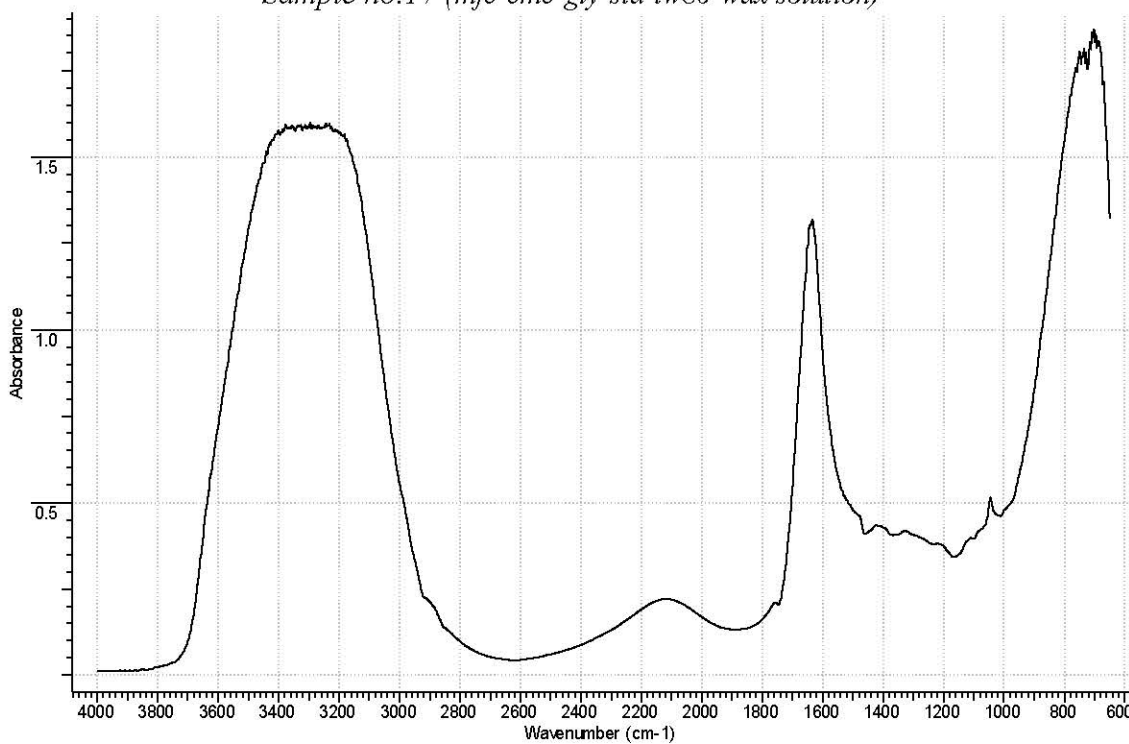
Sample no.18 (mfc2-cmc-gly-sta-tw80-wax solution)

Figure B. 1   (Continued)

(Continued on next page)
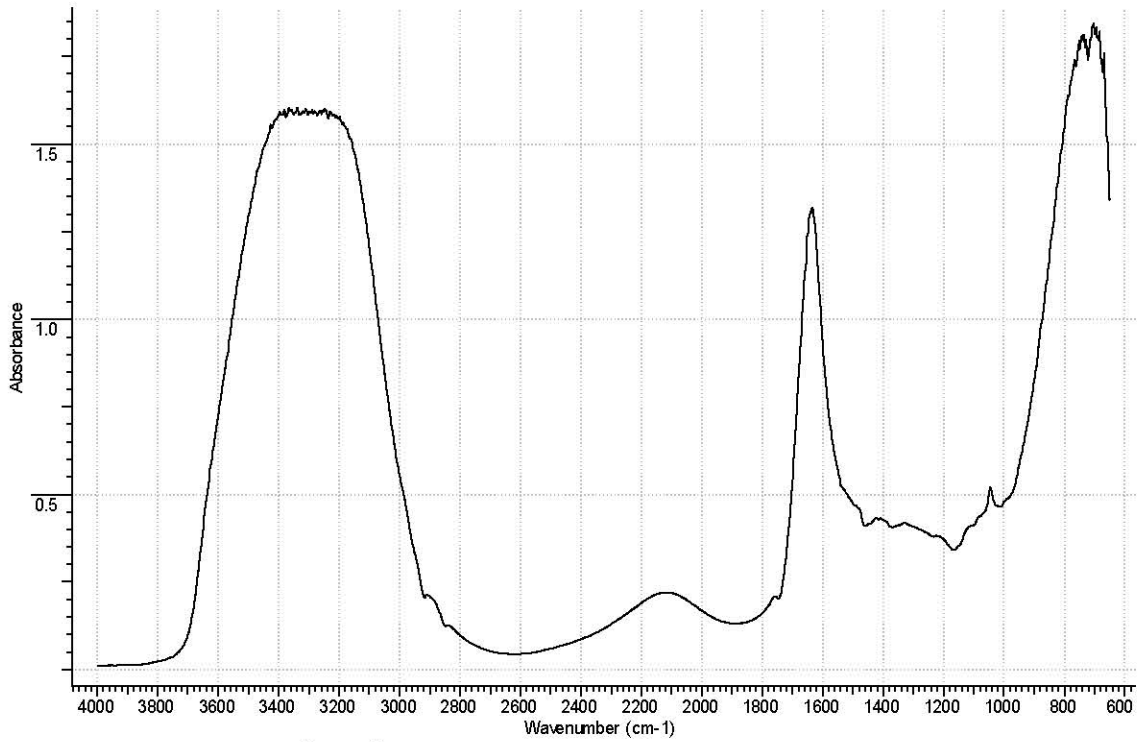
Sample no.19 (mfc-cmc-gly-peg400 solution)
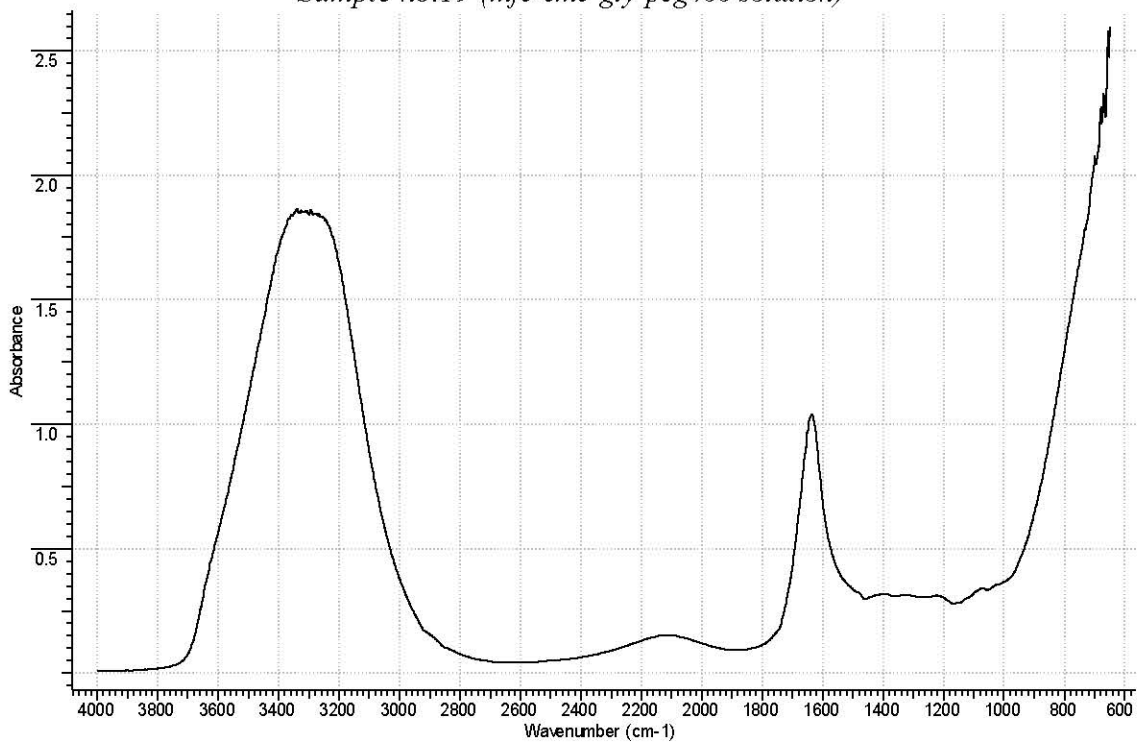
Sample no.20 (2% chitosan solution in ascorbic acid solution)

Figure B. 1   (Continued)

(Continued on next page)
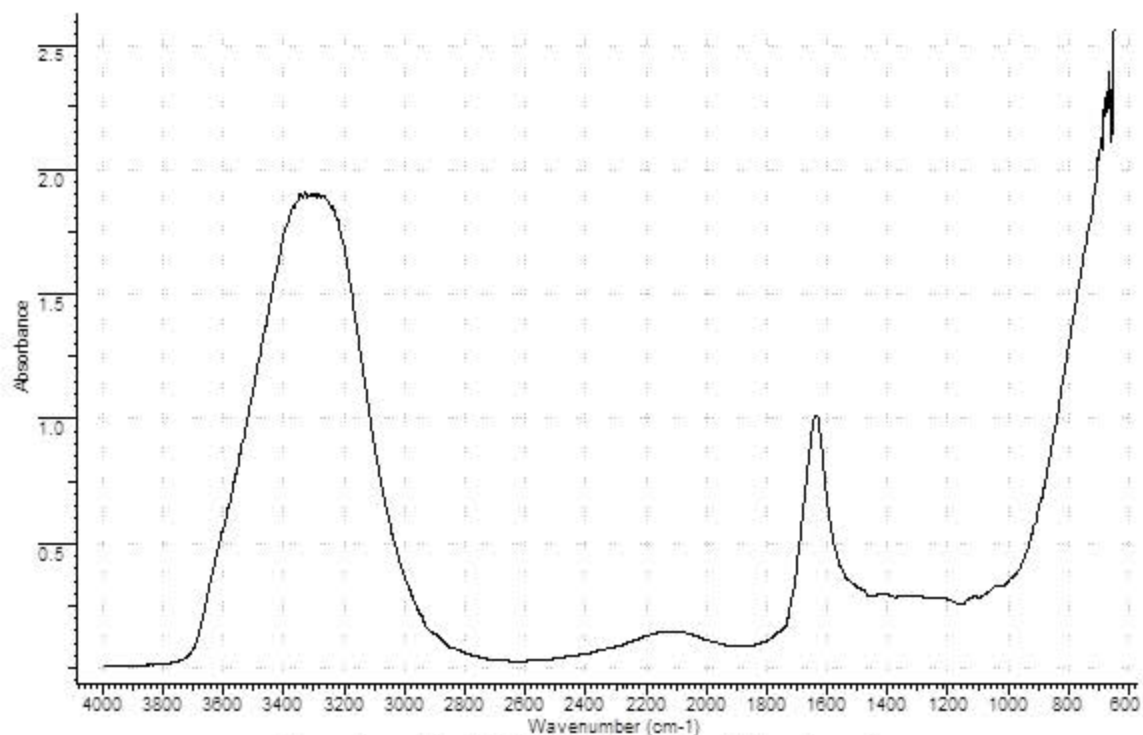
Sample no.21 (1% NCMC + 0.7 % GLY solution)
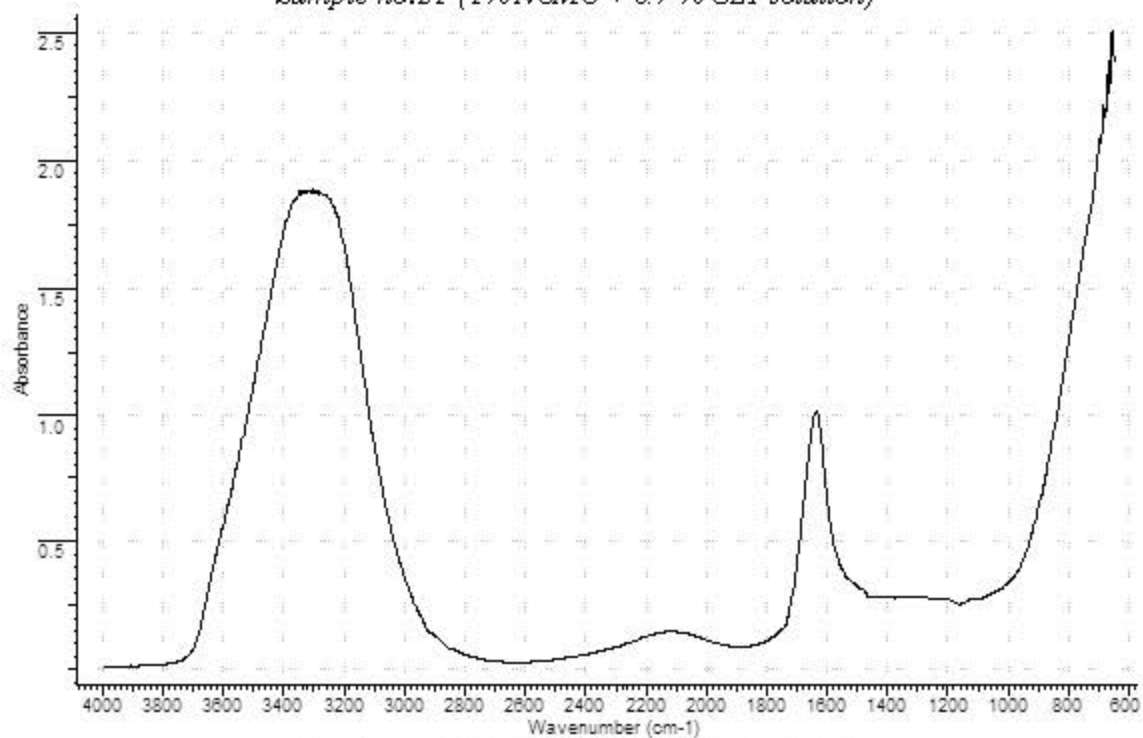
Sample no.22 (0.75 % chitosan solution in DW)

Figure B. 1   (Continued)

(Continued on next page)
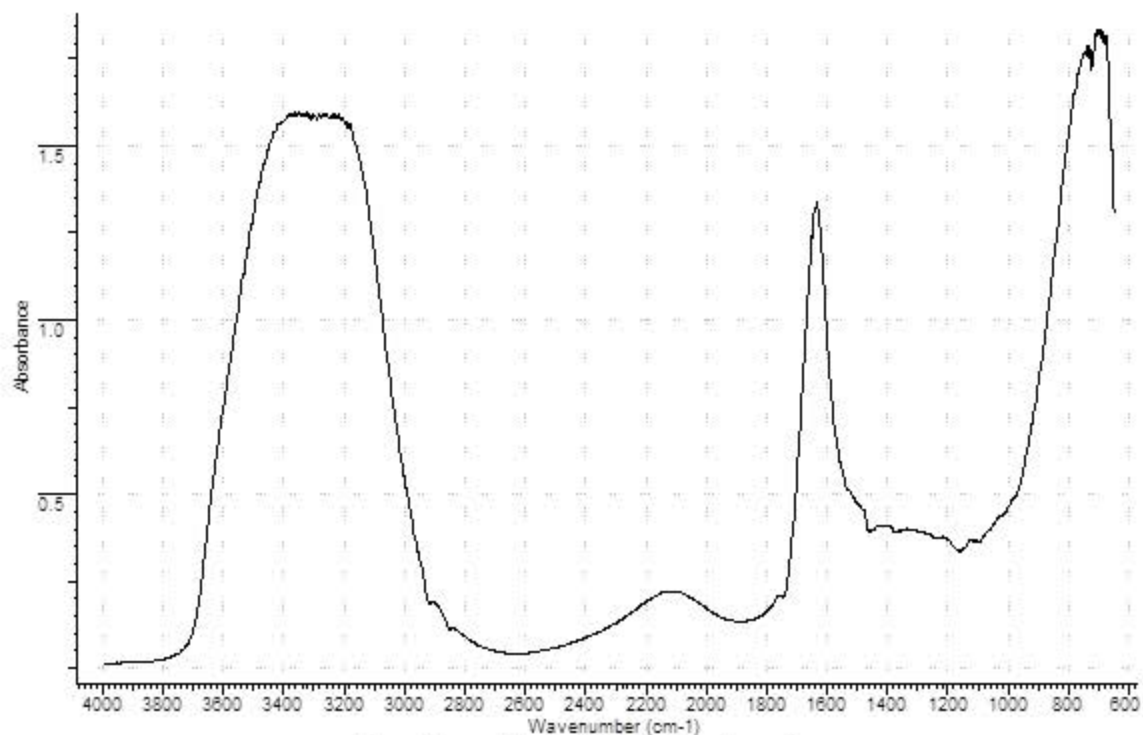
Sample no.23 (1.5 % MFC solution)
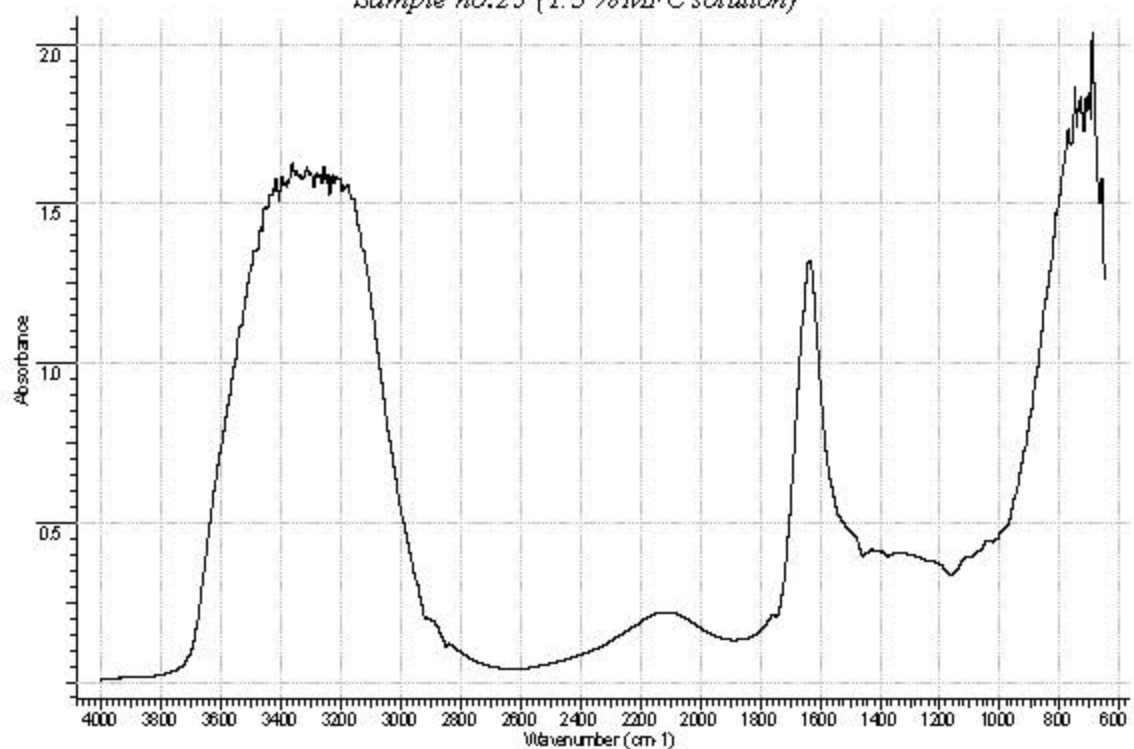
Sample no.24 (1.5 % MFC + 0.7 % GLY + 0.66 % PEG 400 solution)

Figure B. 1   (Continued)

(Continued on next page)

143
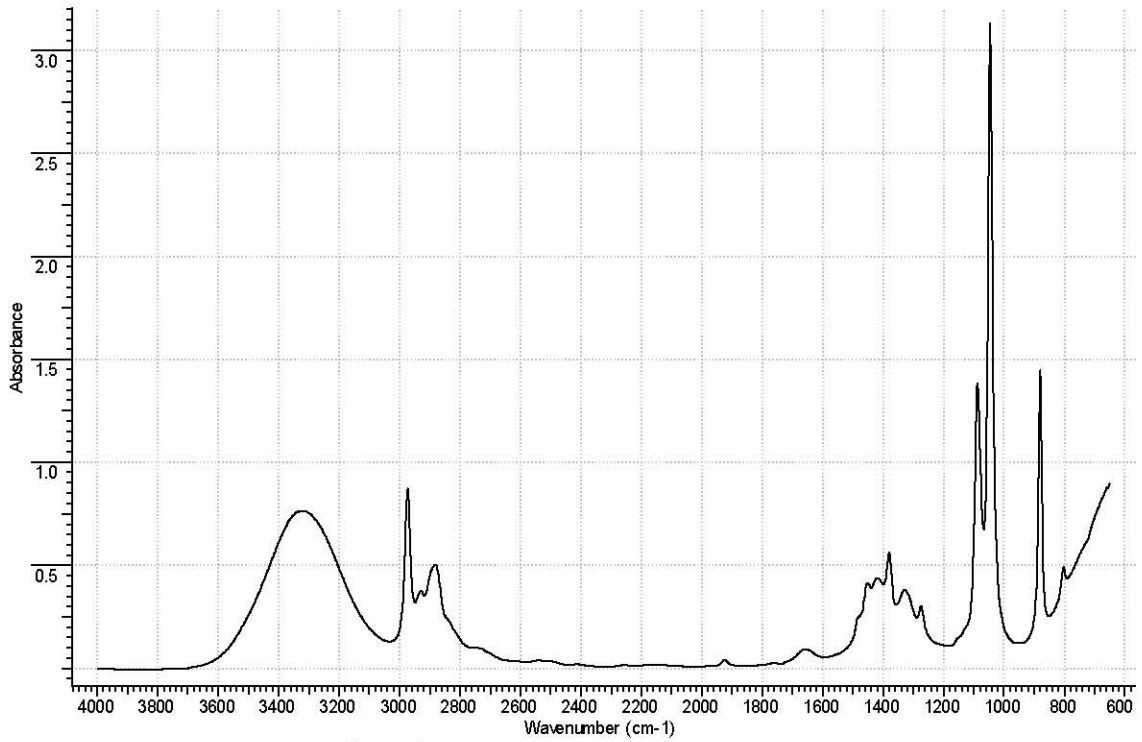
Sample no.25 ((70 : 30) Et-OH : DW)
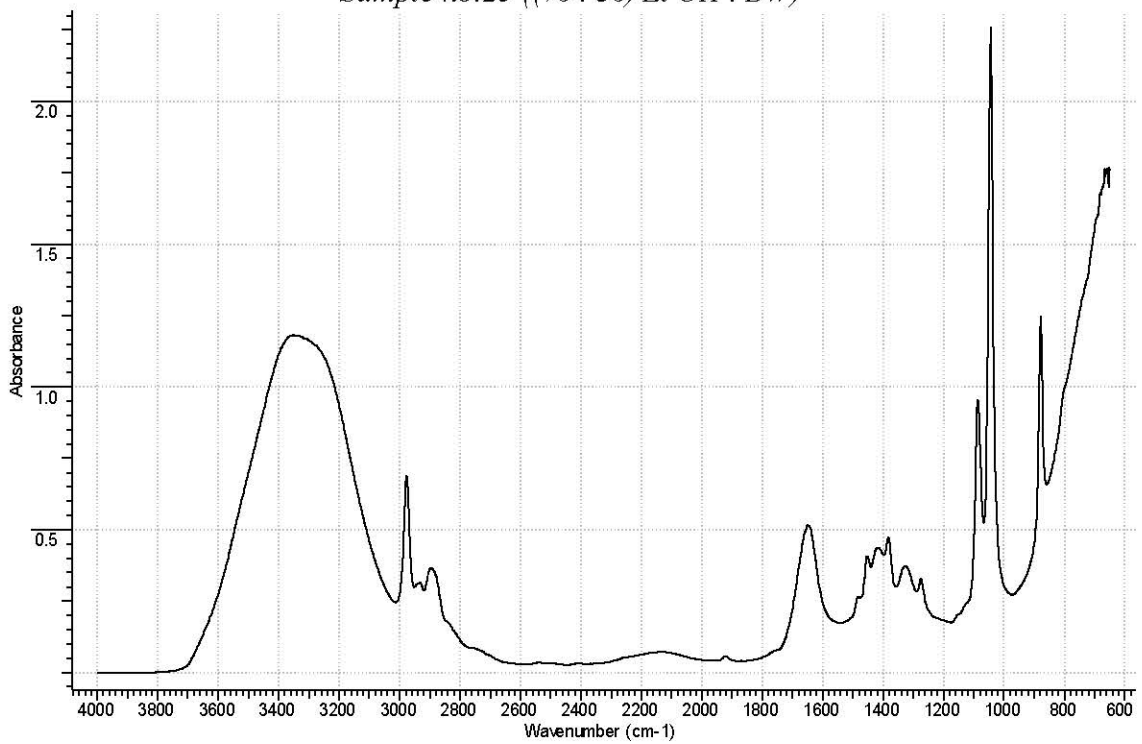
Sample no.26 (Et-OH)

Figure B. 1   (Continued)
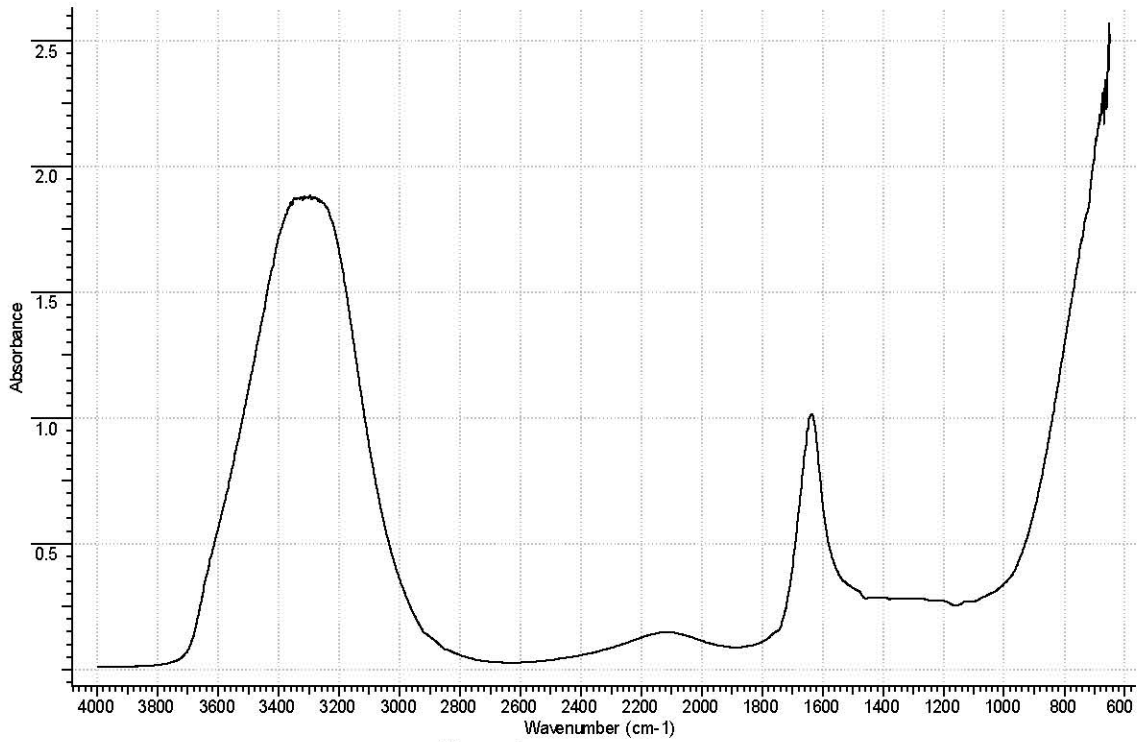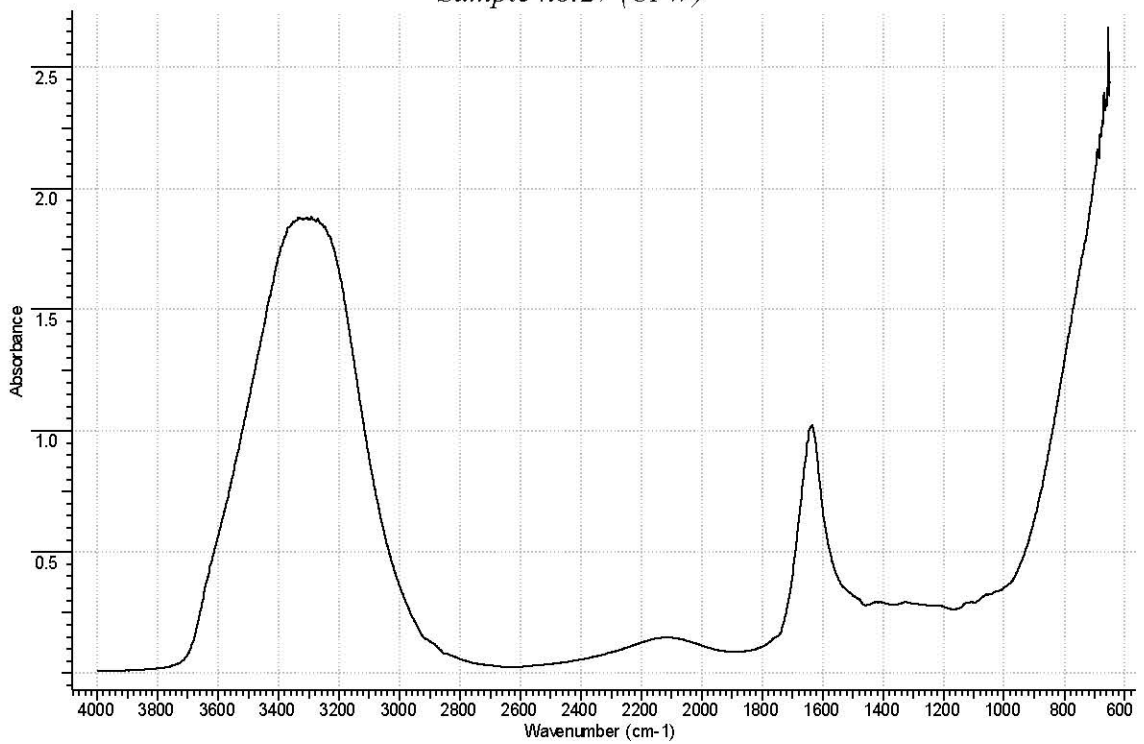
Sample no.27 (UPW)

Sample no.28 (1.6 % Na-CMC)

Figure B. 1   (Continued)

(Continued on next page)
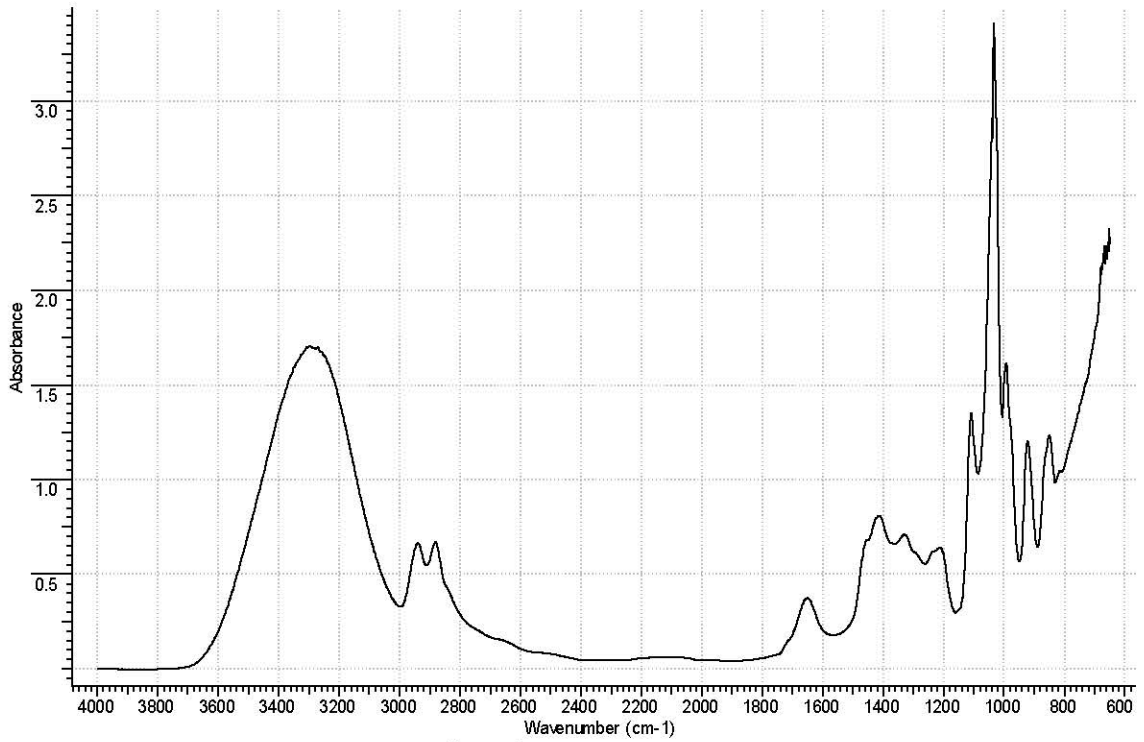
Sample no.29 (GLY)
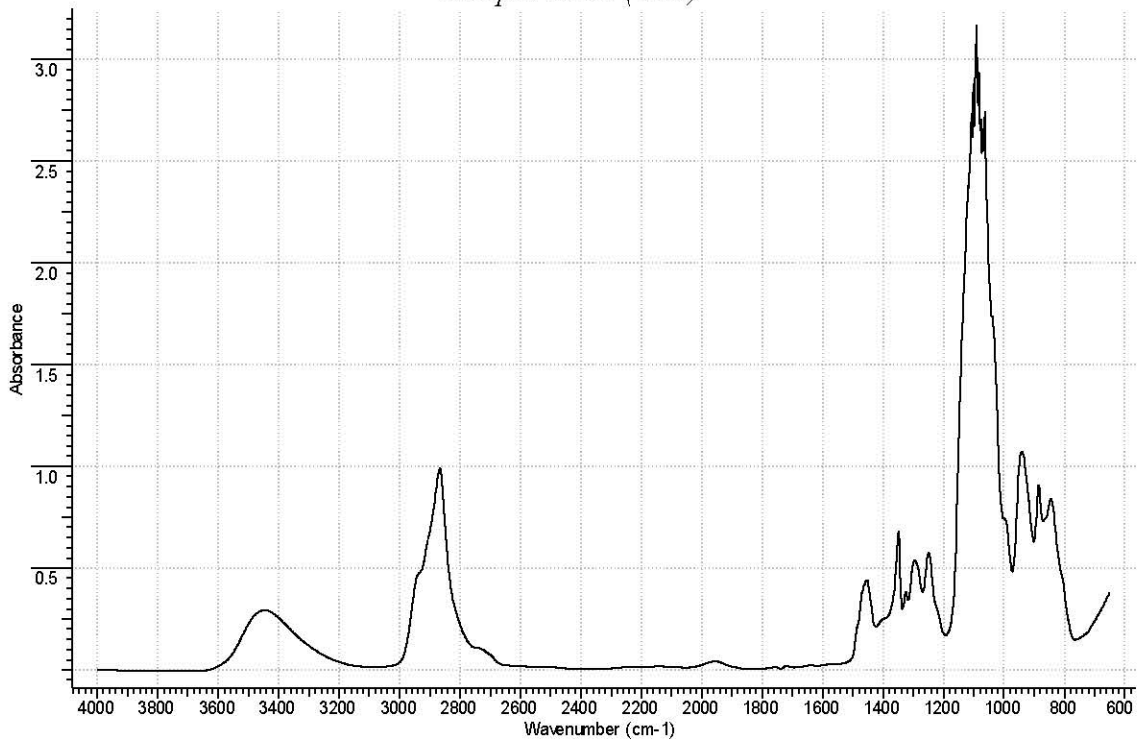
Sample no.30 (peg 400)

Figure B. 1 (Continued)

(Continued on next page)
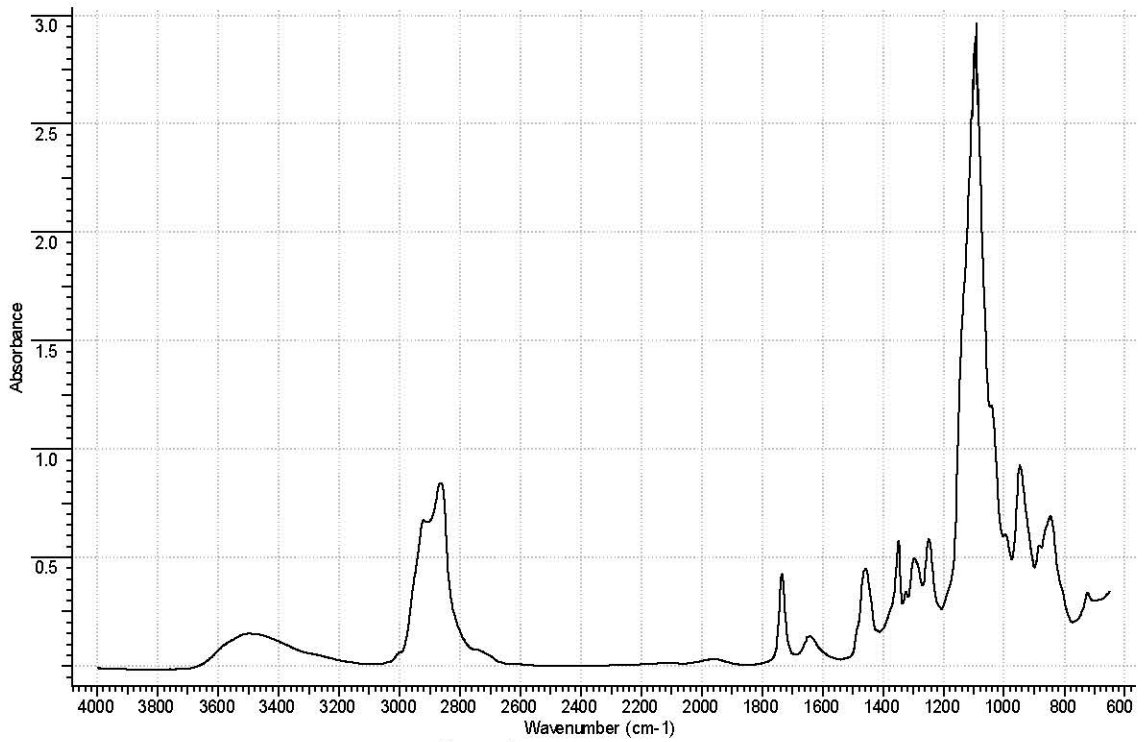
Sample no.31 (Tw 80)
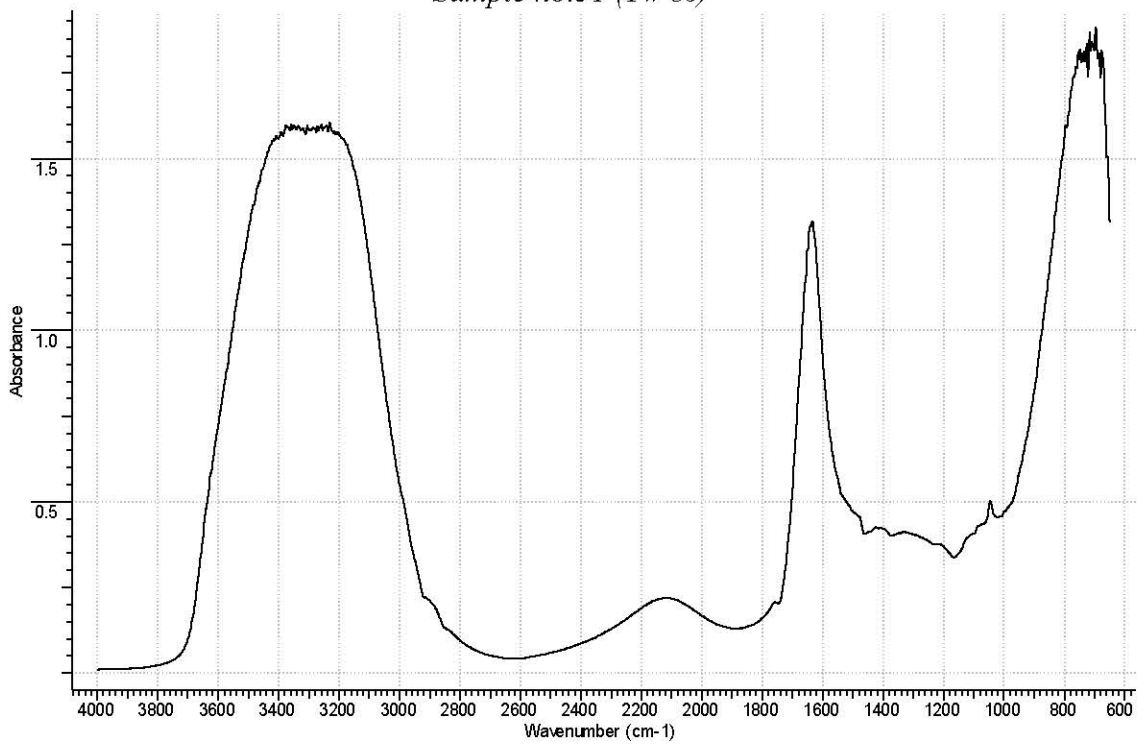
Sample no.32 (mfc2-cmc-gly-peg400 solution)

Figure B. 1   (Continued)

Table B. 1 ATR-FTIR peak assignments for artichoke fiber (Fiore 2011)

Wavelength (cm⁻¹)	Bonds	Component
3342	O-H stretching vibration, H bond	OH groups
2923 , 2854	C-H stretching vibration	CH and CH_2 in cellulose, hemicellulose
1737	carbonylic group C=O stretching vibration of linkage of carboxylic acid	lignin or ester group in hemicellulose
1594		water in the fibres
1506	C=C stretching	aromatic ring of the lignin
1422	CH_2 symmetric bending	cellulose
1372 , 1318	bending vibration	C-H and C-O groups of the aromatic ring in polysaccharides
1245	C-O stretching vibration	acetyl group in lignin
intense band centred at 1035	C-O stretching	OH and ether groups in cellulose
892	β-glycosidic linkages	monosaccharides
598	C-OH bending	

APPENDIX C. Thermal Evaluation of Powdered and Film Products

Temperatures at those phase transition occur for mentioned powdered or film products were listed below. Peaks were extracted from TGA/Dtg, DSC diagrams those presented at results section.

Table C.1 DSC Peaks for cellulose and AFB

Sample name	peak (°C)	onset (°C)	endset (°C)	heat (mj)	heat (j/g)
Cellulose fiber	64.44	25.99	103.29	-547.13	-210.43
	319.38	258.21	347.68	1.88 J	722.65
Artichoke leaf powder	61.26	-114.13	102.55	-325.09	-108.36
	332.58	293.64	370.95	1.54	513.11

Table C.2 DSC results for films-1

Sample name	peak (°C)	onset (°C)	endset (°C)	heat (mj)	heat (j/g)
mfc2-cmc-gly-peg400-wax	72.6	39.8	111.81	-626.49	-208.83
	207.68	155.64	299.7	-707.93	-235.98
	333.09	314.7	353.21	-139.65	-46.55
	402.64	355.4	370.13	-374.39	-124.8
	462.68	463.12	465.68	-2.19	-0.73
mfc-cmc-gly-peg400-wax - 30ml	83.29	33.57	118.01	-641.28	-200.4
	212.95	158.26	297.88	-987.82	-308.69
	333.52	314.64	354.69	-201.04	-62.82
	408.88	363.56	429.64	-373.14	-116.61
mfc-cmc-gly-peg400-wax - 40ml	83.88	35.58	118.53	-619.75	-193.67
	221.64	156.7	307.9	-1.23	-384.08
	331.85	317.66	351.34	-72.45	-22.64
	353.75	357.56	444.03	-454.21	-141.94
	76.19	31.6	121.3	-673.74	-210.54
	208.82	161.09	229.49	-659.4	-206.06
	332.23	320.29	351.53	-86.43	-27.01
	402.44	357.77	434.3	-274.95	-85.92
	456.8	440.21	462.7	-17.67	-5.52
	68.78	37.03	109.2	-420.79	-127.51
	207.43	156.39	294.49	-822.67	-249.29
	329	311.13	347.75	-113.83	-34.49
	404.26	355.52	447.1	-350.59	-106.24

Table C.3 DSC results for films-2

Sample name	peak (°C)	onset (°C)	endset (°C)	heat (mj)	heat (j/g)
mfc-cmc-gly-sta-tw80-wax -40ml	70.54	43.65	118.95	-314.27	-112.24
	199.26	154.75	309.52	-798.38	-285.14
	338.8	321.95	362.16	-75.07	-26.81
	392.51	367.82	459.38	-833.64	-297.73
Mfc	65.43	29.8	92.77	261.25	-90.09
	331.09	252.72	321.69	-248.8	-85.79
	378.49	338.52	470.33	-6.65	-2.29
Mfc-gly	98.09	87.28	133.11	-430.83	-143.61
	237.97	218.88	288.88	-779.62	-259.87
	376.71	344.71	497.08	-2.68	-894.55
Mfc2-cmc-gly-sta-tw80-wax	97.86	31.46	136.29	-725.1	-241.7
	235.84	185.17	297.77	-608.95	-202.98
	343.38	324.78	356.09	-41.34	-13.78
	392.52	419.95	429.45	-191.53	-63.84
	439.24	436.69	416.53	-11.05	-3.68
	459.62	453.26	469.29	-37.18	-12.39
Mfc2-cmc-gly-sta-tw80-wax-Lignin-Hmc	64.67	35.6	122.29	-466.8	-160.97
	225.12	218.31	294.94	-345.53	-119.15
	335.03	316.78	353.81	-74.75	-25.78
	396.71	363.7	435.46	-79.57	-27.44
	471.63	452.89	482.87	-204.23	-70.42
Mfc-cmc-chi-gly-peg400-lignin	89.08	38.46	148.63	-237.97	-79.32
	186.28	171.25	209.87	-48.87	-16.29
	254.92	213.36	246.37	-3.83	-1.28
	330.22	275.79	318.51	5.69	1.9
	365.36	335.89	379.52	-77.45	-25.82
	429.54	413.79	447.45	-14.11	-4.7
Mfc-cmc-aq chi-gly-peg400	106.3	38.56	137.83	-488.36	-162.79
	190.78	163.73	233.71	-308.1	-102.7
	244.85	236.42	290.87	-127.57	-42.52
	367.4	344.24	372.23	-5.57	-1.86
	429.1	378.19	486.31	-657.77	-219.26
mfc-cmc-gly-sta-tw80-wax-30ml	82.57	286.85	123.36	-500.08	-166.69
	220.94	159.45	310.08	-798.48	-266.16
	339.18	323.8	363.14	-83.29	-27.76
	390.76	449.28	460.39	-1.09	-364.55

Table C.4 Dtg Results for film samples

Sample name	temperature (°C)							
Mfc2-cmc-gly-peg400-wax	74.97	228.7	269.99	306.73	382.97			
Mfc-cmc-gly-peg400-wax	66.62	224.07	248.29	261.03	290.5	310.33	333.65	377.09
	66.18	164.31	211.01	232.28	257.52	340.11	379.02	
	76.1	211.17	232.98	324.64	382.27			
	74.71	227.43	277.11	326.1	382.66			
Mfc-gly	81.58	233.07	359.37					
Mfc	68.98	277.1	342.94	458.46				
Mfc-cmc-gly-chi-peg400-lignin	72.06	321.4	383.22	396.2	423.77			
cmc-mfc2-sta-tw80-wax	76.1	230.22	327.24	388.07				
cmc-mfc-sta-tw80-wax-40ml	81.02	229.43	256.15	330	382.64			
cmc-mfc-sta-tw80-wax-30ml	79.33	226.08	260.05	332.35	392.77			
Mfc-cmc-aq chi-gly-peg400	74.63	222.5	262.15	308.97	484.36			

Table C.5   TGA Results for film samples

Sample name	Temp (°C)	W %	Temp(°C)	W %	Temp(°C)	W %
ncmc-chi-mfc-gly-peg400	100	90.247	209.95	75.177	600	25.571
ncmc-chi-mfc-gly-peg400-wax	100	92.035	168.36	86.35	600	20.928
ncmc-mfc-sta-tw80-wax	100	88.951	165.74	83.371	600	25.847
cmc-chi-mfc-gly-peg400-wax	100	98.137	189.28	79.498	600	26.481
cmc-chi-mfc-gly-peg400	100	97.849	170.27	92.035	600	29.036
ncmc-mfc-gly-peg400-wax	100	92.872	175.45	86.93	600	23.042
cmc-mfc-sta-tw80-wax	100	92.153	296.81	43.711	600	25.1
cmc-mfc2-sta-tw80-wax	100	95.324	212.28	83.819	600	24.087
ncmc-mfc2-gly-sta-tw80-wax	100	94.413	156.96	89.58	600	21.321

APPENDIX D. Thickness of Films Produced Used in Various Analyses

Table D.1 Thickness data of solubility tests

sample	n	thickness (mm)
mfc pulp precipitate film pH = 7	10	0.11 ± 0.0108
mfc pulp precipitate film pH = 11	10	0.11 ± 0.0075
mfc-wax film	8	0.06 ± 0.0141
wax sprayed mfc film	8	0.073 ± 0.0158
mfc film	8	0.055 ± 0.0053
sonicated cmc-gly film	8	0.23 ± 0.0504
mfc-cmc-gly-sta-tw80 film	8	0.16 ± 0.02

Table D.2 Film Thickness

sample name	thickness (mm)	n	sample name	thickness (mm)	n
mfc-cmc-sta-tw80-gly	0.11 ± 0.02	4	mfc-cmc-gly-sta	0.19± 0.05	12
mfc-cmc-sta-tw80-gly	0.10 ± 0.01	4	cmc-gly sonicated	0.06± 0.01	8
mfc-cmc-sta-tw80-gly-wax	0.07± 0.01	3	mfc 1%	0.07± 0.02	8
mfc-cmc-sta-tw80-gly-wax	0.10± 0.01	4	wax sprayed mfc	0.06± 0.01	8
mfc-cmc-sta-tw80-gly-wax	0.09± 0.02	8	mfc-wax	0.23± 0.05	8
diluted mfc	0.12± 0.05	9	mfc-cmc-gly-tw80-sta	0.16± 0.02	8
diluted mfc + gly	0.10± 0.04	9	cmc-gly-tw80-sta	0.28± 0.12	4
2 % ncmc	0.10± 0.02	8	mfc-cmc-gly-peg400-chi-20ml	0.23±0.014	3
4 % ncmc	0.24± 0.05	9	mfc-cmc-gly-peg400-chi-30ml	0.30±0.026	3
6 % ncmc	0.35± 0.08	9	mfc-cmc-gly-peg400-chi-40ml	0.43±0.016	3
mfc-cmc-gly-peg400-wax-20ml	0.10±0.000	9	mfc-cmc-gly-sta-tw80-wax-20ml	0.11±0.000	2
mfc-cmc-gly-peg400-wax-30ml	0.13±0.008	3	mfc-cmc-gly-sta-tw80-wax-30ml	0.15±0.020	3
mfc-cmc-gly-peg400-wax-40ml	0.15±0.000	2	mfc-cmc-gly-sta-tw80-wax-40ml	0.22±0.034	3
mfc-cmc-gly-peg400-chi-wax-20ml	0.24±0.013	3	mfc-cmc-gly-peg400-chi-wax-40ml	0.37±0.016	3
mfc-cmc-gly-peg400-chi-wax-30ml	0.30±0.012	3			

APPENDIX E. Opacity of Films

Table E.1 Colour of Different Film Samples (n=4; avg±stdev)

Sample name	side	L *	a*	b*	hue angle
wax sprayed mfc	br	60.90 ± 2.0441	-1.55 ± 0.1821	10.85 ± 1.1486	-1.43 ± 0.0309
	ro	63.99 ± 0.7428	-1.77 ± 0.2259	9.78 ± 0.5263	-1.39 ± 0.0128
cmc-gly sonicated	br	48.52 ± 0.2250	-0.30 ± 0.0115	2.18 ± 0.0379	-1.44 ± 0.0076
	ro	44.70 ± 0.0503	-0.21 ± 0.0551	1.25 ± 0.0404	-1.40 ± 0.0392
mfc 1%	br	60.62 ± 12.9283	-0.58 ± 0.2835	5.13 ± 0.2500	-1.46 ± 0.0577
	ro	48.87 ± 8.7485	-0.47 ± 0.3855	3.57 ± 0.4532	-1.43 ± 0.1275
mfc-cmc-peg400	br	49.27 ± 3.0316	-0.09 ± 0.1153	1.39 ± 0.3323	Nan ± Nan
	ro	42.54 ± 1.0767	0.17 ± 0.0577	0.46 ± 0.2152	1.18 ± 0.1250
mfc-cmc-peg400-5% wax	br	42.71 ± 0.6930	0.02 ± 0.0566	3.13 ± 0.5445	0.00 ± 2.2042
	ro	42.14 ± 0.6505	-0.03 ± 0.0566	3.18 ± 0.2404	0.01 ± 2.2043
mfc-cmc-peg400-1% wax	br	43.45 ± 1.0041	-0.03 ± 0.0000	2.09 ± 0.1485	-1.56 ± 0.0010
	ro	39.17 ± 0.5657	0.03 ± 0.0849	1.52 ± 0.1344	-0.02 ± 2.1635
mfc-cmc-peg400-2% wax	br	41.76 ± 1.3294	-0.37 ± 0.0566	2.26 ± 0.2687	-1.41 ± 0.0055
	ro	39.84 ± 0.0778	-0.28 ± 0.0919	1.88 ± 0.0495	-1.43 ± 0.0442
mfc-cmc-peg400-3% wax	br	41.74 ± 0.4384	-0.52 ± 0.0141	2.04 ± 0.0141	-1.32 ± 0.0049
	ro	41.72 ± 0.7566	-0.60 ± 0.0212	2.47 ± 0.2687	-1.33 ± 0.0167
mfc-cmc-peg400-4% wax	br	42.25 ± 0.2658	-0.39 ± 0.1305	2.22 ± 0.1513	-1.40 ± 0.0473
	ro	41.88 ± 0.2779	-0.38 ± 0.1422	2.27 ± 0.1692	-1.41 ± 0.0515
diluted mfc + gly	br	42.69 ± 0.0762	-0.30 ± 0.0100	1.64 ± 0.0359	-1.39 ± 0.0067
	ro	45.42 ± 0.0275	-0.71 ± 0.0252	2.39 ± 0.0058	-1.28 ± 0.0093
diluted mfc	br	48.95 ± 0.0082	-0.10 ± 0.0050	3.81 ± 0.0082	-1.55 ± 0.0013
	ro	49.00 ± 0.0171	-0.54 ± 0.0150	3.88 ± 0.0100	-1.43 ± 0.0041
mfc-cmc-gly-sta-peg400-wax	br	44.34 ± 0.3245	0.01 ± 0.0585	3.63 ± 0.1879	-0.79 ± 1.5542
	ro	41.73 ± 0.1603	0.01 ± 0.0427	1.79 ± 0.0920	0.00 ± 1.7926
mfc-cmc-gly-sta-peg400-wax	br	44.65 ± 0.3155	0.11 ± 0.0473	3.61 ± 0.1773	1.54 ± 0.0124
	ro	40.66 ± 0.2726	0.08 ± 0.0499	1.72 ± 0.1982	1.52 ± 0.0375
mfc-cmc-gly-sta-peg400	br	45.91 ± 0.0058	0.02 ± 0.0173	3.18 ± 0.0222	Nan ± Nan
	ro	42.13 ± 0.0618	0.01 ± 0.0206	1.63 ± 0.0420	0.00 ± 1.8013
2% Ncmc	Br	43.31 ± 0.0058	1.91 ± 0.0126	6.99 ± 0.0058	1.30 ± 0.0018
	Ro	38.38 ± 0.1100	0.84 ± 0.0311	3.30 ± 0.0744	1.32 ± 0.0038
4% Ncmc	Br	43.81 ± 0.0050	3.81 ± 0.0082	8.17 ± 0.0082	1.13 ± 0.0009
	ro	37.15 ± 0.0350	1.84 ± 0.0173	4.52 ± 0.0359	1.18 ± 0.0015
6% Ncmc	br	63.19 ± 0.0058	4.84 ± 0.0320	17.33 ± 0.0100	1.30 ± 0.0018
	ro	43.03 ± 0.0998	5.19 ± 0.0440	10.54 ± 0.0737	1.11 ± 0.0006
mfc pulp precipitate	br	35.36 ± 3.2454	-0.41 ± 0.2526	3.73 ± 1.2284	-1.43 ± 0.1228
	ro	33.28 ± 2.5586	-0.22 ± 0.1574	2.27 ± 0.6934	-1.48 ± 0.0570
mfc pulp supernatant	br	32.89 ± 1.1682	-0.14 ± 0.0570	1.67 ± 0.0744	-1.49 ± 0.0371
	ro	29.98 ± 4.2042	-0.27 ± 0.1531	1.51 ± 0.2427	-1.39 ± 0.0948

Table E.2 Chromacity and Whiteness Index values of films (n=4)

Sample name	side	L *	a*	b*	c	h
artlp	br	66.76 ± 0.47	2.09 ± 0.04	13.69 ± 0.18	Nan ± Nan	1.42 ± 0.0012
	ro	54.63 ± 0.06	3.67 ± 0.02	14.84 ± 0.03	Nan ± Nan	1.33 ± 0.0015
ncmc-chi-mfc-gly-peg400-wax	br	46.88±2.099	-0.03±0.101	12.67±1.679	12.67±1.68	90.18±0.499
	ro	45.78±1.094	-0.43±0.072	13.10±1.378	13.11±1.38	91.9±0.382
ncmc-mfc-gly-peg400-wax	br	42.13±0.516	0.81±0.545	14.02±1.439	14.05±1.47	86.82±1.806
	ro	39.48±1.563	0.30±0.568	13.36±2.403	13.36±2.42	88.97±2.053
cmc-mfc-gly-peg400-aq chi	br	42.36±0.342	-1.30±0.076	9.24±1.309	9.34±1.303	98.05±0.739
	ro	36.13±1.611	-1.27±0.174	5.71±1.377	5.85±1.379	102.78±1.467
mfc-cmc-peg400-gly-wax-30ml	br	42.38±2.681	-1.07±0.075	4.857±0.155	4.957±0.14	102.58±0.947
	ro	39.83±0.922	-1.18±0.036	3.84±0.873	4.03±0.827	107.32±2.961
mfc-cmc-peg400-gly-wax-40ml	br	43.52±1.64	-0.96±0.036	4.72±0.557	4.817±0.54	101.64±1.042
	ro	37.24±1.542	-0.99±0.049	3.233±0.202	3.403±0.19	107.54±1.285
cmc-mfc-gly-sta-tw80-wax	br	46.37±1.695	-0.75±0.166	12.11±2.449	12.26±2.68	93.6±1.614
	ro	41.04±3.551	-0.88±0.049	10.93±3.533	10.99±3.51	95.093±2.097
cmc-mfc-gly-peg400-chi	br	40.84±2.556	-1.46±0.036	10.9±1.867	10.99±1.86	97.813±1.189
	ro	34.34±1.685	-1.33±0.064	7.327±0.663	7.447±0.653	100.3±0.5515

Table E.3 Chromacity and Whiteness Index values of films (n=4)

sample name	side	chromacity	WI		
wax sprayed mfc	Br	10.96 ± 1.1139	59.39	±	2.04
	Ro	9.94 ± 0.5583	62.64	±	0.74
cmc-gly sonicated	Br	2.20 ± 0.0359	48.48	±	0.23
	Ro	1.27 ± 0.0474	44.69	±	0.05
mfc 1%	Br	5.16 ± 0.2365	60.28	±	12.93
	Ro	3.62 ± 0.3910	48.74	±	8.75
mfc-cmc-peg400	Br	1.39 ± 0.3269	49.25	±	3.03
	Ro	0.49 ± 0.2169	42.54	±	1.08
mfc-cmc-peg400-5% wax	Br	3.13 ± 0.5448	42.62	±	0.69
	Ro	3.18 ± 0.2409	42.05	±	0.65
mfc-cmc-peg400-1% wax	Br	2.09 ± 0.1485	43.41	±	1.00
	Ro	1.52 ± 0.1325	39.15	±	0.57
mfc-cmc-peg400-2% wax	Br	2.29 ± 0.2743	41.71	±	1.33
	Ro	1.90 ± 0.0623	39.81	±	0.08
mfc-cmc-peg400-3% wax	Br	2.11 ± 0.0172	41.70	±	0.44
	Ro	2.54 ± 0.2662	41.66	±	0.76
mfc-cmc-peg400-4% wax	Br	2.26 ± 0.1703	42.20	±	0.27
	Ro	2.30 ± 0.1885	41.84	±	0.28
diluted mfc + gly	Br	1.66 ± 0.0356	42.67	±	0.08
	Ro	2.49 ± 0.0116	45.37	±	0.03
diluted mfc	Br	3.81 ± 0.0082	48.81	±	0.01
	Ro	3.91 ± 0.0084	48.85	±	0.02
mfc-cmc-gly-sta-tw80-wax	Br	3.63 ± 0.1875	44.22	±	0.32
	Ro	1.79 ± 0.0918	41.70	±	0.16
mfc-cmc-gly-sta-tw80-wax	Br	3.61 ± 0.1779	44.53	±	0.32
	Ro	1.72 ± 0.1952	40.64	±	0.27
mfc-cmc-gly-sta-tw80	Br	3.18 ± 0.0222	45.81	±	0.01
	Ro	1.63 ± 0.0419	42.10	±	0.06
artlp	Br	13.85 ± 0.1851	63.99	±	0.47
	Ro	15.29 ± 0.0276	52.13	±	0.06
2% ncmc	Br	7.24 ± 0.0041	42.84	±	0.01
	Ro	3.40 ± 0.0796	38.29	±	0.11
4% ncmc	Br	9.01 ± 0.0082	43.09	±	0.00
	Ro	4.88 ± 0.0392	36.96	±	0.03
6% ncmc	Br	17.99 ± 0.0074	59.03	±	0.01
	Ro	11.75 ± 0.0855	41.83	±	0.10
mfc-cmc-gly-sta-tw80	Br	4.21 ± 0.3153	45.10	±	0.17
	Ro	1.70 ± 0.0926	42.11	±	0.17
mfc pulp precipitate	Br	3.77 ± 1.1888	35.25	±	3.24
	Ro	2.28 ± 0.7011	33.24	±	2.56
mfc pulp supernatant	Br	1.67 ± 0.0712	32.87	±	1.17
	Ro	1.54 ± 0.2497	29.96	±	4.20

APPENDIX F. Colour variations in artichokes

Table F.1 Colour variations in treated and non-treated artichokes (n=4)

t (h)	L *	a*	b*	hue	chrom
DW					
0.5	30.14±0.851	2.46±0.16	10.3±0.462	1.34±1.23	10.59±0.49
17	29.9±0.339	2.37±0.34	9.358±0.235	1.32±0.60	9.65±0.41
22.5	30.63±0.939	2.28±0.54	8.23±1.078	1.30±1.10	8.54±1.21
41.5	34.13±1.121	1.77±0.33	6.933±0.428	1.32±0.92	7.15±0.54
106.5	43.02±1.457	4.66±0.7	12.28±1.355	1.21±1.10	13.13±1.52
	BI	-12.8		ΔL	12.8825
AA					
t (h)	L *	a*	b*	hue	chrom
0.5	31.35±0.5934	0.6175±2.032	12.91±1.856	1.52±0.74	12.92±2.75
17	32.605±0.4032	-0.423±1.5279	13.41±0.418	-1.54±0.27	13.42±1.58
22.5	33.605±1.6609	1.0425±1.4585	13.37±0.346	1.49±0.23	13.41±1.50
41.5	33.085±0.3189	0.3325±1.1101	14.24±0.727	1.55±0.58	14.25±1.33
106.5	40.38±4.789	3.8875±0.6978	8.965±4.404	1.16±1.41	9.77±4.46
	BI	-9.922		ΔL	9.03
SMBS					
t (h)	L *	a*	b*	Hue	chrom
0.5	32.673±1.6761	1.3475±0.9334	15.35±0.81	1.48±0.72	15.41±1.24
17	36.105±1.2462	0.41±0.661	15.61±1.649	1.54±1.19	15.61±1.78
22.5	34.973±0.8517	1.1025±0.4966	16.36±0.526	1.50±0.81	16.40±0.72
41.5	39.54±1.2424	1.2075±0.799	14.85±1.558	1.49±1.10	14.90±1.75
106.5	43.075±2.2572	4.4625±0.8839	14.25±2.215	1.27±1.19	14.93±2.38
	BI	-17.4		ΔL	10.4025
Cys					
t (h)	L *	a*	b*	hue	chrom
0.5	30.945±1.4294	2.178±1.141	11.07±0.8335	1.38±0.63	11.28±1.41
17	32.098±0.4602	2.638±1.053	12.645±0.6961	1.37±0.58	12.92±1.26
22.5	31.87±1.2711	2.53±1.239	13.063±0.4478	1.38±0.35	13.31±1.32
41.5	33.033±1.5871	3.005±1.069	12.625±1.9301	1.34±1.07	12.98±2.21
106.5	43.523±3.0491	4.235±0.66	12.748±1.7935	1.25±1.22	13.43±1.91
	BI	-14.587		ΔL	12.5775
CA					
t (h)	L *	a*	b*	hue	chrom
0.5	30.91±0.912	2.888±0.212	10.8±0.62	1.31±1.24	11.21±0.65
17	31.8±1.503	2.305±0.426	8.8±2.23	1.31±1.38	9.10±2.27
22.5	36.38±1.194	2.41±0.547	7.51±1.43	1.26±1.20	7.88±1.53
41.5	34.47±1.134	2.745±0.506	7.49±1.23	1.22±1.18	7.97±1.33
106.5	40.75±2.445	5.043±0.735	11.4±2.91	1.15±1.32	12.45±3.00
	BI	-10.5		ΔL	9.84

Table F.2 Colour measurement results for fresh artichokes

artichoke	L*	a*	b*	c*	h
Globe no.1	44.35 ± 1.34	-7.33 ± 0.22	12.74 ± 0.09	14.697 ± 0.16	119.93 ± 0.681
Globe no.2	43.58 ± 5.50	-4.96 ± 2.98	10.66 ± 2.27	11.87 ± 3.35	113.48 ± 7.68
heart no.1	60.705 ± 9.34	-0.143 ± 2.44	20.56 ± 1.68	20.675 ± 1.75	90.41 ± 6.52
heart no.2	67.576 ± 4.31	2.278 ± 1.11	23.666 ± 1.83	23.796 ± 1.86	84.57 ± 2.59

VITA

PERSONALITY

Date and Place of Birth: 01.04.1985, İzmir

EDUCATION

2016-2010 (PhD), IZTECH, Dept of Food Eng.

2010-2007(MSci.), IZTECH, Biotechnology & Bioengineering Programme

2007-2003 (BS), Ege University, Dept of Food Eng.

PUBLICATIONS

"Investigating the Potential for Novel Probiotic Bacteria Isolated in Turkey to Impact on the Microbial Ecology of Gastrointestinal Tract" Exchange Visit Report submitted to ENGIHR Scientific Committee & ESF, Aberdeen, İskoçya, Birleşik Krallık (2011) http://www.esf.org/

Şamlı M., Bayraktar O., Korel F., Zeytinyağının Termal Kararlılığının Piyasadaki Diğer Yağlarla Karşılaştırılması, 1. Ulusal Zeytin Kongresi Konferans Bildirileri Kitabı, s. 137-143, 2011, Akhisar, Türkiye

M. Samli, E. Surek, A. O.Buyukkileci, S. Harsa, K.Niranjan, "Extraction Of Lignocellulosic Compounds From Artichoke: Their Potential In Packaging Applications", Proceedings of I.C. FaBE 2013, [vol. 2] ISBN: 978-960-9510-11-0, pg 88-95.

Şamlı, M., Bayraktar, O., Korel, F. (2014): Characterization of silk fibroin based films loaded with rutin–β-cyclodextrin inclusion complexes. J Incl Phenom Macrocycl Chem, 80(1-2), 37-49

İzTech, Food Eng Dept.; İYTEGIDABÜLTEN S-1, Apr 2014, "Antioksidanlar" (Asst. Editor)

İzTech, Food Eng Dept.; İYTEGIDABÜLTEN S-2, August 2014, "Organik Gıdalar" (Editor)

M. Şamlı, E. Sürek, Ali O.Büyükkileci, Ş.Harsa, K.Niranjan. Tarımsal Atıkların Ekolojik Ambalaj Üretiminde Kullanımı, Gıda Teknolojisi Dergisi, Aralık-2014,70-73,

Traditional Fermented Foods from Turkey. By M. Samli & S. (Tellioglu) Harsa. (ENGIHR Conference: The Gut Microbiota throughout Life, , Germany. 2014, (Short Communications)

GRANTS and AWARDS

ESF- Workshop grants (1st ENGIHR Workshop, 2011; 2nd ENGIHR Workshop,2012)

ESF- Exchange visit grant (1 month, UK, 2011)

FEMS Symposium grant (8th INRA-Rowett Symposium, 2012)

"2012 yılı boyunca kütüphaneyi en çok kullanan akademik personel" Award

WORKSHOP ORGANIZATIONS AND VISITS

Visitor, GI Health Research Group, Rowett Institute of Nutrition and Health, UK (2011)

International Workshops on "Food Packaging: Balancing Functionality with Low Environmental Impact", and" Key skills to become a successful research student?", 2014, Izmir.